

EISSN 1305-6441

Indexed in
Web of Science
SCOPUS

Volume: 88 • Issue: 2 • 2025

iupress.istanbul.edu.tr/en/journal/jmed/home



Journal of Istanbul Faculty of Medicine

İstanbul Tıp Fakültesi
Dergisi



İSTANBUL
UNIVERSITY
PRESS



Journal of Istanbul Faculty of Medicine İstanbul Tıp Fakültesi Dergisi

INDEXING AND ABSTRACTING

Web of Science - Emerging Sources Citation Index (ESCI)

Scopus

TÜBİTAK-ULAKBİM TR Dizin

DOAJ

CABI Global Health Database

EBSCO Academic Search Complete

EBSCO Biomedical Index

SOBİAD

Gale Cengage



Journal of Istanbul Faculty of Medicine İstanbul Tıp Fakültesi Dergisi

OWNER

Prof. Dr. Tufan TÜKEK

İstanbul University, İstanbul Faculty of Medicine, İstanbul, Türkiye

RESPONSIBLE MANAGER

Prof. Dr. Bülent BAYRAKTAR

İstanbul University, İstanbul Faculty of Medicine, İstanbul, Türkiye

CORRESPONDENCE ADDRESS

İstanbul University, İstanbul Faculty of Medicine Dean's Office,
Publication Commission, 34093 Capa, Fatih, İstanbul, Türkiye

Phone: +90 (212) 414 21 61

E-mail: itfdergisi@istanbul.edu.tr

<https://dergipark.org.tr/tr/pub/iuitfd>

<https://iupress.istanbul.edu.tr/en/journal/jmed/home>

PUBLISHER

İstanbul University Press

İstanbul University Central Campus,
34452 Beyazıt, Fatih, İstanbul, Türkiye

Phone: +90 212 440 00 00

Authors bear responsibility for the content of their published articles.

The publication languages of the journal is English.

This is a scholarly, international, peer-reviewed and open-access journal published quarterly in January, April, July and October.

Publication Type: Periodical



Journal of Istanbul Faculty of Medicine

İstanbul Tıp Fakültesi Dergisi

EDITORIAL MANAGEMENT BOARD

Editors-in-Chief

Birsen KARAMAN – İstanbul University, İstanbul Faculty of Medicine, İstanbul, Türkiye – bkaraman@istanbul.edu.tr

Ayşe KUBAT ÜZÜM – İstanbul University, İstanbul Faculty of Medicine, İstanbul, Türkiye – ayse.kubat@istanbul.edu.tr

Co-Editors-in-Chief

Halil YAZICI – İstanbul University, İstanbul Faculty of Medicine, İstanbul, Türkiye – halildir@istanbul.edu.tr

Bengüsu MİRASOĞLU – İstanbul University, İstanbul Faculty of Medicine, İstanbul, Türkiye – bengusu.mirasoglu@istanbul.edu.tr

Section Editors

Aydın AYDOSELİ – İstanbul University, İstanbul Faculty of Medicine, İstanbul, Türkiye – aydin.aydoseli@istanbul.edu.tr

Serkan BAYRAM – İstanbul University, İstanbul Faculty of Medicine, İstanbul, Türkiye – dr.serkanbayram89@gmail.com

Nalan ÇAPAN – İstanbul University, İstanbul Faculty of Medicine, İstanbul, Türkiye – nalan.capan@istanbul.edu.tr

Ali Fuat Kaan GÖK – İstanbul University, İstanbul Faculty of Medicine, İstanbul, Türkiye – afkgok@istanbul.edu.tr

Funda GÜNGÖR UĞURLUCAN – İstanbul University, İstanbul Faculty of Medicine, İstanbul, Türkiye – funda.gungor@istanbul.edu.tr

Çiğdem KEKİK ÇINAR – İstanbul University, İstanbul Faculty of Medicine, İstanbul, Türkiye – cigdem.kekik@istanbul.edu.tr

Gonca KESKİNDEMİRCİ – İstanbul University, İstanbul Faculty of Medicine, İstanbul, Türkiye – gonca.keskindemirci@istanbul.edu.tr

Lütfiye ÖKSÜZ – İstanbul University, İstanbul Faculty of Medicine, İstanbul, Türkiye – oksuzl@istanbul.edu.tr

Nuray ÖZGÜLNAR – İstanbul University, İstanbul Faculty of Medicine, İstanbul, Türkiye – nuray.ozgulnar@istanbul.edu.tr

Bilge Şadan ÖZSAİT SELÇUK – İstanbul University, İstanbul Faculty of Medicine, İstanbul, Türkiye – ozsaitb@istanbul.edu.tr

Ayşe PALANDUZ – İstanbul University, İstanbul Faculty of Medicine, İstanbul, Türkiye – apalanduz@istanbul.edu.tr

İsmail Cem SORMAZ – İstanbul University, İstanbul Faculty of Medicine, İstanbul, Türkiye – ismail.sormaz@istanbul.edu.tr

Nermin Görkem ŞİRİN İNAN – İstanbul University, İstanbul Faculty of Medicine, İstanbul, Türkiye – nermingo@istanbul.edu.tr

Tzevat TEFİK – İstanbul University, İstanbul Faculty of Medicine, İstanbul, Türkiye – tztefik@istanbul.edu.tr

Yasemin YALÇINKAYA – İstanbul University, İstanbul Faculty of Medicine, İstanbul, Türkiye – yasemin.yalcinkaya.78@istanbul.edu.tr

Cafer Sadık ZORKUN – İstanbul University, İstanbul Faculty of Medicine, İstanbul, Türkiye – zorkun@istanbul.edu.tr

Ethics Editor

Arın NAMAL – İstanbul University, İstanbul Faculty of Medicine, İstanbul, Türkiye – arinn@istanbul.edu.tr

Statistics Editor

Halim İŞSEVER – İstanbul University, İstanbul Faculty of Medicine, İstanbul, Türkiye – hissever@istanbul.edu.tr

Publicity Managers

Bengüsu MİRASOĞLU – İstanbul University, İstanbul Faculty of Medicine, İstanbul, Türkiye – bengusu.mirasoglu@istanbul.edu.tr

Birgül TAŞTEMİR – İstanbul University, İstanbul Faculty of Medicine, Publishing Office, İstanbul, Türkiye – itfdergisi@istanbul.edu.tr

Editorial Assistant

Birgül TAŞTEMİR – İstanbul University, İstanbul Faculty of Medicine, Publishing Office, İstanbul, Türkiye – itfdergisi@istanbul.edu.tr



Journal of Istanbul Faculty of Medicine

İstanbul Tıp Fakültesi Dergisi

EDITORIAL BOARD

- Mehmet Emin ADIN – Yale University, School of Medicine, New Haven, CT, USA – mehmet.adin@yale.edu
- Sema AŞKIN KEÇELİ – Kocaeli University, Faculty of Medicine, Kocaeli, Türkiye – sema.keceli@kocaeli.edu.tr
- Pınar BAYRAK TOYDEMİR – University of Utah School of Medicine, ARUP Laboratories, Salt Lake USA – pinar.bayrak@aruplab.com
- Nilgün BOZBUĞA – İstanbul University, İstanbul Faculty of Medicine, İstanbul, Türkiye – nilgun.bozbuga@istanbul.edu.tr
- Mehmet Furkan BURAK – Harvard Medical School, Boston, USA - mfburak@hsph.harvard.edu
- Yaşar ÇALIŞKAN – Saint Louis University, School of Medicine, St. Louis, USA – yasar.caliskan@health.slu.edu
- Şükrü H. EMRE – Yale University, Yale School of Medicine, New Haven, CT, USA – sukru.emre@yale.edu
- Simin GÖRAL – Perelman School of Medicine University of Pennsylvania USA – simin.goral@uphs.upenn.edu
- Nilüfer GÖZÜM – İstanbul University, İstanbul Faculty of Medicine, İstanbul, Türkiye – nilgozum@istanbul.edu.tr
- Hülya GÜL – İstanbul University, İstanbul Faculty of Medicine, İstanbul, Türkiye – hulyagul@istanbul.edu.tr
- Ayten KANDİLCİ – Gebze Technical University, Department of Molecular Biology and Genetics, İstanbul, Türkiye – akandilci@gtu.edu.tr
- Özge KARADAĞ – Columbia Climate School, New-York, USA - ok2267@columbia.edu
- Fahrettin KELEŞTEMUR – Yeditepe University, Faculty of Medicine, İstanbul, Türkiye – kelestemur@yeditepe.edu.tr
- Dildar KONUKOĞLU – İstanbul University-Cerrahpaşa, Cerrahpaşa Faculty of Medicine, İstanbul, Türkiye – dkonuk@iuc.edu.tr
- Abdullah KUTLAR – Augusta University, Medical College, Georgia, Augusta, USA – akutlar@augusta.edu
- Sacit Bülent OMA – Yale University, Yale School of Medicine, New Haven, CT, USA – sacit.omay@yale.edu
- Betigül ÖNGEN – İstanbul University, İstanbul Faculty of Medicine, İstanbul, Türkiye – ongenb@istanbul.edu.tr
- Beyza ÖZÇINAR – İstanbul University, İstanbul Faculty of Medicine, İstanbul, Türkiye – bozcinar@istanbul.edu.tr
- Altay SENCER – İstanbul University, İstanbul Faculty of Medicine, İstanbul, Türkiye – altayser@istanbul.edu.tr
- Yasemin ŞANLI – İstanbul University, İstanbul Faculty of Medicine, İstanbul, Türkiye – yasemin.sanli@istanbul.edu.tr
- M.Öner ŞANLI – İstanbul University, İstanbul Faculty of Medicine, İstanbul, Türkiye – sanlio@istanbul.edu.tr
- Esra ŞEKETOĞLU – Health Sciences University, İstanbul, Türkiye – caglaes@yahoo.com
- Reha TOYDEMİR – University of Utah, School of Medicine, Salt Lake City, USA – rehatoy@yahoo.com
- E. Murat TUZCU – Cleveland Clinic, Abu Dhabi, UAE – tuzcue@ccf.org
- Tolga TÜRKER – University of Arizona College of Medicine, Tucson, Arizona, USA – tturker@ortho.arizona.edu
- Bernd WOLLNIK – Göttingen University, Göttingen, Germany – bernd.wollnik@med.uni-goettingen.de
- Pınar YAMANTÜRK ÇELİK – İstanbul University, İstanbul Faculty of Medicine, İstanbul, Türkiye – ymntrkp@istanbul.edu.tr
- Meral YİRMİBEŞ KARAOĞUZ – Gazi University, Faculty of Medicine, Ankara, Türkiye – karaoguz@gazi.edu.tr
- Hengameh ZANDI - Shahid Sadoughi University of Medical Sciences, School of Medicine, Department of Microbiology, Yazd, Iran - hengameh_zandi@yahoo.com



Journal of Istanbul Faculty of Medicine İstanbul Tıp Fakültesi Dergisi

AIMS SCOPE AND PUBLICATION STANDARDS

Journal of Istanbul Faculty of Medicine (J Ist Faculty Med) an international, scientific, open access periodical published in accordance with independent, unbiased, and double-blinded peer-review principles. The journal is the official publication of İstanbul University, İstanbul Faculty of Medicine and it is published quarterly on January, April, July and October. The publication language of the journal is English.

Journal of Istanbul Faculty of Medicine (J Ist Faculty Med) aims to contribute to the literature by publishing manuscripts at the highest scientific level on all fields of medicine. The journal publishes original experimental and clinical research articles, reports of rare cases, reviews articles by invited researchers who have a reputable place in the international literature in their field, and letters to the editors as well as brief reports on a recently established method or technique or preliminary results of original studies related to all disciplines of medicine from all countries.

The journal's target audience includes researchers, physicians and healthcare professionals who are interested or working in all medical disciplines.

The editorial and publication processes of the journal are shaped in accordance with the guidelines of the International Committee of Medical Journal Editors (ICMJE), World Association of Medical Editors (WAME), Council of Science Editors (CSE), Committee on Publication Ethics (COPE), European Association of Science Editors (EASE), and National Information Standards Organization (NISO). The journal is in conformity with the Principles of Transparency and Best Practice in Scholarly Publishing (doaj.org/bestpractice).

Journal of Istanbul Faculty of Medicine is currently indexed in Web of Science - Emerging Sources Citation Index (ESCI), Scopus, TUBITAK ULAKBIM TR Index, DOAJ, CABI Global Health Database, EBSCO-Academic Search Complete, EBSCO Biomedical Index, SOBIAD and Gale Cengage.

Processing and publication are free of charge with the journal. No fees are requested from the authors at any point throughout the evaluation and publication process.

All expenses of the journal are covered by the İstanbul University.

Statements or opinions expressed in the manuscripts published in Journal of Istanbul Faculty of Medicine reflect the views of the author(s) and not the opinions of the editors, the editorial board, or the publisher; the editors, the editorial board, and the publisher disclaim any responsibility or liability for such materials. The final responsibility in regard to the published content rests with the authors.

All published content is available online, free of charge.

Editor: Birsen Karaman
Address: İstanbul University, İstanbul Faculty of Medicine Deanery, Turgut Özal Cad. 34093, Çapa, Fatih, İstanbul, Türkiye
Phone: +90 212 414 21 61
E-mail: itfdergisi@istanbul.edu.tr

Publisher: İstanbul University Press
Address: İstanbul University Central Campus, 34452 Beyazıt, Fatih/İstanbul, Türkiye
Phone: +90 212 440 00 00



CONTENTS

RESEARCH ARTICLES

- 90** CORTICAL THICKNESS ALTERATIONS IN ALZHEIMER'S PROGRESSIVE MEMORY IMPAIRMENT CONTINUUM: A NETWORK PERSPECTIVE
ALZHEIMER'İN İLERLEYİCİ BELLEK BOZUKLUĞU SÜREKLİLİĞİNDE KORTİKAL KALINLIK DEĞİŞİMLERİ: AĞ PERSPEKTİFİ
Gözde KIZILATEŞ EVİN, Ali BAYRAM, Elif KURT, Emre HARI, Çiğdem ULAŞOĞLU YILDIZ, Hakan GÜRVİT, Tamer DEMİRALP
- 98** EFFECTS OF PLATELET-RICH PLASMA AND OZONE THERAPY ON PAIN AND QUALITY OF LIFE IN KNEE OSTEOARTHRITIS: A RETROSPECTIVE TRIAL
DİZ OSTEOARTRİTİNDE TROMBOSİTTEN ZENGİN PLAZMA VE OZON TEDAVİSİNİN AĞRI VE YAŞAM KALİTESİ ÜZERİNE ETKİLERİ: RETROSPEKTİF ÇALIŞMA
Aylin AYYILDIZ, Selda ÇİFTÇİ İNCEOĞLU, Banu KURAN
- 102** DO TRACTION-INTERNAL ROTATION X-RAYS HAVE AN AFFECT ON THE TREATMENT OPTIONS OF PROXIMAL FEMUR FRACTURES AMONG ORTHOPEDIC SURGEONS WITH DIFFERENT LEVELS OF EXPERTISE?
PROKSİMAL FEMUR KIRIKLARINDA ÇEKİLEN TRAKSİYON-İÇ ROTASYON GRAFİSİ FARKLI TECRÜBEDEKİ ORTOPEDİ HEKİMLERİNİN TEDAVİ SEÇENEKLERİNİ ETKİLİYOR MU?
Emre KOCAZEYBEK, Taha Furkan YAĞCI, Mehmet DEMİREL, Yavuz SAĞLAM, Cengiz ŞEN
- 108** ENHANCING RISK PERCEPTIONS AND KNOWLEDGE IN WOMEN WITH RISK PREGNANCIES: EDUCATIONAL INTERVENTION
RİSKLİ GEBELERDE RİSK ALGISINI VE BİLGİ DÜZEYİNİ ARTIRMAK: BİR EĞİTİM MÜDAHALESİ ÇALIŞMASI
Osman KÜÇÜKKELEPÇE, Hülya DOĞAN TİRYAKI, Osman KURT Bengü Nehir BUĞDAYCI YALÇIN, Erdoğan ÖZ
- 118** SYNTHESIS, CHARACTERISATION AND INVESTIGATION OF THE ANTICANCER POTENTIAL OF CARMOFUR-LOADED SILVER NANOPARTICLES
KARMOFUR YÜKLÜ GÜMÜŞ NANOPARTİKÜLLERİNİN SENTEZİ, KARAKTERİZASYONU VE ANTİKANSER POTANSİYELİNİN ARAŞTIRILMASI
Ferdane DANIŞMAN KALINDEMİRTAŞ, İshak Afşin KARİPER, Dilşad ÖZERKAN, Dürdane Serap KURUCA
- 128** HOW DID THE PANDEMIC LOCKDOWN AFFECT THE DEVELOPMENT OF INFANTS' SOCIAL AND COMMUNICATION SKILLS? A RETROSPECTIVE STUDY FROM TÜRKİYE
PANDEMİ KARANTİNASI BEBEKLERİN SOSYAL VE İLETİŞİM BECERİLERİNİN GELİŞİMİNİ NASIL ETKİLEDİ? TÜRKİYE'DEN RETROSPEKTİF BİR ÇALIŞMA
Öykü ÖZBÖRÜ AŞKAN, Gonca KESKİNDEMİRCİ, Melike METE, Ümran ÇAKIROĞLU, Shabnam ALİYEVA, Pınar YEŞİL, Gülbin GÖKÇAY
- 135** A COMPREHENSIVE MORPHOLOGICAL AND MORPHOMETRIC STUDY OF THE SPINOGLENOID NOTCH AND LIGAMENT/MEMBRANE: POSSIBLE CLINICAL RELEVANCE OF SUPRASCAPULAR NERVE ENTRAPMENT
SPİNOGLENÖİD ÇENTİK VE LİGAMENT/MEMBRAN ÜZERİNE KAPSAMLI MORFOLOJİK VE MORFOMETRİK BİR ÇALIŞMA: SUPRASKAPULAR SINIR BASISI AÇISINDAN OLASI KLİNİK ÖNEMİĞİ: TEK MERKEZ DENEYİMİ
Osman COŞKUN, İlke Ali GÜRSES, Özcan GAYRETLİ, Ayşin KALE, Adnan KINA, Ahmet USTA, Kayıhan ŞAHİNOĞLU, Adnan ÖZTÜRK
- 146** INVESTIGATION OF ACANTHAMOEBA SPP. WITH CULTURE AND MOLECULAR METHODS IN THE ENVIRONMENTAL WATER SAMPLES
ÇEVRESEL SU ÖRNEKLERİNDE ACANTHAMOEBA SPP.'NİN KÜLTÜR VE MOLEKÜLER YÖNTEMLER İLE ARAŞTIRILMASI
Şeyma EFE, Özden BORAL, Halim İŞSEVER
- 155** LATEST ADVANCES FOR TREATING CONGENITAL ADRENAL HYPERPLASIA DUE TO 21-HYDROXYLASE DEFICIENCY
21-HİDROKSİLAZ EKSİKLİĞİNE BAĞLI KONJENİTAL ADRENAL HİPERPLAZİ TEDAVİSİNDEKİ YENİLİKLER
Ecesu ÇETİN, Mehmet Furkan BURAK



CONTENTS

REVIEW

- 164** EPIGENETIC REGULATION BY CURCUMIN IN OVARIAN CANCER: A FOCUS ON miRNA NETWORKS, HISTONE MODIFICATIONS AND DNA METHYLATION
OVER KANSERİNDE KURKUMİN İLE EPIGENETİK DÜZENLEME: miRNA AĞLARI, HİSTON MODİFİKASYONLARI VE DNA METİLASYONU ÜZERİNE BİR İNCELEME
Özlem TİMİRCİ KAHRAMAN, Deryanaz BİLLUR, Esin BAYRALI ÜLKER

CASE REPORT

- 172** SPONTANEOUS DISAPPEARANCE OF A CAUDATE NUCLEUS ARTERIOVENOUS MALFORMATION FOLLOWING EXTERNAL VENTRICULAR DRAINAGE: A CASE REPORT AND LITERATURE REVIEW
EKSTERNAL VENTRİKÜLER DRENAJ SONRASI SPONTAN KAYBOLAN KAUDAT ÇEKİRDEK ARTERİOVENÖZ MALFORMASYONU: OLGU SUNUMU VE LİTERATÜR İNCELEMESİ
Duygu DÖLEN, Sefa ÖZTÜRK, Alperen POYRAZ, Cafer İkbal GÜLSEVER, Tuğrul Cem ÜNAL, İlyas DOLAŞ, Mehmet BARBUROĞLU, Pulat Akın SABANCI

LETTER TO THE EDITOR

- 176** CASE REPORTS AS AN ARTICLE: A FORLORN CAUSE?
YAYIN OLARAK OLGU SUNUMLARI: YETERİNCE DEĞER GÖRMÜYOR MU?
Manas BAJPAI

CORTICAL THICKNESS ALTERATIONS IN ALZHEIMER'S PROGRESSIVE MEMORY IMPAIRMENT CONTINUUM: A NETWORK PERSPECTIVE

ALZHEIMER'İN İLERLEYİCİ BELLEK BOZUKLUĞU SÜREKLİLİĞİNDE KORTİKAL KALINLIK DEĞİŞİMLERİ: AĞ PERSPEKTİFİ

Gözde KIZILATEŞ EVİN^{1,2} , Ali BAYRAM³ , Elif KURT³ , Emre HARI⁴ , Çiğdem ULAŞOĞLU YILDIZ³ , Hakan GÜR VİT⁵ , Tamer DEMİRALP⁴ 

¹Istanbul University, Graduate School of Health Sciences, İstanbul, Türkiye

²Istanbul University, Hulusi Behcet Life Sciences Research Laboratory, Neuroimaging Unit, İstanbul, Türkiye

³Istanbul University, Aziz Sançar Institute of Experimental Medicine, Department of Neuroscience, İstanbul, Türkiye

⁴Istanbul University, İstanbul Faculty of Medicine, Department of Physiology, İstanbul, Türkiye

⁵Istanbul University, İstanbul Faculty of Medicine, Department of Neurology, Behavioral Neurology and Movement Disorders Unit, İstanbul, Türkiye

ORCID IDs of the authors: G.K.E. 0000-0001-5518-6015; A.B. 0000-0002-6588-3479; E.K. 0000-0003-1956-575X; E.H. 0000-0002-8329-5507; Ç.U.Y. 0000-0003-1849-0055; H.G. 0000-0003-2908-8475; T.D. 0000-0002-6803-734X

Cite this article as: Kızılateş Evin G, Bayram A, Kurt E, Hari E, Ulaşoğlu Yıldız Ç, Gürvit H, et al. Cortical thickness alterations in Alzheimer's progressive memory impairment continuum: A network perspective. J Ist Faculty Med 2025;88(2):90-97. doi: 10.26650/IUITFD.1581821

ABSTRACT

Objective: Alzheimer's Progressive Memory Impairment Continuum (PMIC) is typically the clinical reflection of the neurofibrillary tangle (NFT) spread of Alzheimer's disease (AD), which starts with subtle memory complaints of subjective cognitive impairment (SCI), passes through objectifiable memory problems of the amnesic mild cognitive impairment (aMCI), and finally reaches the dementia stage of multiple cognitive deficits with an amnesic core (ADD). This study evaluated the patterns of cortical thickness changes across the PMIC, using a network perspective to unravel structural and functional disruptions.

Material and Methods: The study included 88 participants: 21 with mild ADD, 34 with aMCI, and 33 with SCI. Clinical and neuropsychiatric evaluations were conducted, followed by structural MRI scanning for cortical thickness measurements. Vertex-wise cortical thickness analyses were conducted using ANCOVA. Age, gender, and education were covariates.

Result: The results showed significant cortical thinning across the PMIC, with more pronounced reductions in the ADD group. The cortical thinning overlapped with the Default Mode Network (DMN), Ventral Attention Network (VAN), and Frontopari-

ÖZET

Amaç: Alzheimer'ın İlerleyici Bellek Bozukluğu Sürekliliği (İBBS), Alzheimer hastalığında (AH) nörofibriler yumak (NFY) yayılımının klinik yansımasıdır. Bu süreç, subjektif kognitif bozukluk (SKB) olarak bilinen hafif bellek şikayetleriyle başlayıp, amnestik hafif kognitif bozukluk (aHKB) olarak adlandırılan belirginleşmiş bellek problemlerine, nihayetinde amnestik bir çekirdekle karakterize edilen çoklu kognitif bozuklukları içeren demans aşamasına (AHD) ulaşır. Bu çalışma, İBBS boyunca kortikal kalınlık değişim paternlerini ağ perspektifiyle değerlendirerek yapısal ve fonksiyonel bozulmaları ortaya çıkarmayı amaçlamıştır.

Gereç ve Yöntem: Bu çalışmaya, 21 hafif AHD, 34 aHKB ve 33 SKB olmak üzere 88 katılımcı dahil edilmiştir. Klinik ve nöropsikiyatrik değerlendirmeler yapıldıktan sonra, kortikal kalınlık ölçümleri için yapısal MRG taraması gerçekleştirilmiştir. Verteks-temelli kortikal kalınlık analizleri ANCOVA kullanılarak yapılmıştır. Yaş, cinsiyet ve eğitim kovaryet değişkenlerdi.

Bulgular: Sonuçlar, İBBS boyunca anlamlı kortikal incelme olduğunu ve bu incelmenin AHD grubunda daha belirgin olduğunu göstermiştir. Kortikal incelme Olağan Durum Ağı (ODA), Ventral Dikkat Ağı (VDA) ve Frontoparyetal Ağ (FPA) ile örtüşmektedir.

Corresponding author/İletişim kurulacak yazar: Gözde KIZILATEŞ EVİN – gozde.kizilates@gmail.com

Submitted/Başvuru: 09.11.2024 • **Revision Requested/Revizyon Talebi:** 28.11.2024 •

Last Revision Received/Son Revizyon: 29.11.2024 • **Accepted/Kabul:** 03.12.2024 • **Published Online/Online Yayın:** 13.03.2025



Content of this journal is licensed under a Creative Commons Attribution-NonCommercial 4.0 International License.

etal Network (FPN). The comparison between the SCI and aMCI groups revealed no significant difference.

Conclusion: Cortical thinning was evident across different stages of PMIC, with more extensive thinning in later stages. The observed network-wide pattern of atrophy that AD-like deterioration affects broader neural systems rather than isolated regions. The findings highlight the importance of a network-based approach to understand AD-related structural changes and the potential for future research to integrate multimodal imaging to explore functional connectivity alongside structural atrophy.

Keywords: Alzheimer's disease, mild cognitive impairment, structural magnetic resonance imaging, cortical thickness

SKB ve aHKB grupları arasındaki karşılaştırmada anlamlı bir fark bulunamamıştır.

Sonuç: Kortikal incelleme, IBBS'nin farklı evrelerinde belirgindir ve özellikle ileri evrelerde daha yaygın görülmektedir. Ağ genelinde gözlemlenen atrofi paterni, AH-benzeri bozulmanın yalnızca izole bölgeleri değil, daha geniş sinir sistemlerini etkilediğini göstermektedir. Bulgular, AH ile ilişkili yapısal değişiklikleri anlamak için ağ tabanlı bir yaklaşımın önemini vurgulamakta ve yapısal atrofının yanı sıra fonksiyonel bağlantısallığı keşfetmek için gelecekteki araştırmalara çoklu modalite görüntülemeyi entegre etme potansiyeline dikkat çekmektedir.

Anahtar Kelimeler: Alzheimer hastalığı, hafif kognitif bozukluk, yapısal manyetik rezonans görüntüleme, kortikal kalınlık

INTRODUCTION

Alzheimer's disease (AD) is a neurodegenerative process causing progressive cognitive impairment. The initiating event is the accumulation of amyloid during the pre-clinical stage. The clinical stages start with the formation and spread of the hyperphosphorylated tau-containing neurofibrillary tangles (NFTs) (1). In the most common AD phenotype, which constitutes 90% of cases (typical AD), the transentorhinal and entorhinal limbic cortices are the initial targets of NFTs corresponding to the I and II Braak and Braak stages, followed by progressive spread along the nodes of the episodic memory neural network, comprising the intrinsic hippocampal circuitry and the larger Papez circuit of the paralimbic cortices, corresponding to Braak and Braak III and IV stages. Finally, neocortical spread starts with stage V and is completed in stage VI by the invasion of virtually all the association cortices (2, 3). Clinically, this spread pattern manifests as an insidious onset progressive memory impairment. Stages I-II are the pre-clinical stage of the disease continuum, which comprises cognitively normal (CN) individuals and those with subjective cognitive impairment (SCI), who have subjective memory complaints but normal performance in neuropsychological testing (4). The mid-stages III-IV generally correspond to the amnesic subtype of mild cognitive impairment (aMCI) stage, where memory impairment, isolated or accompanied by other cognitive deficits with lesser severity can be demonstrated. Activities of daily living (ADLs) must be preserved during the MCI stage (5-7). aMCI was shown to be double the risk of conversion to dementia in a 3-year long longitudinal study, which found the overall rate as 29% (8). Therefore, we deemed aMCI as the representative of the mid-stage along the AD continuum. Finally, the neocortical stages V-VI correspond to the dementia stage, where multiple cognitive deficits with an amnesic core are severe enough to cause ADL impairment. This dementia subtype is typical for AD and is called probable AD dementia (ADD). This particular progression of cognitive impairment leading to dementia can be named as "progressive memory impairment continuum (PMIC)", which in the presence of positive

biomarkers can also be named as "Alzheimer's continuum." Early recognition of Alzheimer's continuum-related SCI and MCI is crucial for timely interventions, as these stages offer a potential window for disease-modifying treatments before irreversible neuronal damage occurs (4, 9-12).

Complementing these neuropathological and clinical stages, structural magnetic resonance imaging (sMRI) is widely used to detect and quantify brain atrophy associated with AD. Among the key imaging biomarkers assessed by sMRI, cortical thickness is particularly relevant. Cortical thinning, especially in regions such as the entorhinal cortex, hippocampus proper and its sub-sectors, and temporoparietal areas, is one of the earliest detectable structural changes in individuals at risk for AD (13). Studies have shown that cortical thinning is strongly correlated with both the clinical progression of cognitive decline and the presence of AD pathology, such as tau and amyloid deposition. Cortical atrophy is particularly pronounced in patients transitioning from MCI to ADD. By measuring cortical thickness changes, sMRI provides valuable insights into the disease's progression and can be used to predict MCI progression to ADD (14, 15).

In the progression of ADD, alterations in the intrinsic connectivity networks (ICNs) connectivity patterns of the brain play a critical role in the clinical and pathological manifestations of the disease. Two of the most well-studied networks that show disrupted connectivity are the Default Mode Network (DMN) and the Salience/Ventral Attention Network (SN/VAN), although other networks such as the Frontoparietal Network (FPN) and Hippocampal-Cortical Networks are also affected. Early disruptions in DMN connectivity are linked to amyloid pathology in pre-clinical AD. It was shown that not only amyloid positivity as detected by amyloid PET imaging leads to DMN connectivity disruptions in CN individuals as severe as those with ADD, being mere APOE-ε4 carrier in CN individuals with negative amyloid status causes the same DMN connectivity disruption (16, 17). Longitudinal studies have also revealed a progressive shift in the balance

of within-network and inter-network connectivity, particularly within the DMN and hippocampal networks, which deteriorates over time. At the same time, compensatory increases in inter-network connectivity between the DMN and VAN are observed in the early phases of the disease, followed by a global decrease in network integration as the disease advances (18).

In this study, we aimed to evaluate and discuss patterns of cortical thickness changes from a network perspective along the continuum of AD, providing a more integrated understanding of structural and functional disruptions.

MATERIALS AND METHODS

Participants

This study included a total of 88 patients, comprising 21 with mild ADD, 34 with aMCI, and 33 with SCI, all of whom were followed up at the Behavioral Neurology and Movement Disorders Unit of the Department of Neurology, İstanbul University, İstanbul Faculty of Medicine. All participants were thoroughly informed about the study. Written informed consent was obtained before the clinical evaluation. Detailed neuropsychiatric evaluations were conducted, and study groups were determined based on scores from the Clinical Dementia Rating (CDR), the Mini-Mental State Examination (MMSE), and the Free and Cued Selective Reminding Test (FCSRT) (19-22). Additionally, all participants' FLAIR and T2-weighted structural MRI images were reviewed by an expert neurologist for the presence of hyperintensities. The ADD group included patients diagnosed with very mild and mild AD according to the NIA-AA criteria, while the aMCI group included patients diagnosed based on Petersen's criteria (23-25). The SCI group comprised individuals with self-reported memory complaints (26). The criteria of the groups are detailed in Table 1. The exclusion criteria for the study included significant neuropsychiatric disorders such as major depression or schizophrenia, systemic diseases or unstable medical conditions, neurological comorbidities, a history of stroke or head injury, and white matter hyperintensities with Fazekas scores ≥ 1 on clinical MRI examinations. The study protocol was approved by the Clinical Research Ethics Committee

Table 1: The criteria for determining study groups

Group	CDR	SOB	FCS-RT-TFR
ADD	0.5 or 1	≥ 2 (very mild ADD) or 1 (mild ADD)	-
aMCI	0.5	0.5 or 1	≤ 24
SCI	0	-	> 24

ADD: Alzheimer's disease dementia, aMCI: Amnesic mild cognitive impairment, SCI: Subjective cognitive impairment, CDR: Clinical Dementia Rating, SOB: Sum of Boxes, FCSRT-TFR: Free and Cued Selective Reminding Test-Total Free Recall

of İstanbul University, İstanbul Faculty of Medicine (Date: 09.09.2022, No: 16). This study was conducted according to the ethical principles of the latest version of the Declaration of Helsinki.

MRI acquisition

The MRI data were collected at Hulusi Behçet Life Sciences Research Laboratory, İstanbul University using a 3 Tesla MRI system (Phillips, Achieva, Best, The Netherlands) with a 32-channel SENSE head coil. T1-weighted MRI images were acquired with 3D FFE (Fast Field Echo) sequence with the following parameters: TR/TE (ms) = 8.3/3.8, flip angle = 8° , FoV = 220x240 mm, 1 mm³ isotropic voxels, 180 axial slices.

Preprocessing and cortical thickness estimation

Cortical surfaces from high-resolution T1-weighted images were extracted using the Computational Anatomy Toolbox (CAT12, version 12.9 (r1932), Structural Brain Imaging Group, University of Jena, <https://neuro-jena.github.io/cat/>) within Statistical Parametric Mapping (SPM12, r7771, Statistical Parametric Mapping, Wellcome Trust Centre for Neuroimaging, United Kingdom, <https://www.fil.ion.ucl.ac.uk/spm/>) run with MATLAB (R2022b; MathWorks, Natick, MA, USA).

A fully automated approach of CAT12 enables the cortical thickness estimation and the central surface reconstruction of the grey matter (GM) in a single step. This method uses tissue segmentation to determine the distance from the white matter (WM) to the cortical surface, then projecting the local maxima, representing the cortical thickness, onto the outer GM voxels based on neighbour relationship. This projection-based thickness (PBT) technique effectively manages sulcal blurring and partial volume effects without requiring explicit sulcal reconstruction (27).

All T1 images were corrected for bias-field inhomogeneities, automatically segmented into GM, WM, and CSF (28), and spatially aligned to a Montreal Neurological Institute standard space (MNI-152 template) using the Diffeomorphic Image Registration Algorithm (DARTEL) within SPM12 (29). The cortical thickness values were also estimated for each hemisphere. All data appeared to be of good quality, so all participants' data were used for cortical surface reconstructions. After subject-level thickness estimation, group-level analysis was performed. For group comparisons, the subject-specific results were transformed into a common space and smoothed with a 15-mm Gaussian kernel (30, 31).

Statistical analysis

The vertex-wise thickness was analysed with the General Linear Model (GLM) as part of the statistical inference using CAT12. A one-way ANCOVA model was created. Age, gender, and education were covariates. A cluster

forming threshold at $p_{\text{uncorr}} < 0.001$ and the cluster level threshold at $p_{\text{FWE-corrected}} < 0.05$ were applied.

Statistical analyses of the demographic data were conducted using SPSS 26.0 (IBM SPSS Corp., Armonk, NY, USA). Age, education, gender, and MMSE and FCSRT-TFR scores were compared among the study groups. Age was analysed using ANOVA, while education, MMSE, and FCSRT-TFR scores were compared using the Kruskal-Wallis test. Gender distribution among the groups was assessed using a chi-square test. Post hoc t-tests were performed using a 0.05 alpha threshold. The Bonferroni correction was applied for multiple comparisons.

RESULTS

Demographic and clinical results

Age, gender, and education did not differ statistically, but there were significant differences in MMSE and FCSRT-TFR scores among the groups (Table 2). Post-hoc analyses revealed that there was a significant reduction in both MMSE and FCSRT-TFR scores from SCI to ADD among the 3 groups ($p < 0.005$).

Cortical thickness comparisons

According to the ANCOVA results, widespread cortical thinning was observed among the groups in the cortical areas overlapping with DMN, VAN, and FPN (Figure 1). The cluster size, peak F value, and MNI coordinate of the statistically significant clusters are listed in Table 3.

Post hoc comparisons revealed a significant decrease in the cortical thickness in individuals with ADD compared with those with aMCI and SCI. The mean cortical thickness value of the aMCI group was lower than that of the SCI group, however this difference was not statistically significant (Figure 2).

DISCUSSION

This study investigated the surface-based morphometry analysis along the PMIC. The study revealed a widespread reduction in the cortical thickness among subjects diagnosed with ADD, aMCI, and SCI. These decreases corresponded to the VAN, FPN, and DMN regions of Yeo's 7-network atlas (32). Moreover, pairwise compari-

sons between the groups showed that this reduction was significantly greater in ADD than in aMCI and SCI.

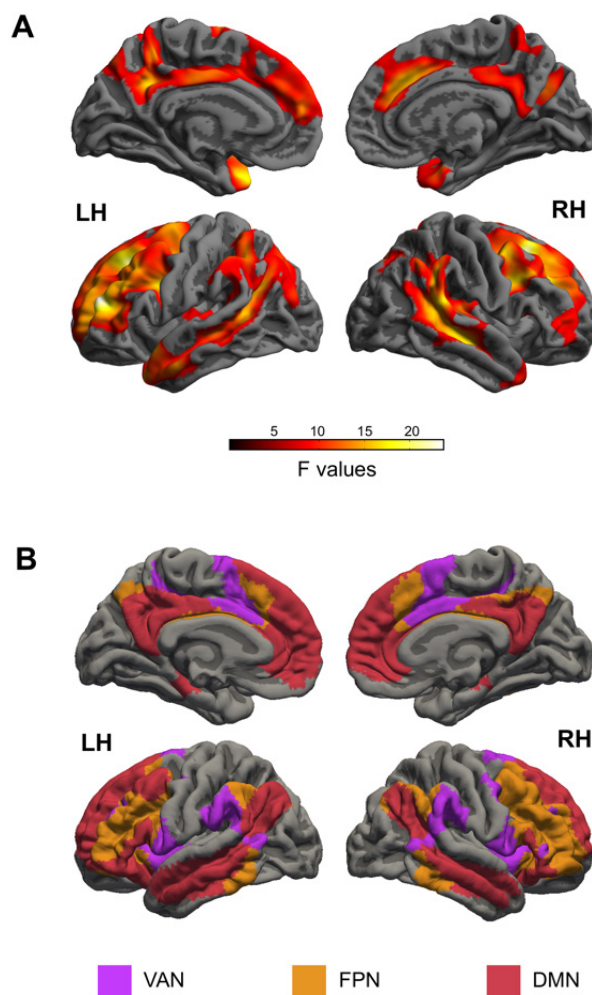


Figure 1: **A)** The areas with significant cortical thickness differences among the groups (cluster forming threshold at $p_{\text{uncorr}} < 0.001$, the cluster level threshold at $p_{\text{FWE-corrected}} < 0.05$). **B)** Yeo 7-Network Template maps comprising VAN, FPN and DMN. LH: Left Hemisphere, RH: Right Hemisphere, VAN: Ventral Attention Network, FPN: Frontoparietal Network, DMN: Default Mode Network

Table 2: Demographical and clinical characteristics of the groups

	ADD (n=21)	aMCI (n=34)	SCI (n=33)	Comparison
Age	67.43±9.938	63.79±7.176	63.12±8.019	F=1.921 ^a , p=0.153
Gender (F/M)	10/11	13/21	22/11	$\chi^2=5.554^b$, p=0.062
Education	10.86±4.629	10.94±4.936	13.12±4.722	$\chi^2=2.911^c$, p=0.233
MMSE	23.33±3.799	27.91±1.712	28.94±1.391	$\chi^2=37.315^c$, p<0.001
FCSRT-TFR	8.14±7.255	18.35±4.389	30.85±4.424	$\chi^2=68.957^c$, p<0.001

^aOne-way ANOVA test, ^bPearson's Chi-Square test, ^cKruskal-Wallis test, F: Female, M: Male, MMSE: Mini-Mental State Examination

Table 3: Clusters with cortical thickness differences among groups

Cortical areas	Hemisphere	Cluster p value	Cluster size	Peak F value	MNI coordinates (x y z)
Superior frontal Rostral middle frontal Inferior parietal Superior parietal	L	<0.0001	11476	23.73171	-22 22 41
Inferior parietal Supramarginal Superior temporal Middle temporal	R	<0.0001	4285	17.28386	65 -37 18
Superior frontal Rostral middle frontal Caudal middle frontal	R	<0.0001	3393	21.96116	23 19 51
Precuneus Posterior cingulate Isthmus cingulate	R	<0.0001	941	12.79864	20 -69 26
Pars opercularis Pars triangularis Insula	R	0.0083	223	12.96585	38 18 10
Precuneus	R	0.0173	191	9.51841	8 -49 63
Superior parietal	R	0.0260	173	9.45733	21 -68 41

MNI: Montreal Neurological Institute, L: Left, R: Right

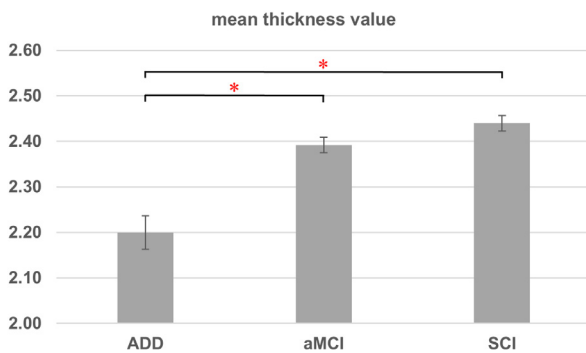


Figure 2: Mean thickness values of all significant clusters. Error bars show the standard error of the thickness values (Significance threshold * $p < 0.001$). ADD: Alzheimer's disease dementia, aMCI: Amnesic mild cognitive impairment, SCI: Subjective cognitive impairment

Many studies have explored cortical thickness changes in AD using ROI-based or surface-based morphometry approaches, highlighting significant patterns of localised atrophy. Dickerson et al. indicated that specific regions of the brain, particularly the ventromedial temporal and inferior parietal cortices, reveal cortical atrophy even in individuals with very mild AD. This regional atrophy correlated with clinical measures of memory impairment, that specific areas may serve as biomarkers for distinguishing different stages of cognitive decline. This suggests that these areas are among the first to be affected by the disease, even before more pronounced symptoms appear (14).

Additionally, Vogt et al. demonstrated significant cortical thickness reductions in individuals with ADD, particularly in the bilateral frontal, parietal, and temporal regions, as well as in the limbic areas, compared to healthy individuals and those with MCI. The cortical thickness comparison between the MCI group and controls indicated no significant difference (33).

Montal et al. reported that healthy control subjects demonstrated increased cortical thickness in middle temporal gyrus, precuneus, and superior parietal areas, indicating preserved structural integrity in the early stages. In contrast, individuals with MCI progressing to ADD show significant atrophy in critical areas such as the middle temporal gyrus, indicating early neurodegenerative changes. Furthermore, patients with dementia exhibit widespread cortical atrophy across multiple regions, reflecting the advanced and progressive nature of neurodegeneration in AD (34).

Moreover, Bakkour et al. investigated the cortical signature of thinning associated with MCI and its predictive value for the progression to mild AD dementia. The study found that the thickness of the medial temporal lobe showed the best performance to predict the progression. Additionally, the mean thickness of the AD-signature regions also performed well (35).

The findings we obtained are consistent with previous research in the literature; however, a network-based interpretation of cortical thickness alterations may provide

a more comprehensive understanding than a strictly regional approach. Specifically, our analysis revealed that the observed cortical thickness reductions were predominantly distributed across the three neural networks. This pattern indicates that neurodegenerative changes in AD may manifest not as isolated focal atrophy but rather as network-wide disruptions that reflect the vulnerability of particular ICNs to the underlying pathophysiology.

Although this study did not directly address functional changes within networks, previous literature highlights the critical role of disrupted functional connectivity in the DMN, VAN, and FPN as underlying features of AD, contributing to its cognitive symptoms. The DMN is crucial in ageing-related fMRI studies because it contains brain areas linked to AD, where amyloid buildup is first observed, even in individuals showing no symptoms (36-39). Greicius et al. was one of the first to identify that the DMN activity was disrupted in ADD as compared to CN individuals (40). Villemagne et al. showed that amyloid deposition as detected by PET was particularly evident in midline cerebral structures, which are also the major hubs of DMN, and during follow-up they observed that cognitive decline was weakly correlated with amyloid burden in patients with ADD and MCI and in CN individuals (41). Onoda et al. revealed that resting-state functional connectivity between the anterior cingulate cortex and bilateral insula, regions linked to SN, decreases with age (42). Berier et al. demonstrated that AD is linked not only to a reduction in connectivity within individual networks but also to decreased correlations between different networks. This pattern of decline becomes more pronounced as the disease progresses, reflecting a broader disruption in the functional integrity of brain networks (43). Moreover, Nebizadeh et al. reported that lower functional connectivity correlates with tau spread (44).

Our findings support the existing literature by demonstrating that reduced cortical thickness accompanies the diminished connectivity observed across these networks. This suggests a parallel relationship between cortical atrophy and decreased network connectivity, potentially reflecting the broader impact of neurodegenerative processes on the anatomical and functional integrity of the brain.

Future research could benefit from a multimodal approach by examining the relationship between cortical thickness alterations and functional network changes. This integrated analysis would offer a more comprehensive perspective, potentially elucidating how structural atrophy corresponds to disruptions in functional connectivity and contributes to the progression of neurodegenerative processes. Such an approach could provide deeper insights into the mechanisms linking anatomical and functional network changes in cognitive decline.

CONCLUSION

This study demonstrates that cortical thinning occurs across the PMIC, from SCI to aMCI and ADD, with more pronounced reductions in the later stages. The observed cortical atrophy is not restricted to specific brain regions but is distributed across key networks, including the DMN, VAN, and FPN. This network-wide pattern of cortical thinning indicates that AD impacts broader neural systems, potentially underlying the cognitive and functional deficits seen in affected individuals. Our findings emphasise the importance of a network-based approach to understanding the structural changes associated with AD. Future research should incorporate multimodal imaging techniques to explore the relationship between structural atrophy and functional connectivity disruptions, which may offer deeper insights into the mechanisms driving neurodegenerative processes.

Ethics Committee Approval: Ethics committee approval was received for this study from the İstanbul University, İstanbul Faculty of Medicine (Date: 09.09.2022, No: 16).

Informed Consent: Written informed consent was obtained from all participants who participated in this study.

Peer Review: Externally peer-reviewed.

Author Contributions: Conception/Design of Study- G.K.E., A.B., E.H., H.G., T.D.; Data Acquisition- E.K., Ç.U.Y.; Data Analysis/Interpretation – G.K.E., A.B.; Drafting Manuscript- G.K.E., A.B., E.K., E.H., Ç.U.Y.; Critical Revision of Manuscript- H.G., T.D.; Final Approval and Accountability- G.K.E., A.B., E.K., E.H., Ç.U.Y., H.G.; Supervision- H.G., T.D.

Conflict of Interest: The authors have no conflict of interest to declare.

Financial Disclosure: This work was supported by İstanbul University Research University Support Program (Grant #: TSA-2022-39128).

REFERENCES

1. Jack CR Jr, Knopman DS, Jagust WJ, Shaw LM, Aisen PS, Weiner MW, et al. Hypothetical model of dynamic biomarkers of the Alzheimer's pathological cascade. *Lancet Neurol* 2010;9(1):119-28. [\[CrossRef\]](#)
2. Braak H, Braak E. Neuropathological staging of Alzheimer-related changes. *Acta Neuropathol* 1991;82(4):239-59. [\[CrossRef\]](#)
3. Braak H, Thal DR, Ghebremedhin E, Del Tredici K. Stages of the pathologic process in Alzheimer disease: age categories from 1 to 100 years. *J Neuropathol Exp Neurol* 2011;70(11):960-9. [\[CrossRef\]](#)
4. Sperling RA, Aisen PS, Beckett LA, Bennett DA, Craft S, Fagan AM, et al. Toward defining the preclinical stages of Alzheimer's disease: Recommendations from the National Institute on Aging-Alzheimer's Association workgroups on diagnostic guidelines for Alzheimer's disease. *Alzheimers Dement* 2011;7(3):280-92. [\[CrossRef\]](#)

5. Petersen RC. Mild cognitive impairment as a diagnostic entity. *J Intern Med* 2004;256(3):183-94. [\[CrossRef\]](#)
6. Petersen RC, Doody R, Kurz A, Mohs RC, Morris JC, Rabins PV, et al. Current concepts in mild cognitive impairment. *Arch Neurol* 2001;58(12):1985-92. [\[CrossRef\]](#)
7. Winblad B, Palmer K, Kivipelto M, Jelic V, Fratiglioni L, Wahlund LO, et al. Mild cognitive impairment--beyond controversies, towards a consensus: report of the International Working Group on Mild Cognitive Impairment. *J Intern Med* 2004;256(3):240-6. [\[CrossRef\]](#)
8. Ravaglia G, Forti P, Maioli F, Martelli M, Servadei L, Brunetti N, et al. Conversion of mild cognitive impairment to dementia: predictive role of mild cognitive impairment subtypes and vascular risk factors. *Dement Geriatr Cogn Disord* 2006;21(1):51-8. [\[CrossRef\]](#)
9. Rabin LA, Smart CM, Amariglio RE. Subjective cognitive decline in preclinical Alzheimer's disease. *Annu Rev Clin Psychol* 2017;13(1):369-96. [\[CrossRef\]](#)
10. Jessen F, Amariglio RE, Van Boxtel M, Breteler M, Ceccaldi M, Chételat G, et al. A conceptual framework for research on subjective cognitive decline in preclinical Alzheimer's disease. *Alzheimers Dement* 2014;10(6):844-52. [\[CrossRef\]](#)
11. Petersen RC, Lopez O, Armstrong MJ, Getchius TS, Ganguli M, Gloss D, et al. Practice guideline update summary: Mild cognitive impairment: Report of the Guideline Development, Dissemination, and Implementation Subcommittee of the American Academy of Neurology. *Neurology* 2018;90(3):126-35. [\[CrossRef\]](#)
12. Albert MS, DeKosky ST, Dickson D, Dubois B, Feldman HH, Fox NC, et al. The diagnosis of mild cognitive impairment due to Alzheimer's disease: Recommendations from the National Institute on Aging-Alzheimer's Association workgroups on diagnostic guidelines for Alzheimer's disease. *Alzheimers Dement* 2011;7(3):270-9. [\[CrossRef\]](#)
13. Hari E, Kurt E, Ulasoglu-Yildiz C, Bayram A, Bilgic B, Demiralp T, et al. Morphometric analysis of medial temporal lobe subregions in Alzheimer's disease using high-resolution MRI. *Brain Struct Funct* 2023;228(8):1885-99. [\[CrossRef\]](#)
14. Dickerson BC, Bakkour A, Salat DH, Feczko E, Pacheco J, Greve DN, et al. The cortical signature of Alzheimer's disease: regionally specific cortical thinning relates to symptom severity in very mild to mild AD dementia and is detectable in asymptomatic amyloid-positive individuals. *Cereb Cortex* 2009;19(3):497-510. [\[CrossRef\]](#)
15. Desikan RS, Cabral HJ, Hess CP, Dillon WP, Glastonbury CM, Weiner MW, et al. Automated MRI measures identify individuals with mild cognitive impairment and Alzheimer's disease. *Brain* 2009;132(8):2048-57. [\[CrossRef\]](#)
16. Sheline YI, Morris JC, Snyder AZ, Price JL, Yan Z, D'Angelo G, et al. APOE4 allele disrupts resting state fMRI connectivity in the absence of amyloid plaques or decreased CSF Aβ42. *J Neurosci* 2010;30(50):17035-40. [\[CrossRef\]](#)
17. Sheline YI, Raichle ME, Snyder AZ, Morris JC, Head D, Wang S, et al. Amyloid plaques disrupt resting state default mode network connectivity in cognitively normal elderly. *Biol Psychiatry* 2010;67(6):584-7. [\[CrossRef\]](#)
18. Pievani M, de Haan W, Wu T, Seeley WW, Frisoni GB. Functional network disruption in the degenerative dementias. *Lancet Neurol* 2011;10(9):829-43. [\[CrossRef\]](#)
19. Buschke H. Cued recall in amnesia. *J Clin Exp Neuropsychol* 1984;6(4):433-40. [\[CrossRef\]](#)
20. Folstein MF, Folstein SE, McHugh PR. "Mini-mental state": a practical method for grading the cognitive state of patients for the clinician. *J Psychiatr Res* 1975;12(3):189-98. [\[CrossRef\]](#)
21. Ivnik RJ, Smith GE, Lucas JA, Tangalos EG, Kokmen E, Petersen RC. Free and cued selective reminding test: MOANS norms. *J Clin Exp Neuropsychol* 1997;19(5):676-91. [\[CrossRef\]](#)
22. Morris JC. The Clinical Dementia Rating (CDR) current version and scoring rules. *Neurology* 1993;43(11):2412-4. [\[CrossRef\]](#)
23. McKhann GM, Knopman DS, Chertkow H, Hyman BT, Jack CR Jr, Kawas CH, et al. The diagnosis of dementia due to Alzheimer's disease: Recommendations from the National Institute on Aging-Alzheimer's Association workgroups on diagnostic guidelines for Alzheimer's disease. *Alzheimers Dement* 2011;7(3):263-9. [\[CrossRef\]](#)
24. Grober E, Sanders AE, Hall C, Lipton RB. Free and cued selective reminding identifies very mild dementia in primary care. *Alzheimer Dis Assoc Disord* 2010;24(3):284-90. [\[CrossRef\]](#)
25. Petersen RC. Mild cognitive impairment as a diagnostic entity. *J Intern Med* 2004;256(3):183-94. [\[CrossRef\]](#)
26. Jessen F, Wolfsgruber S, Wiese B, Bickel H, Mösch E, Kaduszkiewicz H, et al. AD dementia risk in late MCI, in early MCI, and in subjective memory impairment. *Alzheimers Dement* 2014;10(1):76-83. [\[CrossRef\]](#)
27. Dahnke R, Yotter RA, Gaser C. Cortical thickness and central surface estimation. *Neuroimage* 2013;65:336-48. [\[CrossRef\]](#)
28. Ashburner J, Friston KJ. Unified segmentation. *Neuroimage* 2005;26(3):839-51. [\[CrossRef\]](#)
29. Ashburner J. A fast diffeomorphic image registration algorithm. *Neuroimage* 2007;38(1):95-113. [\[CrossRef\]](#)
30. Yotter RA, Dahnke R, Thompson PM, Gaser C. Topological correction of brain surface meshes using spherical harmonics. *Hum Brain Mapp* 2011;32(7):1109-24. [\[CrossRef\]](#)
31. Yotter RA, Thompson PM, Gaser C. Algorithms to improve the reparameterization of spherical mappings of brain surface meshes. *J Neuroimaging* 2011;21(2): e134-e147. [\[CrossRef\]](#)
32. Yeo BT, Krienen FM, Sepulcre J, Sabuncu MR, Lashkari D, Hollinshead M, et al. The organization of the human cerebral cortex estimated by intrinsic functional connectivity. *J Neurophysiol* 2011;106(3):1125-65. [\[CrossRef\]](#)
33. Vogt NM, Hunt JF, Adluru N, Dean DC III, Johnson SC, Asthana S, et al. Cortical microstructural alterations in mild cognitive impairment and Alzheimer's disease dementia. *Cereb Cortex* 2020;30(5):2948-60. [\[CrossRef\]](#)
34. Montal V, Vilaplana E, Alcolea D, Pegueroles J, Pasternak O, González-Ortiz S, et al. Cortical microstructural changes along the Alzheimer's disease continuum. *Alzheimers Dement* 2018;14(3):340-51. [\[CrossRef\]](#)
35. Bakkour A, Morris JC, Dickerson BC. The cortical signature of prodromal AD: regional thinning predicts mild AD dementia. *Neurology* 2009;72(12):1048-55. [\[CrossRef\]](#)
36. Ferreira LK, Busatto GF. Resting-state functional connectivity in normal brain aging. *Neurosci Biobehav Rev* 2013;37(3):384-400. [\[CrossRef\]](#)
37. Ferreira LK, Busatto GF. Neuroimaging in Alzheimer's disease: current role in clinical practice and potential future applications. *Clinics* 2011;66:19-24. [\[CrossRef\]](#)

38. Mevel K, Chételat G, Eustache F, Desgranges B. The default mode network in healthy aging and Alzheimer's disease. *Int J Alzheimers Dis* 2011;2011:535816. [\[CrossRef\]](#)
39. Buckner RL, Andrews-Hanna JR, Schacter DL. The brain's default network: anatomy, function, and relevance to disease. *Ann N Y Acad Sci* 2008;1124(1):1-38. [\[CrossRef\]](#)
40. Greicius MD, Srivastava G, Reiss AL, Menon V. Default-mode network activity distinguishes Alzheimer's disease from healthy aging: Evidence from functional MRI. *Proc Natl Acad Sci USA* 2004;101(13):4637-42. [\[CrossRef\]](#)
41. Villemagne VL, Pike KE, Chételat G, Ellis KA, Mulligan RS, Bourgeat P, et al. Longitudinal assessment of Abeta and cognition in aging and Alzheimer disease. *Ann Neurol* 2011;69(1):181-92. [\[CrossRef\]](#)
42. Onoda K, Ishihara M, Yamaguchi S. Decreased functional connectivity by aging is associated with cognitive decline. *J Cogn Neurosci* 2012;24(11):2186-98. [\[CrossRef\]](#)
43. Brier MR, Thomas JB, Snyder AZ, Benzinger TL, Zhang D, Raichle ME, et al. Loss of intranetwork and internetwork resting state functional connections with Alzheimer's disease progression. *J Neurosci* 2012;32(26):8890-9. [\[CrossRef\]](#)
44. Nabizadeh F. Disruption in functional networks mediated tau spreading in Alzheimer's disease. *Brain Commun* 2024;6(4):fcae198. [\[CrossRef\]](#)

EFFECTS OF PLATELET-RICH PLASMA AND OZONE THERAPY ON PAIN AND QUALITY OF LIFE IN KNEE OSTEOARTHRITIS: A RETROSPECTIVE TRIAL

DİZ OSTEOARTRİTİNDE TROMBOSİTTEN ZENGİN PLAZMA VE OZON TEDAVİSİNİN AĞRI VE YAŞAM KALİTESİ ÜZERİNE ETKİLERİ: RETROSPEKTİF ÇALIŞMA

Aylin AYYILDIZ¹ , Selda ÇİFTÇİ İNCEOĞLU² , Banu KURAN² 

¹Başakşehir Çam and Sakura City Hospital, Physical Medicine and Rehabilitation, İstanbul, Türkiye

²Hamidiye Şişli Etfal Training and Research Hospital, Physical Medicine and Rehabilitation, İstanbul, Türkiye

ORCID IDs of the authors: A.A. 0000-0002-7163-8234; S.Ç.İ. 0000-0002-0387-3558; B.K. 0000-0003-2273-1018

Cite this article as: Ayyıldız A, Çiftçi İnceoğlu S, Kuran B. Effects of platelet-rich plasma and ozone therapy on pain and quality of life in knee osteoarthritis: A retrospective trial. J Ist Faculty Med 2025;88(2):98-101. doi: 10.26650/IUITFD.1567904

ABSTRACT

Objective: There are many methods for treating knee osteoarthritis (KOA). However, especially among conservative treatments, intra-articular injection methods have not been shown to be superior to each other. In our study, we compared the effects of ozone therapy and platelet-rich plasma on pain and functionality.

Material and Methods: This retrospective clinical study included patients aged 30-70 years who received ozone and Platelet-Rich Plasma (PRP) for the treatment of knee osteoarthritis. Both groups received three sessions of ultrasound-guided intra-articular injection. The demographic characteristics of the patients, such as age and gender, were recorded. Pain was assessed with a numerical rating scale (NRS) before and three months after treatment, functionality with the Western Ontario and McMaster Universities Osteoarthritis Index (WOMAC), and quality of life with the Short Form-12 (SF-12).

Results: The mean age of the 54 patients included in the study was 58.53±8.25 years. No significant difference was found between the two groups in terms of age, gender, pre-treatment NRS, WOMAC, and SF-12 values. There were significant differences in the NRS, WOMAC, and SF-12 values in both ozone and PRP groups after treatment compared to before treatment. However, this difference was not found to be significant between the groups.

Conclusion: Both PRP and ozone therapy are effective short-term treatments for KOA. There is no evidence that one is more effective than the other.

Keywords: Knee osteoarthritis, ozone, pain, platelet-rich plasma,

ÖZET

Amaç: Diz osteoartritinin (DOA) tedavisi için birçok yöntem vardır. Ancak özellikle konservatif tedaviler arasında eklem içi enjeksiyon yöntemlerinin birbirlerine üstünlüğü gösterilememiştir. Çalışmamızda, ozon tedavisi ve trombositlen zengin plazmanın ağrı ve fonksiyonellik üzerindeki etkilerini karşılaştırmayı amaçladık.

Gereç ve Yöntem: Bu retrospektif klinik çalışmaya diz osteoartriti tedavisi için ozon ve trombositlen zengin plazma (PRP) alan 30-70 yaş arası hastalar dahil edildi. Her iki gruba da üç seans ultrason eşliğinde eklem içi enjeksiyon uygulandı. Hastaların yaş ve cinsiyet gibi demografik özellikleri kaydedildi. Ağrı tedaviden önce ve üç ay sonra sayısal derecelendirme ölçeği (NRS) ile, işlevsellik Western Ontario ve McMaster Üniversiteleri Osteoartrit İndeksi (WOMAC) ile ve yaşam kalitesi Kısa Form-12 (SF-12) ile değerlendirildi.

Bulgular: Çalışmaya dahil edilen 54 hastanın yaş ortalaması 58,53±8,25 yıl idi. İki grup arasında yaş, cinsiyet, tedavi öncesi NRS, WOMAC ve SF-12 değerleri açısından anlamlı bir fark bulunmadı. Hem ozon hem de PRP gruplarında tedavi sonrası NRS, WOMAC ve SF-12 değerlerinde tedavi öncesine göre anlamlı farklılıklar vardı. Ancak bu fark gruplar arasında anlamlı bulunmamıştır.

Sonuç: Hem PRP hem de ozon tedavisi DOA için etkili kısa süreli tedavilerdir. Birinin diğerinden daha etkili olduğuna dair bir kanıt saptanmamıştır.

Anahtar kelimeler: Diz osteoartriti, ozon, ağrı, trombositlen zengin plazma, yaşam kalitesi

Corresponding author/İletişim kurulacak yazar: Aylin AYYILDIZ – aylin.mrt93@gmail.com

Submitted/Başvuru: 15.10.2024 • **Revision Requested/Revizyon Talebi:** 31.10.2024 •

Last Revision Received/Son Revizyon: 01.12.2024 • **Accepted/Kabul:** 14.12.2024 • **Published Online/Online Yayın:** 15.04.2025



Content of this journal is licensed under a Creative Commons Attribution-NonCommercial 4.0 International License.

INTRODUCTION

Knee osteoarthritis (KOA) is a common degenerative joint disorder that leads to chronic pain and reduced function, particularly in older populations (1). With an estimated prevalence of 3.8%, KOA affects over 300 million people globally, a number expected to rise due to increased life expectancy and obesity rates (2-4).

Treatment approaches for KOA fall into two broad categories: conservative and surgical. Surgery offers a definitive solution but is typically reserved as a last resort due to its cost and higher risk of complications (5, 6). Among the conservative methods, intra-articular injections have gained attention although current research does not establish any one injection as superior. While many studies have focused on individual injectate, few have compared different types, such as ozone, platelet-rich plasma (PRP), corticosteroids, and hyaluronic acid. This gap often leaves clinicians to make treatment decisions based on experience rather than high-level evidence (7). This is because the study methods employed have often focused on the effect of a single injectate. The number of studies examining the comparative efficacy of intra-articular injection types, including ozone, PRP, corticosteroid, and hyaluronic acid, in terms of pain and functional status is limited (5). This lack of evidence-based research results in clinicians organising treatment plans based on their personal experiences rather than on treatments with a high level of evidence. In response, this study aimed to compare the efficacy of PRP and ozone therapy in managing KOA-related pain and functional impairment.

MATERIAL AND METHODS

This retrospective comparative study was conducted between August and September 2024 at the Physical Medicine and Rehabilitation Clinic of Şişli Hamidiye Etfal Training and Research Hospital. Ethical approval was granted by the Clinical Research Ethics Committee of Şişli Hamidiye Etfal Training and Research Hospital (Date: 09.07.2024, No: 2691), and all participants provided informed consent.

The initial screening phase involved the evaluation of 72 patients, aged between 30-70 years, who had presented at the outpatient clinic for the purpose of receiving treatment for KOA and had been administered an intra-articular injection as part of a PRP or ozone therapy between January and April 2024. Only patients diagnosed with stage 2 or 3 KOA, according to the Kellgren-Lawrence grading system. Patients with KOA flares, stages 1 or 4 osteoarthritis, recent knee surgery or injections within the last three months, infections, malignancies, bleeding disorders, or cognitive impairments were excluded.

Demographic and clinical data, including age, gender, occupation, gonarthrosis stage, and symptom duration,

were collected through hospital records. Pain levels were recorded using the Numeric Rating Scale (NRS), functionality was assessed via the WOMAC index, and quality of life was evaluated using the Short Form-12 (SF-12) before treatment and three months afterward. Patients were divided into two groups: one receiving intra-articular leukocyte-poor PRP and the other ozone therapy. Each group received three weekly injections administered under ultrasound guidance. The ozone group was given 15 µg/mL of ozone, delivered in 10 cc volumes, while PRP was prepared using a two-step centrifugation process. In the PRP group, blood was drawn from the patients, placed in citrated tubes, and spun at low speed to separate platelets. After the first centrifugation, the plasma containing the platelets was transferred to new tubes and subjected to higher-speed centrifugation, after which the platelet-rich fraction was injected into the knee under ultrasound guidance, with the knee flexed at 20°.

Statistical analysis

Sample size calculations, with an alpha significance level of 0.05 and 95% power, indicated that at least 54 participants were required. Descriptive statistics included means, standard deviations, medians, minimums, maximums, frequencies, and percentages. The Kolmogorov-Smirnov test was used to assess the data distribution. The Mann-Whitney U test was applied to the independent quantitative variables, and the Wilcoxon and Student-t tests were used for the dependent data. The chi-square test and Fisher's exact test were used to analyse qualitative data when the chi-square assumptions were unmet.

RESULTS

Of the 72 patients screened, 27 patients who met the inclusion criteria were included in the PRP group, and 27 patients were included in the ozone group. Of the 18 patients excluded from the study, 12 had undergone ozone therapy and 6 had received PRP. The retrospective data study revealed that no adverse effects were reported following the injection.

The average age of participants was 58.53±8.25 years. The ozone group had a mean age of 58.2±8.54, and the PRP group had a mean age of 58.9±8.11. Age differences between the groups were not statistically significant ($p>0.05$). In terms of gender, 49 patients (90.7%) were female and 5 (9.3%) were male, with no significant difference in gender distribution between the groups ($p>0.05$). Both groups showed no significant pre-treatment differences in NRS scores, WOMAC scores, Kellgren-Lawrence stages, or SF-12 mental and physical component scores ($p>0.05$).

Post-treatment results indicated significant improvements in the ozone group across the NRS, WOMAC, and SF-12 physical and mental component scores ($p<0.05$). Similarly, the PRP group demonstrated signif-

icant improvements in these same measures ($p < 0.05$). However, when comparing the magnitude of change in the NRS and WOMAC scores between the groups, no statistically significant differences were identified ($p > 0.05$). The only notable difference between the groups was found in the SF-12 mental component scores, where the ozone group saw a significant increase, while the PRP group experienced a decrease, creating a statistically significant divergence between the two groups ($p < 0.05$). These findings are summarised in Table 1.

Table 1: Comparison of the ozone and PRP groups in terms of pain, functionality, and quality of life

	Ozone group (n=27) Mean±SD	PRP group (n=27) Mean±SD	p
Pre-treatment NRS for pain	7.52±0.753	7±0.877	
Post-treatment NRS for pain	5.89±1.739	5.22±1.761	
Intra-group changes	mean difference: 2.00	mean difference: 2.00	0.483 ^M
Intra-group p	<.001^W	<.001^W	
Pre-treatment WOMAC	53.7±16.134	50.26±6.746	
Post-treatment WOMAC	44.22±15.2	42.15±12.654	
Intra-group changes	mean difference: 9.00	mean difference: 8.41	0.614 ^M
Intra-group p	<.001^W	<.001^W	
Pre-treatment SF-12 PCS	33.47±5.722	34.27±6.087	
Post-treatment SF-12 PCS	37.02±7.871	39.35±6.732	
Intra-group changes	mean difference: -3.55	mean difference: -5.46	0.400 ^T
Intra-group p	0.019^P	<.001^W	
Pre-treatment SF-12 MCS	48.3±6.719	51.27±7.589	
Post-treatment SF-12 MCS	51.8±6.176	49.89±8.263	
Intra-group changes	mean difference: -3.50	mean difference: 1.31	0.003^M
Intra-group p	0.018^P	0.011^W	

NRS: Numeric Rating Scale, WOMAC: Western Ontario and McMaster Universities Osteoarthritis Index, SF-12: Short Form-12, PCS: Physical Component Score, MCS: Mental Component Score, PRP: Platelet-Rich Plasma SD: Standard deviation, M: Mann-Whitney U Test, T: Student-t Test, P: Paired T test, W: Wilcoxon Test

DISCUSSION

This study highlights that both ozone therapy and PRP are effective in managing pain and improving functional status in patients with KOA over the short term. Our findings indicate significant improvements in pain relief and functionality after treatment in both groups, with no substantial evidence revealing that one therapy is more effective than the other. These results align with existing literature, including a meta-analysis by Rahimzadeh et al., which found both treatments effective in the short term, although PRP demonstrated superior long-term outcomes for KOA (8). Similarly, Raeissadat et al.'s randomised clinical trial also supported our results, indicating that ozone therapy produces rapid relief, with comparable early-stage outcomes to PRP. However, in the later stages, PRP shows a tendency to yield more sustained benefits (3). This distinction is echoed in other research, such as a meta-analysis by Lin et al., where PRP outperformed other intra-articular therapies for treating KOA (5).

In a study examining ozone therapy, Arias-Vazquez et al. observed a marked reduction in pain following intra-articular ozone injections, although the improvements in functionality were temporary (9). Our study also demonstrated significant improvements in pain and function, but as we only evaluated patients over a 3-month period, longer-term assessments are required to fully gauge these effects. In a meta-analysis comparing PRP with corticosteroids, which have proven their effectiveness in the treatment of KOA for years, although intra-articular corticosteroid injection and PRP showed similar effects in terms of pain and functionality in the early period, the superiority of PRP over corticosteroids was shown in the longer term, and this is thought to increase the effectiveness of PRP as a treatment method (10). A study by Khuba et al. demonstrated that PRP is an effective treatment for pain reduction and functional improvement in early KOA, with benefits lasting up to six months after a single dose application (11). The effectiveness of PRP is influenced by numerous factors, such as the patient's initial pain level, the concentration of white blood cells, and the platelet count in the prepared PRP. The researches show that a platelet concentration of at least 10 billion is required to achieve meaningful therapeutic effects in KOA (12, 13). In our study, PRP was prepared in line with these recommendations, and the ozone doses administered also correspond to those cited in the existing literature (14).

Moreover, some studies have explored the combination of PRP and ozone therapy. For example, Dernek et al. found that combining these therapies resulted in similar improvements in pain and function as PRP alone, although the ozone group reported reduced pain after injections. This supports the idea that PRP is also effective as a monotherapy for KOA (15).

One of the key limitations of this study is its short-term follow-up period. Although our evaluations were performed three months post-treatment, longer-term studies are necessary to understand the sustained effects of both therapies. Additionally, this study was not a randomised controlled trial, and there was no blinding, which could introduce bias. Future studies should address these limitations by employing randomised controlled designs with extended follow-up periods.

CONCLUSION

This study demonstrated that both PRP and ozone therapy are effective short-term treatments for KOA, providing significant improvements in pain and functionality. No clear evidence demonstrates that one treatment is more effective than the other within the evaluated period. However, further long-term studies are needed to assess whether the benefits of these therapies persist over time.

Ethics Committee Approval: Ethics committee approval was received for this study from the Şişli Hamidiye Etfal Training and Research Hospital (Date: 09.07.2024, No: 2691).

Informed Consent: Written informed consent was obtained from all participants who participated in this study.

Peer Review: Externally peer-reviewed.

Author Contributions: Conception/Design of Study- A.A.; Data Acquisition- A.A., S.Ç.; Data Analysis/Interpretation – A.A., B.K.; Drafting Manuscript- A.A.; Critical Revision of Manuscript- A.A.; Final Approval and Accountability- A.A., B.K.; Technical or Material Support- S.Ç.; Supervision- B.K.

Conflict of Interest: The authors have no conflict of interest to declare.

Financial Disclosure: The authors declared that this study received no financial support.

REFERENCES

- Hunter DJ, Bierma-Zeinstra S. Osteoarthritis. *Lancet* 2019;393(10182):1745-59. [\[CrossRef\]](#)
- Lawrence RC, Felson DT, Helmick CG, Arnold LM, Choi H, Deyo RA, et al. Estimates of the prevalence of arthritis and other rheumatic conditions in the United States. Part II. *Arthritis Rheum* 2008;58(1):26-35. [\[CrossRef\]](#)
- Raeissadat SA, Ghazi Hosseini P, Bahrami MH, Salman Roghani R, Fathi M, Gharooee Ahangar A, et al. The comparison effects of intra-articular injection of platelet rich plasma (PRP), plasma Rich in growth factor (PRGF), Hyaluronic Acid (HA), and ozone in knee osteoarthritis; a one year randomized clinical trial. *BMC Musculoskelet Disord* 2021;22(1):134. [\[CrossRef\]](#)
- Blaga FN, Nutiu AS, Lupsa AO, Ghiurau NA, Vlad SV, Ghitea TC. Exploring Platelet-rich plasma therapy for knee osteoarthritis: An in-depth analysis. *J Funct Biomater* 2024;15(8):221. [\[CrossRef\]](#)
- Lin X, Zhi F, Lan Q, Deng W, Hou X, Wan Q. Comparing the efficacy of different intra-articular injections for knee osteoarthritis: A network analysis. *Medicine (Baltimore)* 2022;101(31):e29655. [\[CrossRef\]](#)
- Meheux CJ, McCulloch PC, Lintner DM, Varner KE, Harris JD. Efficacy of Intra-articular Platelet-rich plasma injections in knee osteoarthritis: A systematic review. *Arthroscopy* 2016;32(3):495-505. [\[CrossRef\]](#)
- Bannuru RR, Osani MC, Vaysbrot EE, Arden NK, Bennell K, Bierma-Zeinstra SMA, et al. OARSI guidelines for the non-surgical management of knee, hip, and polyarticular osteoarthritis. *Osteoarthritis Cartilage* 2019;27(11):1578-89. [\[CrossRef\]](#)
- Rahimzadeh P, Imani F, Azad Ehyaei D, Faiz SHR. Efficacy of oxygen-ozone therapy and platelet-rich plasma for the treatment of knee osteoarthritis: A meta-analysis and systematic review. *Anesth Pain Med* 2022;12(4):e127121. [\[CrossRef\]](#)
- Arias-Vázquez PI, Tovilla-Zárate CA, Hernández-Díaz Y, González-Castro TB, Juárez-Rojop IE, López-Narváez ML, et al. Short-Term Therapeutic Effects of ozone in the management of pain in knee osteoarthritis: A meta-analysis. *PM R* 2019;11(8):879-87. [\[CrossRef\]](#)
- Bensa A, Sangiorgio A, Boffa A, Salerno M, Moraca G, Filardo G. Corticosteroid injections for knee osteoarthritis offer clinical benefits similar to hyaluronic acid and lower than platelet-rich plasma: a systematic review and meta-analysis. *EFORT Open Rev* 2024;9(9):883-95. [\[CrossRef\]](#)
- Khuba S, Khetan D, Kumar S, Garg KK, Gautam S, Mishra P. Role of platelet rich plasma in management of early knee osteoarthritis pain: A retrospective observational study. *Interv Pain Med* 2023;2(4):100297. [\[CrossRef\]](#)
- Kikuchi N, Yoshioka T, Arai N, Sugaya H, Hyodo K, Taniguchi Y, et al. A Retrospective analysis of clinical outcome and predictive factors for responders with knee osteoarthritis to a single injection of leukocyte-poor platelet-rich plasma. *J Clin Med* 2021;10(21):5121. [\[CrossRef\]](#)
- Berrigan W, Tao F, Kopcow J, Park AL, Allen I, Tahir P, et al. The effect of platelet dose on outcomes after platelet rich plasma injections for musculoskeletal conditions: A systematic review and meta-analysis. *Curr Rev Musculoskelet Med* 2024. 2024/09/27. doi: 10.1007/s12178-024-09922-x. [\[CrossRef\]](#)
- Lino VTS, Marinho DS, Rodrigues NCP, Andrade CAF. Efficacy and safety of ozone therapy for knee osteoarthritis: an umbrella review of systematic reviews. *Front Physiol* 2024;15:1348028. [\[CrossRef\]](#)
- Dernek B, Kesiktas FN. Efficacy of combined ozone and platelet-rich-plasma treatment versus platelet-rich-plasma treatment alone in early stage knee osteoarthritis. *J Back Musculoskelet Rehabil* 2019;32(2):305-11. [\[CrossRef\]](#)

DO TRACTION-INTERNAL ROTATION X-RAYS HAVE AN AFFECT ON THE TREATMENT OPTIONS OF PROXIMAL FEMUR FRACTURES AMONG ORTHOPEDIC SURGEONS WITH DIFFERENT LEVELS OF EXPERTISE?

PROKSİMAL FEMUR KIRIKLARINDA ÇEKİLEN TRAKSİYON-İÇ ROTASYON GRAFİSİ FARKLI TECRÜBEDEKİ ORTOPEDİ HEKİMLERİNİN TEDAVİ SEÇENEKLERİNİ ETKİLİYOR MU?

Emre KOCAZEYBEK^{1,2} , Taha Furkan YAĞCI² , Mehmet DEMİREL² , Yavuz SAĞLAM² , Cengiz ŞEN² 

¹Haseki Training and Research Hospital, Clinic of Orthopedics and Traumatology, İstanbul, Türkiye

²İstanbul University, İstanbul Faculty of Medicine, Department of Orthopedics and Traumatology, İstanbul, Türkiye

ORCID IDs of the authors: E.K. 0000-0001-5861-8653; T.F.Y. 0000-0002-5097-2241; M.D. 0000-0003-1131-7719; Y.S. 0000-0003-4475-8211; C.Ş. 0000-0001-9788-580X

Cite this article as: Kocazeybek E, Yağcı TF, Demirel M, Sağlam Y, Şen C. Do traction-internal rotation X-rays have an affect on the treatment options of proximal femur fractures among orthopedic surgeons with different levels of expertise? J Ist Faculty Med 2025;88(2):102-107. doi: 10.26650/IUITFD.1583403

ABSTRACT

Objective: The purpose of the current study was to investigate whether the traction-internal rotation X-ray used in proximal femur fractures actually alters the implant choice among 12 different levels of expertise orthopaedic surgeons.

Material and Methods: The radiographs of 50 patients who were treated due to proximal femur fracture in our clinic were identified retrospectively. Twelve orthopaedic surgeons evaluated the patient X-rays in two different rounds, two weeks apart. Each observer was asked to independently examine the anteroposterior radiographs of both hips in the first round and the traction-internal rotation radiographs in the second round. Inter-observer agreement was determined using the Fleiss' Kappa statistic, while intra-observer agreement was calculated using the Kappa statistic.

Results: A total of 50 patients with proximal femur fractures were included in our study. 26 of the patients were female (52%) and 24 (48%) were male. The average age of the participants was 70 (50±94). The implant options were as follows: total hip arthroplasty, hemiarthroplasty, proximal femur nail, long femur nail, 95° AO blade plate, anatomical plate, cannulated screw and dynamic hip screw. The intraobserver agreement was found to be moderate to substantial ($\kappa=0.44-0.68$) in consultant trauma surgeons, moderate in senior orthopaedic surgeons ($\kappa=0.47-0.56$) and fair to moderate ($\kappa=0.24-0.59$) in orthopaedic residents. The

ÖZET

Amaç: Bu çalışmanın amacı, proksimal femur kırıklarında kullanılan traksiyon-iç rotasyon röntgeninin, 12 farklı uzmanlık seviyesindeki ortopedik cerrahlar arasında implant seçimini gerçekten değiştirip değiştirmediğini araştırmaktır.

Gereç ve Yöntem: Kliniğimizde proksimal femur kırığı nedeniyle tedavi edilen 50 hastanın radyografileri retrospektif olarak belirlendi. Hasta röntgenleri 12 ortopedik cerrah tarafından iki hafta arayla iki farklı turda değerlendirildi. İlk turda her gözlemciden her iki kalçanın ön-arka radyografilerini, ikinci turda ise traksiyon-iç rotasyon radyografilerini bağımsız olarak incelemeleri istendi. Gözlemciler arası uyum için Fleiss Kappa istatistiği, gözlemciler içi uyum için Cohen Kappa kat sayısı kullanıldı.

Bulgular: Çalışmamıza proksimal femur kırığı olan toplam 50 hasta dahil edildi. Hastaların 26'sı (%52) kadın, 24'ü (%48) erkekti. Katılımcıların yaş ortalaması 70 (50±94) idi. İmplant seçenekleri total kalça artroplastisi, hemiarthroplasti, proksimal femur çivisi, uzun femur çivisi, 95° AO blade plak, anatomik plak, kanüllü vida ve dinamik kalça vidası olarak belirlendi. Gözlemciler içi uyum danışman travma cerrahlarında orta ila önemli ($\kappa=0,44-0,68$), kıdemli ortopedi cerrahlarında orta ($\kappa=0,47-0,56$) ve ortopedi asistanlarında ortanın altı ve orta ($\kappa=0,24-0,59$) olarak saptandı. Gözlemciler arasında uyum ise danışman travma cerrahları arasında orta ila önemli düzeyde ($\kappa=0,56-0,62$), kıdemli ortopedi cerrahlar

Corresponding author/İletişim kurulacak yazar: Emre KOCAZEYBEK – emrekc2@gmail.com

Submitted/Başvuru: 12.11.2024 • **Revision Requested/Revizyon Talebi:** 05.01.2025 •

Last Revision Received/Son Revizyon: 04.03.2025 • **Accepted/Kabul:** 04.03.2025 • **Published Online/Online Yayın:** 16.04.2025



Content of this journal is licensed under a Creative Commons Attribution-NonCommercial 4.0 International License.

inter-observer agreement was moderate to substantial between consultant trauma surgeons ($\kappa=0.56-0.62$), moderate agreement between senior orthopaedic surgeons and fair agreement between orthopaedic residents respectively ($\kappa=0.45$, $\kappa=0.30$).

Conclusion: Traction radiography is crucial in the proper classification of proximal femur fractures in accordance with the literature. This study shows that as professional experience increases, traction radiography increases the consistency in surgical implant selection.

Keywords: Hip fracture, traction-internal rotation X-ray, proximal femur

INTRODUCTION

Hip fractures are one of the most common trauma referrals to orthopaedic emergency departments (1). With the development of technology, an increase in the incidence of hip fractures is observed because of the prolonged life expectancy in the human population (1, 2). These hip fractures can occur in two different segments of the population (1). While a minority of the cases occurred in the younger generation usually caused by high-energy trauma, the major remaining part happened in the elderly due to numerous factors along with age-associated reduced bone quality (3). With the early diagnosis and correct treatment algorithm, this burden on the health system can be significantly reduced.

Several methods exist in the classification of proximal femoral fractures based on plain radiographs, but none has been shown to be practical with satisfactory reproducibility and reliability in literature reviews (4, 5).

In a suspected hip fracture, evaluation begins with a standard pelvis AP (anteroposterior) X-ray. In some clinics, cross table lateral is added in addition to the pelvis Anteroposterior (AP) X-ray (1). In rare cases, CT and MRI are also used in some occult hip fractures (6). Recognising the pattern of the fracture on radiographs is essential to determine the surgical treatment. The affected limbs of patients with proximal femur fractures usually appear in a short and externally rotated posture. The position of the extremity, considering the natural anteversion of the femur, the fracture pattern can be difficult to understand. Therefore, traction-internal rotation projection corrects the femoral anteversion and aligns the fracture.

Our aim in this study was to investigate whether the traction-internal rotation X-ray used in proximal femur fractures actually alters the treatment plan among 12 different levels of expertise orthopaedic surgeons.

MATERIAL AND METHODS

Study design and setting

This single-centre retrospective study was performed in the Department of Orthopaedics and Traumatology with permission of İstanbul Faculty of Medicine Clinical Research Ethics Committee (Date: 26.01.2024, No: 2).

arasında orta derecede ve ortopedi asistanları arasında ortanın altı düzeyde ($\kappa=0,45$, $\kappa=0,30$) idi.

Sonuç: Traksiyon radyografisi proksimal femur kırıklarının literatüre uygun olarak doğru sınıflandırılmasında önemlidir. Bu çalışma mesleki deneyim arttıkça traksiyon radyografisinin cerrahi implant seçiminde tutarlılığı arttırdığını göstermektedir.

Anahtar kelimeler: Kalça kırığı, traksiyon-iç rotasyon röntgeni, proksimal femur

Patient selection

Patients with fractures of 31A1/2/3 and its subtypes according to the new AO/OTA classification between 2022 and 2023 were retrospectively analysed (7). Standard plain Pelvis AP, cross table lateral and AP traction-internal rotation radiograph of 50 randomly selected patients were chosen from our hospital database via the Picture Archive and Communication System (PACS) and formed into two electronic folders. Demographic data of these patients including age and gender were also recorded (Table 1).

Table 1: Demographics of the patients

	Mean±SD	Min-Max
Age, years	74.7±10	50-94
Gender, F/M	26/24 (52%-48%)	
Side (R/L)	33/17 (66%-34%)	

F: Female, M:Male, R: Right, L: Left

Inclusion criteria:

- Patients older than 18 years old
- Patients with fractures of 31A1/2/3 and its subtypes

Exclusion criteria:

- Patients younger than 18 years old
- Patients with concomitant proximal and diaphyseal or distal femur fractures
- Patients with femoral head fracture

The techniques of the images are given below.

AP pelvis (Figure 1a): Patient in supine position with the beam perpendicular to the pelvis and feet positioned in 15°-20° of internal rotation.

Cross table lateral (Figure 1b): Patient in the supine position with the radiation beams parallel to the table, the unaffected hip is abducted and flexed to >80°. With the affected limb in 15o internal rotation, the X-ray tube is placed at the foot of the opposite extremity and the beam is parallel to the table and 45° to the extremity.



Figure 1a: Anteroposterior (AP) X-ray of the hip



Figure 1c: Traction- internal rotation X-ray of the hip



Figure 1b: Cross-table lateral X-ray of the hip

Traction-internal rotation radiograph (Figure 1c): Patient in supine position with the beam perpendicular to the pelvis, the first assistant holds the patient from the armpits and the other assistant applies traction to the affected limb from the ankle until the limb length is equal to the other.

The X-rays were prepared in the digital platform and sent to the participants by e-mail. The operation technique and implant choice were asked participants with a 2-week interval. The operation techniques were consisted of three different modalities including open reduction-internal fixation group such as Dynamic hip screw (DHS), Screw fixation, 95 or 130 AO Blade, Anatomical Proximal Femur plate, intramedullary nailing (Short or

long Intramedullary Nailing), arthroplasty (Hemiarthroplasty or Total Hip Replacement) which formed the treatment options.

Twelve observers were selected in accordance with their orthopaedic experience as following; five consultant trauma surgeons, three senior orthopaedic surgeons and four orthopaedic residents

In the first step, the fracture side was shown randomly to the twelve orthopaedic physicians via standard pelvis radiograph and asked their surgical options. In the second step, all radiographs were mixed in a randomised sequence and the traction-internal rotation X-rays were added next to the standard pelvis AP radiograph and showed the participants two weeks after the initial survey. In this step, we asked about their surgical options again. In this way, the surgical preferences of each observer were obtained twice, two weeks apart, regardless of their initial choice.

Statistical analysis

The statistical data were analysed using SPSS (Statistical Package for the Social Sciences) version 27.0 (IBM SPSS Corp., Armonk, NY, USA). The mean, minimum–maximum, standard deviation (SD), and percentage were used as descriptive statistics. The value of $p < 0.05$ was considered statistically significant. Inter-observer agreement was determined with The Fleiss' Kappa statistic, while intra-observer agreement was calculated with the Kappa statistic (Cohen's Kappa coefficient) in two time points (one month interval) individually (Table 2) (8).

RESULTS

A total of 50 patients with proximal femur fractures were included in our study. 26 of the patients were female (52%) and 24 (48%) were male. The average age of the participants was 70 (50–94) (Table 1).

Table 2: Kappa statistic agreement scores

Value of κ	Agreement
<0	Poor agreement
0.00-0.20	Slight agreement
0.21-0.40	Fair agreement
0.41-0.60	Moderate agreement
0.61-0.80	Substantial agreement
0.81-1.00	Almost perfect agreement

The inter-observer analysis for the first and second observational points are shown in Table 3, respectively. The inter-observer agreement was moderate to substantial between the consultant trauma surgeons ($\kappa=0.56-0.62$) (Table 3). On the other hand, moderate agreement was found between senior orthopaedic surgeons and fair agreement was found in orthopaedic residents respectively ($\kappa=0.45$, $\kappa=0.30$). When all the observers were taken into consideration, the interobserver agreement was found to be fair.

Intra-observer analysis of all participants is given in Table 4. The intra-observer agreement of the consultant trauma surgeons was found to be moderate to substantial ($\kappa=0.44-0.68$) (Table 4).

The intra-observer agreement of orthopaedic surgeons was found to be moderate ($\kappa=0.47-0.56$) (Table 4).

The intra-observer agreement of orthopaedic residents was found to be fair to moderate ($\kappa=0.24-0.59$) (Table 4).

Table 3: Inter-observer analyses for the comparison of the two observational points

Status	Fleiss' kappa (95% CI)	Level of agreement
All observers		
First assessment	0.32 (0.31-0.34)	Fair
Second assessment	0.40 (0.37-0.41)	Fair
Consultant trauma surgeons (O-1, O-2, O-3, O-4, and O-5)		
First assessment	0.56 (0.60-0.69)	Moderate
Second assessment	0.64 (0.6-0.68)	Substantial
Senior orthopaedic surgeons (O-6, O-7, and O-8)		
First assessment	0.52 (0.43-0.60)	Moderate
Second assessment	0.45 (0.37-0.54)	Moderate
Orthopaedic residents (O-9, O-10, O-11, and O-12)		
First assessment	0.32 (0.26-0.37)	Fair
Second assessment	0.30 (0.23-0.35)	Fair

DISCUSSION

The most important finding of our study is that intra- and inter-observer agreement is higher in experienced orthopaedic surgeons (consultants and seniors) after the use of traction radiography in the treatment choice of proximal femur fractures. Diagnosing and classifying proximal femur fractures has a significant impact on determining the optimal method of treatment and the overall prognosis of the patient (9).

Table 4: Intra-observer analyses for the comparison of the two observational points

	Observer	Cohen's K value (95% CI)	Level of agreement
Consultant trauma surgeons	O-1	0.68	Substantial
	O-2	0.53	Moderate
	O-3	0.64	Substantial
	O-4	0.59	Moderate
	O-5	0.44	Moderate
Senior orthopaedic surgeons	O-6	0.56	Moderate
	O-7	0.53	Moderate
	O-8	0.47	Moderate
Orthopaedic residents	O-9	0.24	Fair
	O-10	0.59	Moderate
	O-11	0.42	Moderate
	O-12	0.28	Fair

Dr. Witze identified the use of traction-internal rotation radiography in the diagnosis of hip fractures in 1974 (10). Although Dr. Witze originally identified it with its use of the diagnosis of subtle proximal femur fractures, it later began to be part of the standard radiographic series obtained for hip fracture at several departments of orthopaedics and traumatology (11).

A number of studies examining the necessity of traction X-ray were found in the literature review (12-14). A study by Koval et al. reported that routine traction radiography in proximal femur fractures is more accurate in fracture classification. Moreover, they also stated that this has a direct impact on accurate surgical planning and implant choice (12). Even though their study was conducted with 15 orthopaedic residents, in our study, fair agreement was found in the evaluation of implant selection with traction X-rays between resident physicians. A similar study was conducted by Khurana et al. in 2018 (13). X-rays were evaluated by 2 musculoskeletal radiologists. It was re-

ported in the study that traction radiography increased accuracy in proximal femur fracture classification even among radiologists. On the other hand, the universal classification of pertrochanteric fractures is the AO/OTA. Two recent studies were published about the reliability of the classification (15, 16). Both studies revealed that internal rotation traction X-rays did not improve the reliability of the new AO/OTA classification for pertrochanteric fractures as assessed by inter- and intra-observer agreement between different levels of expertised surgeons.

The unique aspect of our study was to examine the effects of traction X-rays on surgical implant choice among three groups of orthopaedic surgeons. Traction X-rays are important to distinguish whether the fracture is stable or unstable, especially in proximal femur fractures. Based on the literature, while DHS and intramedullary nails can be applied to stable fractures, intramedullary devices are more preferred for unstable fractures due to their biomechanical superiority (17, 18). A recent study similar to ours was conducted by Garcia-Serrano et al (14). In their study, 3 different groups of orthopaedic physicians (residents, seniors and trauma specialists) evaluated the necessity of traction radiography and found that traction X-rays can be used to modify the choice of the implant in pertrochanteric fractures.

Our study has some limitations. First, it is a retrospective study with a relatively small number of each type of fracture and not all the subgroups in the AO classification were included. This may have created a selection bias. Second, as it is known, lateral wall competency is a criterion for instability of the proximal femur fractures and is not taken into account when choosing an implant by the participants. Third, the interpretation was not based on computed tomography images, and the misdiagnosis of the classification may have affected the implant selection.

CONCLUSION

The accurate diagnosis of proximal femoral fractures is important in selecting the optimal surgical treatment. This study shows that traction radiography increases the agreement of implant selection of the proximal femur fractures, especially among experienced trauma surgeons. In this way, it becomes an important guide in the treatment algorithm.

Ethics Committee Approval: Ethics committee approval was received for this study from the İstanbul Faculty of Medicine Clinical Research Ethics Committee (Date: 26.01.2024, No: 2).

Informed Consent: Due to the retrospective design of the study, informed consent was not taken.

Peer Review: Externally peer-reviewed.

Author Contributions: Conception/Design of Study- Y.S., M.D.; Data Acquisition- T.F.Y., E.K.; Data Analysis/Interpretation – E.K., T.F.Y.; Drafting Manuscript- Y.S., E.K., M.D.; Critical Revision of Manuscript- E.K., Y.S., M.D.; Final Approval and Accountability- Y.S., M.D., C.Ş.; Technical or Material Support- M.D., Y.S.; Supervision- C.Ş., M.D., Y.S.

Conflict of Interest: The authors have no conflict of interest to declare.

Financial Disclosure: The authors declared that this study received no financial support.

REFERENCES

1. Emmerson BR, Varacallo MA, Inman D. Hip Fracture Overview. In: StatPearls. Treasure Island (FL): StatPearls Publishing; 2023.
2. Johnell O, Kanis JA. An estimate of the worldwide prevalence and disability associated with osteoporotic fractures. *Osteoporos Int* 2006;17(12):1726-33. [\[CrossRef\]](#)
3. Deandrea S, Lucenteforte E, Bravi F, Foschi R, La Vecchia C, Negri E. Risk factors for falls in community-dwelling older people: a systematic review and meta-analysis. *Epidemiology* 2010;21(5):658-68. [\[CrossRef\]](#)
4. Blundell CM, Parker MJ, Pryor GA, Hopkinson-Woolley J, Bhonsle SS. Assessment of the AO classification of intracapsular fractures of the proximal femur. *J Bone Joint Surg Br* 1998;80(4):679-83. [\[CrossRef\]](#)
5. Andersen E, Jorgensen LG, Hededam LT. Evans' classification of trochanteric fractures: an assessment of the interobserver and intraobserver reliability. *Injury* 1990;21(6):377-8. [\[CrossRef\]](#)
6. Deleanu B, Prejbeanu R, Tsiroidis E, Vermesan D, Crisan D, Haragus H, et al. Occult fractures of the proximal femur: imaging diagnosis and management of 82 cases in a regional trauma center. *World J Emerg Surg* 2015;10:55. [\[CrossRef\]](#)
7. Meinberg EG, Agel J, Roberts CS, Karam MD, Kellam JF. Fracture and dislocation classification compendium-2018. *J Orthop Trauma* 2018;32(Suppl 1):S1-170. [\[CrossRef\]](#)
8. Landis JR, Koch GG. The measurement of observer agreement for categorical data. *Biometrics* 1977;33(1):159-74. [\[CrossRef\]](#)
9. Ly T, Swionkowski M. Intracapsular hip fractures. *Skeletal trauma: basic science, management, and reconstruction Fifth Edit Philadelphia, PA: Saunders. 2014:1607-81.*
10. Wiltse LL. Internal rotation for the diagnosis of impacted fracture of the hip. *Clin Orthop Relat Res* 1974;(103):20. [\[CrossRef\]](#)
11. Mitchell PM, Gavrilova SA, Dodd AC, Attum B, Obrebsky WT, Sethi MK. The impact of resident involvement on outcomes in orthopedic trauma: An analysis of 20,090 cases. *J Clin Orthop Trauma* 2016;7(4):229-33. [\[CrossRef\]](#)
12. Koval KJ, Oh CK, Egol KA. Does a traction-internal rotation radiograph help to better evaluate fractures of the proximal femur? *Bull NYU Hosp Jt Dis* 2008;66(2):102-6.
13. Khurana B, Mandell JC, Rocha TC, Duran-Mendicuti MA, Jimale H, Rosner B, et al. Internal rotation traction radiograph improves proximal femoral fracture classification accuracy and agreement. *AJR Am J Roentgenol* 2018;211(2):409-15. [\[CrossRef\]](#)

14. Garcia-Serrano MC, Garcia-Guerrero LF, Gomez-Gelvez A, Pinzon-Rendon AA. Diagnostic imaging concordance study: Are traction radiographs necessary in a hip fracture? *Injury* 2021;52(6):1445-9. [\[CrossRef\]](#)
15. Chan G, Hughes K, Barakat A, Edres K, da Assuncao R, Page P, et al. Inter- and intra-observer reliability of the new AO/OTA classification of proximal femur fractures. *Injury* 2021;52(6):1434-7. [\[CrossRef\]](#)
16. Perez-Abdala JI, Huespe I, Vildoza S, Novillo M, Llano L, Carabelli G, et al. The internal rotation traction radiograph does not improve the reliability in the AO classification system for pertrochanteric fractures. An inter- and intra-observer reliability assessment. *Injury* 2023;54(Suppl 6):110779. [\[CrossRef\]](#)
17. Socci AR, Casemyr NE, Leslie MP, Baumgaertner MR. Implant options for the treatment of intertrochanteric fractures of the hip: rationale, evidence, and recommendations. *Bone Joint J.* 2017;99-B(1):128-33. [\[CrossRef\]](#)
18. Alessio-Mazzola M, Traverso G, Coccarello F, Sanguineti F, Formica M. Dynamic hip screw versus intramedullary nailing for the treatment of A1 intertrochanteric fractures: A retrospective, comparative study and cost analysis. *Jt Dis Relat Surg* 2022;33(2):314-22. [\[CrossRef\]](#)

ENHANCING RISK PERCEPTIONS AND KNOWLEDGE IN WOMEN WITH RISK PREGNANCIES: EDUCATIONAL INTERVENTION

RİSKLİ GEBELERDE RİSK ALGISINI VE BİLGİ DÜZEYİNİ ARTIRMAK: BİR EĞİTİM MÜDAHALESİ ÇALIŞMASI

Osman KÜÇÜKKELEPÇE¹ , Hülya DOĞAN TİRYAKİ² , Osman KURT³ , Bengü Nehir BUĞDAYCI YALÇIN¹ , Erdoğan ÖZ⁴ 

¹Adıyaman Provincial Health Directorate, Department of Public Health, Adıyaman, Türkiye

²Gaziantep Provincial Health Directorate, Department of Public Health, Gaziantep, Türkiye

³İnönü University, Department of Public Health, Malatya, Türkiye

⁴Republic of Türkiye Ministry of Health, General Directorate of Public Health, Ankara, Türkiye

ORCID IDs of the authors: O.K. 0000-0002-7138-692X; H.D.T. 0000-0001-8974-8944; O.K. 0000-0003-4164-3611; B.N.B.Y. 0000-0002-5243-9790; E.Ö. 0000-0002-6785-6896

Cite this article as: Küçükkelepçe O, Doğan Tiryaki H, Kurt O, Buğdaycı Yalçın BN, Öz E. Enhancing risk perceptions and knowledge in women with risk pregnancies: Educational intervention. J Ist Faculty Med 2025;88(2):108-117. doi: 10.26650/IUITFD.1554962

ABSTRACT

Objective: We aimed to determine the risk perceptions of women with risky pregnancies. This study aimed to enhance and reevaluate their risk perceptions after providing education about their risks.

Material and Methods: This educational intervention study aimed to engage 336 pregnant women out of a 2,664 population with high-risk pregnancies in Adıyaman, Türkiye. In total, 444 pregnant women participated in the study. Participants completed the sociodemographic questionnaires, a pregnancy risk perception assessment, and a knowledge assessment related to pregnancy risks. The questionnaires were administered twice: once before the educational intervention and again 2-4 weeks after the intervention, allowing us to measure the effectiveness of the education.

Results: After the educational intervention, pregnant women demonstrated a significant increase in both their risk knowledge and risk perception scores ($p<0.001$). Furthermore, we observed a positive correlation between knowledge scores and age ($p<0.001$) as well as first gestational age ($p<0.001$), while a negative correlation was found with gestational age ($p=0.003$). Additionally, a positive correlation emerged between the risk perception score and age ($p=0.008$) and the number of obstetrician visits ($p=0.024$).

Conclusion: To enhance the risk perception, it is crucial to provide them with specialised education on this subject. This is imperative because every woman with a high-risk pregnancy is not only vulnerable to maternal mortality but also places her infant at a higher risk of infant mortality.

Keywords: Risk perception, risky pregnancy, educational intervention, maternal health

ÖZET

Amaç: Bu çalışmada riskli gebelerin risk algılarını belirleme amaçlandı. Çalışma, verilecek eğitim sonrasında risk algısını tekrar değerlendirilmeyi ve risk algısını geliştirmeyi amaçlamıştır.

Gereç ve Yöntem: Bu eğitim müdahale çalışmasında, Adıyaman'da riskli gebeliği olan 2.664 kadından en az 336'sına ulaşmak amaçlandı. Toplamda 444 kadın çalışmaya katıldı. Katılımcılara, sosyodemografik bilgilerini içeren anket ile birlikte gebelik risk algısı ve riskleri ile ilgili anketler uygulandı. Anketler, eğitim müdahalesinden önce ve müdahaleden 2-4 hafta sonra olmak üzere iki kez uygulanarak eğitimin risk algısı üzerinde etkinliği değerlendirildi.

Bulgular: Eğitim müdahalesinden sonra, katılımcıların risk bilgisi ve risk algısı puanlarında anlamlı bir artış görüldü ($p<0.001$). Ayrıca, bilgi puanları ile yaş ($p<0.001$) ve ilk gebelik yaşı ($p<0.001$) arasında pozitif bir korelasyon gözlemlendi, buna karşın gebelik haftası ile negatif bir korelasyon bulundu ($p=0.003$). Ek olarak, risk algısı puanı ile yaş ($p=0.008$) ve obstetrik ziyaret sayısı ($p=0.024$) arasında pozitif bir korelasyon saptandı.

Sonuç: Gebe kadınların risk algısını artırmak için bu konuda onlara özel eğitim sağlamak çok önemlidir. Bu, yüksek riskli gebeliği olan her kadının sadece anne ölümlerine karşı savunmasız olmakla kalmayıp, aynı zamanda bebeğini de bebek ölümleri riski altında bırakması nedeniyle gereklidir.

Anahtar kelimeler: Risk algısı, riskli gebelik, eğitim müdahalesi, anne sağlığı

Corresponding author/İletişim kurulacak yazar: Hülya DOĞAN TİRYAKİ – hdogan4687@gmail.com

Submitted/Başvuru: 24.09.2024 • **Revision Requested/Revizyon Talebi:** 03.12.2024 •

Last Revision Received/Son Revizyon: 24.02.2025 • **Accepted/Kabul:** 08.03.2025 • **Published Online/Online Yayın:** 17.04.2025



Content of this journal is licensed under a Creative Commons Attribution-NonCommercial 4.0 International License.

INTRODUCTION

Risk is the presence of variables that elevate the likelihood of adverse outcomes. Risk perception, on the other hand, refers to an individual's anticipation of the occurrence of an event associated with risk (1). From an alternative perspective, risk perception assesses the likelihood of harm in the absence of precautions (2). Risk perception plays a pivotal role in shaping individuals' health-related decisions and behaviours. Typically, individuals tend to perceive themselves as being at a lower risk than others in similar risk circumstances (1).

Pregnancy and childbirth inherently pose risks due to the physiological changes that affect a woman's body during this period. A pregnancy is considered high-risk if any medical or obstetric condition arises that threatens the health of either the mother or the fetus (3). Globally, around 20 million women experience high-risk pregnancies, and tragically, over 800 of these women lose their lives to perinatal complications every day (4). The incidence of high-risk pregnancies varies from 6% to 33% worldwide and is influenced by regional factors (5). In Türkiye, approximately one-third of pregnancies fall into this high-risk category (6).

Among the complications that can arise during pregnancy, preeclampsia affects 5%–10% of all pregnancies worldwide. The primary objective for women with high-risk pregnancies is to mitigate maternal and infant mortality through comprehensive antenatal care, timely management, treatment, and specialised care during childbirth and the postpartum period (5). Recent studies in Türkiye have revealed a shift in age-specific fertility rates, with the highest rates now occurring in the 25-29 age group, signifying an increase in maternal age as a notable risk factor (6, 7). Even with essential information from healthcare professionals, individual and social factors can alter a pregnant woman's perception of risk (7). Early-stage education to enhance risk perception among women with high-risk pregnancies can help prevent complications for the mother and baby during pregnancy and the postpartum period.

In this study, our objective was to visit the pregnant women mentioned earlier in their residences. During these visits, we aimed to provide information about potential risks, conduct diagnostic procedures such as blood pressure and blood glucose measurements, and, in cases of non-compliance (for those not attending regular appointments or failing to follow healthcare professionals' guidance), involve a family member to the follow-ups. The study's primary focus was to assess the risk perceptions of pregnant women with high-risk conditions and examine how their risk perceptions changed after the receipt of educational interventions.

MATERIAL AND METHODS

This educational intervention study took place in Adıyaman province and its districts within the southeast Anatolia region of Türkiye from October to December 2022.

Sample size

High-risk pregnancies are reported to the Provincial Health Directorate by family physicians. In Adıyaman province, which includes its districts, 5,790 pregnant women were found. Of these, 2,664 (46%) were classified as high-risk. This study focused on the population of 2,664 pregnant women who were considered high-risk due to factors such as comorbid diseases (hypertension, asthma, heart conditions, etc.), economic status, history of miscarriage, multiparity, or having had their last pregnancy within the last two years.

Sample size was determined using a specific universe sampling method. Based on this formula, we assumed that 50% of pregnant women had a certain level of risk perception, with a target of 336 pregnant women with high-risk pregnancies. In this study, we successfully enrolled 464 pregnant women who volunteered to participate. Unfortunately, no second visit could be conducted for 20 women due to the conclusion of their pregnancies or a change of residences. The sampling method was a stratified simple sampling method, with districts serving as strata, and the number of high-risk pregnant women in each district was considered.

Study design and procedures

In this study, pregnant women at risk were diagnosed, and researchers, all of whom were physicians, conducted residential visits to these women. After obtaining their consent, a questionnaire developed by the researchers following a literature review was administered to the at-risk pregnant women via face-to-face interviews. Following the questionnaire, a 30-minute educational session on pregnancy risks was provided. An informative document summarising content from the Ministry of Health's Pregnancy Information Class Training Book was also given to pregnant women during the visits. Each participant was revisited approximately 2-4 weeks after the initial visit, and the questionnaire was completed once again by each participant.

Data collection tools

Personal information form

The personal information form, designed by the researchers following a literature review, encompassed inquiries related to both sociodemographic characteristics (such as age, occupation, educational status, area of residence, family type, duration of marriage, etc.), obstetric characteristics about previous pregnancies (including the total number of pregnancies, total number of births, number of living children, incidents of stillbirth), and current pregnancy (folic acid use, and history of miscarriage).

Perception of pregnancy risk questionnaire (PPRQ)

The risk perception scale, initially developed by Heaman and Gupton, was adapted to Turkish by Evcili and Dağlar (8, 9). While the original scale comprises 11 items, the Turkish version comprises nine items. This visual analog scale employs a linear range from 0 to 100 mm, with the descriptors “no risk at all” to “extremely high risk” for each item. The Cronbach’s alpha coefficient for the entire scale was 0.84 in the original version and 0.87 in the current study. The scale is structured into two factors: the perception of risk to baby, consisting of five items, and the perception of risk to self, consisting of four items.

The total scale scores and their factors were calculated by summing the item scores and dividing by the respective number of items. There are no specific cut-off points on the scale. An increase in the scale score indicates an elevated risk perception for both the pregnant woman and her baby (9).

Risk knowledge of pregnant women

The questionnaire, developed by the researchers, included questions about various medical conditions that may arise during pregnancy. Participants were asked seven short-answer questions related to hypertension, high blood glucose, anaemia, cardiac arrhythmia, dyspnoea, extremity oedema, and proteinuria. Each correct answer was assigned a score of 1 point, while incorrect answers received 0 points. The total score for these questions ranged from 0 to 8, with no specific cut-off point; a higher score indicated greater knowledge. The Cronbach’s alpha value for this study was 0.78.

Ethical approval

Ethical approval for the study was obtained from the Non-Interventional Research Ethics Committee of Firat University (Date: 01.09.2022, No:2022/10-25). Written administrative permission was obtained from Adiyaman Provincial Health Directorate with the date 21.09.2022 and the number E-13389845-771. The study followed the principles outlined in the Declaration of Helsinki.

Statistical analysis

Analysis of the data was performed using the Statistical Package for Social Sciences 22 package program (IBM SPSS Corp., Armonk, NY, USA). In this study, descriptive data were presented as n and percentile values for categorical data, while they were shown as mean±standard deviation (Mean±SD) values for continuous data. Chi-square analysis (Pearson Chi-square) was used to compare categorical variables between groups. The Kolmogorov-Smirnov test was used to evaluate whether the continuous variables had a normal distribution. Student’s t-test was used for normally distributed variables, and the Mann-Whitney U test was used for non-normally distributed variables for comparison of the paired groups. The Pearson correlation test was used for normally distributed

variables and the Spearman’s correlation test for non-normally distributed variables to examine the relationship between continuous variables. The paired samples t-test was used for those with normal distribution and the Wilcoxon test for those without normal distribution to compare scores before and after education. A Linear Regression analysis was conducted to identify the predictors of the Perception of Pregnancy Risk Questionnaire (PPRQ) score and the Risk Knowledge of the Pregnant Women scale score. The Enter method was used to construct the model, and variables that showed significant differences in previous analyses were included in the model. The statistical significance level in the analysis was set as $p < 0.05$.

RESULTS

A total of 444 pregnant women at high risk, with an average age of 31.8 ± 6.5 years (range: 18-53), participated in the study. Among them, 60.8% were under 35 years of age. The majority (84.2%) of these women were housewives, and 58.1% had at least a secondary school education. In terms of residence, 58.3% of the pregnant women lived in the city centre, and 86.5% were from nuclear families. More than half (55%) of the pregnant women reported income below the minimum wage. Regarding obstetric history, 4.5% had experienced infant loss, 5.9% had a history of stillbirth, 34.9% had suffered a miscarriage, and 14.6% had an abortion. The participants’ healthcare practices included tetanus vaccination (59.5%), folic acid use (87.2%), iron supplementation (87.2%), and vitamin D intake (82.2%). Of the participants, 79.1% received information about high-risk pregnancies from family physicians, midwives, or obstetricians, and 84.3% considered this information during their pregnancies. Notably, 66.9% of the women reported that their pregnancies were planned (Table 1).

The mean age at the time of the first pregnancy was 24.1 ± 5.0 years, with a range of 18–42 years. The current mean gestational week was 22.6 ± 9.6 . For prenatal care, the women made an average of 2.3 ± 1.5 visits to their family physician and 4.5 ± 2.7 visits to the gynaecologist.

Among participants, those who were 35 years or older, employed other than as housewives, had a high school education or higher, resided in the province, had an income at or above the minimum wage, who were married for more than five years, experienced infant deaths, had stillbirths, received tetanus vaccination, used folic acid, iron, and vitamin D, were informed about high-risk pregnancies, and had planned pregnancies exhibited significantly higher knowledge scores and PPRQ total scores ($p < 0.05$). Additionally, participants from nuclear families had a higher PPRQ total score ($p = 0.008$), while no significant difference was found in terms of knowledge scores ($p = 0.854$) (Table 2).

Table 1: Characteristics of women with high-risk pregnancies

		Number	%
Age	<35	270	60.8
	≥35	174	39.2
Occupation	Housewife	374	84.2
	Other	70	15.8
Educational status	Secondary school or below	258	58.1
	High school or above	186	41.9
Living place	City centre	259	58.3
	Town/village	185	41.7
Family type	Nuclear family	384	86.5
	Extended family	60	13.5
Total family income	Minimum wage	244	55.0
	Minimum wage or above	200	45.0
Duration of marriage(years)	≤5	174	39.2
	>5	270	60.8
Infant death	Yes	20	4.5
	No	424	95.5
Number of pregnancies	≤2	176	39.6
	>2	268	60.4
Number of births	≤2	323	72.7
	>2	121	27.3
Has a child	Yes	352	79.3
	No	92	20.7
Stillbirth	Yes	26	5.9
	No	418	94.1
Miscarriage	Yes	155	34.9
	No	289	65.1
Abortion	Yes	65	14.6
	No	379	85.4
Tetanus vaccination status	Yes	264	59.5
	No	180	40.5
Folic acid use	Yes	387	87.2
	No	57	12.8
Iron use	Yes	361	87.2
	No	53	12.8
Use of vitamin D	Yes	336	82.2
	No	73	17.8
The status of being briefed about a risky pregnancy by a family doctor, midwife or obstetrician)	Yes	351	79.1
	No	93	20.9
Status of the following advice regarding these risks	Yes	296	84.3
	No	55	15.7
Planned pregnancy	Yes	297	66.9
	No	147	33.1

Table 2: Comparison of pre-educational knowledge and PPRQ scale scores among women with risky pregnancies according to various parameters

		Knowledge score		PPRQ-risk to baby		PPRQ risk to self		PPRQ-total	
		Mean±SD	p*	Mean±SD	p**	Mean±SD	p**	Mean±SD	p**
Age	<35	5.2±2.9	<0.001	27.6±16.4	0.399	33.8±17.9	0.003	30.3±15.4	0.043
	≥35	6.3±2.5		29.0±18.4		39.0±18.7		33.5±16.6	
Occupation	Housewife	5.4±2.9	0.012	27.3±15.7	0.066	34.6±17.6	0.001	30.5±14.6	0.015
	Other	6.8±1.9		32.7±23.2		42.4±21.1		37.0±20.9	
Educational status	Secondary school or below	5.3±3.0	0.009	26.2±14.7	0.008	33.5±17.2	0.002	29.5±13.8	0.002
	High school or above	6.1±2.5		30.8±19.9		39.0±19.5		34.4±18.1	
Living place	City centre	5.9±2.5	0.025	30.0±18.2	0.008	38.3±19.0	0.001	33.7±16.9	0.001
	Town/village	5.2±3.1		25.6±15.5		32.4±16.9		28.6±14.0	
Family type	Nuclear family	5.6±2.8	0.854	28.7±17.6	0.062	36.8±18.5	0.003	32.3±16.2	0.008
	Extended family	5.6±3.0		24.3±14.4		29.3±15.8		26.5±12.8	
Total family income	< Minimum wage	5.4±2.9	0.037	25.9±16.3	0.003	34.0±18.1	0.021	29.5±15.4	0.003
	≥ Minimum wage	5.9±2.6		30.8±17.9		38.1±18.5		34.0±16.3	
Duration of marriage (years)	≤5	4.9±3.1	<0.001	25.4±13.7	0.004	32.5±17.3	0.002	28.6±13.3	0.001
	>5	6.1±2.5		29.9±18.9		38.0±18.8		33.5±17.1	
Infant death	Yes	6.8±2.2	0.041	44.1±29.4	0.02	51.9±25.9	0.009	47.6±26.7	0.011
	No	5.6±2.8		27.4±16.1		35.1±17.6		30.8±14.9	
Stillbirth	Yes	6.2±2.5	0.026	39.0±28.3	0.004	46.2±25.3	0.005	42.2±25.4	0.003
	No	5.6±2.8		27.5±16.1		35.2±17.7		30.9±14.9	
Tetanus vaccination status	Yes	6.0±2.5	0.008	30.5±18.0	0.001	37.7±18.6	0.009	33.7±16.5	0.001
	No	5.1±3.1		24.7±15.4		33.1±17.8		28.4±14.6	
Folic acid use	Yes	5.8±2.7	0.005	29.1±17.5	0.001	36.7±18.4	0.012	32.4±16.0	0.002
	No	4.5±3.3		21.9±13.5		30.1±17.6		25.5±13.8	
Iron use	Yes	5.7±2.7	<0.001	29.6±17.7	0.023	37.1±18.7	0.005	32.9±16.3	0.005
	No	3.9±3.0		23.8±13.7		29.5±15.5		26.3±13.2	
Use of vitamin D	Yes	5.7±2.8	<0.001	29.7±17.9	0.04	37.4±19.0	0.006	33.1±16.5	0.008
	No	4.3±2.8		25.2±14.0		30.8±15.5		27.7±13.4	
Briefed on risky pregnancy	Yes	5.9±2.6	0.007	29.9±17.6	<0.001	38.2±18.0	<0.001	33.5±15.9	<0.001
	No	4.7±3.3		21.6±13.9		27.0±17.0		24.0±13.6	
Planned pregnancy	Yes	6.1±2.5	<0.001	30.1±18.4	<0.001	37.5±19.2	0.004	33.4±16.9	<0.001
	No	4.7±3.2		24.2±13.8		32.5±16.1		27.9±13.0	

*:Mann-Whitney U test, **:Student's t-test was used, PPRQ: Perception of pregnancy risk questionnaire

According to the multiple linear regression analysis results, the predictors of the Knowledge scale score were as follows: not being a housewife ($\beta=0.785$, $p=0.042$), having a high school education or higher ($\beta=0.678$, $p=0.023$), being married for more than five years ($\beta=0.935$, $p=0.002$), having a planned pregnancy ($\beta=1.048$, $p<0.001$), and receiving a tetanus vaccination during pregnancy ($\beta=0.880$, $p=0.002$) (Table 3).

The predictors of the PPRQ total score were being briefed by healthcare professionals about high-risk pregnancy ($\beta=5.737$, $p=0.003$), having a planned pregnancy ($\beta=3.244$, $p=0.048$), and experiencing stillbirth ($\beta=10.759$, $p=0.005$) (Table 4).

There were positive and negative significant correlations between knowledge score and age and first gestational age, and a significant negative correlation between knowledge score and gestational week. A positive significant relationship was found between the PPRQ-risk to baby score and the PPRQ-risk to self-score, gestational age, and number of visits to the obstetrician for pregnancy follow-up. A significant positive correlation was found between PPRQ risk and self-score and age. There was a low significant positive correlation between the PPRQ-total score and age and the number of visits to the obstetrician for pregnancy follow-up (Table 5).

The scores of Knowledge, PPRQ-risk for babies, PPRQ-risk for self-factors, and the PPRQ-total scale of women with risky pregnancies increased significantly after the

education ($p<0.001$) (Figure 1). When evaluating the levels of increase, after the training, the scores showed an increase of 12.5% in Knowledge, 92.8% in PPRQ-risk for the baby, 64.5% in PPRQ-risk for the self, and 78.1% in the PPRQ-total scale.

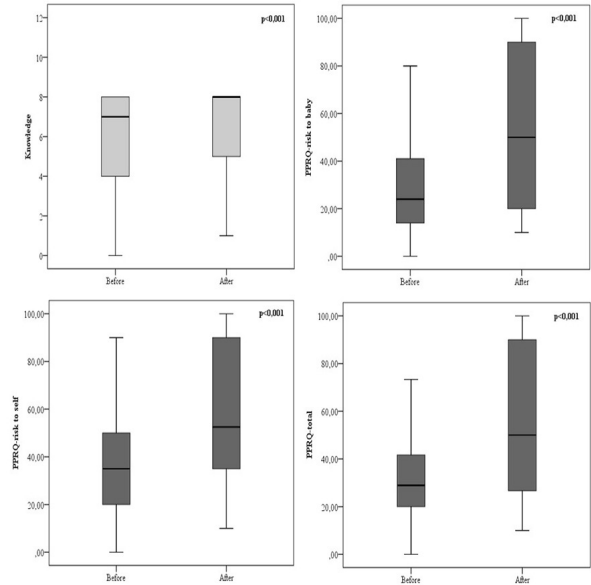


Figure 1: Knowledge and PPRQ scale scores of women with risky pregnancies before and after education
 PPRQ: Perception of the pregnancy risk questionnaire

Table 3: Linear regression analysis of the pre-educational Knowledge Score according to various parameters

	Knowledge score ($R^2=0.205$; $F=6.730$; $p<0.001$)				
	β	SE	Standart β	t	p
Over 35 years old	0.535	0.298	0.092	1.798	0.073
Employed	0.785	0.385	0.102	2.042	0.042
High school or above	0.678	0.298	0.119	2.275	0.023
Resided in city centre	0.445	0.276	0.078	1.615	0.107
Income exceeding the minimum wage	0.095	0.277	0.017	0.343	0.732
Had an infant death	-0.022	0.745	-0.002	-0.030	0.976
Married for over five years	0.935	0.293	0.162	3.196	0.002
Use of iron supplements	0.508	0.512	0.060	0.992	0.322
Folic acid used	0.227	0.407	0.027	0.557	0.578
Vitamin D	0.287	0.437	0.039	0.658	0.511
Briefed about risky pregnancy	0.312	0.331	0.045	0.941	0.347
Had a planned pregnancy	1.048	0.285	0.176	3.678	<0.001
Had a stillbirth	0.246	0.667	0.021	0.368	0.713
Tetanus vaccination	0.880	0.278	0.151	3.162	0.002

R^2 : Coefficient of Determination, F: F-statistic, β : Unstandardised Coefficient, SE: Standard Error, Standard β : Standardised Beta Coefficient

Table 4: Linear Regression Analysis of the pre-educational Total PPRQ Score according to various parameters

	PPRQ total score (R ² =0,199; F=6.491; p<0.001)				
	β	SE	Standart β	t	p
Over 35 years old	1,431	1,708	0.043	0.838	0.403
Employed	1,354	2,206	0.031	0.614	0.540
High school or above	2,461	1,709	0.075	1.440	0.151
Resided in the province	2,164	1,583	0.066	1.367	0.172
Nuclear family	2,998	2,177	0.064	1.377	0.169
Income exceeding the minimum wage	2,057	1,587	0.064	1.296	0.196
Had an infant death	5,597	4,276	0.073	1.309	0.191
Married for over five years	3,237	1,678	0.098	1.929	0.055
Use of iron supplements	1,288	2,939	0.027	0.438	0.661
Folic acid used	3,598	2,335	0.074	1.541	0.124
Vitamin D	0,470	2,505	0.011	0.188	0.851
Briefed about risky pregnancy	5,737	1,901	0.145	3.019	0.003
Had a planned pregnancy	3,244	1,634	0.095	1.986	0.048
Had a stillbirth	10,759	3,826	0.160	2.812	0.005
Tetanus vaccination	1,446	1,597	0.043	0.905	0.366

PPRQ: Perception of the pregnancy risk questionnaire, R²: Coefficient of Determination, F: F-statistic, β: Unstandardised Coefficient, SE: Standard Error, Standard β: Standardised Beta Coefficient

Table 5: Correlation between pre-educational knowledge score and PPRQ scale scores of women with risky pregnancies with the measurement parameters

		Knowledge	PPRQ-risk to baby	PPRQ risk to self	PPRQ-total
PPRQ-risk to baby	r*	-0.074			
	P**	.0120			
PPRQ risk to self	r	-0.0019	0.548		
	p	0.683	<0.001		
PPRQ-total	r	-0.050	0.876	0.872	
	p	0.297	<0.001	<0.001	
Age	r	0.237	0.040	0.189	0.125
	p	<0.001	0.401	<0.001	0.008
First gestational age	r	0.112	-0.047	0.078	0.014
	p	0.018	0.319	0.100	0.765
Gestational week	r	-0.142	0.096	0.038	0.075
	p	0.003	0.042	0.430	0.115
Number of visits to the Family Physician for pregnancy follow-up	r	0.013	0.067	0.030	0.064
	p	0.789	0.161	0.527	0.182
Number of visits to the Obstetrician and Gynaecologist for pregnancy follow-up	r	-0.029	0.123	0.066	0.107
	p	0.541	0.010	0.167	0.024

: Spearman Correlation Analysis Test were used, r: Correlation coefficient, p**: Statistical significance, PPRQ: Perception of the pregnancy risk questionnaire

DISCUSSION

This study looked into what affects how women with high-risk pregnancies perceive the risks they face. Earlier research shows that many pregnant women tend to underestimate these risks and may not have all the necessary information, emphasising the need for better education programs (10). Research shows that when healthcare professionals provide detailed and thorough information, women with high-risk pregnancies tend to have a clearer understanding of the risks they face (11-13). Additionally, regular physician visits tend to reduce anxiety, foster trust between patients and healthcare providers, and potentially induce changes in patient behaviours (13). In our study, we found a positive correlation between the number of visits to Obstetrics and Gynaecology Specialists and both risk perception and knowledge scores. This suggests that pregnant women who perceive a higher risk tend to visit specialists more frequently. Conversely, there was no observed relationship between family physician visits and either risk perception or knowledge scores. This indicates that primary care follow-ups might not be effectively providing the necessary information to women with high-risk pregnancies. Therefore, targeted interventions are needed to improve the awareness and competence of primary care professionals in managing high-risk pregnancy issues. In Türkiye, pregnant women typically have four follow-up appointments with their family physician, whereas those with high-risk pregnancies attend seven. However, studies show that there is no link between the number of family physician visits and women's risk perception an area that clearly warrants further research.

Studies conducted by Gerend et al. in 2004, focusing on pregnant women with chronic diseases, and by Kim et al. in 2007, involving pregnant women with a history of gestational diabetes, revealed no significant correlation between knowledge scores and risk perception (14, 15). Our study yielded similar findings, reinforcing the need for tailored educational content, particularly addressing risk perception, for women facing high-risk pregnancies.

According to the American CDC, the rate of pregnancies among women aged over 35 years increased to 23% in 2014, compared with 9% in 2000. A study that compared risk perception between pregnant women aged 18 years and those aged 18 to 35 found that those under 18 had a significantly higher risk perception than their older counterparts (16). Another study involving nulliparous women revealed a correlation between age, knowledge scores, and risk perception (10). In the present study, we found that the knowledge scores and risk perceptions of pregnant women older than 35 years were higher than those of women younger than 35 years. Given that being under 18 years old and over 35 years old are recognised as

risk factors for pregnancy, it appears that the risk status of pregnant women and their risk perceptions are inter-linked.

In a study conducted in Nepal, the risk perception of pregnant women with a history of infant death and those with complicated obstetric histories was found to be higher (1). Similarly, Silva et al. conducted a study in 2021, which revealed higher risk perceptions among pregnant women who had experienced an incomplete pregnancy, had infants in the neonatal intensive care unit, or experienced infant loss (12). The present study found that knowledge scores and risk perceptions were higher among pregnant women who had experienced a previous miscarriage or infant loss than among those who had not.

In their study, Bayrampour et al. also observed a decrease in risk perception as the gestational age progressed, a trend consistent with our current findings (10). However, another study conducted in Türkiye in 2024 found that risk perception increased as the week of pregnancy progressed (17). This observation may be associated with the increasing belief and optimism among pregnant women who tend to become more confident in their pregnancy as their pregnancy advances towards a positive outcome.

Studies conducted in Nepal in 2021 and by Papiernik et al. in 1997 identified a correlation between socioeconomic status and risk perception and knowledge scores (1, 18). Our study yielded similar results. However, in Heaman and Gupton's 2009 study, no such correlation was found (8). Despite the increased accessibility to information, risk perception may require specific interventions tailored to enhance this perception rather than mere access to information.

Although research on pregnant women's risk perceptions is relatively limited, the findings in the existing literature are mixed. For instance, a 2024 study in Türkiye found that pregnant women's risk perception decreased following health literacy training (19). In contrast, a 2020 study in the United States demonstrated a significant increase in pregnant women's risk perception after training compared to those who did not receive any training (20). Similarly, a 2015 study in Iran reported a substantial increase in pregnant women's risk perception post-training (21). In this study, we observed a significant increase in the pregnant women's perceived risk for themselves and their babies after the training. However, their level of knowledge did not significantly predict their risk perception before the training, nor did it show a noteworthy increase afterward. These findings suggest that pregnant women's risk perception may not be directly influenced by the amount of knowledge they possess and underscore the need for targeted educational interventions explicitly aimed at enhancing risk perception.

Due to the educational sessions being conducted at the participants' residences, creating an ideal learning environment is not always possible. Additionally, there may have been a potential recall bias in the study because the participants were asked to provide retrospective survey responses. Lastly, the lack of a control group in the study is a limitation.

CONCLUSION

In developing countries, a significant proportion of pregnancies are classified as high risk, primarily due to factors like advancing maternal age and the increasing prevalence of chronic diseases. Despite improved access to information, the correlation between knowledge scores and risk perception remained modest. Therefore, comprehensive monitoring of women with high-risk pregnancies during both the pregnancy and postpartum phases is crucial for the well-being of both mothers and their infants. Expanding education and awareness regarding risk perception is essential to empower pregnant women to actively engage in risk perception.

Ethics Committee Approval: Ethical approval for the study was obtained from the Non-Interventional Research Ethics Committee of Firat University (Date: 01.09.2022, No: 2022/10- 5). Written administrative permission was obtained from Adiyaman Provincial Health Directorate with the date 21.09.2022 and the number E-13389845-771. The study followed the principles outlined in the Declaration of Helsinki.

Informed Consent: Consent was obtained from all participants who participated in the study.

Peer Review: Externally peer-reviewed.

Author Contributions: Conception/Design of Study- H.D.T., E.Ö., O.K.; Data Acquisition- H.D.T., B.N.B.Y.; Data Analysis/Interpretation – O.K., O.K.; Drafting Manuscript- O.K., H.D.T.; Critical Revision of Manuscript- B.N.B.Y., E.Ö., O.K.; Final Approval and Accountability- H.D.T., O.K., O.K., B.N.B.Y., E.Ö.; Technical or Material Support- H.D.T.; Supervision- O.K.

Conflict of Interest: The authors have no conflict of interest to declare.

Financial Disclosure: The authors declared that this study received no financial support.

Declaration of Competing Interests: The authors declare that they have no conflicts of interest.

Funding: The authors declare that this study received no financial support.

REFERENCES

1. Rajbanshi S, Norhayati MN, Nik Hazlina NH. Risk perceptions among high-risk pregnant women in Nepal: a qualitative study. *BMC Pregnancy Childbirth* 2021;21(1):1-8. [\[CrossRef\]](#)
2. Lennon SL. Risk perception in pregnancy: A concept analysis. *J Adv Nurs* 2016;72(9):2016-29. [\[CrossRef\]](#)
3. Lee S. Risk perception in women with high-risk pregnancies. *Br J Midwifery* 2014;22(1):8-13. [\[CrossRef\]](#)
4. World Health Organization. Maternal mortality. 2016. December 29, 2022. <https://www.who.int/en/news-room/fact-sheets/detail/maternal-mortality>.
5. Holness N. High-risk pregnancy. *Nurs Clin North Am* 2018;53(2):241-51. [\[CrossRef\]](#)
6. Hacettepe University Institute of Population Studies, Ankara. Turkey Demographics and Health Survey, 2018. 29 Dec 2022. <https://dhsprogram.com/pubs/pdf/FR372/FR372.pdf>
7. Correa-de-Araujo R, Yoon SS. Clinical outcomes in high-risk pregnancies due to advanced maternal age. *J Women Health* 2021;30(2):160-67. [\[CrossRef\]](#)
8. Heaman M, Gupton A. Psychometric testing of the perception of pregnancy risk questionnaire. *Res Nurs Health* 2009;32:493-503. [\[CrossRef\]](#)
9. Evcili F, Dağlar G. Gebelikte Risk Algısı Ölçeği: Türkçe geçerlik ve güvenilirlik çalışması. *Cukurova Med J* 2019;44(1):211-22. [\[CrossRef\]](#)
10. Bayrampour H, Heaman M, Duncan KA, Tough S. Predictors of perception of pregnancy risk among nulliparous women. *J Obstet Gynecol Neonatal Nurs* 2013;42(4):416-27. [\[CrossRef\]](#)
11. Ralston ER, Smith P, Chilcot J, Silverio SA, Bramham K. Perceptions of risk in pregnancy with chronic disease: A systematic review and thematic synthesis. *PLoS One* 2021;16(7):e0254956. [\[CrossRef\]](#)
12. Silva TV, Bento SF, Katz L, Pacagnella RC. "Preterm birth risk, me?" Women risk perception about premature delivery—a qualitative analysis. *BMC Pregnancy and Childbirth* 2021;21:633. [\[CrossRef\]](#)
13. Lee S, Ayers S, Holden D. Risk perception of women during high-risk pregnancy: a systematic review. *Health Risk Soc* 2012;14(6):511-31. [\[CrossRef\]](#)
14. Gerend MA, Aiken LS, West SG, Erchull MJ. Beyond medical risk: Investigating the psychological factors underlying women's perceptions of susceptibility to breast cancer, heart disease, and osteoporosis. *Health Psychol* 2004;23(3):247-58. [\[CrossRef\]](#)
15. Kim C, McEwen LN, Piette JD, Goewey J, Ferrara A, Walker EA. Risk perception for diabetes among women with histories of gestational diabetes mellitus. *Diabetes Care* 2007;30(9):2281-6. [\[CrossRef\]](#)
16. Taghizadeh Z, Cheraghi MA, Kazemnejad A, Pooralajal J, Aghababaei S. Difference in perception of pregnancy risk in two maternal age groups. *J Clin Diagn Res* 2017;11(5):QC09-12. [\[CrossRef\]](#)
17. Maharramova A, Gur EY. The pregnant women's perception of risks and pregnancy stress levels: a cross-sectional study from Turkey. *Rev Assoc Med Bras* (1992) 2024;70(6):e20231270. [\[CrossRef\]](#)
18. Papiernik E, Tafforeau J, Richard A, Pons JC, Keith LG. Perception of risk, choice of maternity site, and socio-economic level of twin mothers. *J Perinat Med* 1997;25(2):139-45. [\[CrossRef\]](#)
19. Şenol DK, Aydin Özkan S, Ağralı C. The effect of the training provided to primiparous pregnant women based on the model on pregnancy risk perception and health literacy. *Women Health* 2024;64(3):283-93. [\[CrossRef\]](#)

20. Adebayo AL, Davidson Mhonde R, DeNicola N, Maibach E. The effectiveness of narrative versus didactic information formats on pregnant women's knowledge, risk perception, self-efficacy, and Information seeking related to climate change health risks. *Int J Environ Res Public Health* 2020;17(19):6969. [\[CrossRef\]](#)
21. Shahnazi H, Sabooteh S, Sharifirad G, Mirkarimi K, Hassanzadeh A. The impact of education intervention on the Health Belief Model constructs regarding anxiety of nulliparous pregnant women. *J Educ Health Promot* 2015;4(1):27. [\[CrossRef\]](#)

SYNTHESIS, CHARACTERISATION AND INVESTIGATION OF THE ANTICANCER POTENTIAL OF CARMOFUR-LOADED SILVER NANOPARTICLES

KARMOFUR YÜKLÜ GÜMÜŞ NANOPARTİKÜLLERİNİN SENTEZİ, KARAKTERİZASYONU VE ANTİKANSER POTANSİYELİNİN ARAŞTIRILMASI

Ferdane DANIŞMAN KALINDEMİRTAŞ¹ , İshak Afşin KARİPER² , Dilşad ÖZERKAN³ , Dürdane Serap KURUCA⁴ 

¹Erzincan Binali Yıldırım University, Faculty of Medicine, Department of Physiology, Erzincan, Türkiye

²Erciyes University, Faculty of Education, Department of Science Education, Kayseri, Türkiye

³Kastamonu University, Faculty of Engineering and Architecture, Department of Genetic and Bioengineering, Kastamonu, Türkiye

⁴Istanbul Atlas University, Faculty of Medicine, Department of Physiology, İstanbul, Türkiye

ORCID IDs of the authors: F.D.K. 0000-0001-7085-8596; İ.A.K. 0000-0001-9127-301X; D.Ö. 0000-0002-0556-3879; D.S.K. 0000-0001-7878-9994

Cite this article as: Danışman Kalindemirtaş F, Kariper İA, Özerkan D, Kuruca DS. Synthesis, characterisation and investigation of the anticancer potential of carmofur-loaded silver nanoparticles. J Ist Faculty Med 2025;88(2):118-127. doi: 10.26650/IUITFD.1567946

ABSTRACT

Objective: The term "triple-negative breast cancer" (TNBC) is used to describe tumours that do not express oestrogen receptor (ER), progesterone receptor (PR), or human epidermal growth factor receptor 2 (HER2). TNBC tends to be more aggressive than other types of breast cancer. Current antineoplastic drugs have limited treatment options for malignant breast cancer owing to their narrow therapeutic index, toxicity, resistance, and non-selectivity. Therefore, there is a need for the prompt development of new medicinal drugs for TNBC. Here, we investigated the growth inhibition potential of carmofur-bonded silver nanoparticles (AgNPs-Car) on two TNBC cell lines, MDA-MB-231 and 4T1, and compared the effects with non-cancerous Human umbilical vein endothelial cells (HUVECs).

Material and Methods: AgNPs-Car were synthesised and characterised by FTIR, DLS, SEM, and EDX. The anticancer effect was evaluated using a 3-(4,5-Dimethylthiazol-2-yl)-2,5-Diphenyltetrazolium Bromide (MTT) assay.

Results: AgNPs-Car was determined to be predominantly more effective than Car alone. Mainly, 4T1 cells were 5.7-fold more sensitive to AgNPs-Car than Car alone. While AgNPs showed no considerable toxicity on HUVECs, they significantly induced the cytotoxicity of MDA-MB-231 and 4T1 cells.

Conclusion: Our results showed that AgNPs-Car is a promising anticancer agent due to its highly potent and selective growth inhibitory effect on TNBC cells.

ÖZET

Amaç: "Üçlü negatif meme kanseri" (TNBC) terimi, östrojen reseptörü (ER), progesteron reseptörü (PR) veya insan epidermal büyüme faktörü reseptörü 2'yi (HER2) ekspres etmeyen tümörleri tanımlamak için kullanılır. TNBC, diğer meme kanseri türlerinden daha agresif olma eğilimindedir. Malign meme kanserinde güncel antineoplastik ilaçların tedavi indeksinin kısıtlayıcı olması, toksisitesi, direnci ve seçici olmaması nedeniyle sınırlı tedavi seçenekleri bulunmaktadır. Bu nedenle, TNBC için yeni tıbbi ilaçların derhal geliştirilmesine ihtiyaç vardır. Burada, MDA-MB-231 ve 4T1 olmak üzere iki TNBC hücre hattı üzerinde karmofur bağlı gümüş nanopartiküllerin (AgNP-Car) büyüme inhibisyonuna etkisini araştırdık ve etkinliklerini kanserli olmayan insan göbek damarı endotel hücreleri (HUVEC) ile karşılaştırdık.

Gereç ve Yöntem: AgNP-Car, FTIR, DLS, SEM ve EDX ile sentezlendi ve karakterize edildi. Anti-kanser etkisi 3-(4,5-Dimetiltiazol-2-il)-2,5-Difeniltetrazolium Bromür (MTT) testi ile değerlendirildi.

Bulgular: AgNP-Car'ın nanopartiküllerin tek başına karmofurdan ağırlıklı olarak daha etkili olduğu belirlendi. Özellikle AgNP-Car uygulanmış 4T1 hücrelerinin, karmofur uygulanmış gruplara göre 5,7 kat daha duyarlı olduğu belirlendi. AgNP'ler HUVEC'ler üzerinde önemli bir toksisite göstermezken; MDA-MB-231 ve 4T1 hücrelerinin sitotoksitesini önemli ölçüde indüklediler.

Corresponding author/İletişim kurulacak yazar: Dilşad ÖZERKAN – dilsadokan@gmail.com

Submitted/Başvuru: 15.10.2024 • **Revision Requested/Revizyon Talebi:** 06.11.2024 •

Last Revision Received/Son Revizyon: 04.03.2025 • **Accepted/Kabul:** 10.03.2025 • **Published Online/Online Yayın:** 18.04.2025



Content of this journal is licensed under a Creative Commons Attribution-NonCommercial 4.0 International License.

Keywords: Silver nanoparticles, antiproliferative, anticancer, Carmofur, triple-negative breast cancer cells

Sonuç: Sonuçlarımız, AgNP-Car'ın TNBC hücreleri için oldukça güçlü ve seçici büyüme inhibitörü etkisi nedeniyle umut verici bir anti-kanser ajanı olabileceğini göstermektedir.

Anahtar kelimeler: Gümüş nanopartiküller, antiproliferatif, anti-kanser, karmofur, üçlü negatif meme kanseri hücreleri

INTRODUCTION

Among all cancer types, breast cancer is the most common type among women, and it is very likely to cause death when it progresses (1). Therefore, breast cancer remains one of the most critical health problems in many countries. Triple-negative breast cancer (TNBC) is the most malignant and mortal type of breast cancer compared to its subtypes. TNBCs are known for the deficiency of the expression of oestrogen receptor (ER), progesterone receptor (PR), or human epidermal growth factor receptor 2 (HER2). TNBC exhibits significant genetic heterogeneity. Mutations in key oncogenes and tumour suppressor genes such as *TP53*, *BRCA1/2*, and *PIK3CA* contribute to treatment resistance. Epigenetic changes, including DNA methylation and histone modifications, also play a role in silencing genes critical for drug response. Abnormal activation of signaling pathways such as PI3K/AKT/mTOR, JAK/STAT, and NF- κ B promotes the survival and proliferation of TNBC cells. These pathways often confer resistance by enabling cells to evade apoptosis and sustain growth despite treatment (2-4). TNBC is also defined as aggressive with the rate of upper metastasis and poor prognosis. Overexpression of ATP-binding cassette (ABC) transporters, such as P-glycoprotein (P-gp) and ABCG2, enables TNBC cells to actively pump out chemotherapeutic agents, reducing intracellular drug concentrations (3). The treatment options for TNBC are minimal due to the absence of molecular targets; therefore, these patients cannot be treated with endocrine therapy targeting HER2, and TNBCs are treatment-resistant cancers to usual therapies like chemotherapy and immunotherapy. Consequently, there is a need to develop new treatment approaches for such types of aggressive breast cancer.

The development of nano drug delivery systems can provide great opportunities through the ability of targeted drug delivery and tumour responses to overcome the clinical challenges observed, such as drug resistance of TNBCs (5). By encapsulating drugs within nanoparticles (NPs), nanocarriers can bypass efflux pumps and increase intracellular drug accumulation. For example, nanoparticle formulations of doxorubicin have been shown to evade P-gp-mediated efflux in resistant TNBC cells (3). NPs may selectively affect the tumour tissue because of enhanced permeability and retention (EPR). Hence, the side effects of chemotherapeutics might be decreased

(6). High-dose drugs reach cancer cells to improve therapeutic outcomes while reducing systemic toxicity through delivery systems with lower drug concentrations (5). By selectively targeting TNBC cells and sparing normal tissues, nanodrug delivery systems minimise off-target effects and reduce the toxicity associated with conventional chemotherapy, thus improving patient quality of life.

A drug that has been investigated in treating breast cancer in recent years is carmofur (Car). Car (1-hexylcarbamoyl-5-fluorouracil), a masked form of 5-fluorouracil (5FU), is a pyrimidine analog known as an antineoplastic agent used to treat several cancers (7). Generally, the lipophilic form of 5FU can be taken orally (8). In some countries, Car has also been used as an adjuvant chemotherapy for breast and colorectal cancer (9, 10). In addition, it is a highly strong acid ceramidase (AC) inhibitor (11). The enzyme ceramidase is crucial in sphingolipid synthesis and catalyses the ceramide into sphingosine and fatty acids. Ceramide is a messenger that activates apoptosis and cell differentiation (11-13). Furthermore, it has been reported that Car is more effective in targeting 5FU-resistant cells (14). A hexyl carbamoyl substituent serves as a transport form in the structure of this antimetabolite/Car and supports the entry of 5FU into cells (15). Due to its properties, carmofur has long been used to treat human cancer. In addition, the potential of Car to inhibit cancer cell proliferation has been recognised as an independent attribute of its ability to produce 5FU (16). These factors make it an essential tool for studies in cancer research, supporting the notion that ceramidase should be inhibited for medicinal purposes. Besides all these, AgNPs synthesised with Car have not been evaluated in TNBC or cancer treatment.

Nanocarriers may increase the drug half-life in the biological environment, display enhanced pharmacokinetic activity, and exhibit better patient compliance (17). Besides, nanodrugs prepared with Car or other drugs differ due to some advantages of their physicochemical structure, and they cause various cellular responses in different cell types (18). Among the many nanoparticles, silver nanoparticles have recently attracted significant attention due to their uniqueness and their multiple applications in other fields such as biomedical, food, cosmetics, and engineering (19, 20).

The synthesised silver nanoparticles (AgNPs) altered in size, shape, and other physiological characteristics. The nanosized particles can be catalytic and have electromagnetic capability

many more times. It is considered that the alteration in size plays a significant role in the nanoparticle activity. In addition, the nanoparticle concentration range and agglomeration are important components affecting toxicity induction (21-24). On the other hand, AgNPs have been shown to cause cytotoxicity in a dose-dependent manner (25).

The development of resistance remains a significant challenge for treating TNBC. However, advances in nanotechnology-based drug delivery systems offer innovative solutions to address these hurdles. By enabling targeted delivery, overcoming resistance mechanisms, and improving drug efficacy, nanomedicine holds great potential to transform the therapeutic landscape for TNBC and improve patient outcomes. Therefore, we used AgNPs as drug carriers because of their convenient and low-cost synthesis and biocatalytic-photocatalytic advantages in this study (26-28). We used the highly aggressive MDA-MB-231 (human) and 4T1 (murine) cells as the TNBC cell model (29, 30). We synthesised carmofur-bonded silver nanoparticles (AgNPs-Car), a nanoparticle that has never been found in the literature, with AgNP and Car. Then, we studied the anticancer effects of AgNPs-Car on highly malignant and drug-resistant MDA-MB-231 human breast tumour cells, 4T1 mouse breast tumour cells, and normal HUVEC cells as control cells to investigate whether there is a new treatment option in TNBCs.

MATERIALS AND METHODS

The MDA-MB-231, 4T1, and HUVEC were purchased from American Type Culture Collection (ATCC, USA). Sodium borohydride (NaBH_4), silver nitrate ($\text{Ag}(\text{NO}_3)$), sodium hydroxyl (NaOH), and trisodium citrate (TSC) were obtained from Sigma Aldrich (USA), and 3-[4,5-dimethylthiazol-2-yl]-2,5-diphenyl tetrazolium bromide (MTT) kit, dimethylsulphoxide (DMSO), and Dulbecco's Modified Eagle's Medium (DMEM) were obtained from Sigma (USA). Trypsin, streptomycin (S), penicillin (P), foetal bovine serum (FBS), and phosphate buffer saline (PBS) were obtained from Gibco and Car from Glentham (UK).

Synthesis of the AgNPs-Car

1×10^{-3} M $\text{Ag}(\text{NO}_3)$, 4.3×10^{-3} M trisodium citrate, and 2×10^{-3} M NaBH_4 were prepared and used as stock solutions. The synthesis of AgNPs and AgNPs-Car was prepared using various concentrations of NaBH_4 , TSC, and $\text{Ag}(\text{NO}_3)$. In a dark room, they were combined for 30 min. at 60°C . The $\text{Ag}(\text{NO}_3)$ solution was then added at 90°C drip-by-drip. A 0.1 M NaOH solution was used to bring the pH of the solution down to 10.5 before it was centrifuged at 12,000 rpm for 15 min., rinsed with deionised water, and stored at $+4^\circ\text{C}$.

Characterisation of AgNPs-Car

The Fourier transform infrared spectroscopy (FTIR) spectra of the AgNPs and AgNPs-Car were analysed by a Perkin Elmer Spectrum 400 spectrometer with 4 cm^{-1} res-

olution and ten scans per spectrum. FTIR analyses were taken later, and the samples were dried.

Dynamic light scattering (DLS) examined the nanoparticle size and size distribution of the samples and zeta sizer showed the evaluations at 25°C (Malvern Instruments Ltd., Malvern, UK). The samples were dripped onto the silicon base material for the scanning electron microscope (SEM) analysis. The samples were left overnight to enable the drying of the liquid. Later, the samples were coated with Au/Pd to increase their surface conductivity. SEM and Energy dispersive X-ray (EDX) analysis was started after the samples were prepared with this procedure.

Cell culture analysis

MDA-MB-231, 4T1, and HUVEC cells were used in this study. The cell lines were seeded in T75 flasks with DMEM, including 10% FBS and 1% P/S in 5% CO_2 and 95% relative humidity incubator at 37°C . The cells were treated when they reached 80% confluency.

Cell viability differences in Car, AgNPs, and AgNPs-Car were determined by MTT after 72 h. The 3-[4,5-dimethylthiazol-2-yl]-2,5-diphenyl tetrazolium bromide reduced by live cells to formazan in the MTT, a colorimetric test (31, 32). The subsequent concentrations of Car (3.12, 6.25, 12.5, 25, 50, 70 $\mu\text{g}/\text{mL}$) and AgNPs-Car (3.12, 6.25, 12.5, 25, 50 $\mu\text{g}/\text{mL}$) were applied on MDA-MB-231, 4T1, and HUVEC (Table 1). The Ag concentration in AgNPs-Car is shown in Table 1. MTT solution (10 μl of 5 mg/mL PBS) was added, and the cells were incubated at 37°C for 4 h; the medium was taken, and 100 μL DMSO, which is used to dissolve formazan crystals, was added for lysing. The absorbance was read at 570 nm. The trials were done thrice. Dose-response curves were created to determine the IC_{50} (concentration that inhibits the growth of 50% of cells) for AgNPs-Car. This metric was used to evaluate the effectiveness of AgNPs-Car. The IC_{50} was calculated using the IC_{50} Calculator (AAT Bioquest) (<https://www.aatbio.com/tools/ic50-calculator>). A Nikon Eclipse Ts2 microscope evaluated the morphological changes.

Table 1: AgNPs-Car concentrations used in the cytotoxicity tests

Car stock	AgNPs stock	AgNPs-Car stock	AgNPs-Car $1/2$ diluted	AgNPs-Car $1/4$ diluted	AgNPs-Car $1/8$ diluted
1 mg/mL	108 $\mu\text{g}/\text{mL}$	50 $\mu\text{g}/\text{mL}$ Car+ 5.4 $\mu\text{g}/\text{mL}$ Ag	25 $\mu\text{g}/\text{mL}$ Car+ 2.7 $\mu\text{g}/\text{mL}$ Ag	12.5 $\mu\text{g}/\text{mL}$ Car+ 1.3 $\mu\text{g}/\text{mL}$ Ag	6.25 $\mu\text{g}/\text{mL}$ Car+ 0.6 $\mu\text{g}/\text{mL}$ Ag

Car: Carmofur, AgNPs: Silver nanoparticles, AgNPs-Car: Carmofur loaded silver nanoparticles, Ag: silver

Statistical analysis

One-way ANOVA performed for multiple comparisons of the results of the experiments using the GraphPad Prism 9.1.0 program. The mean of the control group was compared to the mean of the treated groups using the Student's t-test. A $p < 0.05$ was considered statistically significant. Results are given as mean \pm S.D. At least three runs of each test were performed.

RESULTS

The AgNPs displayed proper characterisation results for cancer cell implementation

FTIR results demonstrate the data of AgNPs (Figure 1a) and AgNPs-Car (Figure 1b). In Figure 1a, the first peak was illustrated at 3251 cm^{-1} for the -OH band, the second peak was measured at 1636 cm^{-1} for the carboxylate group of sodium citrate, and the band for -CH vibrations at lower wavelengths. Shifts were detected in Figure 1b compared with Figure 1a. The -OH vibration band determined the amine groups in the AgNPs-Car structure by which shifted from 3251 to 3253 cm^{-1} . Furthermore, characteristic vibration peaks, such as -CN stretching, -OH bending, -CH bending, and -CO stretching, were measured between 1637 - 1015 cm^{-1} in the AgNPs-Car group.

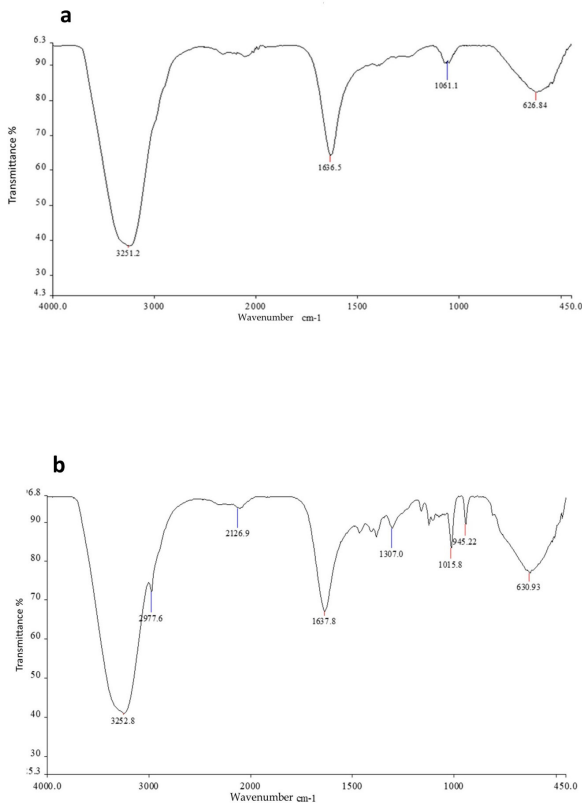


Figure 1: Vibration peaks were determined by FTIR spectroscopic analysis in (a) AgNPs (b) AgNPs-Car groups

At the same time, while the characteristic vibration signal peak of the AgNPs was seen at 626 cm^{-1} in Figure 1b, it was also determined that this vibration signal shifted to 630 cm^{-1} after drug loading.

Car decreased the AgNPs size ideally

Figure 2a shows, however, that when Car was added to the AgNPs in Figure 2b, the particles were found to be more dispersed. Its dimensions were found to range from 10 to 20 nm. This confirms our zeta sizer measurements (Figure 3a, b). The nanoparticle size was examined after being diluted with distilled water. The light scatter measurements were evaluated at 25°C . A Nano ZS and DLS determined the size and size distribution of the AgNPs in the samples. In this study, the average AgNPs-Car size was around 10 nm. As a result of DLS analysis, AgNP and AgNP-Car showed a homogenous distribution in length (Figure 3).

The EDX analysis in Figure 4a shows, together with the base material silicon, that the amount of silver attached to the surface of this base material is around 2%. In Figure 4b, while the amount of silver decreases to 0.5%, the

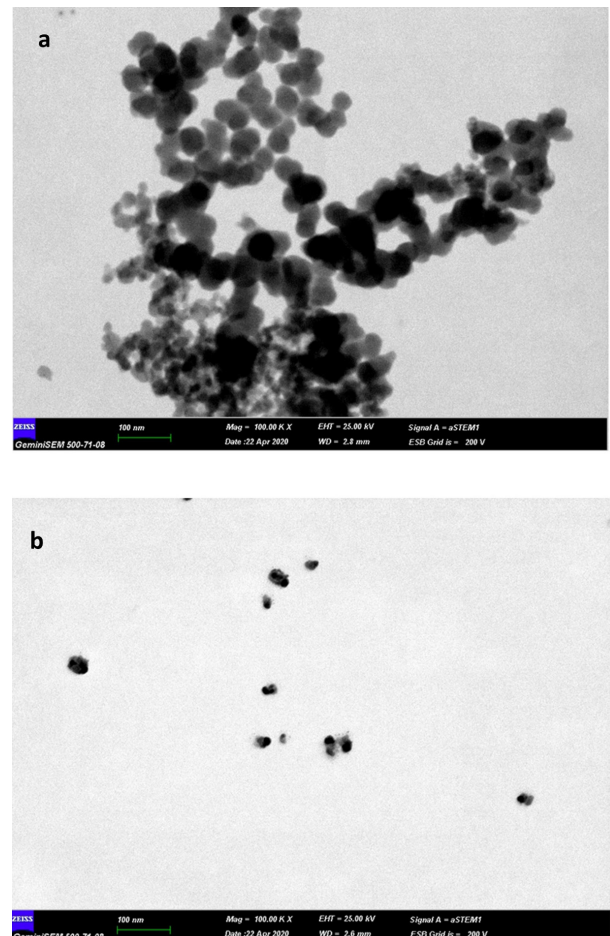


Figure 2: SEM images of (a) AgNPs and (b) AgNPs-Car

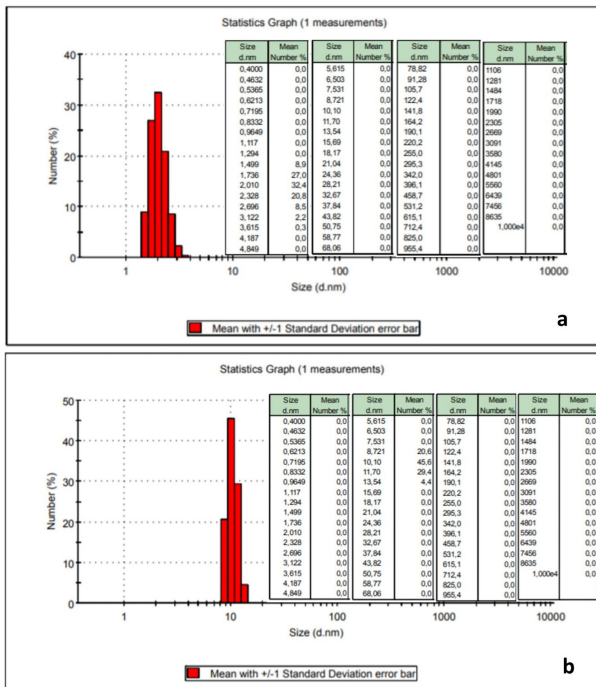


Figure 3: The DLS analyses of (a) AgNPs and (b) AgNPs-Car

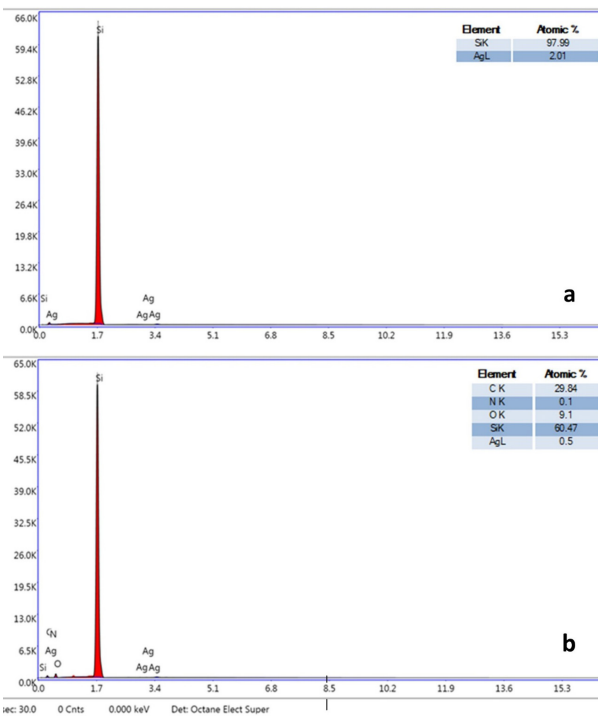


Figure 4: EDX analysis of (a) AgNPs and (b) AgNPs-Car amount of the elements belonging to the AgNPs-bound Car in percentage are also seen on the surface. Elements such as carbon, nitrogen, and oxygen are known to be included in the structure of Car, which confirmed that we successfully bound our drug to AgNPs.

AgNPs-Car are effective agents for cytotoxicity on chemotherapy-resistant TNBC cells

Figure 5 shows the antiproliferative effects of separately Car, AgNPs, and AgNPs-Car that synthesised against MDA-MB-231 and 4T1 cells. As shown in Table 2, AgNPs-Car is several times more effective than Car alone on treatment-resistant TNBC cells. In addition, the fact that AgNPs (without Car) cause no considerable cytotoxicity in any cell group (Figures 5 and 6) indicates that AgNPs will not cause side effects in normal body cells.

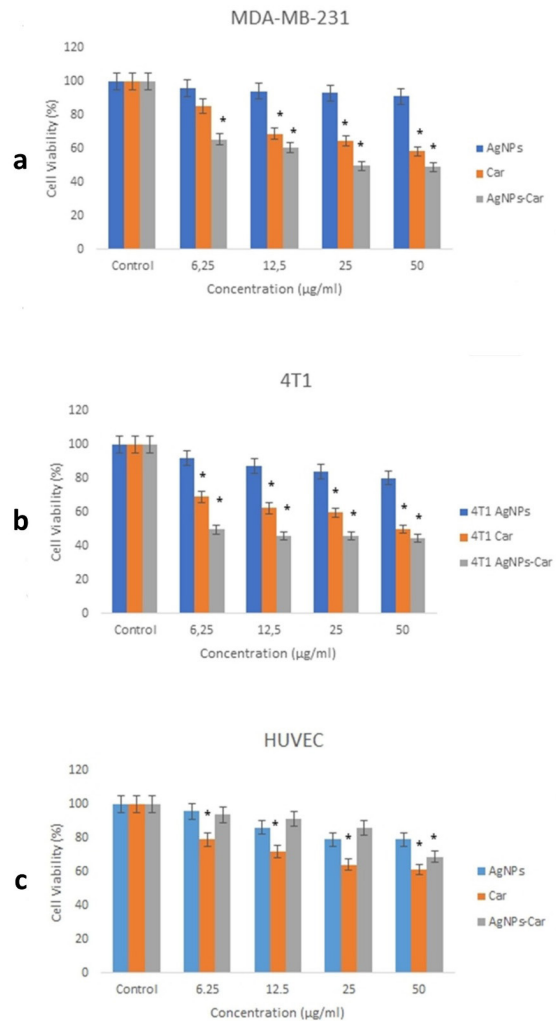


Figure 5: Viability (%) of MDA-MB-231 (a), 4T1 (b) cancer cells, and HUVEC healthy cells (c) incubated with AgNPs, Car, and AgNPs-Car at various concentrations for 72 h. The Car concentrations are indicated on the abscissa of the Figure. AgNPs are also added to the Figure for comparison of the cytotoxicity of the agents, although there is no Car. $P < 0.05$ (*) demonstrated statistical significance compared to the control group. The samples were examined using the Student's t-test. GraphPad Prism 9.1.0 was used for the statistical analysis (GraphPad Software). At least three runs of each test were performed

Notably, AgNPs showed almost no toxicity to non-cancerous HUVEC cells (Figure 6). As mentioned before, many factors determine the toxicity of AgNPs. In addition, the dose of Ag in AgNPs-Car that we used at IC₅₀ concentration is relatively low (3.1 µg / mL for MDA-MB-231, 0.8 µg / mL for 4T1) (Figure 7).

Healthy cells were not affected by AgNPs-Car; therefore, they are ideal agents for breast cancer cell therapy

In our results, Car appears to have an anticancer effect on treatment-resistant MDA-MB-231 and 4T1 breast cancer cells and no toxicity to non-cancerous HUVEC cells at similar concentrations (Figure 5). In addition, it is seen that the AgNPs-Car we synthesised are effective in MDA-MB-231 at a 2.4 times lower concentration than Car alone and 5.7 times lower in 4T1 (Table 2). As a result, AgNPs-Car was found to have anticancer effects on treatment-resistant TNBC cells and non-toxic in non-cancerous HUVEC cells (Table 2). In addition, our results show that AgNPs-Car is much more effective on the murine cancer cell 4T1 than the human cancer cell MDA-MB-231. These Our results displayed that higher doses may be required to treat more complex human organisms.

Table 2: The cytotoxic effect of Car and AgNPs-Car on MDA-MB-231, 4T1, and HUVEC

Cell Lines	*IC ₅₀ (µg/mL)		
	Car	AgNPs-Car	AgNPs
MDA-MB-231	69.381	28.803	Not effective
4T1	43.244	7.580	Not effective
HUVEC	>70	>70	Not effective

Proliferation was examined using an MTT assay for 72 h. * IC₅₀: Concentration that inhibited cell growth by 50%. HUVEC: Human umbilical vein endothelial cells, MDA-MB-231: Human breast adenocarcinoma, 4T1: Mouse breast cancer, stage IV, Car: Carmofur, AgNPs: Silver nanoparticles, AgNPs-Car: carmofur-loaded silver nanoparticles

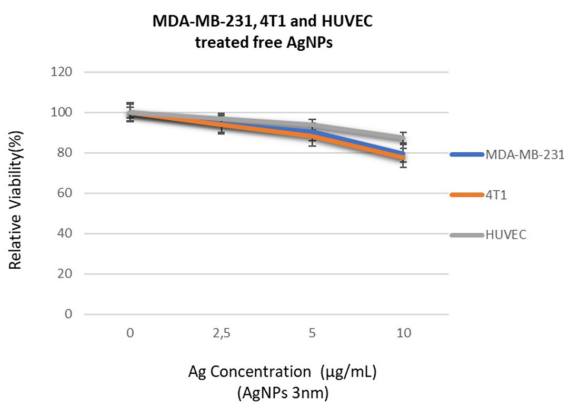


Figure 6: Vitality (%) of MDA-MB-231, 4T1 cancerous cells, and HUVEC non-cancerous cells incubated with free AgNPs at various concentrations for 72 h

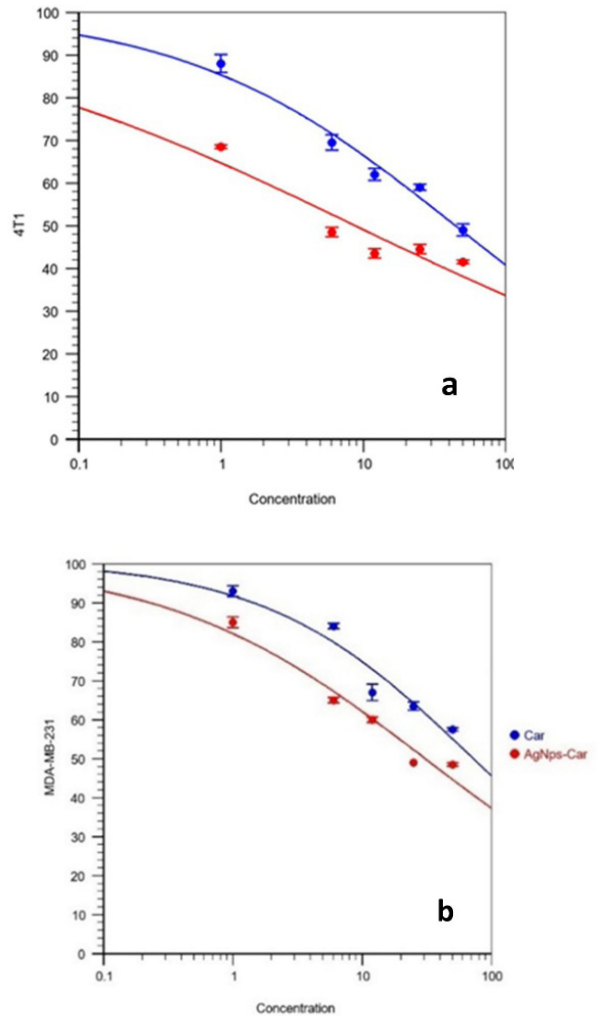


Figure 7: Logarithmic IC₅₀ curves of Car and AgNPs-Car on 4T1 cells (a) and MDA-MB-231 (b) cells. *IC₅₀ values were determined using the AAT Bioquest IC₅₀ calculator

Figure 7 shows that Car and AgNPs-Car had no significant toxicity in normal HUVEC cells. HUVEC lines were interconnected and adhered to the surface in almost all treatment groups. Figure 8 illustrates the morphological differences in MDA-MB-231 and 4T1 cells after incubation in Car and AgNPs-Car at IC₅₀ concentrations and HUVEC cells at 50 µg/mL. After the application, the connections between 4T1 cells appeared to be significantly visibly decreased; intercellular links disappeared, cell integrity was affected, and the shape of the cells shrunk compared with the untreated cells. The number of cells and intercellular connections decreased, and some cells became round and detached from the surface in the MDA-MB-231 cells. The investigation of the effect of drug-free AgNPs showed no change or damage in the cells compared with the control group cells. It is also noteworthy that when Car and AgNPs-Car are administered to TNBC cancer

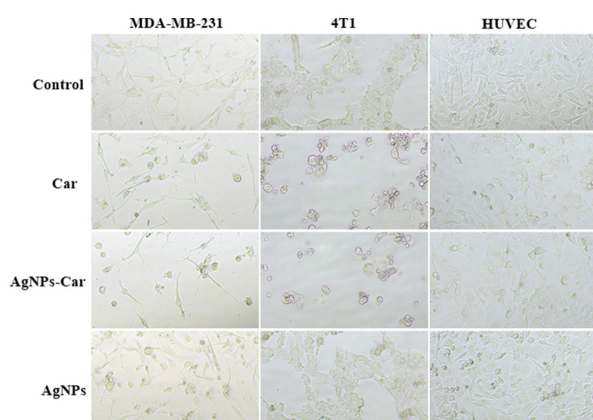


Figure 8: Light microscopy of the MDA-MB-231, 4T1, and HUVEC lines. The cells were incubated with Car and AgNPs-Car, AgNPs for 72 h. Magnification: X100. Car and AgNPs-Car were applied to cancerous MDA-MB-231 and 4T1 cells at IC₅₀ concentrations, as shown in Table 1, and to non-cancerous HUVEC cells at 50 µg/mL

cells, the cell confluency significantly reduces (Figure 8). The number of TNBC cells was remarkably reduced compared with the number of cells in the control group.

DISCUSSION

Triple-negative breast cancer may initially respond to chemotherapy, but it can develop resistance over time. These resistance mechanisms are quite complex and are associated with various biological processes, such as the presence of cancer stem cells, activation of DNA repair mechanisms in TNBCs, epithelial-mesenchymal transition (EMT), and the overexpression of drug efflux pumps like P-gp (33). For these reasons, the treatment of TNBC is complex, and in addition to chemotherapy, new therapeutic strategies are being developed, including immunotherapy and targeted approaches. AgNPs represent a promising new approach to the treatment of breast cancer (32). This nanotechnology-based therapeutic method is particularly noteworthy for its potential to specifically target cancer cells and its reduced side effect profile.

Nanoparticle characterisation is the process of determining the physical, chemical, and biological properties of nanoparticles. The synthesis and characterisation of nanoparticles to ensure biocompatibility directly affect their application success. In this study, AgNPs were characterised using SEM, FTIR, DLS, and EDX analyses (34). FTIR spectral analysis of AgNPs and AgNPs-Car was carried out to investigate the changes in the chemical composition of Car after loading into the AgNPs. According to the EDX data, the structure of Car is known to contain elements like carbon, nitrogen, and oxygen, confirming that we were effective in binding Car to AgNPs. SEM automatically analyzes and classifies the particles in the image while providing high-resolution electron imaging.

This depends on several additional factors in addition to their size and form, including the particles' surface, volume, convexity, and circularity.

In this study, the AgNPs were captured as highly dense. This is because clumps may occur when we drop the sample liquids on the silicone-based material. It is a natural outcome. Because of this clustering, the particles were seen as more prominent in the SEM analysis (35). DLS is the most commonly used for nanoparticle characterisation among the many techniques because of its fast and easy-to-operate methods and sensitivity to small and low-scattering particles (36). The sizes of the nanoparticles are significant because they influence their action and *in vivo* drug circulation (37). Small sizes of nanocarriers facilitate the drug to pass through the plasmalemma and keep away from recognition and degradation by the reticuloendothelial system (RES) and increase the drug circulation half-time (38-40). However, NPs smaller than 10 nm are not preferred in treatment to avoid being eliminated by fast renal clearance. In addition, NPs larger than 100 nm may not reach the tumour site and may be caught by tissue macrophages (41). The nanoparticles we synthesised are small, which is advantageous in cancer treatment (18, 42). In this study, Car decreased the AgNP size ideally to 10 nm. In addition, nanoparticle size plays a significant role in nanoparticle activity (21-24). The synthesised nanoparticles' ideal sizes for drug delivery systems are thus demonstrated. Our results indicate that the AgNPs-Car induced toxicity predominantly towards treatment-resistant TNBC cells, not non-cancerous normal HUVEC cells. These findings show that AgNPs-Car is effective at several times lower concentrations than the Car, specific to breast cancer cells that are more malignant and non-responsive to drugs.

Treatment with AgNPs is known to cause dose-related toxicity, involving the enhancement of reactive oxygen species and insult of DNA, which cannot maintain cell survival (43). In the studies of Swanner et al., AgNPs have been reported to be toxic in increasing concentrations (5, 10, 20, 40 µg/mL) and in different sizes in MDA-MB-231 TNBC cells (44). For TNBCs, AgNPs with 40 µg/mL of silver have been reported to cause higher toxicity, whereas AgNPs containing 5 µg/mL of silver have lower toxicity. The concentration of silver in the AgNPs is critical; the amount of silver is directly proportional to the toxicity, and AgNPs containing 40 µg/mL of silver have been shown to have the highest toxicity. Also, in the same studies, AgNPs were non-toxic in non-cancerous breast cancer cells (44). Although our findings are similar to the results of Swanner et al., the free AgNPs we synthesised appear less toxic than those in the study (44).

Car, a derivative of 5FU, is primarily used for gastrointestinal cancers and some other solid tumours, though it is still being studied for its effects on breast cancer. A preclinical

study has shown that Car can reduce the metastatic potential of breast cancer cells (45). Therefore, this could represent a significant advancement, particularly for aggressive types of breast cancer such as TNBC. Hence, this study used Car-loaded AgNPs, and their efficacy on TNBCs was evaluated. Nevertheless, researchers have shown that Car and its analogs have an anticancer effect non-selectively (even non-cancerous cells) in some studies; however, the number of studies on Car is limited in the literature (10, 11, 46, 47). In a study, Car, an acid ceramidase inhibitor, was used in treating paediatric brain tumours and was highly effective (4.6-50 µM). It was reported that it could be recommended as a new drug for these tumours (46). Morimoto and Koh noted that the adjuvant use of Car is beneficial in early breast cancer (10). N-acylsphingosine amidohydrolase 1 (ASA1), an enzyme involved in ceramide metabolism, has been shown to regulate ceramide levels and decrease tumour growth by causing cell cycle arrest and apoptosis (48). According to a study, ASA1 controls the growth and progression of TNBC by modifying mitogen-activated protein kinase (MAPK). Pharmacological targeting of ASA1 (through the ceramidase inhibitor carmofur) significantly inhibits the growth of TNBC (49). Furthermore, studies on the NPs-Car are very scarce, and no studies were available for AgNPs-Car (50). Thus, AgNPs synthesised with Car have not been evaluated in TNBCs or cancer treatment. Therefore, our findings are essential to the literature. Our results show that AgNPs-Car created a predominant and selective anti-growth effect on treatment-resistant TNBC cells. Our study was evaluated *in vitro* and was limited by the fact that the biodistribution, biocompatibility, and therapeutic efficacy of AgNPs-Car were not investigated in *in vivo* models. In addition, the long-term stability and cellular uptake mechanisms of the nanoparticles were not investigated in detail. In our study, only cell viability was investigated using the MTT assay, and the mechanisms of cell death such as apoptosis and necrosis were not determined. Finally, further large-scale experiments are needed to comprehensively compare the selectivity in different cancer cell lines and healthy cells. In view of this, further studies are required to evaluate the therapeutic potential of AgNPs-Car.

CONCLUSION

TNBC is a challenging cancer to treat due to its high heterogeneity, lack of hormone receptors, and aggressive metastatic potential. Current treatments are often insufficient, with no targeted therapy available. In this study, silver nanoparticles conjugated with carmofur (AgNPs-Car) were synthesised and demonstrated strong anticancer effects on resistant TNBC cell lines. Even at low concentrations, AgNPs-Car was effective without harming normal cells, highlighting its potential as a selective and safe treatment. This nanoplatform offers a promising approach for overcoming chemoresistance in TNBC.

Ethics Committee Approval: Since the commercially purchased cell lines were used in the study, ethics committee approval was not required.

Peer Review: Externally peer-reviewed.

Author Contributions: Conception/Design of Study- F.D.K.; Data Acquisition- F.D.K., İ.A.K.; Data Analysis/Interpretation – D.S.K., İ.A.K., F.D.K.; Drafting Manuscript- D.Ö., F.D.K.; Critical Revision of Manuscript- D.Ö.; Final Approval and Accountability- D.Ö., F.D.K.; Technical or Material Support- İ.A.K., D.S.K.; Supervision- D.S.K.

Acknowledgments: We thank Kadriye Gümüş for her contribution to the English editing of the article at the Istanbul Faculty of Medicine.

Conflict of Interest: The authors have no conflict of interest to declare.

Financial Disclosure: The authors declared that this study received no financial support.

REFERENCES

1. Liyanage PY, Hettiarachchi SD, Zhou Y, Ouhit A, Seven ES, Oztan C, et al. Nanoparticle-mediated targeted drug delivery for breast cancer treatment. *Biochimica Et Biophysica Acta - Reviews on Cancer* 2019;1871(2):419-33. [\[CrossRef\]](#)
2. Jamdade VS, Sethi N, Mundhe N, Kumar P, Lahkar M, Sinha N. Therapeutic targets of triple-negative breast cancer: a review. *Br J Pharmacol* 2015;172(17):4228-37. [\[CrossRef\]](#)
3. Fahmy SA, Mahdy NK, Mohamed AH, Mokhtar FA, Youness RA. Hijacking 5-fluorouracil chemoresistance in triple negative breast cancer via microRNAs-loaded chitosan nanoparticles. *Int J Mol Sci* 2024;25(4):2070. [\[CrossRef\]](#)
4. McGee SF. Understanding metastasis: Current paradigms and therapeutic challenges in breast cancer progression. *RCSI Stud Med J* 2010;3:56-60.
5. Dasari N, Guntuku GS, Pindiprolu SKS. Targeting triple negative breast cancer stem cells using nanocarriers. *Discover Nano* 2024;19(1):41. [\[CrossRef\]](#)
6. Nakamura Y, Mochida A, Choyke PL, Kobayashi H. Nanodrug delivery: Is the enhanced permeability and retention effect sufficient for curing cancer? *Bioconjug Chem* 2016;27(10):2225-38. [\[CrossRef\]](#)
7. Islam MM, Mirza SP. Versatile use of Carmofur: A comprehensive review of its chemistry and pharmacology. *Drug Dev Res* 2022;83(7):1505-18. [\[CrossRef\]](#)
8. Nosrati H, Hamzepoor M, Sohrabi M, Saidijam M, Assari MJ, Shabab N, et al. The potential renal toxicity of silver nanoparticles after repeated oral exposure and its underlying mechanisms. *BMC Nephrology* 2021;22(1):228. [\[CrossRef\]](#)
9. Sakamoto J, Oba K, Matsui T, Kobayashi M. Efficacy of oral anticancer agents for colorectal cancer. *Dis Colon Rectum* 2006;49:82-S91. [\[CrossRef\]](#)
10. Morimoto K, Koh M. Postoperative adjuvant use of Carmofur for early breast cancer. *Osaka City Med J* 2003;49(2):77-83.

11. Realini N, Solorzano C, Pagliuca C, Pizzirani D, Armirotti A, Luciani R, et al. Discovery of highly potent acid ceramidase inhibitors with in vitro tumor chemosensitizing activity. *Sci Rep* 2013;3(1):1035. [CrossRef]
12. Taniguchi M, Okazaki T. Role of ceramide/sphingomyelin (SM) balance regulated through "SM cycle" in cancer. *Cell Signal* 2020;87:110119. [CrossRef]
13. Sharma D, Czarnota GJ. Involvement of ceramide signalling in Radiation-Induced tumour vascular effects and Vascular-Targeted therapy. *Int J Mol Sci* 2022;23(12):6671. [CrossRef]
14. Dementiev A, Joachimiak A, Nguyen HS, Gorelik A, Illes K, Shabani S, et al. Molecular mechanism of inhibition of acid ceramidase by Carmofur. *J Med Chem* 2018;62(2):987-92. [CrossRef]
15. Domracheva I, Muhamadejev R, Petrova MV, Liepin'sh EE, Gulbe A, Shestakova I, et al. 1,2-Dimyristoyl-sn-glycero-3-phosphocholine (DMPC) increases Carmofur stability and in vitro antiproliferative effect. *Toxicol Rep* 2015;2:377-83. [CrossRef]
16. Saied EM, Arenz C. Small molecule inhibitors of ceramidases. *Cellular Physiol Biochem* 2014;34(1):197-212. [CrossRef]
17. Ma P, Mumper RJ. Paclitaxel nano-delivery systems: A comprehensive review. *J Nanomed Nanotech* 2013;4(2):1000164. [CrossRef]
18. Kulkarni SK. Nanotechnology: Principles and practices. Springer eBooks. 2015; 293. <https://doi.org/10.1007/978-3-319-09171-6>. [CrossRef]
19. Arvizo RR, Bhattacharyya S, Kudgus RA, Giri K, Bhattacharya R, Mukherjee P. Intrinsic therapeutic applications of noble metal nanoparticles: past, present and future. *Chem Soc Rev* 2012;41(7):2943. [CrossRef]
20. Dykman LA, Khlebtsov NG. Gold nanoparticles in biomedical applications: recent advances and perspectives. *Chem Soc Rev* 2012;41(6):2256-82. [CrossRef]
21. Limbach LK, Wick P, Manser P, Grass RN, Bruinink AA, Stark WJ. Exposure of engineered nanoparticles to human lung epithelial cells: influence of chemical composition and catalytic activity on oxidative stress. *Environ Sci Tech* 2007;41(11):4158-63. [CrossRef]
22. Pal S, Tak YK, Song JM. Does the antibacterial activity of silver nanoparticles depend on the shape of the nanoparticle? A study of the gram-negative bacterium *Escherichia coli*. *Appl Environ Microbiol* 2007;73(6):1712-20. [CrossRef]
23. Piao MJ, Kang KA, Lee IK, Kim HS, Kim S, Choi JY, et al. Silver nanoparticles induce oxidative cell damage in human liver cells through inhibition of reduced glutathione and induction of mitochondria-involved apoptosis. *Toxicol Lett* 2011;201(1):92-100. [CrossRef]
24. Gliga AR, Skoglund S, Wallinder IO, Fadeel B, Karlsson H. Size-dependent cytotoxicity of silver nanoparticles in human lung cells: the role of cellular uptake, agglomeration and Ag release. *Part Fibre Toxicol* 2014;11:1-17. [CrossRef]
25. Miethling-Graff R, Rumpker R, Richter M, Verano-Braga T, Kjeldsen F, Brewer JR, et al. Exposure to silver nanoparticles induces size- and dose-dependent oxidative stress and cytotoxicity in human colon carcinoma cells. *Toxicol in Vitro* 2014;28(7):1280-9. [CrossRef]
26. Khan AU, Yuan Q, Wei Y, Khan SU, Tahir K, Khan ZUH, et al. Longan fruit juice mediated synthesis of uniformly dispersed spherical AuNPs: cytotoxicity against human breast cancer cell line MCF-7, antioxidant and fluorescent properties. *RSC Advances* 2016;6(28):23775-82. [CrossRef]
27. Ahmad A, Wei Y, Syed F, Khan S, Khan GM, Tahir K, et al. Isatis tinctoria mediated synthesis of amphotericin B-bound silver nanoparticles with enhanced photoinduced antileishmanial activity: A novel green approach. *J Photochem Photobiol B-biology* 2016;161:17-24. [CrossRef]
28. Khatami M, Sharifi I, Nobre MAL, Zafarnia N, Aflatoonian MR. Waste-grass-mediated green synthesis of silver nanoparticles and evaluation of their anticancer, antifungal and antibacterial activity. *Green Chem Lett Rev* 2018;11(2):125-34. [CrossRef]
29. Kang DY, Sp N, Kim DH, Joung YH, Lee HG, Park YM, et al. Salidroside inhibits migration, invasion and angiogenesis of MDA-MB 231 TNBC cells by regulating EGFR/Jak2/STAT3 signaling via MMP2. *Int J Oncol* 2018;53(2):877-85. [CrossRef]
30. Schrörs B, Boegel S, Albrecht C, Bukur T, Bukur V, Holtsträter, C, et al. Multi-Omics characterization of the 4T1 murine mammary gland tumor model. *Front Oncol* 2020;10:1195. [CrossRef]
31. Kumar P, Nagarajan A, Uchil PD. Analysis of cell viability by the MTT Assay. *CSH Protocols* 2018:pdb.prot095505. [CrossRef]
32. Danişman-Kalındemirtaş F, Kariper IA, Hepokur C, Erdem-Kuruca S. Selective cytotoxicity of paclitaxel bonded silver nanoparticle on different cancer cells. *J Drug Deliver Sci Tech* 2021;61:102265. [CrossRef]
33. Ferrari P, Scatena C, Ghilli M, Bargagna I, Lorenzini G, Nicolini A. Molecular mechanisms, biomarkers and emerging therapies for chemotherapy resistant TNBC. *Int J Mol Sci* 2022;23(3):1665. [CrossRef]
34. Clogston JD, Crist RM, Dobrovolskaia MA, Stern ST. Characterization of nanoparticles intended for drug delivery. *Humana Press* 2024;63-70. [CrossRef]
35. Hepokur C, Kariper IA, Misir S, Ay E, Tunoğlu S, Ersez MS, et al. Silver nanoparticle/capecitabine for breast cancer cell treatment. *Toxicol in Vitro* 2019;61:104600. [CrossRef]
36. Fissan H, Ristig S, Kaminski H, Asbach C, Epple M. Comparison of different characterization methods for nanoparticle dispersions before and after aerosolization. *Anal Method* 2014;6(18):7324. [CrossRef]
37. Ramos AP, Cruz MAE, Tovani CB, Ciancaglini P. Biomedical applications of nanotechnology. *Biophysical Rev* 2017;9(2):79-89. [CrossRef]
38. Schmidt C, Storsberg J. Nanomaterials-Tools, technology and methodology of nanotechnology based biomedical systems for diagnostics and therapy. *Biomed* 2015;3(3):203-23. [CrossRef]
39. Hare JI, Lammers T, Ashford M, Puri S, Storm G, Barry ST. Challenges and strategies in anticancer nanomedicine development: An industry perspective. *Adv Drug Deliv Rev* 2017;108:25-38. [CrossRef]
40. Jahan ST, Sadat SMA, Walliser M, Haddadi A. Targeted therapeutic nanoparticles: An immense promise to fight against cancer. *J Drug Deliv* 2017(1):9090325. [CrossRef]
41. Jurj A, Braicu C, Pop L, Tomuleasa C, Gherman C, Berindan-Neagoe I. The new era of nanotechnology, an alternative to change cancer treatment. *Drug Des Devel Ther* 2017;11:2871-90. [CrossRef]
42. Ivanova NA, Gugleva V, Dobрева M, Ivaylo P, Stefanov S, Andonova V. Silver nanoparticles as Multi-Functional Drug

- Delivery Systems. IntechOpen eBooks. 2019; pp. 71-92 London, UK. <https://doi.org/10.5772/intechopen.80238>. [\[CrossRef\]](#)
43. Shelton JR, Lu X, Hollenbaugh JA, Cho JH, Amblard F, Schinazi RF. Metabolism, biochemical actions, and chemical synthesis of anticancer nucleosides, nucleotides, and base analogs. *Chem Rev* 2016;116(23):14379-455. [\[CrossRef\]](#)
 44. Swanner J, Fahrenholtz CD, Tenvooren I, Bernish BW, Sears JJ, Hooker A, et al. Silver nanoparticles selectively treat triple-negative breast cancer cells without affecting non-malignant breast epithelial cells in vitro and in vivo. *FASEB bioAdvances* 2019;1(10):639-60. [\[CrossRef\]](#)
 45. Tominaga T, Kimura M, Asaga T, Yoshida M, Awane H, Koyama H, et al. 1-Hexylcarbonyl-5-fluorouracil + cyclophosphamide + tamoxifen versus CMF + tamoxifen in women with lymph node-positive breast cancer after primary surgery: A randomized controlled trial. *Oncol Rep* 2004;12(4):797-803. [\[CrossRef\]](#)
 46. Doan N, Nguyen HS, Montoure A, Al-Gizawiy MM, Mueller WM, Kurpad S, et al. Acid ceramidase is a novel drug target for pediatric brain tumors. *Oncotarget* 2017;8(15):24753-61. [\[CrossRef\]](#)
 47. Gu T, Lu A, Wang X, Brahan N, Xu L, Zhang L, et al. Synthesis and evaluation of carmofur analogs as antiproliferative agents, inhibitors to the main protease (Mpro) of SARS-CoV-2, and membrane rupture-inducing agents. *bioRxiv* 2024;2024-10. [\[CrossRef\]](#)
 48. Obeid LM, Hannun YA. Ceramide: a stress signal and mediator of growth suppression and apoptosis. *J Cell Biochem* 1995;58:191-8. [\[CrossRef\]](#)
 49. Reddi KK, Chava S, Chabattula SC, Edwards YJ, Singh K, Gupta R. ASAH1 facilitates TNBC by DUSP5 suppression-driven activation of MAP kinase pathway and represents a therapeutic vulnerability. *Cell Death Dis* 2024;15(6):452. [\[CrossRef\]](#)
 50. Çömlekçi E, Kutlu HM, Sezer CV. Toward stimulating apoptosis in human lung adenocarcinoma cells by novel nano-carmofur compound treatment. *Anticancer Drug* 2018;32(6):657-63. [\[CrossRef\]](#)

HOW DID THE PANDEMIC LOCKDOWN AFFECT THE DEVELOPMENT OF INFANTS' SOCIAL AND COMMUNICATION SKILLS? A RETROSPECTIVE STUDY FROM TÜRKİYE

PANDEMİ KARANTİNASI BEBEKLERİN SOSYAL VE İLETİŞİM BECERİLERİNİN GELİŞİMİNİ NASIL ETKİLEDİ? TÜRKİYE'DEN RETROSPEKTİF BİR ÇALIŞMA

Öykü ÖZBÖRÜ AŞKAN¹ , Gonca KESKİNDEMİRCİ² , Melike METE² , Ümran ÇAKIROĞLU³ , Shabnam ALİYEVA³ , Pınar YEŞİL³ , Gülbin GÖKÇAY¹ 

¹Istanbul University, Institute of Child Health, Department of Social Pediatrics, İstanbul, Türkiye

²Istanbul University, İstanbul Faculty of Medicine, Department of Pediatrics, Division of Social Pediatrics, İstanbul, Türkiye

³Istanbul University, İstanbul Faculty of Medicine, Department of Pediatrics, İstanbul, Türkiye

ORCID IDs of the authors: Ö.Ö.A. 0000-0002-4139-5497; G.K. 0000-0003-1797-2802; M.M. 0000-0002-7985-0731; Ü.Ç. 0000-0002-2011-6145; S.A. 0000-0001-9486-6873; P.Y. 0000-0002-8271-4714; G.G. 0000-0003-1042-0407

Cite this article as: Özbörü Aşkan Ö, Keskindemirci G, Mete M, Çakıroğlu Ü, Aliyeva S, Yeşil P et al. How did the pandemic lockdown affect the development of infants' social and communication skills? A retrospective study from Türkiye. J Ist Faculty Med 2025;88(2):128-134. doi: 10.26650/IUITFD.1582447

ABSTRACT

Objective: Limited socialisation during the COVID-19 pandemic is one of the factors that may affect children's social and communication skills. In this study, we assessed the social communication skills of children aged 1-2 years during the COVID-19 pandemic period and compare them with the pre-pandemic era.

Material and Methods: Children who were two years old before the pandemic (Group 1) and children who were two years old during the pandemic quarantine (Group 2) were included in the study. For both groups, demographic information, anthropometric measurements at birth, ages at reaching developmental milestones, Social Communication Area Screening Test for Infants (SCASI) scores at 15 and 24 months [total, pre-speech skills (F1a), vocabulary (F1b), awareness skills scores (F2; n)], and screen time exposure were collected from medical records. Comparative analyses of these variables between the two groups were performed.

Results: A total of 202 children (Group 1; n=123, Group 2; n=79) were included in the study. The rate of girls was higher in Group 2 (p=0.041). No significant difference was found in terms of birth weeks, birth height, weight, head circumference measurements and the initial times of head holding, sitting without support and walking independently. The screen exposure duration for ≥2 hours at 15 and 24 months was higher in Group 2 (p=0.110; p=0.014,

ÖZET

Amaç: COVID-19 pandemisi sırasında sınırlı sosyalleşme, çocukların sosyal ve iletişim becerilerini etkileyebilecek faktörlerden biridir. Bu çalışmada, COVID-19 pandemisi döneminde 1-2 yaş arası çocukların sosyal iletişim becerilerini değerlendirmeyi ve pandemi öncesi dönemle karşılaştırmayı amaçladık.

Gereç ve Yöntem: Pandemi öncesinde iki yaşında olan çocuklar (Grup 1) ve pandemi karantinası sırasında iki yaşında olan çocuklar (Grup 2) çalışmaya dahil edildi. Her iki grup için demografik bilgiler, doğumdaki antropometrik ölçümler, gelişimsel kilometre taşlarına ulaşma yaşları, 15 ve 24 aylık Bebekler İçin Sosyal İletişim Alanı Tarama Testi (SİATT) skorları (toplam, konuşma öncesi beceriler (F1a), kelime kullanımı (F1b), farkındalık becerileri skorları (F2)) ve ekrana maruz kalma süresi tıbbi kayıtlardan toplandı. Bu değişkenlerin iki grup arasında karşılaştırmalı analizleri yapıldı.

Bulgular: Toplam 202 çocuk (Grup 1; n=123, Grup 2; n=79) çalışmaya dahil edildi. Grup 2'de kız çocuklarının oranı daha yüksekti (p=0,041). Doğum haftası, doğum boyu, kilo, baş çevresi ölçümleri ve baş tutma, desteksiz oturma ve bağımsız yürüme başlangıç zamanları açısından anlamlı bir fark bulunmadı. Grup 2'de 15 ve 24. aylarda ≥2 saat ekrana maruz kalma süresi daha yüksek saptandı (sırasıyla p=0,110; p=0,014). Sosyal iletişim de-

Corresponding author/İletişim kurulacak yazar: Öykü ÖZBÖRÜ AŞKAN – oykuozboru@gmail.com

Submitted/Başvuru: 10.11.2024 • **Revision Requested/Revizyon Talebi:** 19.01.2025 •

Last Revision Received/Son Revizyon: 04.03.2025 • **Accepted/Kabul:** 08.03.2025 • **Published Online/Online Yayın:** 17.04.2025



Content of this journal is licensed under a Creative Commons Attribution-NonCommercial 4.0 International License.

respectively). In the Social Communication assessments, the rate of children with risky SCASI results was higher in Group 2, both at 15 and 24 months ($p=0.312$; $p=0.004$, respectively).

Conclusion: Our findings suggest that the COVID-19 pandemic might have an impact on the social communication skills of children aged 1–2 years. It is important to monitor the development of communication skills as a part of paediatric health monitoring and to closely follow up with early interventions.

Keywords: COVID-19, language development, social communication, SCASI

ğerlendirmelerinde, riskli SIATT sonuçları olan çocukların oranı hem 15. hem de 24. ayda Grup 2'de daha yüksekti (sırasıyla $p=0,312$; $p=0,004$).

Sonuç: Bulgularımız, COVID-19 pandemisinin 1-2 yaş arası çocukların sosyal iletişim becerileri üzerinde etkili olabileceğini göstermektedir. Pediatrik sağlık izleminin bir parçası olarak iletişim becerilerinin gelişiminin izlenmesi ve erken müdahalelerle yakından takip edilmesi önemlidir.

Anahtar kelimeler: COVID-19, dil gelişimi, sosyal iletişim, SIATT

INTRODUCTION

Environmental interactions, along with genetic inheritance, play a significant role in children's development (1, 2). Children's interaction with their environment, the variety of stimuli, the social behaviours exhibited in peer and play settings and the freedom to engage in physical activities have a powerful impact on their development. Environmental stressors, such as poverty, limited access to education, environmental exposure, and caregiver characteristics, directly influence the child's development (3, 4).

The Coronavirus Disease 2019 (COVID-19) pandemic has brought about numerous changes in the lives of individuals at various levels (5-7). UNICEF has classified the impact of COVID-19 on children under three main categories: direct transmission of the virus, short-term socioeconomic consequences of preventive measures, and delays in achieving the Sustainable Development Goals (8). Although the direct impact of the virus on children has been less severe, the secondary consequences of the pandemic on children are reported to pose significant risks (9, 10).

Measures such as social isolation, quarantine, and social distancing, taken as protective actions during the pandemic, have been suggested to adversely affect children's development (11). The inability to participate in play and leisure activities outside the home, restricted socialisation, difficulties in understanding facial expressions due to mask-wearing, limitations in communication and language learning and increased screen exposure are all factors that may disrupt the development of children's cognitive, behavioural, social and communication skills (7, 12, 13). This study aimed to evaluate the impact on the social communication skills of children aged 1-2 years during the COVID-19 pandemic and to compare the results with the social communication skills of children aged 1-2 years in the pre-pandemic period.

MATERIALS AND METHODS

This study was conducted retrospectively at the Department of Paediatrics, Division of Social Paediatrics Well-Child Outpatient Clinic, Istanbul University Faculty

of Medicine. The Istanbul University Istanbul Faculty of Medicine Clinical Research Ethics Committee approved the study (Date: 06.09.2024, No: 17).

At the Well-Child Outpatient Clinic, children's growth and development are evaluated from birth until the age of 10. The follow-up intervals were monthly for the first six months, every 3 months from months 6 to 18, every six months from 18 months to six years, and yearly thereafter. If a problem is detected, the follow-up intervals are shortened, and necessary interventions are applied. During each follow-up, weight, height, and head circumference measurements were recorded and plotted on growth charts for continuous growth monitoring. Along with growth, developmental milestones are also assessed. Children are screened to ensure that they have reached developmental milestones for their age. The International Guide for Monitoring Child Development (GMCD) test and the Modified Checklist for Autism Test (M-CHAT) are administered by trained staff in accordance with recommendations from the Turkish Ministry of Health's General Directorate of Public Health (14-16). In addition, the Social Communication Area Screening Test for Infants (SCASI) was used between 6 and 24 months (17). If necessary, the children are referred for multidisciplinary evaluation and appropriate interventions. Furthermore, vaccinations from the Expanded National Immunisation Program, as well as non-routine vaccinations, are administered.

SCASI is a screening test that was developed in 2011 and has been validated for content and construct validity, reliability, and normative studies in Turkish children (17). It was designed as a parent-reported test focusing on the development of social communication to screen the development of children aged 6-24 months. The SCASI consists of 43 items structured under two factors within a single domain. The first factor (F1), "Communication-oriented social skills," is divided into two subgroups: pre-verbal skills (F1a; 26 items) and vocabulary (F1b; 5 items). The second factor (F2), "Awareness Skills" consists of 10 items. Although the last two items are not included in the total score, they serve as red flags, particularly for regression (Supplemented file). After the administration of the SCASI, the scores were compared with appropriate developmental age norms. If a child's score was above

the cut-off point, their development was considered "normal." The children were evaluated as "normal" or "at risk" according to the cut-off score. An "Educational Programme" booklet was provided for children identified as being at risk to assist in developing tailored educational support programs (17).

Children who were born between 1 January 2017 and 31 December 2017 and who had reached two years of age before the pandemic (Group 1) and children who were born between 1 January 2019 and 31 December 2019 and who reached two years of age during the pandemic (Group 2) were included in the study. For both groups, data including demographic information, anthropometric measurements at birth, ages at which developmental milestones were reached, SCASI total and F1a, F1b, and F2 sub scores, and screen time exposure at 15 and 24 months and if there was a diagnosis of speech disorders, autism, bilingualism, in which speech skills could be affected in the follow-up, were collected from their medical records.

Statistical analysis

Statistical Package for the Social Sciences (IBM SPSS Corp., Armonk, NY, USA) version 29 programme was used for statistical analyses. The study data were evaluated using descriptive statistical methods (mean, standard deviation, median, frequency, percentage, minimum, and maximum). The conformity of the continuous variables to the normal distribution was tested by the Shapiro-Wilk test and graphical analyses. The Mann-Whitney U test was used for comparisons of the continuous variables that did not show a normal distribution between the two groups, and the t-test was used for comparisons of the continuous variables that conformed to the normal distribution. The Pearson Chi-Square test and Fisher-Freeman-Halton test were used to compare categorical data. The statistical significance will be set as $p < 0.05$.

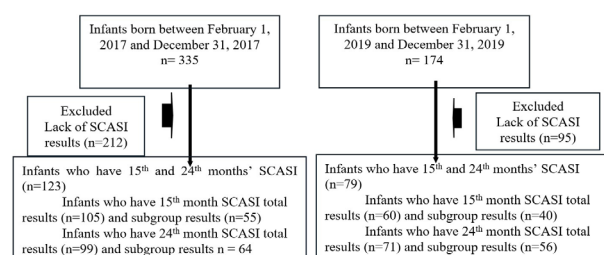


Figure 1: Flow diagram of the study
 SCASI: Social Communication Area Screening Test for Infants

RESULTS

A total of 509 records were evaluated, and 202 infants (Group 1 n=123, Group 2 n=79) were included in the analysis (Figure 1). In Group 1, 105 infants had the 15th-month SCASI total results, 55 had subgroup results, 99

infants had the 24th-month SCASI total results, and 64 had subgroup results. In Group 2, 60 infants had the 15th-month SCASI total results, 40 had subgroup results, 71 infants had the 24th-month SCASI total results, and 56 had subgroup results. In Group 1, 81 infants had both 15th and 24th months of SCASI results, and in Group 2, 52 had.

In the demographic data evaluation, the mean maternal ages were 32.7 (± 5.1) for Group 1 and 32.8 (± 4.7) for Group 2. The maternal age was similar between the groups, but when the maternal educational status was evaluated, the university graduation rate was higher in Group 2 ($p=0.005$). The employment rate of the mothers was higher in Group 2 than in Group 1 (70.9% and 61.8%, respectively), but there was no significant statistical difference ($p=0.185$). The mean paternal ages were 38.5 (± 5.6) for Group 1 and 35.5 (± 5.5) for Group 2, and in both groups, all fathers were employed. There were no significant differences in paternal age, education levels, and employment status between the groups (Table 1).

Among the participants, girls were 42.3% (n=52) and 57% (n=45) in Group 1 and Group 2, respectively. The median age was 86 (± 29) months for infants in Group 1 and 54 (± 2) months in Group 2. The birth weeks, birth height, weight, head circumference measurements and the initial times of head holding, sitting without support and walking independently were not statistically different between the groups. When the duration of screen exposure was compared, it was higher in Group 2 and the difference was statistically significant in the 24th month of age ($p=0.014$). The comparisons of the demographic characteristics among the groups are presented in Table 1.

In Group 1, 10.5% of the children (n=11) in the 15th month exhibited total SCASI values, indicating a potential risk. The rates of children identified as being at risk in the SCASI subgroup assessments were 10.9% for pre-verbal skills (F1a), 32.5% for word usage (F1b), and 16.4% for awareness-containing skills (F2) (Table 2). In Group 1, among the risky children who were assisted with developing a tailored educational support program at 15 months, two were found to be at risk at 24 months. One of these children showed improvement without receiving any other special treatment during the follow-up, while the other was diagnosed with autism and continued to be followed up by child psychiatry. Of the eight children who were found to be at risk at 24 months, two were also found to be at risk at 15 months, while six had a normal SCASI (Table 2).

In Group 2, 15% of the children (n=9) in the 15th month exhibited total SCASI values, indicating a potential risk. The rates of children identified as being at risk in the SCASI subgroup assessments were 17.5% for pre-verbal skills (F1a), 42.5% for word usage (F1b), and 37.5% for awareness-containing skills (F2) (Table 2). In Group 2, among

Table 1: Comparisons of the demographic characteristics among groups

	Group 1	Group 2	p
Maternal age (year); mean (SD)	32.7 (±5.1)	32.8 (±4.7)	0.896*
Paternal age (year); mean (SD)	38.5 (±5.6)	35.5 (±5.5)	0.808*
Maternal education; n (%)			
0 years	1 (0.8)	0 (0)	0.005**
5 years	25 (20.3)	12 (15.4)	
11 years	46 (37.4)	15 (19.2)	
14 years	51 (41.5)	51 (65.4)	
Paternal education; n (%)			
0 years	0 (0)	0 (0)	0.064***
5 years	25 (20.3)	17 (21.8)	
11 years	42 (34.1)	15 (19.2)	
14 years	56 (45.5)	46 (59)	
Gender (Girl); n (%)	52 (42.3)	45 (57)	0.041***
Gestational week; mean (SD)	38.5 (±1.4)	38.3 (±1.2)	0.443*
Birth weight (g); mean (SD)	3276.1 (±447.7)	3264.8 (±444.8)	0.897*
Birth height (cm); mean (SD)	49 (±4.7)	49.3 (±2.2)	0.877*
Birth head circumference (cm); mean (SD)	34.6 (±1.5)	34.5 (±1.3)	0.858*
Head control (months); Median (range)	2 (1-5)	2 (1-4)	0.930*
Sitting without support (months); median (range)	7 (2-9)	7 (5-12)	0.866*
Independent walking (months); Median (range)	12 (9-24)	13 (8-19)	0.379*
15. month screen exposure; n (%)			0.110**
None	31 (43.7)	13 (37.1)	
1 hour	38 (53.5)	17 (48.6)	
≥2 hours	2 (2.8)	5 (14.3)	
24. month screen exposure; n (%)			0.014**
None	35 (47.3)	5 (36.6)	
1 hour	36 (48.6)	17 (41.5)	
≥2 hours	6 (4.1)	9 (22.0)	

SD: Standard Deviation, *: Mann-Whitney U Test, **: Fischer Freeman-Halton Test, ***: Chi-square

Table 2: Risk assessment of children at 15th and 24th months

SCASI		Group 1		p*	Group 2		p*
		15 th month			24 th month		
		n (%)	n (%)		n (%)	n (%)	
F1a	Normal	49 (89.1)	33 (82.5)	0.392	60 (93.7)	48 (85.7)	0.143
	Risky	6 (10.9)	7 (17.5)		4 (6.3)	8 (14.3)	
F1b	Normal	37 (67.5)	23 (57.5)	0.330	54 (84.4)	43 (76.8)	0.292
	Risky	18 (32.5)	17 (42.5)		10 (15.6)	13 (23.2)	
F2	Normal	46 (83.6)	25 (62.5)	0.019	60 (93.7)	48 (85.7)	0.143
	Risky	9 (16.4)	15 (37.5)		4 (6.3)	8 (14.3)	
Total	Normal	94 (89.5)	51 (85.0)	0.392	91 (91.9)	54 (76.1)	0.004
	Risky	11 (10.5)	9 (15.0)		8 (8.1)	17 (23.9)	

SCASI: Social Communication Area Screening Test for Infants

F1a=preverbal skills, F1b=vocabulary skills, F2 = awareness skills, *: Pearson Chi-Square test

the risky children who were assisted with developing a tailored educational support program at 15 months, one child was found to be at risk at 24 months. Except for this at-risk child, the 15-month SCASI scores of the children identified as at-risk at 24 months were normal. No child diagnosed with developmental delay or autism spectrum disorder was found in the follow-up of children with at-risk SCASI scores at 24 months in Group 2.

In the SCASI assessments, the rate of children with risky results was higher in Group 2, both at 15 and 24 months. In the subgroup analyses of the 15th month, the rate of children found at risk was higher in Group 2 for all subgroups: pre-verbal skills (F1a), word usage (F1b), and awareness-containing skills (F2). However, this difference was statistically significant only in awareness-containing skills ($p=0.004$). In the 24th month results, the rate of children with a total SCASI score at risk was statistically significantly higher in Group 2 ($p=0.004$). In the subgroup analyses of the 24th month, the rate of children found at risk was also higher in Group 2 for all subgroups, but no significant difference was found.

DISCUSSION

Our study, which aimed to evaluate the social communication skills of children aged 1–2 years during the COVID-19 pandemic, revealed that children who turned 1–2 years old during the pandemic exhibited a higher risk in social communication skills, particularly at 24 months, as assessed by the SCASI. Additionally, screen time exposure was also notably higher in Group 2, especially at 24 months, suggesting that the pandemic's impact on daily routines has influenced early childhood development in significant ways.

The development of social communication is linked to social engagement. Low levels of social engagement among infants and their caregivers have been associated with developmental delays (18). A qualitative study from the COVID-19 pandemic period reported that social isolation restrictions resulted in 25% of infants not having the chance to meet a child of the same age by their first birthday, leading to a reduction in social peer interaction (19). Because of the isolation measures, it is probable that babies in the COVID-19 era heard a more limited repertoire of speech and were exposed to fewer unmasked faces speaking to them (20). A study examining infant neurodevelopment during the COVID-19 pandemic highlighted that a higher risk of delayed communication development in one-year-old children may be related to experiencing the COVID-19 pandemic and public health strategies for contact isolation during that period (21). In our study, the increased risk of social communication skills in Group 2 aligned with concerns about the pandemic's potential negative effects on child development (22).

As infants spend most of the quarantine in a familiar home environment, it is suggested that they are less likely to encounter new interests that may lead to pointing, for example, parents being in close proximity and anticipating infants' needs before the need to point (20). Byrne et al. also found a reduction in babies' skill in waving bye-bye during the COVID-19 pandemic, which was likely related to reduced opportunities for babies to learn due to limited social contact (20). In our study, the risk status in preverbal skills (F1a), such as pointing, peek-a-boo games, or hand waving, was also higher in Group 2. Early childhood is a critical period for the development of social communication skills, and disruptions in routine social activities and limited peer interactions may have hindered the natural progression of these skills during the pandemic (7, 23).

Increased screen exposure can disrupt natural language development and social engagement in children by limiting face-to-face interaction with caregivers and peers (24, 25). Excessive screen time has also been linked to disrupted sleep patterns, stress, and reduced physical activity, all of which can contribute to developmental challenges in young children (5). Limited screen both for foreground and background exposure for children is recommended, emphasising interactive, non-screen-based activities for healthy development (26). Chonchaiya and Pruksananonda reported that toddlers who started watching TV at <1 year of age and watched >2 h/day were about six times more likely to have speech and language delays (27). In our study, at 24 months, the screen exposure was significantly higher in the group during the pandemic period, which was consistent with the literature (28, 29). The higher screen time in Group 2 could be attributed to parents using digital media as a coping mechanism during lockdowns, potentially impacting children's social communication development.

While higher parental education is generally associated with better developmental outcomes, the higher educational level of the mothers in Group 2 did not mitigate the observed developmental delays (14). The relationship between higher education and higher job opportunities is well known. It can be thought that the mothers in Group 2 are unemployed, have lost their jobs during the pandemic, and this can be a source of stress, which may lead to a decrease in the care of their children. Studies that will evaluate this area on a broader scale can be planned. Despite the mother's higher education, our findings suggest that the extraordinary circumstances of the pandemic may overshadow the impact of protective factors such as parental education (4). The importance of environmental enrichment in early childhood underscores the critical need for social and educational interventions that provide children with structured, interactive learning environments to support children's development (4).

Early identification of delays is crucial to ensure timely interventions, which have been shown to be more effective when applied in early childhood (2). The use of the SCASI tool allowed for the effective identification of children at developmental risk, emphasising the importance of early screening and intervention.

Limitations include the retrospective design and reliance on medical records, which may lack comprehensive data on all potential confounders, including socioeconomic status beyond parental education, parental mental health, and detailed home environment. In addition, the smaller sample size of Group 2 due to the pandemic may affect the generalizability of the results.

CONCLUSION

In conclusion, the COVID-19 pandemic might have an impact on the social communication skills of children aged 1–2 years. The higher rates of delayed communication skills and increased screen exposure in children who reached this age during the pandemic indicate the need for targeted interventions to support early childhood development. It is important to monitor the development of communication skills as a part of paediatric health monitoring and to closely follow up with early interventions.

Ethics Committee Approval: Ethics committee approval was received for this study from the İstanbul University İstanbul Faculty of Medicine Clinical Research Ethics Committee (Date: 06.09.2024, No: 17).

Informed Consent: Due to the retrospective design of the study, informed consent was not taken.

Peer Review: Externally peer-reviewed.

Author Contributions: Conception/Design of Study- Ö.Ö.A., G.K., F.G.; Data Acquisition- Ö.Ö.A., M.M., Ü.Ç., S.A., P.Y.; Data Analysis/Interpretation – Ö.Ö.A., G.K.; Drafting Manuscript- Ö.Ö.A., G.K., M.M., Ü.Ç., S.A., P.Y., G.G.; Critical Revision of Manuscript- Ö.Ö.A., G.K., G.G.; Final Approval and Accountability- Ö.Ö.A., G.K., M.M., Ü.Ç., S.A., P.Y., G.G.; Technical or Material Support- M.M.; Supervision- G.K., G.G.

Conflict of Interest: The authors have no conflict of interest to declare.

Financial Disclosure: The authors declared that this study received no financial support.

REFERENCES

1. Kılıçarslan Törüner E, Büyükgönenç L. Çocuk sağlığı temel hemşirelik yaklaşımları. Ankara: İrem Matbaacılık 2011:1-20.
2. Özmert E. Gelişimin İzlenmesi ve Değerlendirilmesi. In: Gülbin Gökçay UB, editor. İlk Beş Yaşta Çocuk Sağlığı İzlemi. 2nd ed. İstanbul: Nobel Tıp Kitabevleri 2021. p. 53-9.
3. Bundy DA, de Silva N, Horton S, Patton GC, Schultz L, Jamison DT. Child and adolescent health and development: Realizing neglected potential. In: Bundy DA, de Silva N, Horton S, Jamison DT, Patton GC. Child and adolescent health and development. Washington: World Bank; 2017. p.1-25 [CrossRef]
4. Ferguson KT, Cassells RC, MacAllister JW, Evans GW. The physical environment and child development: An international review. *Int J Psychology* 2013;48(4):437-68. [CrossRef]
5. Davico C, Ghiggia A, Marcotulli D, Ricci F, Amianto F, Vitiello B. Psychological impact of the COVID-19 pandemic on adults and their children in Italy. *Front Psychiatry* 2021;12:572997. [CrossRef]
6. Jiao WY, Wang LN, Liu J, Fang SF, Jiao FY, Pettoello-Mantovani M, et al. Behavioral and emotional disorders in children during the COVID-19 epidemic. *J Pediatr* 2020;221:264-6. e1. [CrossRef]
7. Araújo LAd, Veloso CF, Souza MdC, Azevedo JMCd, Taro G. The potential impact of the COVID-19 pandemic on child growth and development: a systematic review. *J Pediatr* 2021;97:369-77. [CrossRef]
8. Birleşmiş Milletler Çocuklara Yardım Fonu, Türkiye. Politika Notu: COVID-19 Salgınının Çocuklar Üzerindeki Etkileri 15 Nisan 2020. [https://www.unicef.org/turkiye/documents/covid-19-salg%C4%B1n%C4%B1n-%C4%B1n-%C3%A7ocuklar-%C3%BCzerindeki-etkileri](https://www.unicef.org/turkiye/documents/covid-19-salg%C4%B1n%C4%B1n%C4%B1n-%C3%A7ocuklar-%C3%BCzerindeki-etkileri)
9. Zemrani B, Gehri M, Masserey E, Knob C, Pellaton R. A hidden side of the COVID-19 pandemic in children: the double burden of undernutrition and overnutrition. *Int J Equity Health* 2021;20:1-4. [CrossRef]
10. Raman S, Harries M, Nathawad R, Kyeremateng R, Seth R, Lonne B. Where do we go from here? A child rights-based response to COVID-19. *BMJ Paediatrics Open* 2020;4(1):e000714. [CrossRef]
11. Konukbay D, Suluhan D. COVID-19 pandemisinde çocuk gelişimini ve bakımı etkileyen süreçler. COVID-19 pandemisi sürecinin çocukların bakımı ve çevresine etkileri 2022;1:8-14.
12. Yogman M, Garner A, Hutchinson J, Hirsh-Pasek K, Golinkoff RM, Baum R, et al. The power of play: A pediatric role in enhancing development in young children. *Pediatrics* 2018;142(3):e20182058. [CrossRef]
13. Borelli JL, Smiley PA, Rasmussen HF, Gómez A. Is it about me, you, or us? Stress reactivity correlates of discrepancies in we-talk among parents and preadolescent children. *J Youth Adolesc* 2016;45:1996-2010. [CrossRef]
14. Ertem IO. The international guide for monitoring child development: enabling individualised interventions. *Early Childhood Matters* 2017;126:83-7.
15. T.C. Sağlık Bakanlığı, Halk Sağlığı Genel Müdürlüğü Çocuk ve Ergen Sağlığı Dairesi Başkanlığı. *Bebek, Çocuk, Ergen İzlem Protokolleri*. Ankara: 2018 https://ekutuphane.saglik.gov.tr/Ekutuphane/kitaplar/Bebek_Cocuk_Ergen_Izlem_Protokolleri_2018.pdf.
16. Kara B, Mukaddes NM, Altınkaya I, Güntepe D, Gökçay G, Özmen M. Using the Modified Checklist for Autism in Toddlers in a well-child clinic in Turkey: Adapting the screening method based on culture and setting. *Autism* 2014;18(3):331-8. [CrossRef]
17. Sertgil NK, Özen DŞ, Gökçay G. Bebeklik ve erken çocukluk döneminde gelişimsel risk tespiti için Sosyal İletişim Alan Tarama Testi (SIATT). *Çocuk Sağlığı ve Hastalıkları Dergisi* 2015;58:87-95.

18. McDonald S, Kehler H, Bayrampour H, Fraser-Lee N, Tough S. Risk and protective factors in early child development: Results from the All Our Babies (AOB) pregnancy cohort. *Res Dev Disabil* 2016;58:20-30. [\[CrossRef\]](#)
19. Sledge H, Lawler M, Hourihane J, Franklin R, Boland F, Dunne S, et al. Parenting a newborn baby during the COVID-19 pandemic: a qualitative survey. *BMJ Paediatrics Open* 2022;6(1):e001348. [\[CrossRef\]](#)
20. Byrne S, Sledge H, Franklin R, Boland F, Murray DM, Hourihane J. Social communication skill attainment in babies born during the COVID-19 pandemic: a birth cohort study. *Arch Dis Child* 2023;108(1):20-4. [\[CrossRef\]](#)
21. Huang P, Zhou F, Guo Y, Yuan S, Lin S, Lu J, et al. Association between the COVID-19 pandemic and infant neurodevelopment: a comparison before and during COVID-19. *Front Pediatr* 2021;9:662165. [\[CrossRef\]](#)
22. Darmiyanti A, Supriadi O, Nurlaeli A. The impact of the Covid-19 pandemic on language and social development for early childhood children age 4-6 years in Karawang District. *IJECES* 2021;10(1):27-32.
23. Yoshikawa H, Wuermlı AJ, Britto PR, Dreyer B, Leckman JF, Lye SJ, et al. Effects of the global coronavirus disease-2019 pandemic on early childhood development: short-and long-term risks and mitigating program and policy actions. *J Pediatr* 2020;223:188-93. [\[CrossRef\]](#)
24. Alroqi H, Serratrice L, Cameron-Faulkner T. The association between screen media quantity, content, and context and language development. *J Child Lang* 2023;50(5):1155-83. [\[CrossRef\]](#)
25. Keskindemirci G, Gökçay G. Screen exposure in children with language delay; results of pilot study. *J Ist Faculty Med* 2020; 83(1):30-4.
26. Guram S, Heinz P. Media use in children: American Academy of Pediatrics recommendations 2016. *Arch Dis Child Educ Pract* 2018;103(2):99-101. [\[CrossRef\]](#)
27. Chonchaiya W, Pruksananonda C. Television viewing associates with delayed language development. *Acta Paediatrica* 2008;97(7):977-82. [\[CrossRef\]](#)
28. Choi EJ, King GK, Duerden EG. Screen time in children and youth during the pandemic: a systematic review and meta-analysis. *Global Pediatrics* 2023;6:100080. [\[CrossRef\]](#)
29. Madigan S, Eirich R, Pador P, McArthur BA, Neville RD. Assessment of changes in child and adolescent screen time during the COVID-19 pandemic: a systematic review and meta-analysis. *JAMA Pediatr* 2022;176(12):1188-98. [\[CrossRef\]](#)

A COMPREHENSIVE MORPHOLOGICAL AND MORPHOMETRIC STUDY OF THE SPINOGLENOID NOTCH AND LIGAMENT/MEMBRANE: POSSIBLE CLINICAL RELEVANCE OF SUPRASCAPULAR NERVE ENTRAPMENT

SPİNOGLENOİD ÇENTİK VE LİGAMENT/MEMBRAN ÜZERİNE KAPSAMLI MORFOLOJİK VE MORFOMETRİK BİR ÇALIŞMA: SUPRASKAPULAR SINİR BASISI AÇISINDAN OLASI KLİNİK ÖNEMİ

Osman COŞKUN¹ , İlke Ali GÜRSES^{1,2} , Özcan GAYRETLİ¹ , Ayşin KALE¹ , Adnan KINA³ , Ahmet USTA^{1,4} , Kayıhan ŞAHİNOĞLU^{1,5} , Adnan ÖZTÜRK^{1,6} 

¹Istanbul University, İstanbul Faculty of Medicine, Department of Anatomy, İstanbul, Türkiye

²Koç University, Faculty of Medicine, Department of Anatomy, İstanbul, Türkiye

³Health Science University, İstanbul Haseki Training and Research Hospital, Department of Radiology, İstanbul, Türkiye

⁴Bahçeşehir University, Faculty of Medicine, Department of Anatomy, Batumi, Georgia

⁵Private Clinic, İstanbul, Türkiye

⁶Istanbul Health and Technology University, Faculty of Medicine, Department of Anatomy, İstanbul, Türkiye

ORCID IDs of the authors: O.C. 0000-0002-0337-4927; İ.A.G. 0000-0001-9188-4662; Ö.G. 0000-0001-7958-3170; A.K. 0000-0002-2305-420X; A.K. 0000-0002-8836-8410; A.U. 0000-0002-2217-0348; K.Ş. 0009-0001-7978-819X; A.Ö. 0000-0002-5819-0543

Cite this article as: Coşkun O, Gürses İA, Gayretli Ö, Kale A, Kına A, Usta A, et al. A comprehensive morphological and morphometric study of the spinoglenoid notch and ligament/membrane: Possible clinical relevance of suprascapular nerve entrapment. J Ist Faculty Med 2025;88(2):135-145. doi: 10.26650/IUITFD.1592664

ABSTRACT

Objective: This study aimed to determine the anatomical features and clinical significance of the spinoglenoid notch and spinoglenoid ligament-membrane as well as the branches of the suprascapular nerve to the infraspinatus muscle as these structures may cause compression of this nerve.

Material and Methods: Fifty sides (25 right and 25 left) were studied on 26 fixed cadavers belonging to the Department of Anatomy, İstanbul University, İstanbul Faculty of Medicine. The suprascapular nerve branches to the infraspinatus muscle and spinoglenoid ligament-membrane were examined in cadavers, and the spinoglenoid notch was investigated in 50 dry scapulae.

Result: The suprascapular nerve had two branches to the infraspinatus muscle in 22 cadavers on 37 sides (74%) and three branches to this muscle in 11 cadavers on 13 sides (26%). On 31 sides the spinoglenoid membrane and on 19 sides the spino-

ÖZET

Amaç: Bu çalışmada, spinoglenoid çentik ve spinoglenoid ligament-membran ile supraskapular sinirin infraspinatus kasına giden dallarının anatomik özellikleri ve klinik öneminin belirlenmesi amaçlanmıştır, çünkü bu yapılar bu sinirin sıkışmasına neden olabilir.

Gereç ve Yöntem: İstanbul Üniversitesi İstanbul Tıp Fakültesi Anatomi Anabilim Dalı'na ait 26 fikse kadavra üzerinde elli taraf (25 sağ ve 25 sol) çalışıldı. Kadavralarda infraspinatus kasına giden supraskapular sinir dalları ve spinoglenoid ligament-membran incelendi ve 50 kuru skapulada spinoglenoid çentik araştırıldı.

Bulgular: Supraskapular sinir, 37 taraftaki 22 kadavrada (%74) infraspinatus kasına iki dal, 13 taraftaki 11 kadavrada (%26) ise bu kasa üç dal verdi. 31 tarafta spinoglenoid membran ve 19 tarafta spinoglenoid ligament gözlemlendi. Spinoglenoid çentik ile ilgili

*This study has been derived from medical speciality thesis which was presented at 15th National Anatomy Congress, Samsun, Türkiye, 5-8 September 2013. (This thesis available at Ulusal Tez Merkezi, Number: 455749)

Corresponding author/İletişim kurulacak yazar: Osman COŞKUN – osmanco@istanbul.edu.tr

Submitted/Başvuru: 28.11.2024 • **Revision Requested/Revizyon Talebi:** 19.01.2025 •

Last Revision Received/Son Revizyon: 24.01.2025 • **Accepted/Kabul:** 29.01.2025 • **Published Online/Online Yayın:** 17.04.2025



Content of this journal is licensed under a Creative Commons Attribution-NonCommercial 4.0 International License.

glenoid ligament were observed. Related to the spinoglenoid notch, the mean width was 17.17 ± 2.17 mm, and the mean depth was 17.45 ± 2.03 mm in calliper measurements on dry bones, while the mean width was 16.99 ± 1.88 mm, the mean depth was 17.73 ± 2 mm and the mean area was 282.04 ± 55.27 mm² in computed tomography measurements.

Conclusion: The presented data regarding the spinoglenoid notch in which the suprascapular nerve is frequently compressed and the branches of the suprascapular nerve to the infraspinatus muscle may guide the surgical treatment of the related entrapment syndrome.

Keywords: Spinoglenoid notch, spinoglenoidal ligament, spinoglenoidal membrane, suprascapular nerve, infraspinatus muscle

olarak kuru kemik üzerinde yapılan dijital kaliper ölçümlerinde ortalama genişlik $17,17 \pm 2,17$ mm, ortalama derinlik $17,45 \pm 2,03$ mm iken, bilgisayarlı tomografi ölçümlerinde ortalama genişlik $16,99 \pm 1,88$ mm, ortalama derinlik $17,73 \pm 2$ mm ve ortalama alan $282,04 \pm 55,27$ mm² olarak bulundu.

Sonuç: Supraskapular sinirin sıklıkla sıkıştığı spinoglenoid çentik ve supraskapular sinirin infraspinatus kasına giden dalları ile ilgili sunulan veriler, ilgili tuzak sendromunun cerrahi tedavisine rehberlik edebilir.

Anahtar Kelimeler: Spinoglenoid çentik, spinoglenoid ligament, spinoglenoid membrane, supraskapular sinir, infraspinatus kası

INTRODUCTION

Due to the complex structure of the shoulder region, anatomical and clinical research is important for a better understanding of the pathologies in this region (1). The suprascapular nerve (SN) is a complex nerve that originates lateral to the superior trunk of the brachial plexus and provides motor and, in some conditions, sensory innervation (2). This nerve passes deep to the omohyoideus and trapezius muscles and extends from the posterior triangle of the neck to the suprascapular notch (SsN). It passes under the superior transverse scapular ligament (STSL) to the suprascapular fossa, and from there, it reaches the infraspinous fossa through the spinoglenoid notch (SGN) located on the outer side of the scapular spine (3-6). During this course, the SN and the accompanying vessels are at risk of compression (7-12). The motor component of the SN innervates the suprascapular and infraspinatus muscles and the articular rami, from which branches reach the shoulder and acromioclavicular joint (4). The suprascapular nerve may rarely have a sensory branch (4). When present, it pierces the deltoid muscle and receives the sensation of the proximal third of the arm. The most common lesion of the suprascapular nerve is neuralgic amyotrophy (4).

Entrapment neuropathy may occur in the scapular notch or because of injury to the SN by trauma to the scapula or shoulder region. Injury to the SN can cause shoulder pain, weakness in the abduction and external rotation, and atrophy of the suprascapular and infraspinatus muscles. Compression of the SN is a common condition that usually requires surgical intervention, and the treatment of this condition varies according to the site of nerve compression. Injuries of the SN may cause shoulder pain, weakness in the abduction and external rotation of the upper extremity, and atrophy of the suprascapular and infraspinatus muscles (9, 10). There are several possible causes, but nerve compression is the most common one, and it can be surgically treated. Shah et al. reported that 71% of their patients reported pain relief after decompression surgery with a follow-up of 22.5 months

in a series of 24 patients with impingement syndrome of SN (11). Other causes include trauma, traction injuries, scapula fractures, ganglion cysts, repetitive overuse, and compressive mass (9, 11-14). The SN is also at risk of iatrogenic damage during shoulder surgery, mainly in case of an anterosuperior or posterior approach, repair of massive rotator cuff tears, and arthroscopic procedures for anterior glenohumeral instability repair (9, 15-17).

The prevalence of the entrapment of the SN is unknown. However, the importance of its entrapment and dysfunction as a pain generator has been approved (11). Entrapment of the SN can occur in two locations: in the SsN (superior compression of the SN) and in the SGN (inferior compression of the SN) (9, 18, 19). Infraspinatus denervation with the preservation of the suprascapular muscle is considered inferior compression around the SGN (20). The surgical treatment regimen for the entrapment of the SN at the SsN differs from the approach for the entrapment of the same nerve at the SGN. Therefore, the underlying pathological condition and location of the nerve entrapment should be well understood preoperatively (21). An original arthroscopic portal has also been described to reveal both sites where the SN is most commonly compressed (9). While the SN entrapment syndrome was first described by Kopell and Thompson in 1959, Ganzhorn et al. described the entrapment syndrome of the SN in the SGN to be causing shoulder pain, weakness in external rotation, and isolated infraspinatus atrophy in 1981 (22-25). A hypertrophic SGN is also among the possible causes in addition to trauma, ganglion cysts, paralabral paralabral cysts, and varicose veins in the SGN (3, 5, 10, 18). Moreover, in the scapular region, as the infraspinatus muscle is the most frequently involved area in myofascial pain syndrome, the branches of the SN innervating this muscle are being explored in order to apply an accurate injection site (26). The spinoglenoid ligament (SGL) is a bilaminar structure that starts from the scapular spine and attaches to the scapular neck. It is affected by the shoulder position and is exposed to maximum pressure when the arm is in full adduction and internal rotation

(27, 28). Bektaş et al. found a prominent ligament structure (SGL) in 16% of cadaveric shoulders and named this structure the spinoglenoid membrane (SGM) in the other cases (29). Won et al. classified this structure as ligament, membrane, or both (30). While the suprascapular artery, vein, and nerve (SN) pass under the SGL/SGM, Aktekin et al. reported that this structure forms a fibroosseous foramen consisting of the scapular spine and the SGL/SGM, where the suprascapular artery occupies 68.5% and the nerve 31.5% (31).

This study investigated the anatomical features of the suprascapular nerve in the SGN region and to complete the limited information in the literature. In line with this aim, morphological and morphometric variations of the SGL/SGM structure significantly affect the suprascapular nerve compression.

MATERIAL AND METHODS

In our study, 50 sides (25 right and 25 left sides) were dissected in 5 female and 21 male cadavers aged between 49 and 88 years, fixed with a mixture of formaldehyde-phenol-ethyl alcohol-glycerine-water, which were used in medical education in the Department of Anatomy, İstanbul Faculty of Medicine.

The skin and subcutaneous tissue of all cadavers were formerly dissected as they had been used in student practices already. The trapezius muscle was separated from the clavicle, acromion, and spine of the scapula. Afterwards, the trapezius and deltoid (spinal part) muscles were removed, exposing the supraspinatus and infraspinatus muscles. The supraspinatus muscle was released from the supraspinous fossa medially, revealing the superior border of the scapulae. We examined the presence of a motor branch to the infraspinatus muscle either directly or by piercing the spinoglenoid ligament. Combining the classifications of Bektaş et al. (SGL, spinoglenoid septum) and Won et al. [SGL, spinoglenoid membrane (SGM), combination of SGL and SGM]), we identified a SGL or spinoglenoid membrane (SGM) (29, 30). A digital calliper (INSIZE Co., Ltd., Taiwan) was used in all measurements, and a digital camera was used for the visualisation of the specific cases.

The presence of either SGL or SGM was first examined macroscopically in SGN. To evaluate the microscopic difference in the macroscopic ligament or membrane, one sample from each macroscopically differentiated type was aimed to be histologically assessed. The specimens were fixed in a 10% phosphate-buffered formaldehyde solution and then dehydrated in ascending grades of ethanol (70%, 90%, 96%, and 100%, respectively) for 24 h before performing the light microscopic examination. They were then kept in 100% ethanol twice for 30 min and clarified in toluol (Merck 1.08323.2500) for 1 h. Subsequently, they

were placed in liquid paraffin (Merck 1.07337.1000) in an oven (Heraeus) at 56°C for 1 h two times and embedded in paraffin blocks. 4 µm thick sections were taken from these blocks with a microtome (LEICA, RM 2255). Masson Trichrome Stain was applied to the sections. Paraffin sections were removed from the paraffin by soaking in toluol for 30 min and then rehydrated by passing through a series of decreasing alcohols (100%, 96%, 90%, and 70%, respectively) in distilled water. Sections were stained in haematoxylin for 4 min and allowed to bruise in tap water for 10 min. They were stained with Ponceau xyloidine-acid fuchsin solution for 5 min and were quickly passed through 1% acetic acid. The sections were stained with Orange G for 10 min, promptly passed through 1% acetic acid, stained with light green for 7 min, and again quickly passed through 1% acetic acid. The sections were then passed through 100% ethanol three times, made transparent with toluol, covered with Canadian balsam, and evaluated under a light microscope to determine the changes in the connective tissue elements.

Fifty (25 right and 25 left) dry scapulae were used for morphometric evaluation of the SGN, where the SN is most frequently compressed. We used two methods (manual measurement with a digital calliper and computed tomography).

For manual measurement with a digital calliper, we determined the anterior and posterior points of the glenoid cavity and the projection of the posterior point on the acromion with the help of a fixed metal needle in a designed plane passing through the spine of the scapula. The distance between the most posterior point of the glenoid cavity and its projection on the acromion was considered the width of the SGN. The shortest distance extending from this width line to the deepest point of the SGN at a perpendicular angle was considered the depth of the SGN. In order to understand the structure of SGN better, the width/depth ratio was calculated (Figure 1).

The computed tomography (CT) scans were performed at the Radiology Clinic using the 16-detector CT acquisition protocol (Somatom Emotion 16, Siemens, AG, Erlanger, Germany). The acquisition parameters were 16x0.75 mm detector collimation, 0.5 s gantry rotation time, and 5 mm slice thickness. The tube voltage was 130 kVp, and the current was 50 mAs. For evaluation, the 5-mm section thickness images were electronically transferred to a workstation (Leonardo, Siemens AG, Erlanger, Germany). At the workstation, reconstruction (MPR: Multiplanar Reconstruction) images were created from these images in axial, coronal, and sagittal planes with 0.75 mm thickness and 0.2 mm reconstruction interval. To evaluate the SGN, images were obtained in the plane passing through the spine of the scapula. In this plane, we determined the

most anterior and posterior edges of the glenoid cavity and the projection of the posterior edge on the acromion. The distance between the posterior border and its projection was considered the width of the SGN, and the perpendicular line drawn from this line to the deepest point of the SGN was regarded as the depth (Figure 1). In addition, we calculated the area under the width of the SGN to determine whether the neurovascular structures passing through the region would affect SN compression. All images were evaluated, and an expert radiologist performed the measurements.

The Clinical Research Ethical Committee of İstanbul Faculty of Medicine approved the study (Date: 08.10.2021, No: 18).

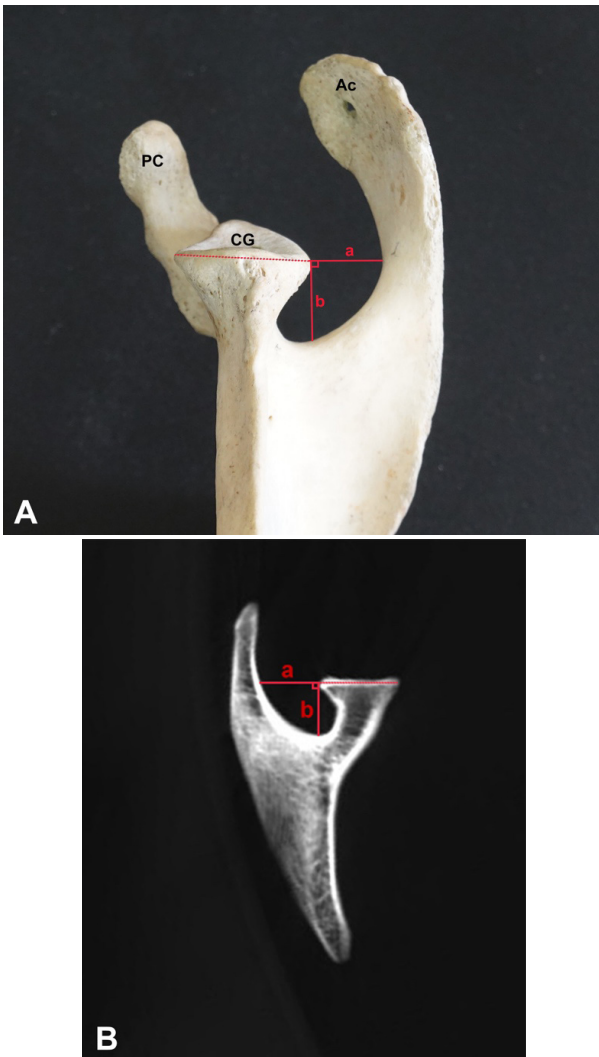


Figure 1: Morphometric measurements of the incisura spinoglenoidale. **A** Manual measurements, **B** Measurements on computed tomography
a: Width, b: Depth, Ac: Acromion, CG: Cavitas glenoidalis, PC: Processus coracoideus

RESULTS

Related to the branches of SN to the infraspinatus muscle, 22 cadavers on 37 sides (74%) had two motor branches and 11 cadavers with 13 sides (26%) had three motor branches (Figure 2). All measurements and evaluations performed on cadavers are shown in Table 1.

In SGN, SGL was macroscopically observed on 19 sides (38%) in 11 cadavers, and SGM was observed on 31 sides (62%) in 18 cadavers (Figure 3). Tight connective tissue arrangement, sparse fibroblasts in between, and the typical corrugated structure seen in the compact connective tissue structure were observed in the sections taken from the specimens macroscopically evaluated as ligaments.

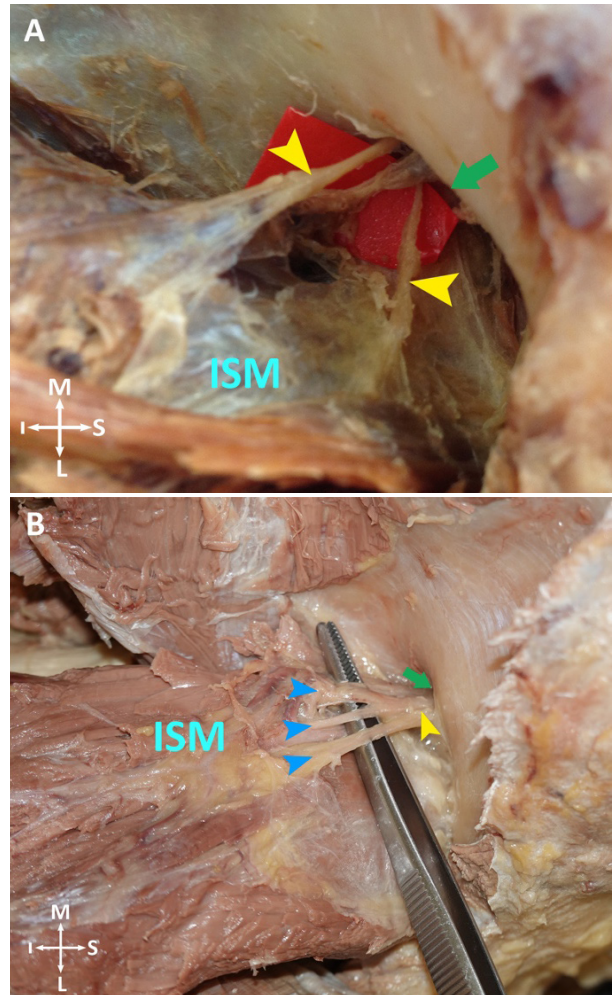


Figure 2: Motor branches to the infraspinatus muscle **A** 2 motor branches to the infraspinatus muscle **B** 3 motor branches to the infraspinatus muscle: infraspinatus muscle (ISM), medial (M), lateral (L), superior (S), inferior (I). Yellow arrows show the motor branches to the infraspinatus muscle. The green arrow shows the spinoglenoid notch. Blue arrows show the motor branches to the infraspinatus muscle

Table 1: Measurements on the cadavers

Cadaver No	Spinoglenoid lig./septum	Branches of SN to the infraspinatus muscle	Cadaver No	Spinoglenoid lig./septum	Branches of SN to the infraspinatus muscle
1-Left	S	3+S	14-Left	S	2
1-Right	S	3	14-Right	S	2
2-Left	L	3	15-Left	S	2
2-Right	L	3	15-Right	S	2
3-Left	S	2	16-Left	L	2
3-Right	S	3	16-Right	L	3
4-Left	S	2	17-Left	L	2
4-Right	S	2	17-Right	S	2
5-Left	L	2	18-Left	S	2
5-Right	L	3	18-Right	S	2
6-Left	S	2	19-Left	S	2
6-Right	L	2	19-Right	S	2
7-Left	S	3	20-Left	S	2
7-Right	S	2	20-Right	S	2
8-Left	S	2	21-Left	S	2
8-Right	S	3	21-Right	S	2
9-Left	L	2	22-Left	L	2
9-Right	L	2	22-Right	L	2
10-Left	L	2	23-Left	L	2
10-Right	L	2	23-Right	L	2
11-Left	L	2	24-Left	S	2
11-Right	L	2	24-Right	S	2
12-Left	S	3	25-Right	S	3
12-Right	L	2	26-Left	S	3
13-Left	S	3			
13-Right	S	2			

S: Spinoglenoid septum **L:** Spinoglenoid ligament

In the sections taken from the specimens macroscopically evaluated as membrane, connective tissue, muscle tissue, and dense fibroblast structures were observed (Figure 3).

The results of the osteometric measurements related to SGN were prepared as the value + standard deviation (minimum value, maximum values).

Related to the spinoglenoid notch; the mean width was 16.91 ± 2.04 mm (13.2, 21.2 mm), and the mean depth was 17.2 ± 2.04 mm (12.6, 20.7 mm) in the 25 right scapula, while the mean width was 17.43 ± 2.3 mm (13.5, 23.5 mm) and the mean depth was 17.71 ± 2.02 mm (14.1, 22.9 mm) in the 25 left scapula. The mean width was 17.17 ± 2.17

mm, and the mean depth was 17.45 ± 2.03 mm regardless of the side. The mean width/depth ratios were 0.98 ± 0.09 (0.79, 1.17) in 25 right scapula, 0.98 ± 0.1 (0.81, 1.32) in 25 left scapula, and 0.98 ± 0.1 total. We collected the data of the manual SGN measurements in a Table (Table 2).

Related to the spinoglenoid notch; the CT evaluation of the same bones (50 scapula) showed that the mean width was 17.26 ± 2.02 mm (14.4, 20.8 mm), the mean depth was 17.66 ± 1.63 mm (14.1, 20.9 mm) and the mean area was $278.04 + 46.05$ mm² (197, 378 mm²) for the right scapula, while the mean width was 16.73 ± 1.74 mm (13.5, 19.7 mm), the mean depth was 17.8 ± 2.35 mm (13.7, 21.4 mm) and the mean area was 286.04 ± 63.9 mm² (201, 375 mm²) for the left scapula. Regardless of the side, the

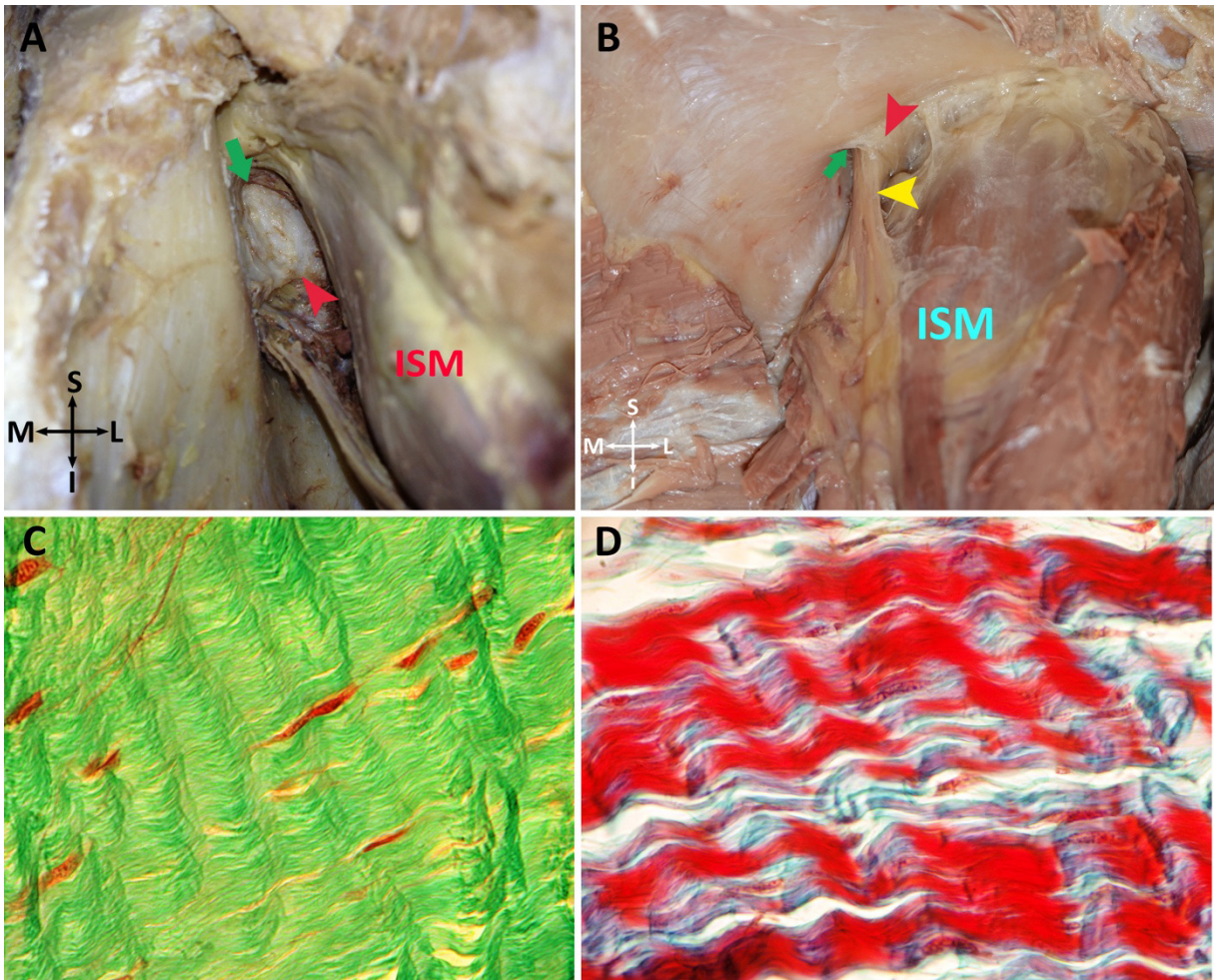


Figure 3: Spinoglenoid ligament and septum, and their histological evaluation **A** Ligament **B** Septum **C** Spinoglenoid ligament (tight connective tissue arrangement, sparse fibroblasts in between, and typical appearance of corrugated structure seen in the compact connective tissue structure) **D** Septum (appearance of connective tissue, muscle tissue, and dense fibroblast structures): infraspinatus muscle (ISM), medial (M), lateral (L), superior (S), inferior (I)

mean width was 16.99 ± 1.88 mm (13.5, 20.8 mm), the mean depth was 17.73 ± 2 mm (13.7, 21.4 mm), and the mean area was 282.04 ± 55.27 mm² (197, 378 mm²). The mean width/depth ratios were 0.98 ± 1.02 (0.10, 1.21) in 25 right scapula, 0.94 ± 0.87 (0.72, 1.16) in 25 left scapula, and 0.96 ± 0.09 totally. The data of the SGN-related measurements performed using CT are shown in a Table (Table 3).

DISCUSSION

The main findings of this study include the number and distribution of the motor branches of the suprascapular nerve to the infraspinatus muscle, macroscopic and microscopic examination of the spinoglenoid ligament (SGL) and spinoglenoid membrane (SGM), and determination of the spinoglenoid notch (SGN) dimensions by manual and CT measurements. These findings are thought to contribute significantly to shoulder surgery, nerve impingement syndromes, and anatomical education.

Morphological and morphometric evaluations

Our study found that the suprascapular nerve gave the infraspinatus muscle two or three motor branches. Two motor branches were observed in 74% (37/50 sides), and three motor branches were observed in 26% (13/50 sides) of the specimens. These findings are consistent with the finding of 70% (14/20) of two branches and 30% (6/20) of three branches reported by Lee et al. (26). However, Warner et al. reported a higher rate by detecting three or four motor branches in 48% (15/31) of the specimens examined (6). These differences may be due to the sample size, methodological differences, or possible anatomical variations. In addition, Warner et al. reported that the branches of the suprascapular nerve to the suprascapular muscle were fewer, shorter, and smaller (6). Our findings support the existing literature regarding the motor innervation of the infraspinatus muscle and provide important anatomical information regarding nerve preservation during surgical procedures (32-35).

Table 2: Data from manual SGN-related measurements

Spinoglenoid Notch							
Cadaver No	Right (mm)		Cadaver No	Left (mm)		Right	Left
	Width	Depth		Width	Depth	Width/Depth	Width/Depth
1	18.4	17.7	1	18.3	18.6	1.039548	0.983871
2	17.9	18.3	2	19.8	19.7	0.9781421	1.005076
3	13.6	12.6	3	14.3	14.1	1.0793651	1.014184
4	18	18.9	4	18.1	16.9	0.952381	1.071006
5	15	14.9	5	17.1	18.8	1.0067114	0.909574
6	15.2	18.4	6	16.3	16.8	0.826087	0.970238
7	14.9	17.9	7	15.8	19.4	0.8324022	0.814433
8	20.4	19.1	8	15.7	16.4	1.0680628	0.957317
9	13.2	14.4	9	14.4	17.3	0.9166667	0.83237
10	18.4	20.7	10	19.5	20.3	0.8888889	0.960591
11	16.3	15.7	11	17.3	17.2	1.0382166	1.005814
12	14.6	14.1	12	15.3	14.4	1.035461	1.0625
13	15	18.9	13	13.5	16.5	0.7936508	0.818182
14	18.6	16.7	14	16.1	15.8	1.1137725	1.018987
15	16.6	17.1	15	18.4	18.1	0.9707602	1.016575
16	19.1	18.3	16	17.6	20.3	1.0437158	0.866995
17	18.7	18.5	17	21	22.9	1.0108108	0.917031
18	18.3	20.2	18	23.5	17.8	0.9059406	1.320225
19	15.7	15	19	15	14.7	1.0466667	1.020408
20	16.4	17.8	20	17.9	17	0.9213483	1.052941
21	16.1	16.2	21	16.4	16.6	0.9938272	0.987952
22	21.2	19.4	22	20.1	18.8	1.0927835	1.069149
23	18.1	16.8	23	17	18.6	1.077381	0.913978
24	17.4	14.8	24	18.8	19.3	1.1756757	0.974093
25	15.7	17.6	25	18.7	16.5	0.8920455	1.133333

The spinoglenoid ligament (SGL) and spinoglenoid membrane (SGM) were analysed macroscopically and microscopically in our study and compared with the literature (33-35). SGL was detected on 19/50 sides (38%), while SGM was observed on 31/50 sides (62%). The presence of SGL has been reported at different rates in the literature. Although Plancher et al. and Aktekin et al. observed SGL in all their specimens (58 fresh frozen shoulders and 36 cadaver shoulders, respectively), Bektaş et al. found significant SGL in only 16% (5/32) (27-29,31). Demirhan et al. reported the presence of SGL in 60.8% (14/23 shoulders), Aiello et al. in 50% and Duparck et al. in 28/30 cadaver shoulders (18, 36, 37). Although the rates in our study contribute to the wide range of variations in the literature, it is noteworthy as one of the few studies that address the distinction between SGL

and SGM at the macroscopic and microscopic levels. We found prominent SGL in 11 cadavers on 19 sides (38%), while we observed SGM in 18 cadavers on 31 sides (62%). The differences in the data presented may be because the SGL-SGM distinction was not made in some studies, and all were accepted as SGL. Moreover, racial disparities and sample size may be responsible for the different results.

From the histological point of view, only Plancher et al. reported that they had histologically examined 8 out of their 58 fresh-frozen specimens (27, 28). They mentioned that the SGL was composed of bundles of collagen fibrils having similar orientations. They also observed that Sharpey fibre bundles of collagen fibres extending from the periosteum to the underlying bone were inserted into the scap-

Table 3: Data of measurements of the spinoglenoid notch performed by computed tomography

	Scapula (Right)	Depth (mm)	Width (mm)	Area (mm ²)	Scapula (Left)	Depth (mm)	Width (mm)	Area (mm ²)	Width/Depth (Right)	Width/Depth (Left)
1		17.6	18.4	272	1	16.2	15.8	245	1.04545455	0.975309
2		20.9	15.7	309	2	19.1	19.7	359	0.75119617	1.031414
3		18.2	22.2	378	3	18.6	18.9	332	1.21978022	1.016129
4		17.1	17.7	290	4	16.9	16.5	259	1.03508772	0.976331
5		16.2	14.4	208	5	14.2	13.5	204	0.88888889	0.950704
6		19.3	17.1	313	6	14.9	15.6	201	0.88601036	1.04698
7		16.1	16.7	226	7	21.4	19.7	400	1.03726708	0.920561
8		19.4	20.6	334	8	17.9	17.8	288	1.06185567	0.994413
9		19.1	18.1	323	9	17.8	17.9	308	0.94764398	1.005618
10		15.2	15.1	197	10	21.2	18.4	375	0.99342105	0.867925
11		18.3	15.1	240	11	18.5	17.7	277	0.82513661	0.956757
12		15.6	15.1	239	12	20.6	18.2	362	0.96794872	0.883495
13		15.7	15.7	233	13	19.7	17.4	317	1.0	0.883249
14		18.7	17.8	301	14	18.3	16	265	0.95187166	0.874317
15		20.1	19.5	334	15	14.3	14.5	202	0.97014925	1.013986
16		14.1	15.4	201	16	17.1	16.7	266	1.09219858	0.976608
17		18.8	17.6	293	17	14.8	13.7	202	0.93617021	0.925676
18		17.9	15.7	283	18	20.2	17.5	314	0.87709497	0.866337
19		18.2	20.8	312	19	22	16	361	1.14285714	0.727273
20		17	18.6	295	20	13.7	16	212	1.09411765	1.167883
21		19	18.5	321	21	16.3	15.9	242	0.97368421	0.97546
22		16.6	15.4	256	22	16.5	13.5	203	0.92771084	0.818182
23		17.9	15.7	265	23	18	16.3	252	0.87709497	0.905556
24		18	17.4	269	24	17.2	17.2	365	0.96666667	1.0
25		16.7	17.3	259	25	19.6	17.9	340	1.03592814	0.913265

ular spine. Plancher et al. did not define different types of SGL (28). In our study, SGL was classified into two types according to the macroscopic examination: SGL (observed on 19 sides (38%) in 11 cadavers) and SGM (on 31 sides (62%) in 18 cadavers). We examined one specimen from each of these two types. In a microscopic examination of the SGL, a tight connective tissue arrangement, sparse fibroblasts in between, and the typical corrugated structure seen in the compact connective tissue structure were observed, and in the sections taken from the SGM, connective tissue, muscle tissue, and dense fibroblast structures were observed. In the literature, we could only reach the study of Plancher et al. to examine the SGL histologically (28). Consequently, we believe that we have provided supplemental microscopic data for types of SGL.

In our study, the mean width of the SGN by the manual measurement method was found to be 17.17 ± 2.17 mm, the mean depth was 17.45 ± 2.03 mm, and the mean width/depth ratio was 0.98 ± 0.1 . From the results of the CT measurements, the mean width of the SGN was determined as 16.99 ± 1.88 mm (13.5, 20.8 mm), the mean depth as 17.73 ± 2 mm (13.7, 21.4 mm), the mean area as 282.04 ± 55.27 mm² (197, 378 mm²) and the mean width/depth ratio as 0.96 ± 0.09 . Yang et al., in their study of 478 patients (266 males, 212 females, 236 left-side and 242 right-side were examined) with thin-section CT, reported that the mean width (AP-the distance between the nadir of the SGN and of the SGN) was 14.63 ± 7.07 mm in males and 13.42 ± 1.89 mm in females while the mean depth on the left side was 13.89 ± 2.19 mm and 12.43 ± 2.03 mm on the right side (38). In their bony study, which was performed by digital callipers on 70 scapulae (58 non-articulated, 12 articulated), Kannapan et al. defined the acromioglennoid (anteroposterior) diameter to be between the supraglenoid tubercle and the highest concavity of the acromion and the lateral diameter (mediolateral) to be located between the posterior rim of the glenoid cavity and the centre of the lateral border of the spine of the scapula. They determined that the anteroposterior and mediolateral diameters of the spinoglenoid notch were found meanly as 3.01 ± 0.4 cm (ranging from 2 to 3.5 cm) and 1.4 ± 0.1 cm (ranging from 1.2 to 1.6 cm), respectively (39). The studies of Yang et al., Kannapan et al., and ours are the only studies we could reach to report both the width and depth of SGN, while there are other studies mentioning their results related to the width of SGN (38, 39). We believe that the difference in the results of these three studies may be due to different measurement methods, different points of measurement, and racial differences, including body size and type.

Defining the acromioglennoid diameter as the distance between the tip of the acromion process and the supraglenoid tubercle, Vinay et al. reported that the acromioglennoid diameter was found meanly as 29.79 ± 4.04 mm and

30.36 ± 4.1 mm, on the right and left sides, respectively, and Dhindsa et al. reported that this diameter was measured meanly as 30.03 ± 3.66 mm and 30.27 ± 4.61 mm on the right and left sides, respectively (40, 41). Mansur et al. defined the acromioglennoid diameter as the distance from the tip of the acromion process to the uppermost point of the glenoid cavity, and they determined that they measured the acromioglennoid diameter meanly as 31.83 ± 3.66 mm and 31.97 ± 3.96 mm, on the right and left sides, respectively (42). We have identified our width differently from other studies as the distance between the most posterior point of the glenoid cavity and its projection on the acromion. We believe that our defining points for the width and the depth may better identify the area where the SN may be impinged.

Bigliani et al., in their cadaver study including 90 (in some measurements, they used 15 cadavers more) cadavers, reported that the suprascapular nerve passed through the spinoglenoid notch approximately 18 mm from the posterior glenoid rim (range: 14–25 mm) (15). Moreover, Bigliani et al. described a safe zone of the posterior glenoid neck. According to them, the safe zone measured 2 cm at the level of the supraglenoid tubercle and decreased to 1 cm at the level of the scapular spine (15). Warner et al. dissected 31 shoulders in 18 cadavers and determined that the palpable posterolateral tip of the acromion to the base of the scapular spine was 4.5 centimeters ± 4 millimetres, adding that this distance might be an appropriate reference point for the location of SN. Warner et al. suggested a posterior incision along the scapular spine just medial to allow dissection in the medial safe zone (6). Because of the narrow passage, even small cysts (0.5–10 mm) may be responsible for causing entrapment (15, 21).

The findings of our study provide comprehensive data on the distribution of the motor branches of the suprascapular nerve, the structural features of the SGL and SGM, and the dimensions of the SGN. This information may contribute to optimising the surgical approach in nerve preservation and decompression procedures in shoulder surgery. It also provides an anatomical basis for understanding the pathophysiology of SN impingement syndromes.

CONCLUSION

This study provided comprehensive data on the anatomy of the suprascapular nerve, the distribution of its motor branches, the macroscopic and microscopic structure of the spinoglenoid ligament and membrane, and the dimensions of the spinoglenoid notch. The failure to detect the cutaneous branch may be because the cadavers were previously used in student practice. Future studies with less damaged cadavers may better reveal the anatomical features of this branch. Our study is an essential anatomical guide for shoulder surgery and nerve decompression operations. We believe our findings significantly contribute to the existing literature both clinically and academically.

Ethics Committee Approval: Ethics committee approval was received for this study from the İstanbul Faculty of Medicine (Date: 08.10.2021, No: 18).

Peer Review: Externally peer-reviewed.

Author Contributions: Conception/Design of Study- O.C., Ö.G., A.K.; Data Acquisition- O.C., İ.A.G., A.K.; Data Analysis/Interpretation – O.C., A.Ö., A.U., K.Ş.; Drafting Manuscript- O.C., Ö.G., İ.A.G., A.K.; Critical Revision of Manuscript- A.Ö., A.K., A.U., K.Ş.; Final Approval and Accountability- O.C., A.Ö., Ö.G., İ.A.G., A.K., A.U., K.Ş.; Technical or Material Support- O.C.; Supervision- A.Ö., A.K.

Acknowledgments: We are so grateful to Latif Sağlam for his valuable contributions. Also, we are eternally thankful to our cadavers for their sacrifice and to their precious families for their patience.

Conflict of Interest: The authors have no conflict of interest to declare.

Financial Disclosure: The authors declared that this study received no financial support.

REFERENCES

1. Chan CW, Peng PW. Suprascapular nerve block: a narrative review. *Reg Anesth Pain Med* 2011;36(4):358-73. [CrossRef]
2. Yang HJ, Gil YC, Jin JD, Ahn SV, Lee HY. Topographical anatomy of the suprascapular nerve and vessels at the suprascapular notch. *Clin Anat* 2012;25(3):359-65. [CrossRef]
3. Demirhan M, Imhoff AB, Debski RE, Patel PR, Fu FH, Woo SL. The spinoglenoid ligament and its relationship to the suprascapular nerve. *J Shoulder Elbow Surg* 1998;7(3):238-43. [CrossRef]
4. Standring S, editor. *Gray's Anatomy. The Anatomical Basis of Clinical Practice*. 41st ed. London: Elsevier; 2016.p.803-4.
5. Titelbaum AR, Ibarra Asencios B, McNeil BE. A circular depression at the spinoglenoid notch of a prehistoric Andean scapula: Plausible evidence of suprascapular nerve entrapment by a paralabral cyst. *Int J Paleopathol* 2019;24:19-24. [CrossRef]
6. Warner JP, Krushell RJ, Masquelet A, Gerber C. Anatomy and relationships of the suprascapular nerve: anatomical constraints to mobilization of the supraspinatus and infraspinatus muscles in the management of massive rotator-cuff tears. *J Bone Joint Surg Am* 1992;74(1):36-45. [CrossRef]
7. Callahan JD, Scully TB, Shapiro SA, Worth RM. Suprascapular nerve entrapment. A series of 27 cases. *J Neurosurg* 1991;74(6):893-6. [CrossRef]
8. Cummins CA, Messer TM, Nuber GW. Suprascapular nerve entrapment. *J Bone Joint Surg Am* 2000;82(3):415-24. [CrossRef]
9. Soubeyrand M, Bauer T, Billot N, Lortat-Jacob A, Gicquelet R, Hardy P. Original portals for arthroscopic decompression of the suprascapular nerve: an anatomic study. *J Shoulder Elbow Surg* 2008;17(4):616-23. [CrossRef]
10. Van Meir N, Fourneau I, Debeer P. Varicose veins at the spinoglenoid notch: an unusual cause of suprascapular nerve compression. *J Shoulder Elbow Surg* 2011;20(7):e21-4. [CrossRef]
11. Shah AA, Butler RB, Sung SY, Wells JH, Higgins LD, Warner JJ. Clinical outcomes of suprascapular nerve decompression. *J Shoulder Elbow Surg* 2011;20(6):975-82. [CrossRef]
12. Gosk J, Urban M, Rutowski R. Entrapment of the suprascapular nerve: anatomy, etiology, diagnosis, treatment. *Ortop Traumatol Rehabil* 2007;9(1):68-74.
13. Natsis K, Totlis T, Tsikaras P, Appell HJ, Skandalakis P, Koebeke J. Proposal for classification of the suprascapular notch: a study on 423 dried scapulas. *Clin Anat* 2007;20(2):135-9. [CrossRef]
14. Steinwachs MR, Haag M, Krug C, Erggelet C, Reichelt A. A ganglion of the spinoglenoid notch. *J Shoulder Elbow Surg* 1998;7(5):550-4. [CrossRef]
15. Bigliani LU, Dalsey RM, McCann PD, April EW. An anatomical study of the suprascapular nerve. *Arthroscopy* 1990;6(4):301-5. [CrossRef]
16. Ebraheim NA, Whitehead JL, Alla SR, Moral MZ, Castillo S, McCollough AL, et al. The suprascapular nerve and its articular branch to the acromioclavicular joint: an anatomic study. *J Shoulder Elbow Surg* 2011;20(2):e13-7. [CrossRef]
17. Vorster W, Lange CP, Briët RJ, Labuschagne BC, du Toit DF, Muller CJ, et al. The sensory branch distribution of the suprascapular nerve: an anatomic study. *J Shoulder Elbow Surg* 2008;17(3):500-2. [CrossRef]
18. Demirkan AF, Sargon MF, Erkula G, Kiter E. The spinoglenoid ligament: an anatomic study. *Clin Anat* 2003;16(6):511-3. [CrossRef]
19. Lichtenberg S, Habermeyer P. Nervenkompressionssyndrome der Schulter : Arthroskopische Dekompressionsverfahren [Nerve compression syndrome of the shoulder: Arthroscopic decompression procedures]. *Orthopade* 2011;40(1):70-8. [CrossRef]
20. Ferretti A, De Carli A, Fontana M. Injury of the suprascapular nerve at the spinoglenoid notch. The natural history of infraspinatus atrophy in volleyball players. *Am J Sports Med* 1998;26(6):759-63. [CrossRef]
21. Moore TP, Hunter RE. Suprascapular nerve entrapment. *Oper Tech Sports Med* 1996;4(1):8-14. [CrossRef]
22. Buyukdogan K, Altintas B, Koyuncu Ö, Eren İ, Birsel O, Fox M, et al. Ultrasound-Guided intralesional methylene blue injection for the arthroscopic decompression of spinoglenoid notch cyst causing suprascapular neuropathy. *Arthrosc Tech* 2020;9(11):e1785-9. [CrossRef]
23. Ganzhorn RW, Hocker JT, Horowitz M, Switzer HE. Suprascapular-nerve entrapment. *J Bone Joint Surg Am* 1981;63(3):492-4. [CrossRef]
24. Kopell HP, Thompson WA. Pain and the frozen shoulder. *Surg Gynecol Obstet* 1959;109(1):92-6.
25. Pillai G, Baynes JR, Gladstone J, Flatow EL. Greater strength increase with cyst decompression and SLAP repair than SLAP repair alone. *Clin Orthop Relat Res* 2011;469(4):1056-60. [CrossRef]
26. Lee HJ, Lee JH, Yi KH, Kim HJ. Anatomical analysis of the motor endplate zones of the suprascapular nerve to the infraspinatus muscle and its clinical significance in managing pain disorder. *J Anat* 2023;243(3):467-74. [CrossRef]
27. Plancher KD, Luke TA, Peterson RK, Yacoubian SV. Posterior shoulder pain: a dynamic study of the spinoglenoid ligament and treatment with arthroscopic release of the scapular tunnel. *Arthroscopy* 2007;23(9):991-8. [CrossRef]

28. Plancher KD, Peterson RK, Johnston JC, Luke TA. The spinoglenoid ligament. Anatomy, morphology, and histological findings. *J Bone Joint Surg Am* 2005;87(2):361-5. [\[CrossRef\]](#)
29. Bektas U, Ay S, Yilmaz C, Tekdemir I, Elhan A. Spinoglenoid septum: a new anatomic finding. *J Shoulder Elbow Surg* 2003;12(5):491-2. [\[CrossRef\]](#)
30. Won HJ, Won HS, Oh CS, Han SH, Chung IH, Yoon YC. Morphological study of the inferior transverse scapular ligament. *Clin Anat* 2014;27(5):707-11. [\[CrossRef\]](#)
31. Aktekin M, Demiryurek D, Bayramoglu A, Tuccar E. The significance of the neurovascular structures passing through the spinoglenoid notch. *Neurosciences (Riyadh)* 2003;8(4):222-4.
32. Ajmani ML. The cutaneous branch of the human suprascapular nerve. *J Anat* 1994;185(Pt 2)(Pt 2):439-42.
33. Cummins CA, Anderson K, Bowen M, Nuber G, Roth SI. Anatomy and histological characteristics of the spinoglenoid ligament. *J Bone Joint Surg Am* 1998;80(11):1622-5. [\[CrossRef\]](#)
34. Horiguchi M. The cutaneous branch of some human suprascapular nerves. *J Anat* 1980;130(Pt 1):191-5
35. Harbaugh KS, Swenson R, Saunders RL. Shoulder numbness in a patient with suprascapular nerve entrapment syndrome: cutaneous branch of the suprascapular nerve: case report. *Neurosurgery* 2000;47(6):1452-5. [\[CrossRef\]](#)
36. Aiello I, Serra G, Traina GC, Tugnoli V. Entrapment of the suprascapular nerve at the spinoglenoid notch. *Ann Neurol* 1982;12(3):314-6. [\[CrossRef\]](#)
37. Duparc F, Coquerel D, Ozeel J, Noyon M, Gerometta A, Michot C. Anatomical basis of the suprascapular nerve entrapment, and clinical relevance of the supraspinatus fascia. *Surg Radiol Anat* 2010;32(3):277-84. [\[CrossRef\]](#)
38. Yang J, Feng Q, Wen YL, Fan QH, Luo B, Jia WL, et al. Morphological measurements and classification of the spinoglenoid notch: A three-dimensional reconstruction of computed tomography in the Chinese population. *Ann Anat* 2019;226:10-5. [\[CrossRef\]](#)
39. Kannappan SGP, Bagoji IB, Kumar S. A morphometric study of spinoglenoid notch, subcoracoacromial arch, and spinous process of the scapula on shoulder impingement. *MGM Journal of Medical Sciences* 2022;9(4):459-64. [\[CrossRef\]](#)
40. Dhindsa G, Gupta V. Morphometric study of the acromion process and its clinical relevance. *Asian J Med Res* 2019;8(3):2. [\[CrossRef\]](#)
41. Vinay G, Sivan S. Morphometric study of the acromion process of scapula and its clinical importance in South Indian population. *Int J Anat Res* 2017;5(3.3):4361-4. [\[CrossRef\]](#)
42. Mansur DI, Khanal K, Haque MK, Sharma K. Morphometry of acromion process of human scapulae and its clinical importance amongst Nepalese population. *Kathmandu Univ Med J (KUMJ)* 2012;10(38):33-6. [\[CrossRef\]](#)

INVESTIGATION OF ACANTHAMOEBA SPP. WITH CULTURE AND MOLECULAR METHODS IN THE ENVIRONMENTAL WATER SAMPLES

ÇEVRESEL SU ÖRNEKLERİNDE ACANTHAMOEBA SPP.'NİN KÜLTÜR VE MOLEKÜLER YÖNTEMLER İLE ARAŞTIRILMASI

Şeyma EFE¹ , Özden BORAL¹ , Halim İŞSEVER² 

¹İstanbul University, İstanbul Faculty of Medicine, Department of Medical Microbiology, İstanbul, Türkiye

²İstanbul University, İstanbul Faculty of Medicine, Department of Public Health, İstanbul, Türkiye

ORCID IDs of the authors: Ş.E. 0009-0009-1233-8619; Ö.B. 0000-0001-7144-1418; H.İ. 0000-0002-5435-706X

Cite this article as: Efe Ş, Boral Ö, İşsever H. Investigation of Acanthamoeba spp. with culture and molecular methods in the environmental water samples. J Ist Faculty Med 2025;88(2):146-154. doi: 10.26650/IUITFD.1583675

ABSTRACT

Objective: *Acanthamoeba* spp. are free-living amoebae found in a variety of environments, including seawater, lakes, rivers, stagnant waters, swimming pools, bottled waters, ventilation ducts, air conditioning units, sewage systems, soil, and in-hospital dialysis and eye wash units. Although infections caused by *Acanthamoeba* spp. are infrequent, they are characterised by high mortality and can lead to serious clinical problems. *Acanthamoeba* causes *Acanthamoeba* keratitis (AK) in healthy individuals and contact lens users. In immunocompromised individuals, it can lead to granulomatous amoebic encephalitis (GAE) and lung and skin infections. In this study, we investigated the presence of *Acanthamoeba* species in environmental water samples collected from various cities across Türkiye. We employed a range of culture and molecular methods for this analysis.

Material and Methods: A total of 100 samples were collected from different cities and water sources in Türkiye. Water samples were filtered through a 0.45 µm diameter cellulose nitrate membrane filter using a vacuum device, allowing approximately 100 ml to pass in about 30 s. The filtered water samples were cultured on Non-Nutrient Agar *E.coli* (NNA-*E.coli*) and Buffered Charcoal Yeast Extract Agar media. Samples that were considered culture-positive were stored at -20 °C for DNA isolation.

Results: Among the 100 samples, 27 (27%) *Acanthamoeba* spp. were detected without differentiation by the media. In the NNA-*E.coli* medium, 22 (22%) *Acanthamoeba* spp. were produced, while 19 (19%) were produced in the BCYE medium. No significant difference was found between the two media. A total of 25 *Acanthamoeba* spp. were detected using RT-PCR (25%). The compatibility of the media with RT-PCR was found to be statistically significant ($p < 0.005$) and bidirectional, as calculated by the kappa coefficient.

ÖZET

Amaç: *Acanthamoeba* spp. serbest yaşayan amiplerden olup çevrede deniz sularında, göllerde, nehirlerde, durgun sularda, yüzme havuzlarında, şişelenmiş sularda, havalandırma kanallarında, klima ünitelerinde, lağım sularında, toprakta, hastanelerin diyaliz üniteleri ve göz yıkama üniteleri gibi çok çeşitli yerlerde bulunabilmektedir. *Acanthamoeba* spp.'ye bağlı enfeksiyonlara az rastlanması-na rağmen yüksek ölüm ile karakterize olup ciddi klinik problemler oluşturmaktadır. *Acanthamoeba* sağlıklı bireylerde ya da kontakt lens kullanıcılarında *Acanthamoeba* keratitine (AK) neden olmaktadır. Bağışıklık sistemi baskılanmış kişilerde granülomatöz amebik ensefalit (GAE), akciğer ve deri enfeksiyonlarına sebep olmaktadır. Çalışmamızda Türkiye'nin çeşitli şehirlerinden toplanan çevresel su örneklerinde, *Acanthamoeba* spp. varlığının farklı kültür ve moleküler yöntem ile araştırılması amaçlanmıştır.

Gereç ve Yöntem: Türkiye'nin farklı şehirlerinden ve su kaynaklarından toplam 100 örnek toplanmıştır. Su örnekleri kültür yöntemi ve DNA izolasyonu için 0.45 µm çapında selüloz nitrat membran filtreden yaklaşık 30 saniyede 100 ml geçecek şekilde vakum cihazı ile filtrelenmiştir. Filtrelenen su örnekleri NNA-*E.coli* ve Tamponlu Kömür Maya Özütlü besiyerlerine kültüre edilmiştir. Kültür sonucu pozitif olarak kabul edilen örnekler DNA izolasyonu için -20 °C dondurucuya kaldırılmıştır.

Bulgular: Toplanan 100 örneğin kültür sonuçları besiyeri ayırımı yapılmaksızın 27 (%27) *Acanthamoeba* spp. tespit edilmiştir. NNA-*E.coli* besiyerinde 22 (%22) BCYE besiyerinde 19 (%19) *Acanthamoeba* spp. üretilmiştir. İki besiyeri arasında anlamlı bir farklılık bulunamamıştır. RT-PCR yöntemi ile toplam 25 *Acanthamoeba* spp. saptanmıştır (%25). Besiyerlerinin RT-PCR ile uyumu kappa katsayısı

Corresponding author/İletişim kurulacak yazar: Şeyma EFE – seymaefe96@gmail.com

Submitted/Başvuru: 12.11.2024 • **Revision Requested/Revizyon Talebi:** 03.02.2025 •

Last Revision Received/Son Revizyon: 17.03.2025 • **Accepted/Kabul:** 18.03.2025 • **Published Online/Online Yayın:** 17.04.2025



Content of this journal is licensed under a Creative Commons Attribution-NonCommercial 4.0 International License.

where the samples were taken were noted on each sample. The collected samples were placed in a thermal bag inbrought to the laboratory of the Department of Parasitology in İstanbul University, İstanbul Faculty of Medicine.

Filtering of the water samples

The water samples that were brought to the Parasitology Laboratory of İstanbul University, İstanbul Faculty of Medicine in sterilised plastic bottles were filtered with a vacuumed device, passing 100 ml approximately in 30 s through a 0.45 µm diameter cellulose nitrate membrane filter (AISIMO, England) for the culturing method and DNA isolation. In order to prevent the drying of the surface of the filter, the filtering process continued until 3-5 ml of water remained on the surface. The surface of the filter membrane was divided into equal parts with a sterile scalpel, and one part was preserved at -20 °C for DNA isolation. The remaining part was divided into two equal parts and one half was placed on Non-Nutrient Agar (NNA) and the other half was placed on Buffered Charcoal Yeast Extract Agar (BCYE) and covered upside down. The edges of the Petri dishes were covered with parafilm to prevent drying. Then, the NNA-*E. coli* was incubated at 30 °C and BCYE was incubated at 37 °C. Images of melting or opening on the surface in areas covered with bacteria were considered suspicious, and the surface was scraped with a sterile scalpel, suspended in approximately 2 ml of Page Saline, vortexed and centrifuged, and then microscopically examined. The samples considered positive were stored at -20 °C for DNA isolation.

Culturing method

Three different media were used in this study. Brain heart infusion agar (BHI) was used to grow *Escherichia coli*, and NNA and Buffered charcoal - yeast extract agar (BCYE) were used to culture the environmental water samples.

Brain heart infusion agar (BHIA) (LABM – United Kingdom)

49 g of powdered BHI was added to 1000 ml of distilled water and mixed well. After adjusting the pH to 7.4±0.2, the prepared mixture was sterilised in an autoclave at 121 °C for 15 min. It was cooled to 47°C, poured into Petri dishes and allowed to dry. It was then covered with parafilm and placed at 4°C.

NNA

Page's saline

A solution was prepared by dissolving 0.12 g NaCl, 0.004 MgSO₄.7H₂O, 0.004 g CaCl₂.2H₂O, 0.142 g Na₂HPO₄, and 0.136 g KH₂PO₄ in 1000 ml distilled water, with the pH adjusted to 6.8±0.1.

NNA

The mixture was prepared by adding 15.0 g agar and 1000 ml of Page's saline, and the pH was adjusted to 7.0±0.2. The prepared mixture was sterilised in an auto-

clave at 121 °C for 15 min. It was then poured into Petri dishes and stored at 4 °C. When the sample was to be planted, 18-24 hours old *E.coli* (ATCC 25922) previously grown on BHIA was suspended densely in 5 ml page saline solution, then autoclaved at 121 °C for 15 min and the suspension was collected with a sterile pipette. 1 ml was taken and spread on the NNA surface with the help of a swab. It was then placed in the oven at 30 °C for 24 h to dry.

Buffered charcoal-yeast extract agar (BCYE) (BD BBL, France)

To prepare BCYE, 2.4 grammes of KOH was added to 1000 ml of distilled water and stirred to dissolve. Then, 38.3 grammes of BCYE was added and mixing continued. Heating and mixing were carried out to completely dissolve the powder. The pH was adjusted to 6.8±0.1 and the prepared mixture was sterilised in an autoclave at 121 °C for 15 min. Then, it was cooled to 45-50 °C and 4 ml of 10% filter-sterilised L-Cysteine HCl solution was added. Then, by mixing, the pH was adjusted to 6.8±0.2. Finally, it was poured into Petri dishes and left to dry. It was then covered with parafilm and placed at 4 °C.

DNA isolation of the culture samples

Isolation of amoebae cultured on NNA medium and BCYE medium was performed according to the procedure steps specified in the QIAamp® DNA Minikit QIAGEN.

Real-time polymerase chain reaction

The real-time polymerase chain reaction (RT-PCR) was performed using the *Acanthamoeba* spp. 18S ribosomal RNA (18S) gene Genesig® Standard Kit.

RESULTS

Water samples brought to the Parasitology Laboratory of İstanbul University Faculty of Medicine under appropriate conditions were filtered with a vacuum device for the culture method, and one half of the filter was inverted onto NNA-*E. coli* and the other half was placed upside down on BCYE medium. The NNA-*E. coli* was incubated at 30 °C, and BCYE was incubated at 37 °C. The NNA-*E. coli* media were incubated for up to 14 days and growth was checked at regular intervals. Since the BCYE medium provided the best growth results between 66 and 72 h and started drying after day 10, the Petri dishes were stored for 10 days. The cyst and trophozoite shapes were observed under a microscope. The examination of the culture results of 100 samples showed that *Acanthamoeba* spp. was detected in 27 water samples regardless of the medium. While 15 cysts and 7 trophozoites belonging to *Acanthamoeba* spp. were observed in the NNA-*E. coli* medium, 9 cysts and 10 trophozoites were detected in the BCYE medium. Cysts/trophozoites were detected in 14 samples in common in both media. Eight samples

were only detected in the NNA-*E. coli* medium, while cysts and trophozoites were observed in five samples in the BCYE medium. The BCYE medium proved to be more effective for trophozoite production.

Acanthamoeba spp. growing in NNA-*E. coli* medium and BCYE medium were statistically compared. The number of samples growing in the two media was calculated by chi-square and a significant degree of concordance was found between the NNA-*E.coli* medium and the BCYE medium (Table 1).

Acanthamoeba spp. were cultured in NNA-*E. coli* medium after identifying the presence of cysts or trophozoites in the sample. Following the passage, the cysts and trophozoites of *Acanthamoeba* were observed again. The cysts were then stained with Lactophenol cotton blue (Figure 2). As illustrated in the figure, the amoeba cyst wall was revealed and stained a darker blue than the surrounding areas.

After the examination of the NNA-*E. coli* and BCYE me-

dia, the samples with *Acanthamoeba* spp. cysts were evaluated in accordance with their morphological criteria. In the classification based on the size and shape of the cysts, the samples identified predominantly belonged to Group II and Group III.

Table 2 shows the location-date information from which the samples were taken and the positivity used in *Acanthamoeba* spp. detection (Table 2).

RT-PCR analysis was performed after DNA isolation of the samples whose media results were observed. RT-PCR results of a total of 25 samples out of 100 were found positive.

The moderate compliance between BCYE and RT-PCR was found to be statistically significant. The compatibility of the NNA-*E. coli* and BCYE media with RT-PCR was evaluated by calculating the kappa coefficient. The detected coefficients showed moderate and potentially significant compliance ranging from 0.30 to 0.60 were found to be statistically significant ($p < 0.001$) (Table 3-4).

DISCUSSION

A total of 100 water samples from various cities in Türkiye, which have intense human contact, were analysed to identify *Acanthamoeba* spp. in environmental water sources. *Acanthamoeba* spp. typically reproduced within an average of 5 days in the samples taken for NNA-*E. coli* and BCYE cultures. The presence of *Acanthamoeba* spp. was detected in 27% of the water samples using both culture methods. The NNA-*E. coli* medium (22/100) showed similar results to the BCYE medium (19/100) in the production of *Acanthamoeba*. Penland and Wilhelmus reproduced the *Pseudomonas aeruginosa* ATCC 27853, *E. aerogenes* ATCC 13048, *Stenotrophomonas maltophilia* ATCC 13637, *E. coli* ATCC 25922, *Staphylococcus aureus* ATCC 25923, *Klebsiella pneumoniae* ATCC 13883 and *Serratia marcescens* B1523 bacteria as alive and dead in non-nutrient medium, and in BCYE and TSA (rabbit blood, sheep blood, horse blood, human blood) in patient samples who were found positive for *Acanthamoeba* spp., and found that the BCYE medium provided more successful results in the production of trophozoites as similarly with our study (7). In our study, we observed 10 trophozoites and 9 cysts of *Acanthamoeba* spp. in the BCYE medium, whereas 15 cysts and 7 trophozoites were found in the heat-killed NNA-*E. coli* medium. There are few studies comparing the growth of *Acanthamoeba* in different culture media. This suggests that new and more accessible culture media could be discovered for cultivating this amoeba.

Tawfeek et al. collected 75 environmental samples and cultured NNA-*E. coli* medium in their study aiming at the genotypic, physiological and biochemical characterisa-

Table 1: Comparison of the positivity of *Acanthamoeba* spp. in NNA-*E. coli* and BCYE Medium

NNA Medium/ <i>E.coli</i>	BCYE Medium				χ^2	P
	No		Yes			
	n	%	n	%		
No	73	93.6	5	6.4	36.515	$p < 0.001$
Yes	8	36.4	14	63.6		

NNA: Non-Nutrient Agar, BCYE: Buffered Charcoal Yeast Extract Agar, χ^2 : chi square, P: chi square p significance value Kappa=0.602: $p < 0.001$, 95% CI : 0.407 and 0.797

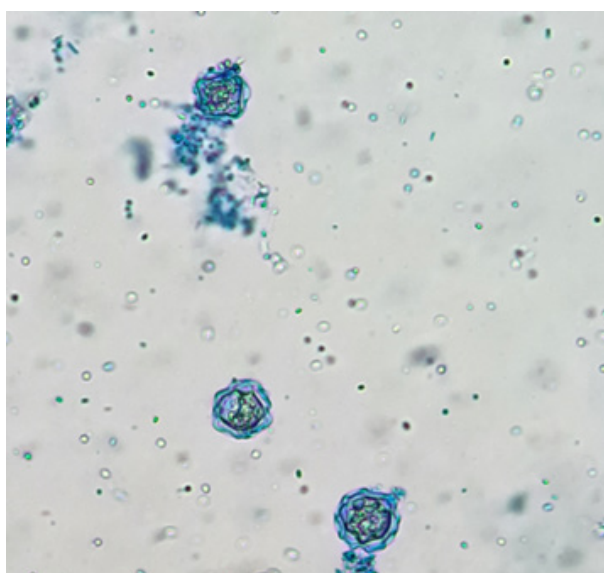


Figure 2: The *Acanthamoeba* cysts (X40) stained with Lactophenol cotton blue in the NNA-*E. coli* medium

Table 2: The location and date of collection of samples and the comparison of positivity of the methods used in the detection of *Acanthamoeba* spp.

Sample no	Source of the water	Type of water	Sampling date	Sampling season	NNA medium/ <i>E. coli</i>	BCYE medium	RT-PCR (C ₁)
1	Mardin	Brackish	27.08.2021	Summer	-	-	-
2	Mardin	Natural spring	27.08.2021	Summer	+	-	+ 23.45
3	Mardin	Tap	27.08.2021	Summer	+	+	+ 21.34
4	Şanlıurfa	Lake	28.08.2021	Summer	+	+	+ 21.12
5	Şanlıurfa	Tap	28.08.2021	Summer	-	-	-
6	Şanlıurfa	Brackish	28.08.2021	Summer	+	+	+ 26.99
7	Şanlıurfa	Dam	28.08.2021	Summer	+	+	+ 29.32
8	Diyarbakır	Thermal	29.08.2021	Summer	+	-	+ 32.21
9	Diyarbakır	Thermal	29.08.2021	Summer	+	+	-
10	Diyarbakır	Natural waterfall	29.08.2021	Summer	+	+	-
11	Diyarbakır	Tap	29.08.2021	Summer	-	-	-
12	Diyarbakır	Stream	29.08.2021	Summer	+	+	-
13	Diyarbakır	River	29.08.2021	Summer	-	-	-
14	Diyarbakır	River	30.08.2021	Summer	-	-	-
15	Diyarbakır	River	30.08.2021	Summer	+	+	-
16	Diyarbakır	Natural spring	30.08.2021	Summer	-	-	-
17	Diyarbakır	Dam	30.08.2021	Summer	-	-	-
18	Diyarbakır	Tap	31.08.2021	Summer	-	-	-
19	Diyarbakır	Tap	31.08.2021	Summer	-	-	-
20	Diyarbakır	Tap	31.08.2021	Summer	-	-	-
21	Diyarbakır	Swimming pool	31.08.2021	Summer	-	-	-
22	Diyarbakır	Tap	31.08.2021	Summer	-	-	-
23	Eskişehir	Tap	25.09.2021	Autumn	-	-	-
24	Eskişehir	Tap	25.09.2021	Autumn	-	-	-
25	Eskişehir	Stream	25.09.2021	Autumn	-	-	-
26	Eskişehir	Bath	25.09.2021	Autumn	-	+	-
27	Antalya	Sea	27.06.2022	Summer	+	+	-
28	Tokat	Tap	22.08.2022	Summer	-	-	-
29	Tokat	Tap	22.08.2022	Summer	-	-	-
30	Tokat	Natural spring	22.08.2022	Summer	-	-	-
31	Afyonkarahisar	Thermal	02.04.2022	Spring	-	-	-
32	Manisa	Tap	03.04.22	Spring	-	-	-
33	Zonguldak	Natural spring	26.08.2022	Summer	-	-	-
34	Zonguldak	Earthy	26.08.2022	Summer	-	-	-
35	Diyarbakır	Earthy	30.08.2021	Summer	-	+	-
36	Bolu	Tap	08.09.2022	Autumn	-	-	-
37	Bolu	Tap	08.09.2022	Autumn	-	-	-
38	Bursa	Tap	18.09.2021	Autumn	-	-	-

Table 2: Continue

Sample no	Source of the sample	Type of water	Sampling date	Sampling season	NNA medium/ <i>E. coli</i>	BCYE medium	RT-PCR (C _t)
39	İstanbul	Hospital tap	22.09.2022	Autumn	-	-	-
40	İstanbul	Tap	07.10.2022	Autumn	-	-	-
41	İstanbul	Hospital tap	10.10.2022	Autumn	-	-	-
42	İstanbul	Hospital tank	10.10.2022	Autumn	+	-	-
43	İstanbul	Hospital tank	10.10.2022	Autumn	-	-	-
44	İstanbul	Drain	10.10.2022	Autumn	-	-	-
45	İstanbul	Potted	13.10.2022	Autumn	+	+	+ 32.39
46	İstanbul	Potted	13.10.2022	Autumn	+	-	+ 20.86
47	İstanbul	Bath	25.10.2022	Autumn	+	+	-
48	İstanbul	Bath	25.10.2022	Autumn	+	-	+ 38.45
49	İstanbul	Tap	25.10.2022	Autumn	-	-	-
50	Van	Lake	10.08.2022	Summer	-	-	-
51	Bitlis	Natural spring	14.08.2022	Summer	-	-	-
52	Siirt	Tap	14.08.2022	Summer	-	-	-
53	Diyarbakır	Tap	02.09.2022	Autumn	-	-	-
54	Diyarbakır	Natural spring	02.09.2022	Autumn	-	-	-
55	Elazığ	Natural spring	06.11.2022	Autumn	-	-	-
56	Elazığ	Lake	06.11.2022	Autumn	-	-	-
57	Malatya	Tap	06.11.2022	Autumn	-	-	-
58	Malatya	Tap	06.11.2022	Autumn	-	-	-
59	İstanbul	Artificial waterfall	26.10.2022	Autumn	-	-	+ 27.65
60	İstanbul	Artificial waterfall	19.11.2022	Autumn	+	+	+ 17.10
61	İstanbul	Potted	20.12.2022	Winter	+	+	+ 30.79
62	İstanbul	Fountain	20.12.2022	Winter	+	-	+ 29.22
63	İstanbul	Fountain	20.12.2022	Winter	-	-	+ 33.77
64	Denizli	Tap	20.12.2022	Winter	-	-	+ 29,67
65	İstanbul	Artificial	04.01.2023	Winter	-	-	+ 30.82
66	İstanbul	Artificial stream	04.01.2023	Winter	-	-	+ 31.73
67	İstanbul	Swimming pool	04.01.2023	Winter	-	-	+ 30.36
68	İstanbul	Brackish	09.01.2023	Winter	-	-	-
69	İstanbul	Brackish	09.01.2023	Winter	-	-	-
70	İstanbul	Tank	10.01.2023	Winter	-	-	-
71	İstanbul	Potted	23.01.2023	Winter	-	-	-
72	İstanbul	Bath	23.01.2023	Winter	-	-	-
73	İstanbul	Bath	23.01.2023	Winter	-	-	-
74	İstanbul	Sea	24.01.2023	Winter	-	-	+ 29.76
75	Ankara	Thermal	28.01.2023	Winter	-	-	-
76	Ankara	Thermal	28.01.2023	Winter	-	-	-
77	Ankara	Thermal	28.01.2023	Winter	-	-	-

Table 2: Continue

Sample no	Source of the sample	Type of water	Sampling date	Sampling season	NNA medium/ <i>E. coli</i>	BCYE medium	RT-PCR (C _t)
78	Ankara	Tap	28.01.2023	Winter	-	-	-
79	İstanbul	Sea	26.02.2023	Winter	-	-	-
80	İstanbul	Sea	26.02.2023	Winter	-	-	-
81	Bolu	Tap	29.01.2023	Winter	-	-	-
82	İstanbul	Lake	26.02.2023	Winter	-	-	-
83	İstanbul	Lake	26.02.2023	Winter	-	-	-
84	İstanbul	Sea	26.02.2023	Winter	-	+	-
85	İstanbul	Sea	26.02.2023	Winter	-	+	+ 38.81
86	İstanbul	Potted	01.03.2023	Spring	-	+	+ 34.82
87	İstanbul	Potted	01.03.2023	Spring	-	-	+ 31.48
88	İstanbul	Potted	01.03.2023	Spring	+	-	+ 29.89
89	İstanbul	Stream	01.03.2023	Spring	+	-	-
90	İstanbul	Ornamental pool	01.03.2023	Spring	-	-	-
91	İstanbul	Swimming pool	14.03.2023	Spring	-	-	-
92	İstanbul	Swimming pool	14.03.2023	Spring	+	+	+ 20.91
93	İstanbul	Ornamental pool	15.03.2023	Spring	-	-	+ 36.01
94	İstanbul	Tap	15.03.2023	Spring	-	-	-
95	İstanbul	Tap	15.03.2023	Spring	-	-	-
96	İstanbul	Bath	15.03.2023	Spring	-	-	-
97	İstanbul	Bath	15.03.2023	Spring	-	-	-
98	İstanbul	Bath	15.03.2023	Spring	-	-	-
99	İstanbul	Ornamental pool	15.03.2023	Spring	-	-	-
100	İstanbul	Tap	15.03.2023	Spring	-	-	-

NNA: Non-Nutrient Agar, BCYE: Buffered Charcoal – Yeast Extract Agar, RT-PCR, (C_t): Real-time polymerase chain reaction (cycle threshold)

Table 3: Comparison of the NNA-*E. coli* and RT-PCR positivity in the detection of *Acanthamoeba* spp.

RT-PCR	NNA- <i>E. coli</i>		χ ²	p
	No	Yes		
No	67	11	22.4	p<0.001
Yes	8	14		
Total	75	25		

NNA: Non-Nutrient Agar, RT-PCR: The real-time polymerase chain reaction, χ²: chi square, P: chi square p significance value Kappa=0.472, p<0.001; 95 % CI 0.270 and 0.675. The compliance between NNA-*E. coli* and RT-PCR was mostly found to be significant

Table 4: Comparison of the BCYE and RT-PCR positivity in the detection of *Acanthamoeba* spp.

RT-PCR	BCYE		χ ²	p
	No	Yes		
No	66	9	9.5	p<0.002
Yes	15	10		
Total	81	19		

BCYE: Buffered Charcoal – Yeast Extract Agar, RT-PCR: The real-time polymerase chain reaction, χ²: chi square, P: Chi square, p significance value Kappa=0.304, p<0.001, 95% CI 0.089 and 0.519

tion of potentially pathogenic *Acanthamoeba* isolated from the environment in Cairo, Egypt. *Acanthamoeba* spp. was found in 11 (31.4%) of the 35 water samples collected in this study (8). Similarly, in our study, a total of 27% culture-positive results were obtained. In Iran, Mahmudi and his colleagues randomly collected 80 water samples

and 20 soil samples from public parks in the districts of Guilan province between May and June 2019, and detected *Acanthamoeba* in 40 (50%) of the 80 water samples (9). Since environmental sources are an important potential risk factor for human infection, examining the prevalence of *Acanthamoeba* in different environments

can be helpful for the control and prevention of the disease in humans. There are differences in the prevalence of *Acanthamoeba* spp., found in many places in the environment. The reason is considered the conditions such as water temperature and climatic conditions in countries and regions with different geographical locations.

In their study, Hajjalilo et al. examined 138 corneal scrapings, contact lens samples, and equipment to isolate and genotype *Acanthamoeba* strains from patients with amoebic keratitis in Iran in 2016. They investigated all clinical samples using both direct microscopy and culturing methods. Among the samples, they classified them based on morphology and predominantly detected cysts belonging to Group II. However, in one isolate, they found a cyst of *Acanthamoeba* spp. belonging to Group I morphology (10).

In another study by Al-Herrawy et al., the presence of *Acanthamoeba* species was investigated in the Damhour drinking water treatment plant in Egypt. Of the 48 water samples analysed, 12 (25%) were positive for *Acanthamoeba*. The results revealed *Acanthamoeba* spp. from Group I, Group II, and Group III in the morphologically classified samples. In our study, which examined 100 different environmental water samples, the morphological classification of 27 *Acanthamoeba* spp. indicated that they primarily belonged to Group II and Group III (11).

In their study, Milanez et al. examined *Acanthamoeba* spp. isolated from 63 drinking water systems in the Philippines from both epidemiological and molecular perspectives. They found a positivity rate of 14.28% (9 out of 63) in the NNA-*E. coli* medium, and the cultures were positive using *Acanthamoeba*-specific primers. Additionally, all samples tested (9 out of 9) were confirmed positive through molecular methods (12).

Meanwhile, Karimi and colleagues investigated the identification and genotyping of *Acanthamoeba* spp. in water resources in Western Iran. They collected and cultured 72 water samples, subsequently performing PCR. They discovered that all 72 samples (100%) were positive for free-living amoebae (FLA) through culture methods. However, only 17 samples (23.6%) tested positive according to the PCR results used to diagnose and identify *Acanthamoeba* from the culture samples (13). In our study, we detected culture positivity in 27 out of 100 samples, while RT-PCR results confirmed that 25 samples were positive for *Acanthamoeba* spp. Additionally, 9 out of 73 samples that did not yield positive results in culture were found to be positive through RT-PCR. Based on our findings, although the culture method is time-consuming, it remains the gold standard for detecting *Acanthamoeba* spp. The discrepancy between the culture and RT-PCR results may be because the cultured samples examined under the microscope could be *Vermamoeba* spp. (formerly known as *Hartmannella*), which have morphological similarities

to *Acanthamoeba* spp. It is also worth noting that *Acanthamoeba* species exhibit numerous genotypes, with new variants continuously being discovered.

Acanthamoeba spp. are found in regions with various climatic characteristics and water resources, and their presence can be influenced by seasonal changes. In a study by Kao et al., the researchers evaluated the presence of *Acanthamoeba* spp. in the Puzih River basin in Taiwan. They collected 136 water samples between July 2009 and March 2010, spanning all four seasons. *Acanthamoeba* spp. was detected in 16 of 136 samples, representing a prevalence of 11.7%.

Seasonally, the findings showed that *Acanthamoeba* spp. was identified in the following proportions: spring (2.9%), summer (32.4%), autumn (2.9%), and winter (8.8%). The organism was most frequently detected during the summer months. In our study, which involved culturing samples collected across the four seasons, *Acanthamoeba* spp. was primarily detected in the summer, yielding 12 positive culture results.

CONCLUSION

In conclusion, 100 different water samples were cultured using NNA-*E. coli* and BCYE media. *Acanthamoeba* spp. were detected in 22 samples (22%) from the NNA-*E. coli* medium and in 22 samples (19%) from the BCYE medium. No significant difference was found between the two types of media. A total of 25 *Acanthamoeba* spp. were identified using the RT-PCR method, representing 25% of the samples. The compatibility of the media with RT-PCR showed a statistically significant result ($p < 0.005$) and was considered bidirectionally acceptable when the kappa coefficient was calculated. There are few studies comparing the growth of *Acanthamoeba* in different culture media, highlighting the need to discover novel and more accessible culture options for this amoeba.

Ethics Committee Approval: Since this study was conducted on environmental water samples, ethics committee approval was not obtained.

Peer Review: Externally peer-reviewed.

Author Contributions: Conception/Design of Study- Ö.B., Ş.E.; Data Acquisition- Ş.E., Ö.B.; Data Analysis/Interpretation – H.İ., Ö.B., Ş.E.; Drafting Manuscript- Ş.E., Ö.B.; Critical Revision of Manuscript- Ö.B., H.İ., Ş.E.; Final Approval and Accountability- Ş.E., Ö.B., H.İ.

Conflict of Interest: The authors have no conflict of interest to declare.

Financial Disclosure: The authors declared that this study received no financial support.

REFERENCES

1. Castrillón JC, Orozco LP. *Acanthamoeba* spp. como parásitos patógenos y oportunistas. *Revista Chil Infectol* 2013;30(2):147-55. [CrossRef]
2. Schuster FL, Visvesvara GS. Free-living amoebae as opportunistic and non-opportunistic pathogens of humans and animals. *Int J Parasitol* 2004;34:1001-27. [CrossRef]
3. Center for Disease Control and Prevention (CDC). *Acanthamoeba* Infections, *Acanthamoeba* Keratitis. 2024 September. <https://www.cdc.gov/acanthamoeba/about/about-acanthamoeba-keratitis.html>
4. Satlin MJ, Graham JK, Visvesvara GS, Mena H, Marks KM, Saal SD, et al. Fulminant and fatal encephalitis caused by *Acanthamoeba* in a kidney transplant recipient: case report and literature review. *Transpl Infect Dis* 2013;15(6):619-26. [CrossRef]
5. Putaporntip C, Kuamsab N, Nuprasert W, Rojrung R, Pattanawong U, Tia T, et al. Analysis of *Acanthamoeba* genotypes from public freshwater sources in Thailand reveals a new genotype, T23 *Acanthamoeba* bangkokensis sp. nov. *Sci Rep* 2021;11(1):17290. [CrossRef]
6. Raju R, Khurana S, Mahadevan A, John DV. Central nervous system infections caused by pathogenic free-living amoebae: An Indian perspective. *Trop Biomed* 2022;39(2):265-80. [CrossRef]
7. Penland RL, Wilhelmus KR. Comparison of axenic and monoxenic media for isolation of *Acanthamoeba*. *J Clin Microbiol* 1997;35(4):915-22. [CrossRef]
8. Tawfeek GM, Bishara SAH, Sarhan RM, Taher EE, Khayyal AE. Genotypic, physiological, and biochemical characterization of potentially pathogenic *Acanthamoeba* isolated from the environment in Cairo, Egypt. *Parasitol Res* 2016;115(5):1871-81. [CrossRef]
9. Mahmoudi MR, Maleki M, Zebardast N, Rahmati B, Ashrafi K, Sharifdini M, et al. Identification of *Acanthamoeba* spp. from water and soil of public parks in the north of Iran. *J Water Health* 2022(10);1604-10. [CrossRef]
10. Hajjalilo E, Behnia M, Tarighi F, Niyayati M, Rezaeian M. Isolation and genotyping of *Acanthamoeba* strains (T4, T9, and T11) from amoebic keratitis patients in Iran. *Parasitol Res* 2016;115(8):3147-51. [CrossRef]
11. Al-Herrawy AZ, Heshmat MG, Abu Kabsha, SH, Gad MA, Lotfy WM. Occurrence of *Acanthamoeba* species in the Damanhour drinking water treatment plant, Behera Governorate (Egypt). *Reports in Parasitology* 2015;4:15-21. [CrossRef]
12. Milanez GD, Masangkay FR, Scheid P, Dionisio JD, Somsak V, Kotepui M, et al. *Acanthamoeba* species isolated from Philippine freshwater systems: epidemiological and molecular aspects. *Parasitol Res* 2020;119(11):3755-61. [CrossRef]
13. Karimi A, Kheirandish F, Mamaghani AJ, Taghipour N, Mousavi SF, Aghajani A, et al. Identification and genotyping of *Acanthamoeba* spp. in the water resources of western Iran. *Parasite Epidemiol Control* 2023;22:e00308. [CrossRef]
14. Kao PM, Chou MY, Tao CW, Huang WC, Hsu BM, Shen SM, et al. Diversity and seasonal impact of *Acanthamoeba* species in a subtropical rivershed. *BioMed Res Int* 2013;2013:405794. [CrossRef]

LATEST ADVANCES FOR TREATING CONGENITAL ADRENAL HYPERPLASIA DUE TO 21-HYDROXYLASE DEFICIENCY

21-HİDROKSİLAZ EKSİKLİĞİNE BAĞLI KONJENİTAL ADRENAL HİPERPLAZİ TEDAVİSİNDEKİ YENİLİKLER

Ecesu ÇETİN¹ , Mehmet Furkan BURAK^{2,3} 

¹Harvard Medical School, Brigham and Women's Hospital, Division of Endocrinology, Diabetes and Hypertension, Postdoctoral Research Fellow, Boston, MA, United States

²Harvard Medical School, Brigham and Women's Hospital, Division of Endocrinology, Diabetes and Hypertension, Principal Investigator, Boston, MA, United States

³Harvard T.H. Chan School of Public Health, Department of Molecular Metabolism, Boston, MA, United States

ORCID IDs of the authors: E.Ç. 0000-0001-7682-3597; M.F.B. 0000-0001-6222-1552

Cite this article as: Çetin E, Burak MF. Latest advances for treating congenital adrenal hyperplasia due to 21-hydroxylase deficiency. J Ist Faculty Med 2025;88(2):155-163. doi: 10.26650/IUITFD.1626109

ABSTRACT

Congenital adrenal hyperplasia (CAH) is a group of inherited diseases characterised by disrupted glucocorticoid (GC) and mineralocorticoid (MC) synthesis in the adrenal glands. Most cases are caused by 21-hydroxylase (21-OH) enzyme deficiency, which leads to diminished cortisol and aldosterone levels, a reactional increase in adrenocorticotrophic hormone (ACTH), resulting in excessive adrenal androgen production. CAH is a challenging condition that often requires supraphysiological doses of GCs to suppress ACTH and subsequent androgen production. It can lead to complications such as short stature and premature puberty during childhood, hyperandrogenism, infertility, and iatrogenic Cushing syndrome in adulthood. This manuscript reviews the current therapeutic landscape, unmet needs, and emerging therapies for CAH, including corticotropin-releasing factor type 1 (CRF1) receptor antagonists, ACTH inhibitors, and investigational gene therapies to replace 21-OH enzymatic activity. The main focus of the pipeline agents is to reduce androgen levels and the need for supraphysiological dosing of GCs. Crinicerfont, a CRF1 receptor antagonist, has recently been approved by the Food and Drug Administration (FDA) after showing significant improvements in androgen levels in adults and paediatric patients aged 4 years and older with classic CAH. The manufacturer claims it is the first novel CAH treatment in 70 years. However, it failed to maintain low androgen levels while reducing GC dosing. Hence, further pipeline is investigating whether it is possible to achieve both goals or cure the disease. The long-term safety and efficacy of these promising

ÖZET

Konjenital adrenal hiperplazi (KAH), adrenal bezlerde glukokortikoid (GC) ve mineralokortikoid (MC) sentezinin bozulmasıyla karakterize bir grup kalıtsal hastalığı ifade eder. Vakaların büyük çoğunluğu, kortizol ve aldosteron seviyelerinin azalmasına yol açan, buna bağlı olarak adrenokortikotropik hormon (ACTH) düzeylerinde reaksiyonel bir artışla adrenal androjen üretiminin fazlaca artmasına neden olan 21-hidroksilaz (21-OH) enziminin eksikliğinden kaynaklanır. KAH, genellikle ACTH'yi ve buna bağlı androjen üretimini baskılamak için fizyolojik sınırların üzerinde GC dozlarının kullanımını gerektiren, yönetimi zor bir hastalıktır. Bu durum, çocukluk döneminde kısa boy ve erken ergenlik, yetişkinlikte ise hiperandrogenizm, infertilite ve iyatrojenik Cushing sendromu gibi komplikasyonlara yol açabilir. Bu makale, KAH için mevcut tedavi seçeneklerini, tedavi alanındaki eksiklikleri ve gelişmekte olan yeni tedavi yaklaşımlarını kapsamlı bir şekilde ele almaktadır. Bunlar arasında kortikotropin salıcı faktör tip 1 (CRF1) reseptör antagonistleri, ACTH inhibitörleri ve 21-OH enzimatik aktivitesini yerine koymayı hedefleyen deneysel gen tedavileri bulunmaktadır. Yeni geliştirilen ajanların ana hedefi, androjen seviyelerini azaltmak ve suprafizyolojik GC dozlarına duyulan ihtiyacı en aza indirmektir. CRF1 reseptör antagonisti olan crinicerfont, androjen seviyelerinde önemli iyileşmeler göstermesi nedeniyle; 4 yaş ve üzeri çocuk ve yetişkin klasik KAH hastalarında kısa bir süre önce Amerikan Gıda ve İlaç Dairesi (FDA) tarafından onaylanmıştır. Üretici firma, bu ilacın son 70 yıl içerisinde onaylanan ilk yenilikçi KAH tedavisini olduğunu öne sürmektedir. Ancak, bu tedavi yöntemi, GC dozlarını azaltırken düşük androjen seviyelerini sürdürebilme hedefini karşılayama-

Corresponding author/İletişim kurulacak yazar: Mehmet Furkan BURAK – mfburak@hsph.harvard.edu

Submitted/Başvuru: 24.01.2025 • **Revision Requested/Revizyon Talebi:** 27.01.2025 •

Last Revision Received/Son Revizyon: 30.01.2025 • **Accepted/Kabul:** 07.02.2025 • **Published Online/Online Yayın:** 11.03.2025



Content of this journal is licensed under a Creative Commons Attribution-NonCommercial 4.0 International License.

therapeutic approaches require further investigation and elucidation.

Keywords: Congenital adrenal hyperplasia, 21-hydroxylase, melanocortin type 2 receptor, CRF receptor type 1, gene therapy

miştir. Bu nedenle, güncel araştırmalar, her iki hedefe aynı anda ulaşıp ulaşılamayacağı veya hastalığın tamamen tedavi edilip edilemeyeceği sorularına yanıt aramaktadır. Bu umut verici tedavi yaklaşımlarının uzun vadeli güvenliği ve etkinliği daha fazla araştırma ile kapsamlı bir şekilde değerlendirilmelidir.

Anahtar Kelimeler: Konjenital adrenal hiperplazi, 21-hidroksilaz eksikliği, melanokortin tip 2 reseptörü, kortikotropin salgılatıcı faktör, gen terapisi

INTRODUCTION

Congenital adrenal hyperplasia (CAH) is a group of inherited diseases that are characterised by the disruption of physiological cortisol and aldosterone synthesis in the adrenal glands. A deficiency in the 21-hydroxylase (21-OH) enzyme causes more than 95% of CAH cases (1). This leads to decreased negative feedback to the Hypothalamic-Pituitary-Adrenal (HPA) axis (Figure 1) (2). This form of CAH is the primary focus of this review.

Diminished serum cortisol levels in patients with 21-OH deficiency trigger a compensatory increase in the pituitary secretion of adrenocorticotrophic hormone (ACTH). This, in turn, promotes hyperstimulation of the adrenal gland, resulting in hyperplasia. ACTH-dependent overstimulation of the adrenal gland shifts steroid synthesis to excessive androgen production in a setting of 21-OH deficiency (3). The clinical manifestations vary greatly depending on the severity of the enzymatic defect and the degree of androgen excess. 21-OH deficiency-associated CAH is mainly categorised into classic and non-classic subtypes. The classic form is a severe and potentially life-threatening disorder that arises from a lack of both cortisol and aldosterone. If untreated, the classic form can be fatal due to adrenal crises during the initial two weeks after birth. Additionally, with some enzymatic activity, patients may exhibit ambiguous genitalia at birth, as well as clinical manifestations of hyperandrogenism resulting from early adrenarche and gonadotropin-independent precocious puberty. These manifestations often include the premature appearance of pubic hair and rapid growth progression (4). Non-classic CAH represents a less severe form of the condition, arising from genetic mutations that preserve 20–50% of 21-OH activity. It is frequently asymptomatic but may occasionally exhibit signs of androgen overproduction in females. When present, the symptoms typically emerge during childhood or early adulthood, resulting in a less immediate diagnosis compared with classic CAH (4, 5). 21-OH deficiency is a common genetic condition (1). Its prevalence differs significantly across different demographic groups and regions, ranging from as rare as 1 in 28,000 to as common as 1 in 280 (6, 7).

The diagnosis of CAH typically begins with newborn screening to enable an early identification of affected in-

dividuals. Beyond infancy, the initial evaluation in symptomatic patients often includes measuring early-morning serum 17-hydroxyprogesterone (17-OHP) levels. This approach is adopted because 21-OH, the enzyme responsible for converting 17-OHP into cortisol and aldosterone precursors, is deficient in most cases of CAH. As a result, the absence of 21-OH activity leads to the accumulation of 17-OHP, making its measurement a key diagnostic marker for the condition. If the initial 17-OHP measurement is inconclusive, it is advised to evaluate for potential deficiencies in other enzymes. Genetic testing is generally reserved for inconclusive results, unreliable tests, or counselling (8). Once the diagnosis is established, the primary goals of management are to prevent adrenal crises through a balanced hormone replacement therapy, normalise adrenal androgen production, and ensure appropriate physical and sexual development for children. For the treatment of CAH in children, hydrocortisone is the preferred therapy. Suspension forms of hydrocortisone, as well as long-acting potent glucocorticoids (GCs), are not recommended due to their effects on the suppression of growth (2, 8). In infancy, fludrocortisone and sodium chloride supplements are incorporated in addition to GCs. The treatment regimen in adults includes hydrocortisone and/or long-acting GCs, supplemented with mineralocorticoids (MCs) where needed (8). Additionally, modified-release hydrocortisone, approved in the United Kingdom and Europe but not in the US, has demonstrated some potential therapeutic benefits (9, 10). However, achieving adequate suppression of the HPA axis often necessitates GC dosages that exceed physiological levels. Otherwise, insufficient suppression of ACTH secretion can result in hyperstimulation of the adrenal gland and hyperandrogenism (5, 11). Maintaining the appropriate balance of GC treatment is challenging, as excess doses can lead to iatrogenic Cushing's syndrome or inadequate GC dosing can lead to hyperandrogenism. Consequently, the therapeutic window for GC replacement is significantly narrower compared with other forms of adrenal insufficiency without concomitant androgen excess (2, 3, 5, 11). This review examines the limitations of current treatments for CAH and explores promising emerging therapies.

An overview of the HPA axis

The HPA axis is a complex neuroendocrine system that regulates vital functions. These include the secretion of

stress hormones and the production of sex hormones. It also coordinates metabolism and maintains homeostasis (12). This important axis is a direct drug target for CAH treatment (Figure 1). Corticotropin-releasing factor (CRF), also referred to as corticotropin-releasing hormone (CRH), is a peptide hormone that is mainly responsible for regulating the HPA axis (13). Neurosecretory parvocellular neurons of the paraventricular nucleus of the hypothalamus release CRF into the hypothalamohypophyseal portal system (12). The physiological actions of CRH are mediated through two distinct receptor subtypes, CRF-1 and CRF-2. CRF-1 is primarily expressed centrally, serving as the main receptor subtype responsible for mediating the endocrine stress response of CRH. The binding of CRF to CRF1 on the anterior pituitary stimulates ACTH production from its precursor protein, proopiomelanocortin (POMC), and its subsequent secretion into the systemic circulation (12, 13). Circulating ACTH targets the adrenal cortex, where it binds to the melanocortin type 2 receptor (13). This activation promotes the secretion of corticosteroids from the zona fasciculata, MCs from the zona glomerulosa, and androgens predominantly from the zona reticularis (12). This HPA axis is regulated through negative feedback mechanisms involving GCs, which are impacted by their concentration, duration, and rhythmic release patterns (12, 13). Additionally, the HPA axis can be regulated by CRH-binding proteins commonly present in the circulation and expressed in the pituitary and hypothalamus (12). If this negative feedback mechanism is impaired, such as in the case of CAH due to the inability to synthesise corticosteroids, ACTH exerts chronic stimulation in the adrenal cortex and promotes hyperplasia.

Treatment landscape for CAH and management challenges

Current CAH management is associated with numerous adverse outcomes. These complications arise from either undertreatment of the disease, excessive adrenal androgen levels, or the supraphysiological administration of GCs and MCs to suppress the HPA axis (5). CAH management is particularly challenging in the paediatric population due to the intricate balance required between dynamic growth patterns and premature sexual development. In paediatrics, hydrocortisone is the preferred short-acting GC; however, its rapid clearance often results in periods of androgen rebound between doses (8, 14). Inadequate management in boys can lead to central precocious puberty, while in girls, it may result in delayed puberty (15). Both excessive GC therapy, leading to growth suppression, and insufficient GC therapy, resulting in elevated androgen levels accelerating skeletal development prematurely, impair final adult height attainment (4, 5). In adulthood, males typically do not seek medical help. In contrast, females mostly seek help primarily for hyperandrogenism and infertility and often

end up experiencing GC overdosing. In the long term, affected individuals are at an elevated risk of a broad spectrum of multisystem complications. Cardiovascular and metabolic risks are significantly elevated, characterised by higher rates of obesity, insulin resistance, hypertension, dyslipidemia, and cardiovascular disease (16, 17). Bone health is frequently compromised due to prolonged GC therapy, leading to microarchitectural alterations, increased fracture susceptibility, and osteoporosis (4, 18, 19). Additionally, the hypersecretion of ACTH not only drives adrenal hyperplasia but may also predispose individuals to adrenal tumour development over time (5, 20). Gonadal dysfunction is another significant concern, presenting as hypogonadotropic hypogonadism and infertility, while excess adrenal androgen levels in females may lead to additional manifestations such as acne, hirsutism, irregular menstrual cycles, and voice deepening (4, 5, 21). In males, elevated ACTH could contribute to testicular adrenal rest tumours (TART), which results in gonadal dysfunction (21). These challenges demonstrate the critical need to develop innovative therapeutic strategies that can mitigate the long-term effects and enhance the overall outcomes for individuals living with CAH.

Evolving treatment pipeline for CAH

Novel therapeutic approaches are being explored in CAH to further improve outcomes for patients as well as reduce excessive GC and androgen exposure. These newer strategies target the hypothalamic–pituitary–adrenal axis through alternative mechanisms and provide more effective management options for patients. Figure 1 demonstrates an overview of the hypothalamic–pituitary–adrenal axis and the targets of emerging therapies (Figure 1). In summary, these agents target the ACTH and consecutive overstimulation of the adrenal gland. Multiple ACTH inhibition approaches have emerged. They either decrease the secretion via CRF1 antagonism or directly inhibit ACTH through antibody neutralisation or ACTH receptor antagonism. These approaches aim for better disease management and control of androgen levels while continuing GC and MC therapy. The ultimate cure for the disease is to restore enzyme activity, which is also under development.

CRF1 receptor antagonists

Crinicerfont

Crinicerfont is an oral CRF1 receptor antagonist that offers a nonsteroidal approach to managing 21-OH deficiency (Figure 1) (22, 23). In a Phase II trial with adults, crinicerfont demonstrated substantial, dose-dependent reductions in ACTH, 17-OHP, and androstenedione levels. It also decreased the testosterone levels in female patients and reduced the androstenedione/testosterone ratio in the male. Remarkably, these effects occurred in the early morning, which is a notoriously difficult period for attaining effective disease management with physio-

logic GC regimens (22). Following this, another Phase II study in adolescent participants demonstrated comparable results, which is an important step for early intervention to support healthy development (24).

The CAHtalyst phase 3 trial included 182 participants (2:1 crinecerfont 100 mg vs placebo twice per day) across 54 international centres. The study involved a 24-week treatment period, beginning with 4 weeks of stable GC dosing to assess androstenedione reduction. During this initial phase, crinecerfont significantly decreased androstenedione concentrations (-47% active arm vs +7.7% for placebo). The following 20 weeks focused on GC dose optimisation to achieve the lowest dose while maintaining androstenedione control. By week 24, GC doses were reduced by 27.3% in the crinecerfont group compared with 10.3% in the placebo group. Notably, 62.7% of participants in the crinecerfont group reached physiological GC levels with androstenedione control, compared to 17.5% in the placebo. There was no increase in the incidence of adrenal crises. The commonly observed side effects were headache and fatigue (23). Similar benefits were demonstrated in the paediatric population. In a phase 3 study involving 103 paediatric participants, crinecerfont decreased androstenedione levels by 6.9 nmol/litre by week 4, while levels were elevated by 2.5 nmol/litre in the placebo. Crinecerfont reduced the GC dose by 18.0% to physiological levels while still controlling androstenedione levels. In comparison, the placebo group experienced a 5.6% increase in the GC dose (14). The results show that crinecerfont therapy enabled meaningful decreases in GC doses to physiological levels or decreases in androgen levels with stable GC dosing in both paediatric and adult patients with classic CAH. However, once GC doses were reduced in the phase 3 trial, there was a rebound increase in androgen levels. Further investigation is needed to determine if crinecerfont could lower GC doses to levels necessary for intensive management (23). Importantly, in December 2024, The U.S. Food and Drug Administration (FDA) granted approval for crinecerfont for use in conjunction with GCs in adult and paediatric patients aged 4 years and above diagnosed with CAH (25). This approval was focused solely on hyperandrogenism, rather than lowering GC doses.

Tildacerfont

Tildacerfont is an orally administered second-generation antagonist of the CRF1 receptor (Figure 1). It attaches selectively to CRF1 receptors located in the pituitary gland and has a strong affinity. Initially, it was proposed as a once-daily dosing regimen to differentiate it from Crinecerfont, which requires a twice-daily regimen. Two Phase 2 trials have demonstrated that tildacerfont might decrease the levels of ACTH, 17-OHP, and androstenedione in individuals with inadequately managed CAH. The initial study established a proof-of-concept through

the decrease in ACTH, and the results of the subsequent study further corroborated these findings. Patients with poorly controlled CAH at baseline experienced marked improvements in biomarkers while maintaining a stable dose of GC treatment, with some even reaching ACTH and androstenedione normalisation. However, in both studies, patients with a well-controlled disease only had slight biomarker improvements. Hence, their studies failed to show a robust efficacy. Longer-term studies will be needed to assess the clinical endpoints and the possibility of lowering GC dosages. Another concern is that tildacerfont was found to interact with dexamethasone, a commonly used medication in adult CAH management (26).

ACTH antagonists

Atumelnant (CRN04894)

Atumelnant (CRN04894) is a nonpeptide orally bioavailable small molecule. It is a potent and subtype-selective first-in-class antagonist of the ACTH receptor (27, 28). Atumelnant acts on the melanocortin 2 receptor (MC2R) located in the adrenal cortex (Figure 1). It inhibits the action of ACTH on this receptor and disrupts the downstream signaling cascade (28). In a placebo-controlled study of healthy participants, administering 80 mg of atumelnant once-daily for 10 days reduced the average 24-h serum cortisol by 51% and androstenedione levels by 40%, despite an approximately fivefold elevation in the 24-h average ACTH levels. Furthermore, the median 24-h urinary-free cortisol was reduced by 75% (29). Expanding upon these results, an ongoing phase 2 dose-finding study has been evaluating atumelnant in 30 adult patients with CAH (30). The preliminary findings indicate that a once-daily dose of 120 mg for 12 weeks led to an 80% reduction in androstenedione levels and a 65% decrease in 17-OHP concentrations (31). In contrast to the findings

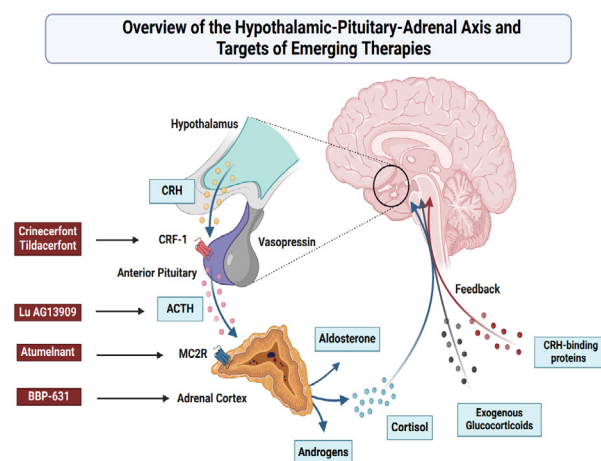


Figure 1: The figure depicts the hypothalamic–pituitary–adrenal axis and the targets of the novel emerging therapies

from the healthy participant trial, ACTH levels did not significantly change in patients with CAH (32). Remarkably, eight out of 13 female participants with elevated baseline testosterone levels achieved normalisation by week 12. Additionally, six of eleven affected female patients experienced a return of their regular menstrual cycles. The study also reported a significant decrease in the adrenal gland volume and androgen-related polycythaemia resolved in five of six affected participants (31). Overall, atumelnant was tolerated well. The most frequently reported adverse events were headache and fatigue (31, 32). These results are promising for its potential use for treating CAH.

Lu AG13909

Lu AG13909 is an IgG1 monoclonal antibody that targets ACTH with high affinity and specificity, thereby interrupting MC2R signaling (Figure 1) (33, 34). Taking this further, a Phase 1 study of Lu AG13909 is undergoing to evaluate its safety profile, tolerability, and efficacy. The study is being conducted in adult patients with CAH who have baseline elevated 17-OHP concentrations and are on a stable GC and MC regimen. Each participant receives up to six doses of intravenous Lu AG13909 over 28-to 35-day intervals (33, 35). Moreover, a Phase 2 trial is assessing the effects of Lu AG13909, administered both intravenously and subcutaneously, on cortisol concentrations in adult patients with Cushing's disease (36).

Gene therapy: BBP-631

BBP-631 is an investigational gene therapy using an AAV5 capsid serotype (AAV5) vector to deliver a functional copy of the single-stranded DNA of the human CYP21A2 transgene (Figure 1). This gene encodes the 21-OH enzyme (37, 38). In a CAH mouse model of 21-OH deficiency, BBP-631 therapy demonstrated early and durable effects in correcting the enzyme deficiency. It also achieved persistent human CYP21A2 gene expression in the adrenal cortex of non-human primates (37). Previous studies demonstrated that the correction of adrenal function was transient in animal models. These findings, along with the limitations of preclinical studies, raised concerns that advancing to clinical trials of gene therapy for CAH might have been premature (39). The Phase 1/2 study revealed that individuals with CAH could produce endogenous cortisol levels up to 11 µg/dL following the administration of BBP-631. Biochemical improvements supported the sustained effect of gene therapy. These included lasting elevations in the product of 21-OH, 11-deoxycortisol, which increased up to 99 times the baseline levels. The results demonstrated the promising potential of gene therapy for treating CAH. However, they did not meet the threshold required to continue investing in and developing BBP-631 for CAH, leading to the discontinuation of this program (40). This initial effort proved that CAH patients with complete 21-OH deficiency could syn-

thesise their own cortisol and that gene therapy could be safely administered. This approach requires long-term development efforts for dosing, duration optimisation, and long-term safety evaluation.

DISCUSSION

CAH is a significantly challenging and common endocrine disorder affecting both paediatric and adult populations. The current standard of care includes different formulations of GC and MC replacement with limited efficacy on ACTH and subsequent androgen level suppression. In adults, males generally do not seek much help and tend to lose follow-up. Females primarily seek help with infertility and hyperandrogenism. In the paediatric population, the unmet need is even higher with challenging growth and sexual development complications regardless of gender. Recently, there have been great efforts to increase awareness and willingness to treat rare genetic disorders. CAH is one of the most common genetic disorders, which is included in newborn screening. Recent efforts for drug development against CAH have focused on ACTH inhibition and hyperandrogenism with the hope of reducing GC dosing to prevent iatrogenic Cushing syndrome. Recently, crinecerfont was approved by the FDA to lower androgen levels in CAH and has been recorded as the first approved drug for any rare disorder in the last 70 years (41). This is a very encouraging development for the entire rare disease field. Even though crinecerfont offers a very promising and safe approach to lower androgen levels, it failed to achieve both the initial goals of lowering GC and androgen levels at the same time. The use of crinecerfont allowed for the reduction of GC doses to physiological levels (14, 22-24). It also effectively reduced androstenedione levels in two Phase 2 trials (22, 24). However, in the subsequent Phase 3 trial involving adults, the average androstenedione levels increased from 316 ng/dL to 607 ng/dL after the reduction of GC doses (23). The fact that average androgen levels only dropped by around 50% (not fully normalised) and that lowering GC doses caused rebound elevations suggests that the trialled regimen of 100 mg twice daily was perhaps not enough for maximum efficacy. The question remains whether the field will try higher doses in separate trials or pursue off-label use for severe cases. At the same time, any potential increase in adverse effects from dose escalation would need to be carefully evaluated. For now, this regimen adds two more pills to the patients' daily routine without decreasing the GC and MC doses. Hence, some patients might struggle with compliance due to the pill burden. Given the significant economic cost of the treatment, consideration should be given to individual patients and treatment goals when using crinecerfont in a hyperandrogenism-centric manner. We should also consider that the most common side effects of crinecerfont are fatigue, headache, dizziness, and low

appetite (42). These side effects are already bothersome for CAH patients with fluctuating GC dosing and overlap with the symptoms of adrenal insufficiency. Males with TART or females seeking help for infertility due to hyperandrogenism would be a prioritised special group to be treated, yet the potential outcome remains uncertain.

In another aspect, crinicerfont showed similar trends in insulin sensitivity and body weight across adult and paediatric trials. In adults, reductions in prolonged high-dose GC therapy improved weight and insulin sensitivity. However, these changes did not reach statistical significance. It is worth noting that these outcomes were secondary endpoints, and the 24-week duration of the trial may have been insufficient for a full assessment (23). Supporting this, in the paediatric trial, notable improvements in BMI and insulin resistance were observed. This occurred despite the limited duration of GC dose reduction (14). Variations in GC dose changes within the placebo groups may explain the discrepancy in statistical significance between the adult and paediatric populations. In the adult trial, the placebo group also reduced their GC dose, albeit less than the crinicerfont group. This potentially diminished the contrast between the two groups (23, 43). Conversely, in the paediatric trial, the placebo group slightly increased their baseline GC dose (14).

In summary, crinicerfont would be utilised significantly for hyperandrogenism, but atumelnant could offer some advantages with once-daily dosing and more direct inhibition of ACTH via its end-organ receptors (Figure 1). Atumelnant has also been evaluated for ACTH-dependent Cushing's syndrome and showed strong inhibition of ACTH despite very high circulating levels (4045 pg/mL) in an early Phase 1 trial (29, 44). It could be harder to lower actual ACTH synthesis and secretion but more likely to block its receptors. This approach might overcome the rebound elevation of androgens seen with crinicerfont, given its strong blockage of ACTH receptors. The mechanistic basis of its effectiveness is mediated by the selective antagonism of MC2R. Notably, this receptor is only expressed in the adrenal cortex (27, 45). Such specificity establishes its antagonism as a potentially optimal therapeutic strategy. Another promising finding from the initial results of the Phase 2 study is the improvement in androgen-mediated polycythaemia in most affected participants (31). This may reduce the cardiovascular risk, which is an important long-term complication for individuals with CAH (16, 17, 46). Additionally, the data showing that 55% of affected women experienced spontaneous return of their menses is promising for infertility indication. However, its true clinical impact will depend on outcomes from advanced trials, particularly Phase 3 studies, which aim to determine whether sufficient androgen suppression can be achieved under reduced GC dosing. One important point for consideration is the ho-

mology MC2R shares with other melanocortin receptors, specifically 45% with MC3R and 38% with MC4R (27, 47). Off-target binding appears less likely given these low homology rates and its target specificity. However, this is particularly concerning because of the risk of adverse effects mediated through MC3R or MC4R activation, which would affect food intake and energy expenditure. Although ACTH elevation was observed in the Phase 1 study (29), no such increase was seen in the initial results of the Phase 2 study (32). It will be important to monitor whether ACTH elevation occurs in the remaining Phase 2 and upcoming Phase 3 trials. If persistent ACTH elevation is noted in subsequent studies, the potential downstream effects, including the risk of hyperpigmentation, will require careful evaluation (48). The consequences of elevated, long-standing circulating ACTH levels are unknown in the setting of blocked MC2R. Some literature indicates adrenal gland-independent effects of ACTH, which will require careful consideration in the long term (49). In summary, a comparison with simulations from the stoichiometry of atumelnant dose-response studies suggests that the ACTH increase in a setting of lower GC dosing might not result in a rebound increase in androgen levels if MC2R is fully or mostly blocked. This approach could address the current unmet need of lowering both GC doses and androgen levels simultaneously.

Another emerging therapy, Lu AG13909, represents a first-in-class anti-ACTH monoclonal that disrupts MC2R signaling (33). Unlike atumelnant, it neutralises ACTH-driven signaling across all five melanocortin receptor subtypes (34). This raises concerns about potential unintended adverse effects from interactions with melanocortin receptors other than MC2R. Future clinical trials will need to carefully evaluate this possibility.

Finally, although gene therapy treatments represent the most promising approach with their potential to provide a curative solution, the development of BBP-631 has been discontinued by the manufacturing company (40). Regrettably, the regenerative nature of the adrenal cortex poses a significant challenge for achieving sustained benefit with recombinant adeno-associated viral vector gene therapy for CAH. The constant cellular renewal within the adrenal gland makes it difficult to maintain genetic modifications over the long term (50). Overcoming this physiological barrier may require innovative strategies to realise the full potential of gene therapy. However, findings from the trial reported increased cortisol production and durable BBP-631 transgene activity. These findings show that the challenge may be surmountable (40). Recent advancements in gene editing technologies might help create alternative strategies for AAV gene delivery. Moving forward, further studies will provide guidance in understanding the efficacy and durability of gene therapies.

CONCLUSION

The management of CAH due to 21-OH deficiency remains a significant challenge, as current treatments, though effective, are suboptimal and linked to long-term adverse outcomes. Pipeline therapies, such as ACTH and CRF1 receptor antagonists, demonstrate the potential to normalise adrenal androgen levels without requiring supraphysiological GC doses. We recommend that clinicians educate their patients about the long-term risks of GC overdose, prefer hydrocortisone, and attempt to titrate down to physiological doses. An additional night-time dose of dexamethasone, a long-acting GC, is commonly used for ACTH suppression but contributes to GC-related harm. Instead, clinicians should consider using novel agents such as crinecerfont to lower androgen levels. Treatment goals should be personalised, and patients should be informed about newer treatments. Higher doses of crinecerfont have not been tested, leaving an open question for researchers. Atumelnant has promising early data but has not been tested in a setting of lowered GC dosing; hence, more investigation is needed in a timely manner. These newer agents are expensive and require insurance authorization. Therefore, advocacy for access is also critical. Moreover, gene therapies hold curative potential but require more collective efforts to bring them into clinical practice. Importantly, the long-term safety and efficacy of these emerging approaches remain to be fully elucidated.

Peer Review: Externally peer-reviewed.

Author Contributions: Conception/Design of Study- M.F.B.; Data Acquisition- M.F.B., E.Ç.; Drafting Manuscript- M.F.B., E.Ç.; Critical Revision of Manuscript- M.F.B.; Final Approval and Accountability- M.F.B., E.Ç.; Technical or Material Support- M.F.B.; Supervision- M.F.B.

Acknowledgements: We thank all the patient advocacy organisations and rare disease researchers, and clinicians for their invaluable contributions to CAH patients. Figure 1 was created using BioRender (Çetin, E. (2025) <https://BioRender.com/f70g748>).

Conflict of Interest: The authors have no conflict of interest to declare.

Financial Disclosure: The authors declared that this study received no financial support.

REFERENCES

- Merke DP, Auchus RJ. Congenital adrenal hyperplasia due to 21-Hydroxylase deficiency. *N Engl J Med* 2020;383(13):1248-61. [CrossRef]
- El-Maouche D, Arlt W, Merke DP. Congenital adrenal hyperplasia. *Lancet* 2017;390(10108):2194-210. [CrossRef]
- Prete A, Auchus RJ, Ross RJ. Clinical advances in the pharmacotherapy of congenital adrenal hyperplasia. *Eur J Endocrinol* 2021;186(1):R1-14. [CrossRef]
- Pofi R, Ji X, Krone NP, Tomlinson JW. Long-term health consequences of congenital adrenal hyperplasia. *Clin Endocrinol (Oxf)* 2024;101(4):318-31. [CrossRef]
- Nordenstrom A, Lajic S, Falhammar H. Long-term outcomes of congenital adrenal hyperplasia. *Endocrinol Metab (Seoul)* 2022;37(4):587-98. [CrossRef]
- Lee HH, Kuo JM, Chao HT, Lee YJ, Chang JG, Tsai CH, et al. Carrier analysis and prenatal diagnosis of congenital adrenal hyperplasia caused by 21-hydroxylase deficiency in Chinese. *J Clin Endocrinol Metab* 2000;85(2):597-600. [CrossRef]
- Pang S, Murphey W, Levine LS, Spence DA, Leon A, LaFranchi S, et al. A pilot newborn screening for congenital adrenal hyperplasia in Alaska. *J Clin Endocrinol Metab* 1982;55(3):413-20. [CrossRef]
- Speiser PW, Arlt W, Auchus RJ, Baskin LS, Conway GS, Merke DP, et al. Congenital adrenal hyperplasia due to steroid 21-hydroxylase deficiency: an endocrine society clinical practice guideline. *J Clin Endocrinol Metab* 2018;103(11):4043-88. [CrossRef]
- Merke DP, Mallappa A, Arlt W, Brac de la Perriere A, Linden Hirschberg A, Juul A, et al. Modified-release hydrocortisone in congenital adrenal hyperplasia. *J Clin Endocrinol Metab* 2021;106(5):e2063-77. [CrossRef]
- Mallappa A, Merke DP. Management challenges and therapeutic advances in congenital adrenal hyperplasia. *Nat Rev Endocrinol* 2022;18(6):337-52. [CrossRef]
- Yogi A, Kashimada K. Current and future perspectives on clinical management of classic 21-hydroxylase deficiency. *Endocr J* 2023;70(10):945-57. [CrossRef]
- Sheng JA, Bales NJ, Myers SA, Bautista AI, Roueinfar M, Hale TM, et al. The Hypothalamic-pituitary-adrenal axis: development, programming actions of hormones, and maternal-fetal interactions. *Front Behav Neurosci* 2020;14:601939. [CrossRef]
- Smith SM, Vale WW. The role of the hypothalamic-pituitary-adrenal axis in neuroendocrine responses to stress. *Dialogues Clin Neurosci* 2006;8(4):383-95. [CrossRef]
- Sarafoglou K, Kim MS, Lodish M, Felner EI, Martinerie L, Nokoff NJ, et al. Phase 3 trial of crinecerfont in pediatric congenital adrenal hyperplasia. *N Engl J Med* 2024;391(6):493-503. [CrossRef]
- Kulshreshtha B, Eunice M, Ammini AC. Pubertal development among girls with classical congenital adrenal hyperplasia initiated on treatment at different ages. *Indian J Endocrinol Metab* 2012;16(4):599-603. [CrossRef]
- Torky A, Sinaii N, Jha S, Desai J, El-Maouche D, Mallappa A, et al. Cardiovascular disease risk factors and metabolic morbidity in a longitudinal study of congenital adrenal hyperplasia. *J Clin Endocrinol Metab* 2021;106(12):e5247-57. [CrossRef]
- Barbot M, Mazzeo P, Lazzara M, Ceccato F, Scaroni C. Metabolic syndrome and cardiovascular morbidity in patients with congenital adrenal hyperplasia. *Front Endocrinol (Lausanne)* 2022;13:934675. [CrossRef]
- Li L, Bensing S, Falhammar H. Rate of fracture in patients with glucocorticoid replacement therapy: a systematic review and meta-analysis. *Endocrine* 2021;74(1):29-37. [CrossRef]
- Sun X, Wu Y, Lu L, Xia W, Zhang L, Chen S, et al. Bone microarchitecture and volumetric mineral density assessed by HR-pQCT in patients with 21- and 17alpha-hydroxylase deficiency. *Calcif Tissue Int* 2023;113(5):515-25. [CrossRef]

20. Nerموen I, Falhammar H. Prevalence and characteristics of adrenal tumors and myelolipomas in congenital adrenal hyperplasia: a systematic review and meta-analysis. *Endocr Pract* 2020;26(11):1351-65. [CrossRef]
21. Claahsen-van der Grinten HL, Stikkelbroeck N, Falhammar H, Reisch N. Management of endocrine disease: Gonadal dysfunction in congenital adrenal hyperplasia. *Eur J Endocrinol* 2021;184(3):R85-97. [CrossRef]
22. Auchus RJ, Sarafoglou K, Fechner PY, Vogiatzi MG, Imel EA, Davis SM, et al. Crinicerfont lowers elevated hormone markers in adults with 21-hydroxylase deficiency congenital adrenal hyperplasia. *J Clin Endocrinol Metab* 2022;107(3):801-12. [CrossRef]
23. Auchus RJ, Hamidi O, Pivonello R, Bancos I, Russo G, Witchel SF, et al. Phase 3 trial of crinicerfont in adult congenital adrenal hyperplasia. *N Engl J Med* 2024;391(6):504-14. [CrossRef]
24. Newfield RS, Sarafoglou K, Fechner PY, Nokoff NJ, Auchus RJ, Vogiatzi MG, et al. Crinicerfont, a CRF1 receptor antagonist, lowers adrenal androgens in adolescents with congenital adrenal hyperplasia. *J Clin Endocrinol Metab* 2023;108(11):2871-8. [CrossRef]
25. U.S. Food and Drug Administration. FDA approves new treatment for congenital adrenal hyperplasia 2024. 01.20.2025. <https://www.fda.gov/news-events/press-announcements/fda-approves-new-treatment-congenital-adrenal-hyperplasia>.
26. Sarafoglou K, Barnes CN, Huang M, Imel EA, Madu IJ, Merke DP, et al. Tildacerfont in adults with classic congenital adrenal hyperplasia: results from two phase 2 studies. *J Clin Endocrinol Metab* 2021;106(11):e4666-79. [CrossRef]
27. Kim SH, Han S, Zhao J, Wang S, Kusnetzow AK, Reinhart G, et al. Discovery of CRN04894: A novel potent selective MC2R antagonist. *ACS Med Chem Lett* 2024;15(4):478-85. [CrossRef]
28. Fowler MA, Kusnetzow AK, Han S, Reinhart G, Kim SH, Johns M, et al. Effects of CRN04894, a nonpeptide orally bioavailable ACTH antagonist, on corticosterone in rodent models of ACTH excess. *J Endocr Soc* 2021;5(Supplement_1):A167. [CrossRef]
29. Trainer P, Ferrara-Cook C, Ayala A, Luo R, Miller S, Wang Y, et al. CRN04894: an oral, nonpeptide adrenocorticotrophic hormone (ACTH) receptor antagonist decreases basal and stimulated cortisol secretion in healthy volunteers. *Endocrine Abstracts* 2022;86:344. [CrossRef]
30. ClinicalTrials.gov. Evaluate the safety, efficacy, and pharmacokinetics of CRN04894 in participants with congenital adrenal hyperplasia (TouCAHn). 11.03.2024. <https://clinicaltrials.gov/study/NCT05907291?term=NCT05907291&rank=1>.
31. Pharmaceuticals C. Topline phase 2 results from atumelant in congenital adrenal hyperplasia (CAH). 17.01.2025. <https://ir.crinetics.com/static-files/62ecfe1f-0938-4de5-a73e-0436f5ecd127>.
32. Auchus RJ, Trainer PJ, Lucas KJ, Bruera D, Marko J, Ayala A, et al. 12537 Once daily oral atumelant (CRN04894) induces rapid and profound reductions of androstenedione and 17-hydroxyprogesterone in participants with classical congenital adrenal hyperplasia: initial results from a 12-week, phase 2, open-label study. *J Endocr Soc* 2024;8(Supplement_1):bvae163.249. [CrossRef]
33. Srirangalingam U, Velusamy A, Louise Binderup M, Baker B, Folden Flensburg M, Pickering Boserup L, et al. 12484 safety and pharmacokinetics of Anti-ACTH antibody Lu AG13909 in patients with classic congenital adrenal hyperplasia: phase 1 open-label, multiple-ascending-dose trial protocol. *J Endocr Soc* 2024;8(Supplement_1):bvae163.285. [CrossRef]
34. Feldhaus AL, Anderson K, Dutzar B, Ojala E, McNeill PD, Fan P, et al. ALD1613, a novel long-acting monoclonal antibody to control ACTH-Driven pharmacology. *Endocrinology* 2016;158(1):1-8. [CrossRef]
35. ClinicalTrials.gov. Study of Lu AG13909 in participants with congenital adrenal hyperplasia. 11.04.2024. <https://clinicaltrials.gov/study/NCT05669950?term=Lu%20AG13909&rank=1>.
36. ClinicalTrials.gov. A Trial of Lu AG13909 in Adult Participants With Cushing's Disease (BalanCeD). 11.04.2024. <https://clinicaltrials.gov/study/NCT06471829?term=Lu%20AG13909&rank=2>.
37. Merke DP, Auchus RJ, Sarafoglou K, Geffner ME, Kim MS, Escandon RD, et al. Design of a phase 1/2 open-label, dose-escalation study of the safety and efficacy of gene therapy in adults with classic congenital adrenal hyperplasia (CAH) due to 21-hydroxylase deficiency through administration of an adeno-associated virus (AAV) serotype 5-based recombinant vector encoding the human CYP21A2 gene. *J Endocr Soc* 2021;5(Suppl_1):A82. [CrossRef]
38. Bharucha K, Weinstein D, Kirby K, Auchus R, Geffner M, Kim M, et al. ODP046 Initial lessons from a prescreening protocol to identify participants with classic CAH potentially eligible for gene therapy treatment with BBP-631, an adeno-associated virus (AAV) serotype 5-based recombinant vector encoding the human CYP21A2 gene. *J Endocr Soc* 2022;6(Suppl_1):A60-1. [CrossRef]
39. White PC. Emerging treatment for congenital adrenal hyperplasia. *Curr Opin Endocrinol Diabetes Obes* 2022;29(3):271-6. [CrossRef]
40. Philippidis A. Astellas Shutting Gene Therapy facility in South San Francisco, CA. *Hum Gene Ther* 2024;35(19-20):777-80. [CrossRef]
41. Halsey G. FDA Approves Crinicerfont for Congenital Adrenal Hyperplasia in Adults and Children in Landmark Decision. *Patient Care (Online)*. 2024.
42. U.S. Food and Drug Administration. Highlights of prescribing information. 01.29.2025. https://www.accessdata.fda.gov/drugsatfda_docs/label/2024/218808s000,218820s000lbl.pdf.
43. Auchus RJ, Sturgeon J, Lin VH. Crinicerfont in adult congenital adrenal hyperplasia. Reply. *N Engl J Med* 2024;391(16):1557-8. [CrossRef]
44. Elenius H, McGlotten R, Moore C, Ayala A, Wu Y, Trainer PJ, et al. Atumelant (CRN04894) induces rapid and sustained reductions in serum and urine cortisol in patients with ACTH-Dependent Cushing Syndrome during a phase 1b/2a, single center, 10-day, inpatient, open-label study. 01.29.2025. https://crinetics.com/wp-content/uploads/2024/05/Elenius-et-al_ENDO2024_CS-Poster_FINAL.pdf. [CrossRef]
45. Malik S, Dolan TM, Maben ZJ, Hinkle PM. Adrenocorticotrophic hormone (ACTH) responses require actions of the melanocortin-2 receptor accessory protein on the extracellular surface of the plasma membrane. *J Biol Chem* 2015;290(46):27972-85. [CrossRef]

46. Ory J, Nackeeran S, Balaji NC, Hare JM, Ramasamy AR. Secondary Polycythemia in men receiving testosterone therapy increases risk of major adverse cardiovascular events and venous thromboembolism in the first year of therapy. *J Urol* 2022;207(6):1295-301. [\[CrossRef\]](#)
47. Yang Y. Structure, function and regulation of the melanocortin receptors. *Eur J Pharmacol* 2011;660(1):125-30. [\[CrossRef\]](#)
48. Hunt G, Donatien PD, Lunec J, Todd C, Kyne S, Thody AJ. Cultured human melanocytes respond to MSH peptides and ACTH. *Pigment Cell Res* 1994;7(4):217-21. [\[CrossRef\]](#)
49. Hasenmajer V, Bonaventura I, Minnetti M, Sada V, Sbardella E, Isidori AM. Non-canonical effects of ACTH: Insights into adrenal insufficiency. *Front Endocrinol (Lausanne)* 2021;12:701263. [\[CrossRef\]](#)
50. van Dijk EB, Ginn SL, Alexander IE, Graves LE. Genome editing in the adrenal gland: a novel strategy for treating congenital adrenal hyperplasia. *Exploration of Endocrine and Metabolic Diseases* 2024;1(3):101-21. [\[CrossRef\]](#)

EPIGENETIC REGULATION BY CURCUMIN IN OVARIAN CANCER: A FOCUS ON miRNA NETWORKS, HISTONE MODIFICATIONS AND DNA METHYLATION

OVER KANSERİNDE KURKUMİN İLE EPİGENETİK DÜZENLEME: miRNA AĞLARI, HISTON MODİFİKASYONLARI VE DNA METİLASYONU ÜZERİNE BİR İNCELEME

Özlem TİMİRCİ KAHRAMAN¹ , Deryanaz BİLLUR^{1,2} , Esin BAYRALI ÜLKER^{1,2,3} 

¹Istanbul University, Aziz Sancar Institute of Experimental Medicine, Department of Molecular Medicine, İstanbul, Türkiye

²Istanbul University, Institute of Graduate Studies in Health Sciences, Department of Molecular Medicine, İstanbul, Türkiye

³The Ohio State University, James Comprehensive Cancer Center, College of Medicine, Columbus, OH, USA

ORCID IDs of the authors: Ö.T.K. 0000-0002-2641-5613; D.B. 0000-0002-6079-8224; E.B.Ü. 0000-0001-8457-1430

Cite this article as: Timirci Kahraman Ö, Billur D, Bayralı Ülker E. Epigenetic regulation by curcumin in ovarian cancer: A focus on miRNA networks, histone modifications and DNA methylation. J Ist Faculty Med 2025;88(2):164-171. doi: 10.26650/IUITFD.1631708

ABSTRACT

Ovarian cancer remains a leading cause of gynaecological cancer-related deaths, driven by its late-stage diagnosis, high metastatic potential, and frequent development of chemoresistance. Current therapeutic strategies often fail to address the intricate mechanisms underlying tumour progression, necessitating innovative approaches. Curcumin, a bioactive polyphenol derived from *Curcuma longa*, has emerged as a potent epigenetic regulator with multifaceted anticancer properties. This review highlights curcumin's ability to modulate key epigenetic mechanisms such as microRNA (miRNA/miR) regulation, histone modifications, and DNA methylation, which are central to ovarian cancer pathogenesis. Curcumin selectively reprograms miRNA networks, restoring tumour-suppressive miRNAs while downregulating oncogenic miRNAs, thereby mitigating epithelial-mesenchymal transition and chemoresistance. In addition, curcumin inhibits histone deacetylase (HDACs) and EZH2-mediated histone methylation, reactivating critical tumour-suppressor genes like *BRCA1*. Through its suppression of DNA methyltransferase (DNMT) activity, curcumin reverses promoter hypermethylation, further enhancing tumour-suppressor gene expression. These synergistic epigenetic modulations disrupt oncogenic pathways, improve chemotherapy sensitivity, and restore the immune recognition of tumour cells. Despite its promise, poor bioavailability limits the clinical translation of curcumin, but advanced formulations, including nanoparticles

ÖZET

Over kanseri, geç evrede teşhis edilmesi, yüksek metastaz potansiyeli ve genellikle gelişen kemoterapi direnci nedeniyle, jinekolojik kanserlerden kaynaklanan ölümlerin başlıca nedenlerinden biri olmaya devam etmektedir. Mevcut tedavi yaklaşımları, tümör ilerlemesinin altında yatan karmaşık mekanizmaları yeterince ele alamamakta ve bu durum yenilikçi stratejilere olan ihtiyacı ortaya koymaktadır. Zerdeçalın (*Curcuma longa*) biyoaktif bir polifenolü olan kurkumin, çok yönlü anti-kanser özellikleri ile güçlü bir epigenetik düzenleyici olarak öne çıkmıştır. Bu derlemede, kurkuminin over kanseri patogenezinde önemli rol oynayan mikroRNA (miRNA/miR) düzenlemesi, histon modifikasyonları ve DNA metilasyonu gibi temel epigenetik mekanizmaları nasıl modüle ettiğine dikkat çekilmektedir. Kurkumin, tümör baskılayıcı miRNA'ları yukarı regüle ederken, onkogenik miRNA'ları aşağı regüle ederek miRNA ağlarını seçici şekilde yeniden programlamaktadır. Bu sayede, epitel-mezenkimal dönüşümü ve kemoterapi direncini azaltabilmektedir. Ayrıca, kurkumin, histon deasetilazları (HDAC'ler) ve EZH2 aracılı histon metilasyonunu inhibe ederek, *BRCA1* gibi kritik tümör baskılayıcı genlerin yeniden aktivasyonunu sağlamaktadır. DNA metiltransferaz (DNMT) aktivitesini baskılayarak, promotör hipermetilasyonunu tersine çevirmekte ve tümör baskılayıcı gen ekspresyonunu artırmaktadır. Kurkuminden kaynaklanan bu sinerjik epigenetik düzenlemeler, onkogenik yolları engellemekte, kemoterapi duyarlılığını artırmakta ve tümör hücrelerinin bağışıklık sistemi tarafından tanınmasını sağlamaktadır. Ancak,

Corresponding author/İletişim kurulacak yazar: Özlem TİMİRCİ KAHRAMAN – ozlemtk@istanbul.edu.tr

Submitted/Başvuru: 03.02.2025 • **Revision Requested/Revizyon Talebi:** 03.03.2025 •

Last Revision Received/Son Revizyon: 06.03.2025 • **Accepted/Kabul:** 07.03.2025 • **Published Online/Online Yayın:** 08.04.2025



Content of this journal is licensed under a Creative Commons Attribution-NonCommercial 4.0 International License.

and liposomes, overcome this limitation. Further research is essential to optimise delivery systems, elucidate long-term epigenetic effects, and validate therapeutic efficacy through clinical trials. This review underscores curcumin's potential to enhance current ovarian cancer therapies by addressing the critical epigenetic mechanisms involved in tumour progression and resistance.

Keywords: Ovarian cancer, curcumin, epigenetics

INTRODUCTION

Ovarian cancer presents a multifaceted challenge to global health. Its high mortality rate, particularly due to late-stage diagnosis, necessitates a concerted effort to improve early detection strategies (1). Furthermore, the significant impact on women's reproductive health and psychological well-being demands a comprehensive approach that tackles not only the physical symptoms of the condition but also the emotional and social challenges faced by those affected (2). Continued research into the underlying biological mechanisms, coupled with the development of personalised treatment plans, is crucial to improve patient outcomes and ultimately reduce the global burden of this devastating malignancy (1).

Ovarian cancer presents significant therapeutic challenges, primarily due to chemoresistance and the propensity for metastasis (3). Chemoresistance, which refers to the capacity of cancer cells to resist the effects of chemotherapy, poses a significant barrier to attaining sustained remission and effective treatment outcomes (4). The mechanisms driving chemoresistance are intricate and multifaceted, encompassing changes in drug absorption, metabolic processes, DNA repair mechanisms, and pathways regulating programmed cell death (5). Moreover, ovarian cancer exhibits a high propensity for metastasis, spreading to distant sites such as the peritoneum, liver, and lungs (6). This metastatic spread significantly contributes to treatment failure and poor patient outcomes. The development of novel therapeutic strategies that can overcome chemoresistance and effectively target metastatic disease remains a critical area of research in ovarian cancer management.

Derived from the rhizome of *Curcuma longa* (turmeric), curcumin, a vibrant yellow pigment, has attracted considerable scientific interest for its diverse pharmacological properties, particularly its significant anti-cancer effects (7). As a polyphenol compound, curcumin exerts its anti-cancer activities through multiple mechanisms, such as inhibiting cell proliferation, inducing programmed cell death, suppressing new blood vessel formation, and modulating various signaling pathways implicated

in tumorigenesis (Figure 1) (8). Curcumin effectively inhibits tumour growth through a multifaceted approach. It interacts with and regulates several key signaling pathways, including PI3K/AKT/mTOR, STAT, and NF- κ B. This involves targeting key cellular processes: apoptosis (through *BCL2* and caspases), cell cycle regulation (via cyclins and CDKs), growth factor signaling (involving *VEGF* and *EGF*), and cytokine production (like interleukins) (8). Furthermore, curcumin exerts a profound impact on gene expression by influencing non-coding RNAs and modifying epigenetic mechanisms, contributing to its broad spectrum of therapeutic benefits (9). As essential regulators of gene expression, microRNAs (miRNAs/miRs) – small, non-coding RNA molecules – are crucial in influencing the behaviour and progression of cancer cells. Our 2024 study demonstrated the potential of curcumin and desmethoxycurcumin to enhance the efficacy of cisplatin in ovarian cancer treatment. Reduced *GSTP-1* and miR-133b levels in cisplatin-resistant cells may contribute to drug resistance, making them potential as therapeutic targets. Dysregulation of miRNAs, such as the observed decrease in miR-133b and its target gene *GSTP-1* in cisplatin-resistant ovarian cancer cells, contributes significantly to tumour development and progres-

Anahtar kelimeler: Over kanseri, kurkumin, epigenetik

in tumorigenesis (Figure 1) (8). Curcumin effectively inhibits tumour growth through a multifaceted approach. It interacts with and regulates several key signaling pathways, including PI3K/AKT/mTOR, STAT, and NF- κ B. This involves targeting key cellular processes: apoptosis (through *BCL2* and caspases), cell cycle regulation (via cyclins and CDKs), growth factor signaling (involving *VEGF* and *EGF*), and cytokine production (like interleukins) (8). Furthermore, curcumin exerts a profound impact on gene expression by influencing non-coding RNAs and modifying epigenetic mechanisms, contributing to its broad spectrum of therapeutic benefits (9). As essential regulators of gene expression, microRNAs (miRNAs/miRs) – small, non-coding RNA molecules – are crucial in influencing the behaviour and progression of cancer cells. Our 2024 study demonstrated the potential of curcumin and desmethoxycurcumin to enhance the efficacy of cisplatin in ovarian cancer treatment. Reduced *GSTP-1* and miR-133b levels in cisplatin-resistant cells may contribute to drug resistance, making them potential as therapeutic targets. Dysregulation of miRNAs, such as the observed decrease in miR-133b and its target gene *GSTP-1* in cisplatin-resistant ovarian cancer cells, contributes significantly to tumour development and progres-



Figure 1: The figure depicts the various mechanisms through which curcumin exerts its anti-cancer effects in ovarian cancer

sion, particularly by promoting drug resistance (10). This highlights the potential of targeting miRNAs to enhance the efficacy of cancer treatments.

Curcumin's anti-cancer properties in ovarian cancer

Curcumin has emerged as a promising anti-cancer agent because of its multifaceted influence on cellular processes. Beyond its anti-oxidant and anti-inflammatory actions, curcumin demonstrates remarkable versatility in modulating gene expression. By downregulating oncogenes like *NF-κB* while simultaneously upregulating tumour suppressors such as *p53*, curcumin disrupts the delicate balance that favours tumour growth (11, 12). This intricate orchestration of gene regulation translates into a cascade of anti-cancer effects, including the inhibition of cell proliferation, induction of apoptosis, and suppression of angiogenesis, all of which are critical steps in cancer development. Furthermore, curcumin's ability to temper chronic inflammation, a significant contributor to cancer risk, underscores its potential to effectively combat the tumour microenvironment and impede disease progression (13).

Curcumin and chemosensitization

Reduction of the chemoresistance mechanisms

A significant obstacle in managing ovarian cancer is the emergence of resistance to chemotherapy. In this state, cancer cells undergo alterations that enable them to evade the cytotoxic effects of chemotherapy medications, thereby limiting the effectiveness of these treatments (14). Curcumin offers a hopeful avenue for surmounting this obstacle (12). Studies have indicated that curcumin may have the potential to improve the response of ovarian cancer cells to chemotherapy treatments by targeting and overcoming mechanisms that enable cancer cells to resist the effects of these drugs (15). Curcumin has been shown to counteract chemoresistance in ovarian cancer by inhibiting cellular efflux pumps. These transporters, including P-glycoprotein, actively pump chemotherapeutic agents out of cancer cells, thereby reducing drug efficacy. Curcumin's ability to inhibit these efflux pumps leads to increased intracellular drug accumulation, thereby enhancing the effectiveness of chemotherapy in treating ovarian cancer. Additionally, it interferes with the mechanisms that cancer cells use to repair DNA damage, making them more vulnerable to cell death. This multifaceted approach increases the potency of conventional chemotherapy, potentially resulting in better treatment outcomes in individuals with ovarian cancer (16).

Modulation of the key signaling pathways

PI3K/Akt/mTOR pathway modulation by curcumin

The PI3K/Akt/mTOR signaling pathway is crucial in controlling cellular processes such as proliferation, survival, and metabolism. However, in cancers like ovarian cancer, this pathway often exhibits aberrant activation, driv-

en by genetic alterations such as *PIK3CA* mutations or *PTEN* loss. This aberrant activation drives tumorigenesis, promotes metastatic dissemination, and contributes to resistance to conventional therapies (17). Curcumin has emerged as a promising therapeutic agent due to its multifaceted mechanisms of action, including the modulation of the PI3K/Akt/mTOR pathway (18). Curcumin exerts its effects on this pathway through various actions. It can directly target and suppress the key components of the pathway. Furthermore, it can influence upstream regulators that control the activity of these components. Notably, curcumin can also stimulate a counteracting mechanism that helps to dampen the activity of the pathway. Furthermore, curcumin can induce autophagy, a cellular process that can contribute to tumour cell death, by inhibiting *mTORC1* activity. By targeting this critical pathway, curcumin demonstrates significant anti-proliferative and pro-apoptotic effects in ovarian cancer cells, offering a potential adjuvant therapeutic strategy for this challenging malignancy. A key mechanism underlying curcumin's anti-cancer effects in ovarian cancer involves the modulation of the PI3K/Akt/mTOR signaling pathway. The function of this pathway is indispensable for supporting essential cellular activities, such as cell growth, proliferation, and the ability of cells to survive and thrive (17).

STAT3/NF-κB/iNOS/COX-2 signaling pathway

Curcumin has been shown to effectively modulate this pathway, which is a key contributor to inflammation and tumorigenesis in ovarian cancer (18). This pathway plays a critical role in promoting cell proliferation, survival, and angiogenesis. It exerts its inhibitory effects by suppressing the activation of *STAT3* and *NF-κB*, key transcription factors that regulate the expression of downstream inflammatory mediators such as *iNOS* (inducible nitric oxide synthase) and *COX-2* (cyclooxygenase-2). By downregulating this pathway, curcumin can effectively inhibit tumour growth, induce apoptosis, and suppress tumour invasion and metastasis. This multifaceted modulation of inflammatory signaling pathways highlights the significant therapeutic potential of curcumin in ovarian cancer management (18).

The intricate interplay of signaling pathways, including *STAT3* and *NF-κB*, plays a pivotal role in orchestrating the complex cascade of events that underpin malignant transformation. The aberrant activation of *NF-κB*, a key regulator of inflammatory responses, drives the overexpression of pro-inflammatory factors such as *COX-2*, *iNOS*, cytokines (including *TNF-α*), and other inflammatory mediators, thereby fostering a pro-tumorigenic microenvironment (18, 19). Curcumin, a polyphenol derived from turmeric, has emerged as a compelling therapeutic candidate due to its ability to effectively modulate these critical signaling pathways. By inhibiting *NF-κB* activa-

tion, curcumin suppresses the expression of downstream target genes such as *p53*, *VEGF*, *Bcl-2*, *COX-2*, *iNOS*, *cyclin D1*, *TNF- α* , interleukins, and *MMP-9*, thereby exerting anti-proliferative and anti-metastatic effects (18). This inhibitory action extends to the *STAT3* pathway, further contributing to the suppression of tumour growth and metastasis. Mechanistically, curcumin inhibits the DNA-binding capacity of *NF- κ B* by altering its subunit composition, while simultaneously downregulating *AP-1* transcription factors. Furthermore, in preclinical models, curcumin has been demonstrated to induce apoptosis through the activation of caspase-3, an effect closely associated with the inhibition of *NF- κ B* activity and the subsequent downregulation of *COX-2* and *cyclin D1* expression (18). These findings collectively underscore the significant potential of curcumin as a therapeutic agent in various cancers by effectively targeting and disrupting the intricate network of signaling pathways that drive tumorigenesis and progression.

NF- κ B/PRL-3 pathway and its impact on tumour proliferation and migration

The signaling pathway involving *NF- κ B* and *PRL-3* plays a significant role in the aggressive behaviour of ovarian tumours. Curcumin can disrupt this pathway. *NF- κ B*, a protein that regulates gene expression, is often abnormally active in ovarian cancers. This excessive activity stimulates the production of various genes that promote tumour growth, including the gene for *PRL-3* (20). *PRL-3*, an enzyme that removes phosphate groups from proteins, has been implicated in the progression of various cancers, including ovarian cancer. This enzyme has been shown to contribute to key aspects of cancer development, such as uncontrolled cell growth, metastasis, and the ability of cancer cells to penetrate and invade surrounding tissues (21). Curcumin inhibits *NF- κ B* activation, leading to a subsequent downregulation of *PRL-3* expression. By targeting this critical signaling axis, curcumin may effectively suppress tumour growth and metastasis in ovarian cancer. Curcumin nanoparticles (CUR-NPs) are emerging as a novel therapeutic approach in ovarian cancer treatment. Studies have shown that CUR-NPs can effectively inhibit tumour growth and metastasis by targeting the *NF- κ B/PRL-3* signaling pathway. By suppressing the overactivation of *NF- κ B* and consequently downregulating *PRL-3* expression, CUR-NPs demonstrate a promising strategy for developing innovative and targeted therapies for ovarian cancer (22).

Curcumin-induced ferroptosis

Ferroptosis, a regulated form of cell death driven by iron, is gaining attention as a potential therapeutic approach for ovarian cancer. It was first described in 2012 by Dixon et al., and is characterised by lipid peroxidation, iron overload, and glutathione depletion (23). Curcumin, a natural substance found in turmeric, has powerful anti-cancer effects. This includes its ability to induce ferroptosis, a

cell death process that can selectively eliminate cancer cells (24). The mechanisms underlying curcumin-induced ferroptosis in ovarian cancer are likely multifaceted and may involve the disruption of cellular redox homeostasis through the depletion of glutathione and the inhibition of glutathione peroxidase 4 (*GPX4*). This results in the buildup of lipid peroxidation byproducts and reactive oxygen species, eventually causing oxidative stress and cellular death. Furthermore, curcumin may modulate iron metabolism within cancer cells, potentially increasing iron availability and worsening ferroptosis. Understanding the precise mechanisms of curcumin-induced ferroptosis in ovarian cancer is crucial for optimising its therapeutic potential and developing novel therapeutic strategies that exploit this unique form of cell death (25).

Curcumin derivative NL01 and ferroptosis induction through HCAR1/MCT1 signaling

NL01, a potent curcumin derivative, induces ferroptosis in ovarian cancer cells by targeting the *HCAR1/MCT1* signaling axis (25-28). *HCAR1* (hydroxycarboxylic acid receptor 1) and *MCT1* (monocarboxylate transporter 1) are critical for cellular metabolism. By disrupting this axis, NL01 disrupts cellular metabolism, leading to iron accumulation and lipid peroxidation, ultimately triggering ferroptotic cell death (29). Furthermore, NL01 downregulates *HCAR1* and *MCT1*, activating the *AMPK-SREBP1* signaling axis, leading to *GPX4* suppression and lipid peroxidation, ultimately triggering ferroptosis (30). These findings highlight NL01's potent anti-tumour activity and provide a novel therapeutic strategy for ovarian cancer by exploiting the ferroptotic pathway.

Curcumin and epigenetic regulation in ovarian cancer

Epigenetic dysregulation is a hallmark of ovarian cancer, contributing to tumour progression, metastasis, and therapeutic resistance (31). By targeting these aberrations, curcumin, a naturally derived bioactive compound, offers a promising approach to restoring the balance of gene expression. Among its mechanisms, curcumin's influence on miRNA expression, histone modifications, and DNA methylation highlights its potential to reprogram the cancer epigenome, disrupt oncogenic pathways, and enhance therapeutic efficacy (32). This section explores these epigenetic interactions, emphasising their implications for ovarian cancer management.

miRNA regulation by curcumin

miRNAs are non-coding RNA molecules that regulate gene expression post-transcriptionally, influencing various cellular processes such as proliferation, apoptosis, and metastasis (33). In ovarian cancer, the deregulation of miRNAs has been implicated in tumour progression and chemoresistance. Curcumin, a natural polyphenolic compound, has shown potential in modulating miRNA expression to exert anti-cancer effects.

Curcumin upregulates tumour-suppressive miRNAs such as miR-9, which targets the Akt/FOXO1 signaling axis, leading to increased apoptosis and reduced cell proliferation. Studies on SKOV3 ovarian cancer cells have shown that curcumin-induced expression of miR-9 inhibits the phosphorylation of Akt and FOXO1, thereby suppressing cell survival pathways and promoting caspase-3-mediated apoptosis (34). Another important miRNA modulated by curcumin is miR-199a-5p. Through its downregulation of the discoidin domain receptor 1 (DDR1), miR-199a-5p suppresses migration, epithelial-to-mesenchymal transition, and activation of the NF- κ B pathway, thus impairing ovarian cancer cell invasiveness (35).

In addition, curcumin influences the circRNA-miRNA-mRNA regulatory axis. For instance, curcumin enhances the expression of circ-*PLEKHM3*, which acts as a sponge for miR-320a, an oncogenic miRNA overexpressed in ovarian cancer. By reducing miR-320a levels, curcumin restores the tumour-suppressive function of *SMG1*, a kinase involved in apoptosis and cell cycle arrest. This regulatory network underscores the ability of curcumin to modulate non-coding RNA interactions in ovarian cancer progression (36).

Moreover, curcumin affects chemoresistance by targeting extracellular vesicle-mediated miRNA transfer. In cisplatin-resistant ovarian cancer cells, curcumin inhibits the transfer of miR-214 while upregulating the lncRNA *MEG3*, reversing drug resistance and sensitising cells to chemotherapy. The modulation of these miRNAs demonstrates curcumin's potential as an adjunct to standard ovarian cancer therapies, providing a multifaceted approach to targeting tumour growth and resistance mechanisms (37). When combined with dihydroartemisinin (DHA), curcumin synergistically enhances apoptosis in SKOV3 ovarian cancer cells by modulating miR-124 expression and targeting midkine (MK), a heparin-binding growth factor implicated in tumorigenesis and poor prognosis. The co-treatment significantly upregulates miR-124, which directly binds to MK mRNA, leading to its degradation and a subsequent reduction in MK protein levels. This mechanism promotes apoptotic cell death independent of caspase-3 activation and highlights the therapeutic potential of curcumin and DHA as a combinatorial strategy for ovarian cancer. Importantly, the combination not only demonstrated efficacy in vitro but also effectively suppressed tumour growth in vivo without notable toxicity, reinforcing its clinical promise for ovarian cancer treatment (38). Notably, curcumin modulates miR-133b, an miRNA implicated in drug resistance through its regulation of *GSTP-1*. *GSTP-1*, a key enzyme in glutathione metabolism, confers cisplatin resistance in ovarian cancer cells. By downregulating *GSTP-1* expression via miR-133b, curcumin increases the sensitivity of both cisplatin-sensitive and cisplatin-resistant ovarian cancer cells to chemotherapy (10).

Through its ability to selectively target and modulate miRNA expression, curcumin reprograms the molecular landscape of ovarian cancer cells, mitigating tumour progression and resistance. This dual modulation of oncogenic and tumour-suppressive miRNAs underscores curcumin's therapeutic potential, not only as a standalone epigenetic regulator and as an adjunct to existing treatment modalities. These findings pave the way for further exploration of miRNA-focused therapeutic strategies leveraging curcumin in ovarian cancer.

Histone modifications and DNA methylation

Epigenetic alterations, including histone modifications and DNA methylation, are pivotal in regulating gene expression and chromatin structure. These processes are frequently dysregulated in ovarian cancer, leading to the aberrant silencing of tumour-suppressor genes and the activation of oncogenes (12). Curcumin, with its established role as an epigenetic modulator, exerts profound effects on both histone acetylation and DNA methylation, offering a promising therapeutic avenue for ovarian cancer.

Histone modifications

Histone modifications, such as acetylation, methylation, phosphorylation, and ubiquitination, play pivotal roles in regulating chromatin structure and gene transcription. These dynamic changes determine whether chromatin adopts an open (euchromatin) or closed (heterochromatin) conformation, thereby controlling the accessibility of transcription factors to DNA. Among these modifications, histone acetylation is particularly well-studied due to its central role in maintaining transcriptional activity. Histone acetylation is catalysed by histone acetyltransferase (HATs), which add acetyl groups to lysine residues on histones, and reversed by histone deacetylase (HDACs), which remove these groups. Dysregulated HDAC activity in ovarian cancer leads to chromatin compaction and transcriptional silencing of critical tumour-suppressor genes, contributing to cancer progression, metastasis, and resistance to therapy (39, 40).

Curcumin has been shown to inhibit HDACs, which are often overexpressed in ovarian cancer, leading to the hypoacetylation of histones and the transcriptional silencing of tumour suppressor genes (9). By inhibiting HDACs, curcumin promotes the acetylation of histones H3 and H4, thereby enhancing chromatin accessibility and reactivating the silenced genes. For example, curcumin treatment increases the acetylation of histone H3 in the promoter regions of tumour suppressor genes such as *p21*, restoring their expression and inducing cell cycle arrest and apoptosis (9, 41).

In addition to its effects on acetylation, curcumin influence histone methylation. Histone methylation, particularly trimethylation at lysine residues such as H3K27me3,

is associated with transcriptional repression. Curcumin reduces the levels of H3K27me3 by downregulating the activity of histone methyltransferases (HMTs), such as *EZH2*, a key component of the polycomb repressive complex 2. This demethylation effect reactivates epigenetically silenced genes involved in tumour suppression and cell differentiation (42).

Furthermore, curcumin modulates the interplay between histone acetylation and methylation. Studies have demonstrated that curcumin alters the expression of epigenetic “writers” (HMTs), “erasers” (HDACs), and “readers” (bromodomain proteins), thereby exerting a broad impact on histone modification landscapes (43, 44). For example, the combination of curcumin with other agents, such as DNA demethylating drugs like decitabine, has been shown to synergistically alter histone and DNA methylation patterns, further enhancing tumour suppressor gene reactivation (43).

These findings underscore curcumin’s potential as a therapeutic agent in ovarian cancer by reversing aberrant histone modifications, thereby restoring normal gene expression and enhancing the efficacy of existing treatments. Future studies should focus on elucidating the precise molecular mechanisms of curcumin’s effects on histone-modifying enzymes and exploring its combination with other epigenetic therapies.

DNA methylation

DNA methylation, the addition of a methyl group to the fifth carbon of cytosine within CpG dinucleotides, is a crucial epigenetic mechanism that regulates gene expression without altering the DNA sequence. DNA methyltransferases (DNMTs), including *DNMT1*, *DNMT3A*, and *DNMT3B*, primarily mediate this process. Aberrant DNA methylation, characterised by hypermethylation of tumour suppressor genes and hypomethylation of oncogenes, is a hallmark of ovarian cancer and contributes to tumour progression, metastasis, and chemoresistance (43).

Curcumin modulates DNA methylation by targeting DNMTs. Studies indicate that curcumin directly inhibits DNMT activity, leading to the reactivation of silenced tumour suppressor genes such as *PTEN* and *p16INK4a*. For instance, in ovarian cancer, curcumin treatment was found to reduce CpG island hypermethylation in gene promoters, restoring normal transcriptional activity and inducing apoptosis (43, 44).

In addition to its DNMT inhibitory effects, curcumin enhances DNA demethylation through the activation of ten-eleven translocation (TET) enzymes, which convert 5-methylcytosine to 5-hydroxymethylcytosine. This dynamic regulation further contributes to the reversal of aberrant methylation marks in cancer cells (45).

Curcumin’s potential to enhance the efficacy of other epigenetic therapies has garnered significant attention. When combined with DNMT inhibitors like 5-aza-2'-deoxycytidine, curcumin synergistically amplifies the re-expression of tumour suppressor genes, addressing the limitations of monotherapy such as incomplete gene reactivation and off-target toxicity. Furthermore, curcumin’s inhibition of HDACs complements its suppression of DNMTs, creating a permissive chromatin environment conducive to the transcriptional activation of silenced genes. This dual modulation is particularly evident in the reactivation of *BRCA1*, which enhances DNA repair mechanisms and sensitises ovarian cancer cells to chemotherapy (44, 46).

These findings highlight curcumin’s multifaceted role in regulating DNA methylation, from reactivating tumour suppressor genes to restoring the global methylation balance. Its ability to synergize with other epigenetic therapies further underscores its potential as a powerful adjunct in ovarian cancer treatment. Future research should explore the precise molecular mechanisms underpinning curcumin’s epigenetic effects and assess its clinical utility in combination regimens.

Clinical implications and future directions

The ability of curcumin to modulate miRNAs, histone modifications, and DNA methylation highlights its potential as a multi-targeted epigenetic therapy for ovarian cancer. However, challenges such as curcumin’s limited bioavailability and rapid metabolism hinder the translation of curcumin research into clinical settings. To overcome these limitations, advanced curcumin formulations, including nanoparticles, liposomes, and conjugates with other carriers, are being developed to enhance its stability, solubility, and targeted delivery (47, 48). These innovations improve curcumin’s therapeutic efficacy *in vivo*.

Another promising avenue is the use of curcumin in combination therapies. Preclinical studies show that curcumin enhances the efficacy of standard chemotherapy agents, such as cisplatin and paclitaxel, by sensitising cancer cells through epigenetic reprogramming. For example, the combined use of curcumin and DNMT inhibitors has shown synergistic effects in restoring the expression of silenced tumour-suppressor genes, while its HDAC-inhibitory properties complement the actions of conventional drugs to disrupt tumour-promoting pathways (48). These combinatory approaches not only improve therapeutic outcomes but also mitigate the toxicity of high-dose chemotherapy.

Future research should also explore the long-term effects of curcumin on epigenetic regulation and its potential role in preventing relapse by maintaining tumour-suppressor gene activation. Large-scale clinical trials are needed to validate preclinical findings and establish

standardised protocols for curcumin-based therapies. By addressing these challenges and leveraging curcumin's multi-faceted epigenetic actions, this natural compound holds significant promise for improving outcomes in ovarian cancer treatment.

CONCLUSION

In conclusion, this review highlights the multifaceted role of curcumin in modulating key signaling pathways and epigenetic mechanisms implicated in ovarian cancer pathogenesis. Curcumin exhibits potent anti-proliferative, anti-metastatic, and pro-apoptotic effects in ovarian cancer cells, primarily through the inhibition of critical signaling pathways such as PI3K/Akt/mTOR, NF- κ B, and STAT3. Furthermore, curcumin exerted significant epigenetic effects, including the modulation of DNA methylation, histone modifications, and miRNA expression, as evidenced by the observed downregulation of miR-133b in combination with other treatments in cisplatin-resistant ovarian cancer cells. Curcumin contributes to the reversal of chemoresistance by modulating the miRNA expression profiles. Given its favourable safety profile and promising preclinical data, curcumin holds significant potential as an adjunct therapy for ovarian cancer, either alone or in combination with conventional treatments. Future research should focus on optimising curcumin delivery systems to enhance its bioavailability and target specific tumour microenvironments. In addition, comprehensive clinical trials are warranted to evaluate the efficacy and safety of curcumin in ovarian cancer patients. By further elucidating the underlying mechanisms of curcumin's action, including its impact on miRNA expression, and conducting rigorous clinical investigations, we can pave the way for the translation of this promising natural compound into an effective therapeutic strategy for ovarian cancer.

Peer Review: Externally peer-reviewed.

Author Contributions: Conception/Design of Study- Ö.T.K., D.B., E.B.Ü.; Data Acquisition- Ö.T.K., D.B., E.B.Ü.; Drafting Manuscript- Ö.T.K., D.B., E.B.Ü.; Critical Revision of Manuscript- Ö.T.K.; Final Approval and Accountability- Ö.T.K., D.B., E.B.Ü.; Technical or Material Support- Ö.T.K.; Supervision- Ö.T.K.

Conflict of Interest: The authors have no conflict of interest to declare.

Financial Disclosure: The authors declared that this study received no financial support.

REFERENCES

1. López-Portugués C, Montes-Bayón M, Díez P. Biomarkers in ovarian cancer: towards personalized medicine. *Proteomes* 2024;12(1):8. [CrossRef]
2. Lutkiewicz K, Bieleninik Ł, Kaloeti DVS, Bidzan M. Editorial: Reproductive health and well-being from a life span perspective. *Front Psychol* 2023;14:1289603. [CrossRef]
3. Yeung TL, Leung CS, Yip KP, Au Yeung CL, Wong ST, Mok SC. Cellular and molecular processes in ovarian cancer metastasis. A Review in the theme: Cell and molecular processes in cancer metastasis. *Am J Physiol Cell Physiol* 2015;309(7):C444-56. [CrossRef]
4. Kigawa J. New strategy for overcoming resistance to chemotherapy of ovarian cancer. *Yonago Acta Med* 2013;56:43-50.
5. Yang L, Xie HJ, Li YY, Wang X, Liu XX, Mai J. Molecular mechanisms of platinum-based chemotherapy resistance in ovarian cancer (Review). *Oncol Rep* 2022;47(4):82. [CrossRef]
6. Cancer Research UK. Stage 4 ovarian cancer. 2025 Jan 19. <https://www.cancerresearchuk.org/about-cancer/ovarian-cancer/stages-grades/stage-4>.
7. Cancer Research UK. Turmeric and cancer. 2025 Jan 19. <https://www.cancerresearchuk.org/about-cancer/treatment/complementary-alternative-therapies/individual-therapies/turmeric>
8. Farghadani R, Naidu R. Curcumin: Modulator of key molecular signaling pathways in hormone-independent breast cancer. *Cancers (Basel)* 2021;13:3427. [CrossRef]
9. Ravindran F, Mhatre A, Koroth J, Narayan S, Choudhary B. Curcumin modulates cell type-specific miRNA networks to induce cytotoxicity in ovarian cancer cells. *Life Sci* 2023;334:122224. [CrossRef]
10. Ülker EB, Aktaş EÇ, Seyhan MF, Isbir T, Billur D, Timirci-Kahraman Ö. Effects of curcumin and its analogue desmethoxycurcumin on miR-133b and its target gene GSTP-1 in cisplatin-resistant ovarian cancer cells. *Anticancer Res* 2024;44(12):5351-9. [CrossRef]
11. Sultana S, Munir N, Mahmood Z, Riaz M, Akram M, Rebezov M, et al. Molecular targets for the management of cancer using curcuma longa Linn. phytoconstituents: A Review. *Biomed Pharmacother* 2021;135:111078. [CrossRef]
12. Liu X, Qi M, Li X, Wang J, Wang M. Curcumin: a natural organic component that plays a multi-faceted role in ovarian cancer. *J Ovarian Res* 2023;16:47. [CrossRef]
13. Wilken R, Veena MS, Wang MB, Srivatsan ES. Curcumin: A review of anti-cancer properties and therapeutic activity in head and neck squamous cell carcinoma. *Mol Cancer* 2011;10:12. [CrossRef]
14. Nara K, Taguchi A, Yamamoto T, Hara K, Tojima Y, Honjoh H, et al. Heterogeneous effects of cytotoxic chemotherapies for platinum-resistant ovarian cancer. *Int J Clin Oncol* 2023;28(9):1207-17. [CrossRef]
15. Yallapu MM, Maher DM, Sundram V, Bell MC, Jaggi M, Chauhan SC. Curcumin induces chemo/radio-sensitization in ovarian cancer cells and curcumin nanoparticles inhibit ovarian cancer cell growth. *J Ovarian Res* 2010;3:11. [CrossRef]
16. Farghadani R, Naidu R. Curcumin as an enhancer of therapeutic efficiency of chemotherapy drugs in breast cancer. *Int J Mol Sci* 2022;23(4):2144. [CrossRef]
17. Porta C, Paglino C, Mosca A. Targeting PI3K/Akt/mTOR signaling in cancer. *Front Oncol* 2014;4:64. [CrossRef]
18. Golmohammadi M, Zamanian MY, Al-Ani AM, Jabbar TL, Kareem AK, Aghaei ZH, et al. Targeting STAT3 signaling

- pathway by curcumin and its analogues for breast cancer: A narrative review. *Animal Model Exp Med* 2024;7(6):853-867. [CrossRef]
19. Fan Y, Mao R, Yang J. NF- κ B and STAT3 signaling pathways collaboratively link inflammation to cancer. *Protein Cell* 2013;4(3):176-85. [CrossRef]
 20. Harrington BS, Annunziata CM. NF- κ B Signaling in ovarian cancer. *Cancers (Basel)* 2019;11(8):1182. [CrossRef]
 21. Liu H, Li X, Shi Y, Ye Z, Cheng X. Protein Tyrosine Phosphatase PRL-3: A key player in cancer signaling. *Biomolecules* 2024;14(3):342. [CrossRef]
 22. Liu S, Zhou S, Wang B, Jia Z. Effects of curcumin nanoparticles on the proliferation and migration of human ovarian cancer cells assessed through the NF- κ B/PRL-3 signaling pathway. *Int Immunopharmacol* 2024;141:112964. [CrossRef]
 23. Dixon SJ, Lemberg KM, Lamprecht MR, Skouta R, Zaitsev EM, Gleason CE, et al. Ferroptosis: an iron-dependent form of nonapoptotic cell death. *Cell* 2012;149(5):1060-72. [CrossRef]
 24. Zhang Y, Yu C, Peng C, Peng F. Potential roles and mechanisms of curcumin and its derivatives in the regulation of ferroptosis. *Int J Biol Sci* 2024;20(12):4838-52. [CrossRef]
 25. Li L, Qiu C, Hou M, Wang X, Huang C, Zou J, et al. Ferroptosis in ovarian cancer: A novel therapeutic strategy. *Front Oncol* 2021;11:665945. [CrossRef]
 26. Stockwell BR, Friedmann Angeli JP, Bayir H, Bush AI, Conrad M, Dixon SJ, et al. Ferroptosis: A regulated cell death nexus linking metabolism, redox biology, and disease. *Cell* 2017;171(2):273-85. [CrossRef]
 27. Tang S, Chen L. The recent advancements of ferroptosis of gynecological cancer. *Cancer Cell Int* 2024;24(1):351. [CrossRef]
 28. Kapper C, Oppelt P, Arbeithuber B, Gyunesh AA, Vilusic I, Stelzl P, et al. Targeting ferroptosis in ovarian cancer: Novel strategies to overcome chemotherapy resistance. *Life Sci* 2024;349:122720. [CrossRef]
 29. Zhao Y, Li M, Yao X, Fei Y, Lin Z, Li Z, et al. HCAR1/MCT1 Regulates tumor ferroptosis through the lactate-mediated AMPK-SCD1 activity and its therapeutic implications. *Cell Rep* 2020;33(10):108487. [CrossRef]
 30. Shi M, Zhang MJ, Yu Y, Ou R, Wang Y, Li H, et al. Curcumin derivative NL01 induces ferroptosis in ovarian cancer cells via HCAR1/MCT1 signaling. *Cell Signal* 2023;109:110791. [CrossRef]
 31. Kwon MJ, Shin YK. Epigenetic regulation of cancer-associated genes in ovarian cancer. *Int J Mol Sci* 2011;12(2):983-1008. [CrossRef]
 32. Reuter S, Gupta SC, Park B, Goel A, Aggarwal BB. Epigenetic changes induced by curcumin and other natural compounds. *Genes Nutr* 2011;6(2):93-108. [CrossRef]
 33. Hussen BM, Hidayat HJ, Salihi A, Sabir DK, Taheri M, Ghafouri-Fard S. MicroRNA: A signature for cancer progression. *Biomed Pharmacother* 2021;138:111528. [CrossRef]
 34. Zhao SF, Zhang X, Zhang XJ, Shi XQ, Yu ZJ, Kan QC. Induction of microRNA-9 mediates cytotoxicity of curcumin against SKOV3 ovarian cancer cells. *Asian Pac J Cancer Prev* 2014;15(8):3363-8. [CrossRef]
 35. Ravindran F, Koroth J, Manjunath M, Narayan S, Choudhary B. Curcumin derivative ST09 modulates the miR-199a-5p/DDR1 axis and regulates proliferation and migration in ovarian cancer cells. *Sci Rep* 2021;11(1):23025. [CrossRef]
 36. Sun S, Fang H. Curcumin inhibits ovarian cancer progression by regulating circ-*PLEKHM3*/miR-320a/SMG1 axis. *J Ovarian Res* 2021;14(1):158. [CrossRef]
 37. Zhang J, Liu J, Xu X, Li L. Curcumin suppresses cisplatin resistance development partly by modulating extracellular vesicle-mediated transfer of MEG3 and miR-214 in ovarian cancer. *Cancer Chemother Pharmacol* 2017;79(3):479-87. [CrossRef]
 38. Zhao J, Pan Y, Li X, Zhang X, Xue Y, Wang T, et al. Dihydroartemisinin and curcumin synergistically induce apoptosis in SKOV3 cells Via upregulation of MiR-124 targeting midkine. *Cell Physiol Biochem* 2017;43(2):589-601. [CrossRef]
 39. Vijayalakshmi P, Gowdham M, Dinesh DC, Sibiya A, Vaseeharan B, Selvaraj C. Unveiling the guardians of the genome: The dynamic role of histones in DNA organization and disease. *Adv Protein Chem Struct Biol* 2025;143:39-68. [CrossRef]
 40. Skrzypczak M, Wolinska E, Adaszek Ł, Ortmann O, Treec O. Epigenetic modulation of estrogen receptor signaling in ovarian cancer. *Int J Mol Sci* 2024;26(1):166. [CrossRef]
 41. Yen HY, Tsao CW, Lin YW, Kuo CC, Tsao CH, Liu CY. Regulation of carcinogenesis and modulation through Wnt/ β -catenin signaling by curcumin in an ovarian cancer cell line. *Sci Rep* 2019;9(1):17267. [CrossRef]
 42. Al-Yousef N, Shinwari Z, Al-Shahrani B, Al-Showimi M, Al-Moghrabi N. Curcumin induces re-expression of BRCA1 and suppression of γ synuclein by modulating DNA promoter methylation in breast cancer cell lines. *Oncol Rep* 2020;43(3):827-38. [CrossRef]
 43. Hassan FU, Rehman MS, Khan MS, Ali MA, Javed A, Nawaz A, et al. Curcumin as an alternative epigenetic modulator: Mechanism of action and potential effects. *Front Genet* 2019;10:514. [CrossRef]
 44. Irshad R, Husain M. Natural products in the reprogramming of cancer epigenetics. *Toxicol Appl Pharmacol* 2021;417:115467. [CrossRef]
 45. Prasanth MI, Sivamaruthi BS, Cheong CSY, Verma K, Tencomnao T, Brimson JM, et al. Role of epigenetic modulation in neurodegenerative diseases: implications of phytochemical interventions. *Antioxidants (Basel)* 2024;13(5):606. [CrossRef]
 46. Kumar V, Kesharwani R, Patel DK, Verma A, Mehanna MG, Mohammad A, et al. Epigenetic impact of curcumin and thymoquinone on cancer therapeutics. *Curr Med Chem*. Published online April 4, 2024. doi:10.2174/0109298673288542240327112351. [CrossRef]
 47. Hegde M, Kumar A, Girisa S, Aswani BS, Vishwa R, Sethi G, et al. Nanoformulations of curcumin: An alliance for effective cancer therapeutics. *Food Biosci* 2023;56:103095. [CrossRef]
 48. Hosokawa M, Seiki R, Iwakawa S, Ogawara KI. Combination of azacytidine and curcumin is a potential alternative in decitabine-resistant colorectal cancer cells with attenuated deoxycytidine kinase. *Biochem Biophys Res Commun* 2021;578:157-62. [CrossRef]

SPONTANEOUS DISAPPEARANCE OF A CAUDATE NUCLEUS ARTERIOVENOUS MALFORMATION FOLLOWING EXTERNAL VENTRICULAR DRAINAGE: A CASE REPORT AND LITERATURE REVIEW

EKSTERNAL VENTRİKÜLER DRENAJ SONRASI SPONTAN KAYBOLAN KAUDAT ÇEKİRDEK ARTERİOVENÖZ MALFORMASYONU: OLGU SUNUMU VE LİTERATÜR İNCELEMESİ

Duygu DÖLEN¹ , Sefa ÖZTÜRK¹ , Alperen POYRAZ¹ , Cafer İkbal GÜLSEVER^{1,2} , Tuğrul Cem ÜNAL¹ , İlyas DOLAŞ¹ , Mehmet BARBUROĞLU³ , Pulat Akın SABANCI¹ 

¹İstanbul University, İstanbul Faculty of Medicine, Department of Neurosurgery, İstanbul, Türkiye

²Hakkari State Hospital, Clinic of Neurosurgery, Hakkari, Türkiye

³İstanbul University, İstanbul Faculty of Medicine, Department of Radiodiagnostik, Division Neuroradiology, İstanbul, Türkiye

ORCID IDs of the authors: D.D. 0000-0002-6929-4401; S.Ö. 0000-0001-5583-0384; A.P. 0000-0002-3885-5894; C.İ.G. 0000-0002-9246-1378; T.C.Ü. 0000-0001-6228-1379; İ.D. 0000-0002-3425-3220; M.B. 0000-0002-8715-1893; P.A.S. 0000-0002-0283-0927

Cite this article as: Dölen D, Öztürk S, Poyraz A, Gülsever Cİ, Ünal TC, Dolaş İ, et al. Spontaneous disappearance of a caudate nucleus arteriovenous malformation following external ventricular drainage: A case report and literature review. J Ist Faculty Med 2025;88(2):172-175. doi: 10.26650/IUITFD.1623147

ABSTRACT

Brain arteriovenous malformations (AVMs) are congenital vascular anomalies that can cause life-threatening haemorrhages. Spontaneous AVM thrombosis is extremely rare and is not fully understood. A 15-year-old female presented with severe headache and confusion. Computed tomography (CT) revealed intraventricular haemorrhage, leading to urgent external ventricular drainage (EVD). Digital subtraction angiography (DSA) confirmed an AVM located in the right caudate nucleus head, supplied by the lateral lenticulostriate artery and draining into the deep venous system. At the 2-month follow-up, DSA showed complete disappearance of the AVM. This case highlights the rare phenomenon of spontaneous AVM thrombosis, potentially influenced by haemorrhage, venous outflow obstruction, and EVD placement. While spontaneous resolution is possible, long-term imaging follow-up is essential due to the risk of delayed recanalization.

Keywords: Arteriovenous malformation, external ventricular drainage, intraventricular haemorrhage, spontaneous thrombosis

ÖZET

Beyin arteriovenöz malformasyonları (AVM), yaşamı tehdit eden kanamalara yol açabilen konjenital vasküler anomalilerdir. AVM'lerin kendiliğinden tromboze olması son derece nadir görülen ve yeterince anlaşılamayan bir durumdur. On beş yaşında bir kız hasta, şiddetli baş ağrısı ve bilinç bulanıklığı ile acil servise başvurdu. Bilgisayarlı tomografi (BT), intraventriküler kanama varlığı gösterdi ve acil eksternal ventriküler drenaj (EVD) uygulandı. Dijital substraksiyon anjiyografi (DSA), sağ kaudat çekirdek başına yerleşmiş, lateral lentikülostriat arter tarafından beslenen ve derin venöz sisteme drene olan bir AVM varlığını doğruladı. İki ay sonra yapılan kontrol takibinde DSA'da AVM'nin tamamen kaybolduğu gözlemlendi. Bu olgu, kanama, venöz drenaj tıkanıklığı ve EVD uygulamasının AVM trombozunu nasıl tetikleyebileceğini gösteren nadir bir örnektir. AVM'lerin kendiliğinden kaybolması mümkün olmakla birlikte, geç rekürrens riski nedeniyle uzun süreli görüntüleme takibi gereklidir.

Anahtar kelimeler: Arteriovenöz malformasyon, eksternal ventriküler drenaj, intraventriküler kanama, spontan tromboz

Corresponding author/İletişim kurulacak yazar: Cafer İkbal GÜLSEVER – cafer.gulsever@gmail.com

Submitted/Başvuru: 19.01.2025 • **Accepted/Kabul:** 08.03.2025 • **Published Online/Online Yayın:** 17.04.2025



Content of this journal is licensed under a Creative Commons Attribution-NonCommercial 4.0 International License.

INTRODUCTION

Brain arteriovenous malformations (AVMs) are congenital vascular anomalies characterised by abnormal tangles of arteries and veins lacking an intervening capillary network (1). Rupture of AVMs is a well-known cause of intracerebral haemorrhage (ICH) and is the most common cause of ICH in the paediatric population. Symptoms of AVMs, including headache, seizures, and motor weakness, are non-specific and can mimic other neurological conditions (2).

AVMs are classified into five grades based on three features: size (<3 cm, 3–6 cm, >6 cm), location (eloquent vs. non-eloquent), and venous drainage (superficial vs. deep). Diagnosis is typically achieved through computed tomography angiography (CTA), magnetic resonance angiography (MRA), and digital subtraction angiography (DSA), with DSA being the gold standard (3).

In this study, we report a case of an AVM with a small nidus located in the caudate nucleus head, presenting with an intraventricular haematoma that disappeared spontaneously following external ventricular drain (EVD) placement.

CASE PRESENTATION

A 15-year-old woman with no known comorbidities presented to the paediatric emergency unit with headache and confusion. Neurological examination revealed spontaneous breathing, spontaneous eye opening, isochoric pupils with positive light reflex, uncooperativeness, flexor response to painful stimuli, and nonsensical vocalisation (GCS: 8, E2M4V2). The patient was promptly intubated and stabilised.

A non-contrast cranial computed tomography (CT) scan demonstrated diffuse intraventricular haemorrhage. An EVD was immediately placed, with the evacuation of the high-pressure haemorrhagic fluid. The drainage rate was adjusted to 10–15 cc/h. A contrast-enhanced cranial CT angiography scan was subsequently performed, revealing an AVM in close proximity to the right caudate nucleus head and near the EVD catheter (Figure 1).

Diagnostic DSA confirmed an AVM in the same region, receiving arterial supply from the lateral lenticulostriate artery. The nidus measured approximately 6 mm in diameter, with a 1.2 mm aneurysm within it. Venous drainage occurred via the deep circulation through the thalamostriate vein. The AVM was classified as Spetzler-Martin Grade 2 and Lawton-Young Score 1.

The patient was transferred to the intensive care unit (ICU), where sedation was gradually reduced. By the second day post-haemorrhage, she was extubated. The patient's neurological examination was intact (GCS: 15), with no motor deficits or cognitive impairment.

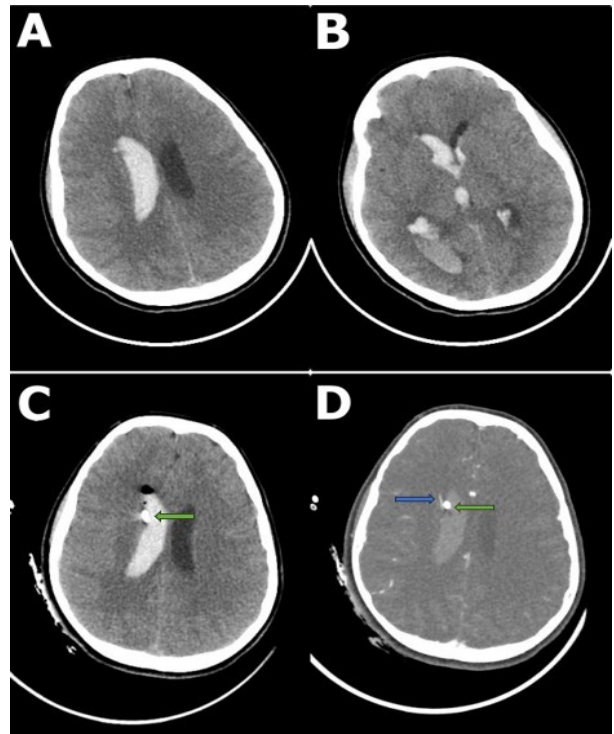


Figure 1: A, B: Preoperative CT scans demonstrating acute intraventricular haemorrhage. (C) Postoperative CT scan confirming persistent intraventricular haemorrhage with the EVD catheter (green arrow) positioned within the ventricle. D: Postoperative CT angiography revealing intraventricular haemorrhage, a suspected AVM nidus (blue arrow) at the head of the right caudate nucleus, and the close proximity of the EVD catheter (green arrow) to the AVM drainage vein within the ventricle

Follow-up imaging showed a gradual reduction in intraventricular haematoma volume. The EVD was removed on the seventh day post-haemorrhage. The patient had an uneventful recovery, with no wound infections, fever, or additional complaints. She was discharged on day 20 with a scheduled follow-up DSA after 2 months.

At the 2-month follow-up, repeat DSA revealed complete disappearance of the previously identified AVM adjacent to the right caudate nucleus head (Figure 2).

DISCUSSION

Management options for AVMs include microsurgical resection, stereotactic radiosurgery, endovascular embolisation, or a combination of these approaches. The Spetzler-Martin and Lawton-Young grading systems guide treatment selection by assessing the AVM size, location, venous drainage, patient age, and haemorrhage history (4).

In the Spetzler-Martin grading system, microsurgical resection is typically preferred for low-grade AVMs (Grades

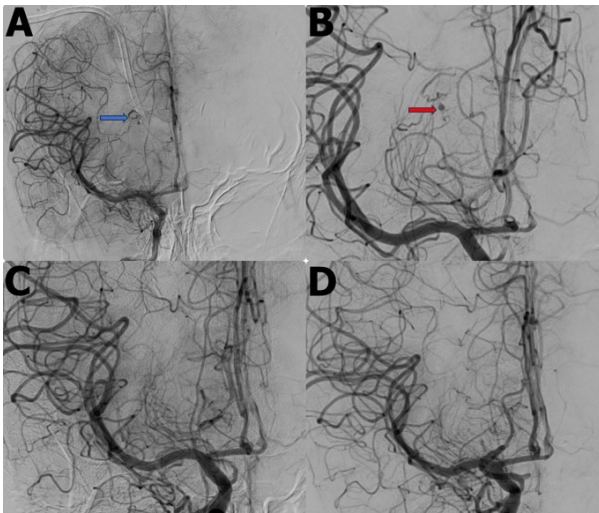


Figure 2: A, B: Preoperative diagnostic DSA scans showing an AVM (blue arrow) adjacent to the right caudate nucleus head, supplied by the lateral lenticulostriate artery. The nidus measured approximately 6 mm in diameter, with a 1.2 mm aneurysm (red arrow) identified within it, and drainage occurred via the thalamostriate vein. The AVM was also noted to be in close proximity to the EVD catheter and its drainage vein within the ventricle. C, D: Follow-up DSA at 2 months demonstrating complete disappearance of the previously identified AVM near the right caudate nucleus head

I–III) because of the relatively low surgical risk. Conversely, high-grade AVMs (Grades IV–V) may be unsuitable for surgery, and alternative treatments such as stereotactic radiosurgery or endovascular embolisation are preferred (5). Lawton et al. introduced the Supplemented Spetzler-Martin grade, which incorporates additional factors such as patient age, haemorrhage history, and nidus type to improve surgical risk assessment (4).

Spontaneous AVM disappearance

Spontaneous regression of brain AVMs is exceptionally rare, with an estimated incidence of 0.1%. Small AVMs with a single superficial draining vein and prior haemorrhage have a higher likelihood of spontaneous thrombosis (6).

Following an initial haemorrhage, the mass effect and associated hemodynamic changes may lead to reduced blood flow to the AVM. The subsequent gliotic reaction alters venous drainage and may promote thrombosis. In AVMs with a single draining vein, the lack of alternative outflow pathways may increase the susceptibility to complete thrombosis. This process is believed to be gradual, with thrombosis developing over time rather than as a sudden event (7).

In this case, the presence of a single deep draining vein and the history of previous haemorrhage likely contrib-

uted to the spontaneous AVM thrombosis. Additionally, the proximity of the EVD catheter to the AVM nidus may have facilitated thrombosis, potentially due to localised hemodynamic alterations or inflammatory responses.

Clinical implications and follow-up

The annual haemorrhage rate of AVMs is estimated to be 2.2%–4.5% per 100 patient-years, increasing significantly after an initial rupture. The risk of rehemorrhage within the first year post-rupture ranges from 6% to 15.8%, emphasising the importance of early intervention in high-risk cases (8). However, given the extremely low likelihood of spontaneous AVM obliteration, conservative management should not be considered a primary strategy. Patients who opt for non-operative management should be informed of the rare but possible outcome of spontaneous resolution (9).

Long-term follow-up is essential because cases of delayed AVM recanalization have been reported up to 39 months after the initial disappearance (10). In this case, no recanalization was observed during the six-month follow-up period. However, continued surveillance with magnetic resonance angiography (MRA) has been recommended to rule out late recanalization.

CONCLUSION

The spontaneous disappearance of brain AVMs is an extremely rare phenomenon, likely influenced by a combination of haemorrhage-induced hemodynamic changes, venous outflow obstruction, and gliotic responses. In this case, the presence of a single deep draining vein, prior bleeding, and the proximity of the EVD catheter to the AVM nidus may have contributed to the thrombosis. While spontaneous resolution is possible, it should not be considered a primary management strategy due to the unpredictable risk of rebleeding or delayed recanalization. Long-term radiological follow-up remains crucial to ensure that the AVM does not reappear, and further research is needed to better understand the mechanisms behind spontaneous AVM obliteration.

Informed Consent: Participant consent was obtained from the patient's family.

Peer Review: Externally peer-reviewed.

Author Contributions: Conception/Design of Study- D.D., S.Ö., A.P., C.İ.G.; Data Acquisition- S.Ö., A.P.; Data Analysis/Interpretation – T.C.Ü., İ.D., M.B., P.A.S.; Drafting Manuscript- S.Ö., A.P., C.İ.G.; Critical Revision of Manuscript- D.D., T.C.Ü., M.B., İ.D., P.A.S.; Final Approval and Accountability- D.D., T.C.Ü., İ.D., M.B., P.A.S.

Acknowledgement: The authors would like to express their gratitude to the neurosurgery and radiology teams involved in the

diagnosis and management of this case. Special thanks to the intensive care unit staff for their dedicated patient care. We also acknowledge the patient and their family for their cooperation and consent in sharing this case for academic and clinical learning purposes.

Conflict of Interest: The authors have no conflict of interest to declare.

Financial Disclosure: The authors declared that this study received no financial support.

REFERENCES

1. Lawton MT, Rutledge WC, Kim H, Stapf C, Whitehead KJ, Li DY, et al. Brain arteriovenous malformations. *Nat Rev Dis Primers* 2015;1:15008. [\[CrossRef\]](#)
2. Panciani PP, Fontanella M, Carlino C, Bergui M, Ducati A. Progressive spontaneous occlusion of a cerebellar AVM: pathogenetic hypothesis and review of literature. *Clin Neurol Neurosurg* 2008;110(5):502-10. [\[CrossRef\]](#)
3. Buis DR, Van Den Berg R, Lycklama G, Van Der Worp HB, Dirven CMF, Vandertop WP. Spontaneous regression of brain arteriovenous malformations--a clinical study and a systematic review of the literature. *J Neurol* 2004;251(11):1375-82. [\[CrossRef\]](#)
4. Lawton MT, Kim H, McCulloch CE, Mikhak B, Young WL. A supplementary grading scale for selecting patients with brain arteriovenous malformations for surgery. *Neurosurgery* 2010;66(4):702-13. [\[CrossRef\]](#)
5. Spetzler RF, Martin NA. A proposed grading system for arteriovenous malformations. *J Neurosurg* 1986;65(4):476-83. [\[CrossRef\]](#)
6. Montalvo-Afonso A, Delgado-López PD, Lista-Araujo MT, Rodríguez-Salazar A. Angiographically occult and spontaneously thrombosed large brain arteriovenous malformation. *Neurocirugia (Astur: Engl Ed)* 2020;32(4):203-8. [\[CrossRef\]](#)
7. Schwartz ED, Hurst RW, Sinson G, Bagley LJ. Complete regression of intracranial arteriovenous malformations. *Surg Neurol* 2002;58(2):139-47. [\[CrossRef\]](#)
8. Agyemang K, Rose A, Olukoya O, Brown J, St George EJ. Spontaneous obliteration of brain arteriovenous malformations: illustrative cases. *J Neurosurg Case lessons* 2022;4(21):CASE22309. [\[CrossRef\]](#)
9. Chen X, Lu X, Yan F, Xu W, Gao L, Zheng J, et al. Spontaneous thrombosis in main draining veins of unruptured cerebral arteriovenous malformations: A case report. *Medicine (Baltimore)* 2019;98(22):e15588. [\[CrossRef\]](#)
10. Mizutani T, Tanaka H, Aruga T. Total recanalization of a spontaneously thrombosed arteriovenous malformation. Case report. *J Neurosurg* 1995;82(3):506-8. [\[CrossRef\]](#)

CASE REPORTS AS AN ARTICLE: A FORLORN CAUSE?

YAYIN OLARAK OLGU SUNUMLARI: YETERİNCE DEĞER GÖRMÜYOR MU?

Manas BAJPAI¹ 

¹Department of Oral Pathology and Microbiology, Rural Dental College, Loni (Maharashtra) India

ORCID IDs of the authors: M.B. 0000-0001-6168-3069

Cite this article as: Bajpai M. Case reports as an article: A forlorn cause?. J Ist Faculty Med 2025;88(2):176-177. doi: 10.26650/IUITFD.1621922

Case reports are defined as brief reports that describe the unique aspects of a medical case and contribute significantly to the existing medical literature and medical education (1).

The academic landscape has long been shaped by the publication of case reports, which have traditionally played a vital role in advancing scientific knowledge and understanding (2). Case reports, which provide detailed accounts of individual patient experiences, have been lauded for their ability to shed light on rare diseases, novel interventions, and unique clinical presentations (1). However, in recent years, there has been a growing concern about the declining importance of case reports in academia (2, 3).

One of the primary reasons for this trend is the perception that case reports do not highly rank in the hierarchy of scientific evidence. In the context of evidence-based medicine, randomised controlled trials and systematic reviews are generally considered to be more robust and reliable sources of information (1, 2). As a result, many high-impact medical journals have become increasingly reluctant to publish case reports, as they are seen as less valuable contributions to the scientific literature. The impact factor is the average number of citations garnered by a journal, an indicator to assess the significance of a particular journal in the academic field. The citation probability of case reports is much lesser compared to the original researches, review articles and meta-analyses (3). The journals have limited spaces due to the limited issues per year/volume; most of the journals publish two or three

case reports in a single issue and with a rapid expansion of scientific community, journals receive huge number of submissions making the selection process significantly competitive. Some journals encourage authors to submit their case reports in a concise form under letter to editor, clinical/radiological/histopathological image and quiz. It is challenging for the editors to find a suitable reviewer for a case report, especially when it deals with a unique and rare case. The assessment of the quality and viability of such case reports becomes a challenge to the editor (Figure 1).

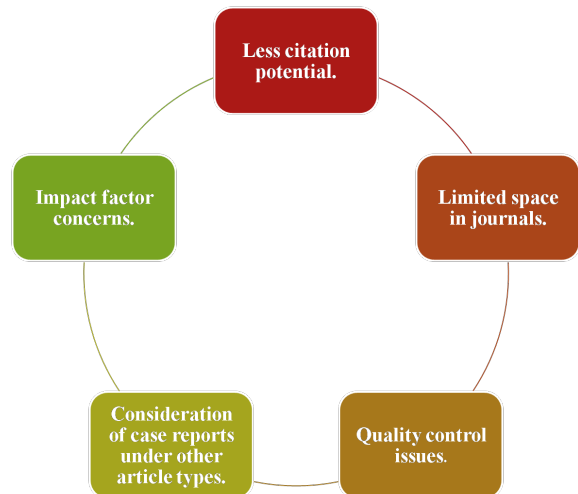


Figure 1: Few probable causes behind the decline of case reports in the scientific literature.

Corresponding author/İletişim kurulacak yazar: Manas BAJPAI – drmb1987@gmail.com

Submitted/Başvuru: 17.01.2025 • **Accepted/Kabul:** 04.02.2025 • **Published Online/Online Yayın:** 24.02.2025



Content of this journal is licensed under a Creative Commons Attribution-NonCommercial 4.0 International License.

Despite this shift, it is important to recognise the significant educational and practical value of case reports. They have long been used as a means of disseminating information on unusual clinical presentations, disease associations, and responses to treatment. Moreover, case reports can serve as a valuable learning experience for both authors and readers, as they provide insights into the practical application of medical knowledge.

REFERENCES

1. Nissen T, Wynn R. The clinical case report: a review of its merits and limitations. *BMC Res Notes* 2014;7:264. [\[CrossRef\]](#)
2. Bradley PJ. Guidelines to authors publishing a case report: the need for quality improvement. *AME Case Rep* 2018;2:10. [\[CrossRef\]](#)
3. Taheri A, Adibi P, Abbasi A, Sabbagh Jaffari M, Rahimi A. Analysis of the reporting requirements of clinical case reports dedicated journals: Towards updating the CARE Guideline. *Adv Biomed Res* 2023;12:41. [\[CrossRef\]](#)